



ANALYTICAL APPROACH TO DIAGNOSE THE INFLUENCE OF THE BURIAL ENVIRONMENT ON THE CONSERVATION STATE OF ARCHAEOLOGICAL REMAINS: FROM LITHIC TO METALLIC OBJECTS

Estefanía Estalayo Mena



eman ta zabal zaku

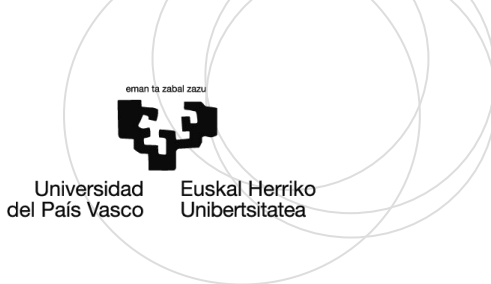


Universidad
del País Vasco

Euskal Herriko
Unibertsitatea



ZTF-FCT
Zientzia eta Teknologia Fakultatea
Facultad de Ciencia y Tecnología



Universidad
del País Vasco

Euskal Herriko
Unibertsitatea

*Department of Analytical Chemistry
Faculty of Science and Technology
University of the Basque Country*

Department of Analytical Chemistry

Analytical approach to diagnose the influence of the burial environment on the conservation state of archaeological remains: From lithic to metallic objects

Dissertation presented for the national PhD degree

Estefania Estalayo Mena

May 2022

Supervised by:

Juan Manuel Madariaga Mota

Julene Aramendia Gutiérrez

Todos tenemos luz y oscuridad en nuestro interior. Lo que importa es que parte decidimos potenciar.

TABLE OF CONTEXT

| | | |
|-----------|---|------------|
| 1. | INTRODUCTION | 2 |
| 1.1 | <i>WORLD HERITAGE.....</i> | 2 |
| 1.2 | <i>PROTECTION AND CONSERVATION OF CULTURAL HERITAGE</i> | 6 |
| 1.3 | <i>DETERIORATION OF CULTURAL HERITAGE</i> | 10 |
| 1.3.1 | Deterioration of Underwater Cultural Heritage | 12 |
| 1.3.1.1 | Physicochemical parameters of the marine environment relevant to the degradation of archaeological pieces | 13 |
| 1.3.1.1.1 | Metallic materials | 16 |
| 1.3.1.1.2 | Wood materials..... | 19 |
| 1.3.2 | Deterioration of the buried cultural heritage..... | 23 |
| 1.3.2.1 | Physicochemical parameters of the buried environment relevant to the degradation of archaeological pieces..... | 24 |
| 1.4 | <i>CHEMISTRY IN ARCHAEOLOGY.....</i> | 37 |
| 1.5 | <i>ANALYTICAL TECHNIQUES.....</i> | 44 |
| 1.6 | <i>BIBLIOGRAPHY</i> | 52 |
| 2. | OBJECTIVES | 70 |
| 3. | MATERIALS AND METHODS | 74 |
| 3.1 | <i>SPECTROSCOPIC INSTRUMENTS FOR IN-SITU ANALYSIS.....</i> | 81 |
| 3.1.1 | Portable Raman Spectroscopy..... | 81 |
| 3.1.2 | Handheld Energy Dispersive X-Ray Fluorescence (EDXRF) | 82 |
| 3.2 | <i>SPECTROSCOPIC INSTRUMENTS FOR LABORATORY ANALYSIS</i> | 83 |
| 3.2.1 | Laboratory Raman Spectroscopy..... | 84 |
| 3.2.2 | Micro-Energy Dispersive X-Ray Fluorescence Spectroscopy (μ -ED-XRF) 86 | |
| 3.2.3 | Scanning Electron Microscope – Energy Dispersive X-Ray Spectroscopy (SEM-EDS) | 88 |
| 3.2.4 | X-Ray diffraction (XRD) | 89 |
| 3.3 | <i>BIBLIOGRAPHY</i> | 91 |
| 4. | SAMPLES AND EMPLACEMENTS | 100 |
| 4.1 | <i>SAMPLES BURIED IN MARINE OR ESTUARINE SEDIMENTS.....</i> | 100 |
| 4.1.1 | Urbieta shipwreck..... | 100 |
| 4.1.1.1 | Historical context | 100 |
| 4.1.1.2 | Emplacement | 105 |
| 4.1.1.3 | Description of the analyzed samples | 106 |

| | | |
|-----------|--|------------|
| 4.1.1.4 | Conservation state and restauration treatments | 107 |
| 4.1.2 | Bakio shipwreck | 108 |
| 4.1.2.1 | Historical context | 108 |
| 4.1.2.2 | Emplacement | 111 |
| 4.1.2.3 | Description of the analyzed samples | 112 |
| 4.1.2.4 | Conservation state and restauration treatments | 117 |
| 4.2 | <i>SAMPLES BURIED IN SOIL</i> | 121 |
| 4.2.1 | Glass beads of Vaccaei culture | 121 |
| 4.2.1.1 | Historical context | 121 |
| 4.2.1.2 | Emplacement | 123 |
| 4.2.1.3 | Description of the analyzed samples | 124 |
| 4.2.1.4 | Conservation state and restauration treatments | 126 |
| 4.2.2 | Lithic tools..... | 127 |
| 4.2.2.1 | Historical context | 127 |
| 4.2.2.2 | Emplacement | 128 |
| 4.2.2.3 | Description of the analyzed samples | 129 |
| 4.2.2.4 | Conservation state and restauration treatments | 131 |
| 4.2.3 | Iron archaeological slags..... | 132 |
| 4.2.3.1 | Historical context | 132 |
| 4.2.3.2 | Emplacement | 133 |
| 4.2.3.3 | Description of the analyzed samples | 136 |
| 4.2.3.4 | Conservation state and restauration treatments | 137 |
| 4.3 | <i>BIBLIOGRAPHY</i> | 138 |
| 5. | RESULTS FROM THE SAMPLES BURIED IN MARINE SEDIMENTS..... | 146 |
| 5.1 | <i>THE URBIETA SHIPWRECK</i> | 149 |
| 5.1.1 | Mineral phases detected in the nails..... | 166 |
| 5.1.2 | Discussion of Urbieta shipwreck analyses | 176 |
| 5.2 | <i>THE BAKIO SHIPWRECK</i> | 181 |
| 5.2.1 | Musket and bullet analysis | 181 |
| 5.2.2 | Detached pieces from the iron anchor and the swivel gun | 195 |
| 5.2.3 | Eight-pounder guns | 209 |
| 5.2.4 | Discussion of Bakio shipwreck analyses | 212 |
| 5.2.4.1 | Musket and bullet analysis..... | 213 |
| 5.2.4.2 | Detached pieces from the iron anchor and the swivel gun | 213 |
| 5.2.4.3 | Eight-pounder guns..... | 214 |
| 5.3 | <i>CONCLUSIONS OF SAMPLES BURIED IN MARINE/ESTUARINE SEDIMENTS</i> | 215 |
| 5.4 | <i>BIBLIOGRAPHY</i> | 218 |
| 6. | RESULTS FROM THE SAMPLES BURIED IN SOIL | 232 |
| 6.1 | <i>GLASS BEADS OF VACCAEI CULTURE</i> | 232 |
| 6.1.1 | Discussion of glass beads of Vaccaei culture analyses | 288 |
| 6.2 | <i>LITHIC TOOLS</i> | 291 |

| | | |
|------------|--|------------|
| 6.2.1 | Discussion of arrowheads analyses | 309 |
| 6.3 | <i>IRON ARCHAEOLOGICAL SLAGS</i> | 311 |
| 6.3.1 | Discussion of iron archaeological slags analyses | 316 |
| 6.4 | <i>CONCLUSIONS OF SAMPLES BURIED IN SOIL</i> | 318 |
| 6.5 | <i>BIBLIOGRAPHY</i> | 320 |
| 7. | INTEGRATED DISCUSSION AND CONCLUSIONS | 324 |
| 7.1 | <i>BIBLIOGRAPHY</i> | 329 |
| 8. | APENDIXES | 332 |
| 8.1 | <i>SCIENTIFIC PUBLICATIONS</i> | 332 |
| 8.1.1 | Articles | 332 |
| 8.1.2 | Book chapters | 332 |
| 8.1.3 | Congresses | 332 |
| 9. | ACKNOWLEDGEMENTS | 336 |
| 10. | BIBLIOGRAPHY | 350 |

CHAPTER 1



1. INTRODUCTION

*“Four things cannot be hidden for long: science, stupidity, wealth, and poverty” –
“Cuatro cosas no pueden ocultarse por mucho tiempo: la ciencia, la estupidez, la
riqueza y la pobreza” – Averroes*

1.1 WORLD HERITAGE

World Heritage is the set of cultural and natural assets that have been inherited from our ancestors, and which allow us to understand and know more about the history, customs, and way of life so far today¹. World Heritage is the base on which humanity builds its collective memory and identity, it is what makes us identify with a culture, with a language and, with a specific way of life. World Heritage is the legacy that we receive from the past, in which we live in the present and what we will pass on to future generations¹. Places as diverse and unique as the Pyramids of Egypt, the Great Barrier Reef in Australia, Galápagos Islands in Ecuador, The Taj Mahal in India, the Grand Canyon in the USA, or the Acropolis in Greece are examples of some natural and cultural places inscribed on the World Heritage List to date¹.

These concepts are defined by UNESCO, the United Nations Educational, Scientific and Cultural Organization for Science and Culture Education. It was created in 1945 with the aim of promoting the identification, protection, and preservation of the Cultural and Natural Heritage of the entire world. At the UNESCO General Conference held in 1972², the countries belonging to the

organization agreed to take the necessary measures to protect these groups and be able to transmit them to future generations. As a result of this conference, the World Heritage Convention was approved in 1975. Initially, 20 states signed it. Nowadays, there are 193 member states and 11 associate members³.

In the previously mentioned UNESCO General Conference, three types of World Heritage were defined: Natural Heritage, Cultural Heritage and Mixed Heritage. According to UNESCO, Cultural Heritage is *in broadest sense, both a product and a process, which provides societies with a wealth of resources that are inherited from the past, created in the present and bestower for benefit of future generations*⁴. In the case of Natural Heritage, UNESCO defined as *natural features consisting of physical and biological formations or groups of such formations, which are outstanding universal value from the aesthetic or scientific point of view*³. In the case of mixed Heritage, UNESCO defined them as *properties that shall be considered as mixed Heritage if they satisfy a part of whole of the definitions of both Cultural and Natural heritage laid out in Articles 1 and 2 of the Convention*⁵. To better understand the types of Universal Heritage that exist and the examples that represent them, Figure 1 shows the mentioned classification.

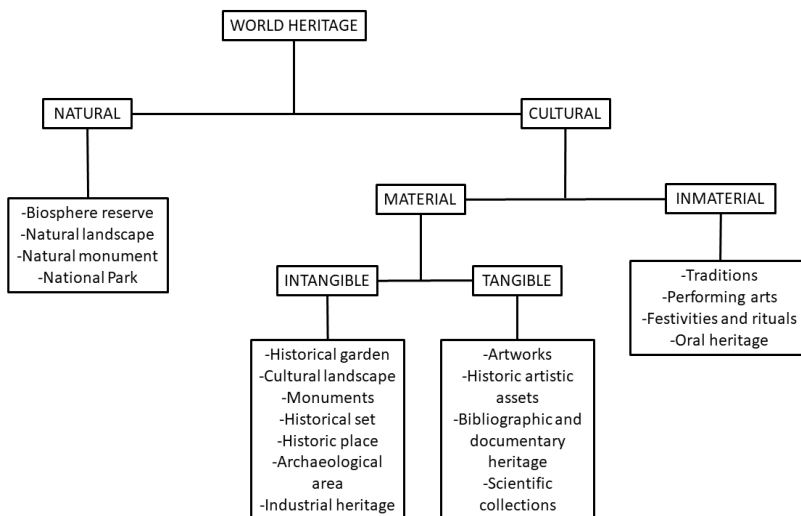


Figure 1 - Classification of the different types of World Heritage

The present PhD is focused on the analytical study of the Cultural Heritage, concretely in intangible material heritage. For this reason, the concept of Cultural Heritage will be explained in greater detail.

According to UNESCO, Cultural Heritage is a term that encompasses *monuments, buildings, sculptures or sites, of an archaeological nature, which are Outstanding Universal Value from the historical, aesthetic, ethnological or anthropological points of view*⁶.

Today, one of the main aims of UNESCO is to promote the identification, protection, and preservation of Cultural and Natural Heritage around the world. In order to fulfill this objective, UNESCO recognizes sites that have exceptional universal value, considering them as World Heritage sites. By means of this distinction, these goods are classified as universal, and their enjoyment, protection and care become recognized by all the people of the world, regardless of the territory in which they are located⁷.

In this way, the countries recognize that the sites located on their territory and inscribed on the World Heritage List constitute a universal heritage in whose protection and safeguard the entire international community has the duty to cooperate. Thanks to the previously mentioned Convention, it has been possible to protect sites with cultural or natural value that have deteriorated due to the lack of resources to preserve them⁷.

In order to understand how Cultural Heritage is protected and conserved in order to prevent its deterioration, loss and/or decline, the next heading focuses on the available tools developed by UNESCO.

1.2 PROTECTION AND CONSERVATION OF CULTURAL HERITAGE

What is the reason to conserve and protect Cultural Heritage? Cultural Heritage provides us information about our ancestors and allows us to study and expand our knowledge of history. Its conservation is crucial for its study and its transfer from one generation to another.

The other key question is, and how is it preserved? Through the creation of an organization like UNESCO and with regulations that protect it, with a wide variety of studies that range from its discovery to its subsequent conservation/preservation.

Both time and changes in natural, social, and historical conditions can cause irreparable damage to Cultural Heritage. This is the reason why conservation has a fundamental role. The vast majority of works of art, sculptures, historical buildings and archaeological sites have undergone some interventions for their preservation since their creation. These interventions have been necessary in order to reduce deterioration and maintain its durability in time. In this way the historical, cultural, artistic and scientific value of Cultural Heritage could be passed from generation to generation.

UNESCO considers well these risks and as previously mentioned, they advocate for the preservation and conservation of Cultural Heritage. In this sense, UNESCO has adopted specific measures at 3 different levels: 1. At the legal level, UNESCO made several recommendations at the General Convention and created several conventions aimed at instituting a general protection regime. 2. On a scientific level, UNESCO proceeds to the study and experimentation of the most modern conservation and restoration techniques. 3. Finally, on a practical level, UNESCO offers assistance to members upon request

to establish and implement programs to highlight monuments and places.

The preservation and conservation of Cultural Heritage is considered an interdisciplinary science requiring the collaboration of professionals from different domains such as materials engineering, environmental engineering, architecture, construction engineering, archaeology, etc. This science ranges from the discovery and/or acquisition of a site or an object to its transfer, exhibition, and valorization. The main objectives of the Cultural Heritage preservation are the classification, protection, research, preservation, and restoration of Cultural Heritage elements⁸.

Nowadays, when the concepts of preservation and restoration are discussed, a new term is employed: *integrated conservation*. This new term advocates for the combination of different perspectives and approaches to achieve the best conservation and preservation of the elements considering conditions for storage or exhibition. This is the reason why research in this field requires interdisciplinary work among different fields⁸.

The concept of integral conservation was used for the first time with reference to the architectural heritage built in a UNESCO motion in 1976 (Concerning the adaptation of laws and regulations to the requirements of integrated conservation of the architectural heritage)⁹ on the adaptation of laws and regulations to the requirements of integrated conservation or architectural heritage. This document was based in some recommendations that governments members promote in the field of the conservation of Cultural Heritage. As described in this document, integrated conservation is based on all possible measures aimed at perpetuating

Cultural Heritage, keeping its use and adaptation to the needs of society as part of the means of life⁸. The principles contained in the mentioned motion were then repeated and defined in article 10 of the Granada Convention (Convention for the Protection of the Archaeological Heritage of Europe, 1985)¹⁰.

Integral conservation has two main objectives.

- a) Heritage conservation through the implementation of protection mechanisms and
- b) the integration of Cultural Heritage in today's society through the implementation of development programs.

The integral conservation principle presents a change with respect to the previous conservation principles, a new focus on **environmental issues**. Today there is growing concern about the effects of climate change^{11,12}. Heritage sites are exposed to the environment and therefore are subjected to interactions with it, which causes changes in their status. Climate is a potential threat to Cultural Heritage as it contributes to deterioration and decomposition phenomena^{12,13}. This is because climate changes can aggravate the physical, chemical, and biological mechanisms that cause degradation by affecting the structure and/or composition of the affected materials¹³. UNESCO has identified several climatic stressors as threats to Cultural Heritage, which led to the creation of a policy document that addresses the effects of climate change and provides organizational solutions for the conservation of heritage sites¹⁴.

In the specific case of archaeology, the European convention for the protection of archaeological heritage (Valleta 1992) requires the state members to establish measures to protect archaeological sites. As archaeological pieces are subjected to hard environmental

changes when extracted from the burial, archaeological sites must be taken into account in environmental impact studies⁸.

In this sense, this PhD is focused on a complete study of some archaeological pieces exposed to different environments. It considers the origin of the samples, their characteristics (both of the different pieces and of the environment where they were found) and different methods of analysis.

1.3 DETERIORATION OF CULTURAL HERITAGE

Cultural Heritage elements are deteriorated over time due to its exposure to different conditions or agents¹¹. These factors/agents which affect the state of conservation can be divided into two groups: external and internal factors. The internal or endogenous factors are based on the possible defects of the materials and on the quality of the technology used in the production process^{8,15}. There are several external or exogenous factors: environmental factors (temperature, precipitation, humidity, air currents), micro-biological and macro-biological factors and natural and anthropogenic pollution factors (chemical, thermal, sonic and radioactive)¹⁵.

These factors can affect differently depending on the type of material involved and the conditions that surrounds it. Moreover, there is another factor which depends directly on the human being and can equally affect any type of Cultural Heritage, the anthropogenic one. It is considered as the most dangerous factor due to the damage it causes to Cultural Heritage. This factor can come from 3 different actions: inadequate displaying, handling, and storing, unauthorized preservation and restoration interventions, and vandalism. The last one is considered the most severe one and the effects of deterioration and degradation that it can cause in most cases are irreversible¹⁵. These possible reasons are summarized in Figure 2.

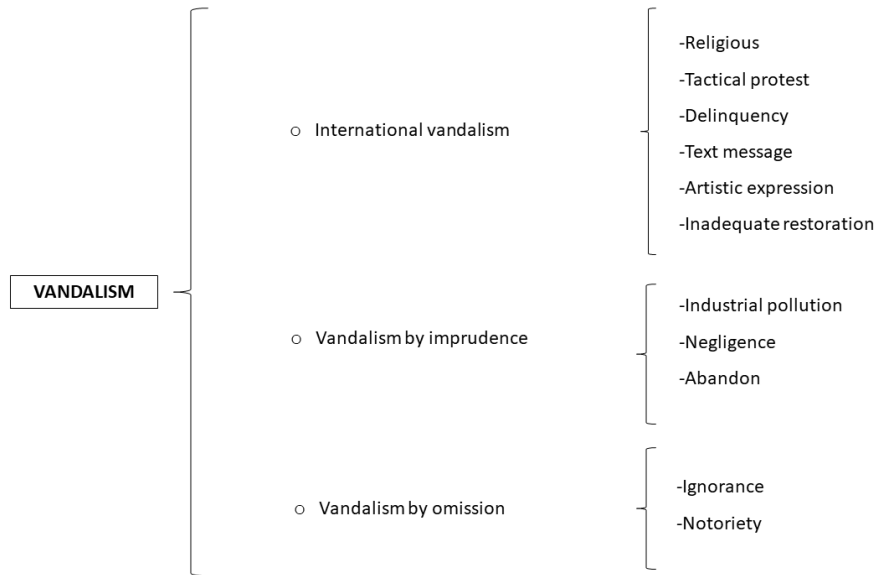


Figure 2 - Different form of vandalism¹⁵

As it can be seen in Figure 2, the act of vandalism can be divided into three groups depending on the intention. On the one hand, there is intentional vandalism, deliberately and consciously produced by those who initiate it. The objective of this act is to destroy or eliminate objects of Cultural Heritage. On the other hand, there is vandalism due to recklessness and omission, in other words, acts generated by ignorance, negligence or disinterest¹⁵.

However, this work is focused on the study of the previously mentioned external and internal factors. All of them may vary depending on the **environment** in which they are found. In order to better understand how the internal and external conditions, affect the materials of the different types of Cultural Heritage that were selected for this work (metallic materials, wood, lithic materials and glassy materials exposed to ground and underwater environments), this

section is divided into two parts, the underwater part and the buried part.

1.3.1 Deterioration of Underwater Cultural Heritage

As previously mentioned, UNESCO defined three general types of Heritage, Cultural, Natural and Mixed Heritages. This work is focused on Cultural Heritage and, one of the types of Cultural Heritage is Underwater Cultural Heritage. UNESCO defined it *as all traces of human existence that have a cultural, archaeological, or historical character and which have been partially or totally underwater, periodically, or continuously for at least 100 years*⁵. Taking into account that the oceans occupy around 95% of the earth's space¹⁶ and which only 5% of them have been analyzed, 90% of the oceans still need to be investigated. Therefore, this type of Heritage is one of the most unknown which has acquired greater importance in recent years. According to UNESCO, it is estimated that there are approximately 3 million wrecks in the oceans¹⁷ some of the being widely recognized as Vasa warship, Mary Rose¹⁸, Fougueux and Bucentaure ships¹⁹, some World War II shipwrecks¹⁷, Qoroq shipwreck²⁰,

For the last decades, and after the adopted UNESCO Convention (Convention on the Protection of the Underwater Cultural Heritage (UCH), 2001)²¹ the protection of underwater materials has been an ongoing challenge. The preservation and conservation of the UCH is essential to preserve the humankind's history and knowledge to future generations²². A great part of the World's Cultural Heritage lies beneath the worldwide sea being vulnerable to the geomorphic marine features. These parameters can promote different reactions in the materials with which they come in contact. In this sense, these

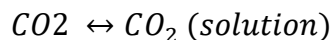
parameters will be previously explained in order to later understand the deterioration processes that the different materials may suffer in the sea.

1.3.1.1 Physicochemical parameters of the marine environment relevant to the degradation of archaeological pieces

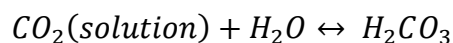
The sea is a complex environment which contains mineral salts, dissolved gases, macro and micro-organisms, suspended organic matter and sediments. The main dissolved gases are oxygen (O_2) and carbon dioxide (CO_2)²³. The concentration of the dissolved oxygen is one of the most important parameters which directly affects to the corrosion phenomena. This gas is physically absorbed into the seawater²⁴ and its concentration varies depending on the geographical place, temperature, depth, and salinity.

In the case of the carbon dioxide, its source comes from the atmosphere and as a product of aerobic respiration. As it occurs with oxygen, the concentration of this component varies depending on various factors such as depth, seasonal or daytime. Moreover, carbon dioxide chemically reacts with the seawater²⁴:

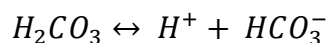
First, CO_2 is dissolved in seawater:



Then, it reacts with water to form carbonic acid:



After, carbonic acid is dissociated in two steps:



The described chemical process is called CO₂-carbonate equilibrium system. This process is the most important equilibrium system in the marine environment. Thanks to that, this system maintains the pH of seawater, controls the depositions of marine sediments and controls the alkalinity of the seawater²⁴.

In addition to dissolved gases, seawater also contains significant concentrations of dissolved salts²⁵. The parameter called salinity is the measure of the content of these salts in saline water. Chloride ions represent a large part of these elements and are mostly represented by NaCl and MgCl₂.

Another important parameter to consider is the pH. Its value in seawater usually varies in the range between 7.5 and 8.4. This parameter is directly related to the depth as it can be observed in the Figure 3. The maximum pH value in the first 100 meters (8.22-8.3) is caused due to air-sea-CO₂ exchange and photosynthesis. The minimum value of pH (7.5-7.7) at 200-1200 meters is promoted due to the zooplankton activity²⁴.

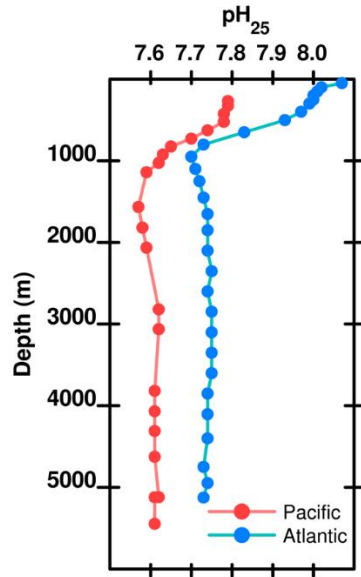


Figure 3 – Depth-sea pH profile²⁶

Among all the salts which composed seawater, most of them are neither acids or bases, so they do not participate in the exchange of protons and therefore do not contribute to the pH of seawater, nevertheless, they contribute to the ionic strength of the marine waters²⁴.

All these parameters affect directly depending on the material. Each material reacts in a different way to the underwater environment. Considering this, the most relevant degradation pathways in the underwater materials considered for this work are resumed hereunder:

1.3.1.1.1 Metallic materials

In the specific case of metallic objects, the interaction between the environment and the metallic object is called corrosion phenomena. In the case of underwater material, the seawater causes a very complex and corrosive medium on the metal surface. Depending on the composition of the metal and the external factors, different corrosion forms can be observed: generalized corrosion affecting the surface, galvanic corrosion (the corrosion formed when two different metals are in contact with a common electrolyte and one of the metals is protected while other experiments corrosion), pitting corrosion²⁷ (a characteristic corrosion formed by cavities or holes) and crevice corrosion (process that arises when water accumulates inside a crack²⁸), the corrosion induced by seawater flow (is the corrosion process produced by the contact between the metal and marine environment, the stress corrosion (is the phenomenon produced by the cracking of a metallic alloy that results from the combined action of a corrosive and traction stress)²⁹, the erosion-corrosion (is the corrosion process produced as a result of the relative movement between the corrosive fluid and the metal surface)³⁰, the fatigue corrosion (the process formed when a metallic component is exposed to a corrosive environment and suffers cyclic stresses³¹) and the corrosion influenced by micro-organisms.

Corrosion can be influenced by physicochemical conditions, such as salinity, dissolved oxygen, temperature, depth and/or microbial activity³².

In the case of salinity, the high concentration of soluble salts can have serious consequences in the corrosion processes of metals in seawater²⁵. Its high concentrations also give the sea a low resistivity,

which favors electrochemical reactions between the medium and the metal sample. It is important to mention that this parameter depends inversely on the concentration of dissolved oxygen, that is, salinity increases with the decrease in dissolved oxygen. This means that the concentration of dissolved salts increases along with the submerged zone and the buried zone.

With respect to dissolved oxygen, this parameter is one of the most severe in terms of corrosion²⁵. Its concentration varies depending on the geographic zone, temperature, depth and salinity. The increase in this parameter produces an increase in the corrosion rate of “active” metals (metals that react strongly or quickly with other substances) such as iron and copper²⁵.

The other important parameter in corrosion process is depth. This parameter is very significant during the first weeks of the immersed object. The metallic surface is not covered immediately by sediments, so two different situations can happen: On the one hand, if the depth is less than 10 meters, the metallic artifact is subjected by wave turbulence and the dissolved oxygen concentration on the metal surface increases its value. Currently, the metal surface becomes very active and further physical erosion of the surface occurs due to the sand or sediments. In this case, the corrosion of the metal parts is high²⁵. On the other hand, if the depth is more than 10 meters, the metal object is not subjected by wave turbulence. Due to this fact, corrosion products can grow up on the surface. In this case, the corrosion rates are reduced due to the formation of corrosion products which act as corrosion protection, such as magnetite in the case of Fe²⁵. Regarding the behavior of an archaeological object, it

could be said that the deeper is located the metal object, the better is the conservation state of the metal.

Besides, it must be highlighted that all the physicochemical parameters are inter-correlated. As mentioned before, the dissolved oxygen, temperature and pH are directly related and it can be said that as depth and salinity increases, their values decrease²⁵. Therefore, there are synergies between the different parameters that lead to unique corrosion conditions.

Apart from these physicochemical parameters, corrosion can be also influenced by microbial activity. Microbially influenced corrosion (MIC) is the result of the confluence of microorganisms, media and metals³³ (Figure 4). It is a phenomena that affects seriously to all underwater metallic objects.

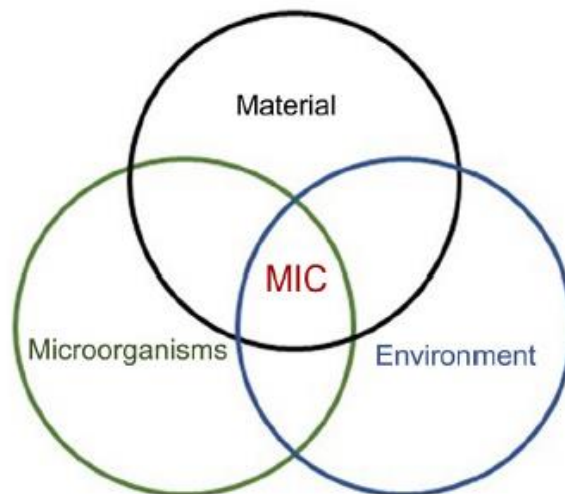


Figure 4 - Factors which affect Microbiological Influenced Corrosion³²

MIC, biological colonization or biocorrosion (different expressions to recognize the corrosion caused by the presence and activities of

microorganisms)³³ is an expected consequence of every metal (biologically non-toxic) immersed in natural seawater²³. This natural process is very fast, since it can be observed after the first hours of immersion of the metallic object in seawater. The first effect it has on the piece is the formation of a biofilm composed of both aerobic and anaerobic bacteria. The biofilm can produce some chemical modifications on the surface of the metallic object, producing local differential aeration sites. These sites can accelerate the local corrosion process. The most corrosive MIC is that generated by sulfate or thiosulfate reducing bacteria (SRB or TRB). In this case, the procedure starts just a few days after immersion when, the surface of the metal is covered by the aforementioned biofilm. Moreover, this attracts microalgae and sediments. The consequences of the biofilm formation on the metal surface can range from corrosion acceleration to complete corrosion inhibition. Microorganisms can accelerate or retard corrosion process by changing the nature or kinetics of the rate-controlling reactions or processes³². Furthermore, it can also cause electrochemical reactions both inside and outside the metallic piece and the alteration of the physicochemical parameters (pH and concentration of dissolved oxygen). Due to the presence of the biofilm, local corrosion processes are accelerated and can promote corrosion by pitting or cracking in the metal^{23,25}.

1.3.1.1.2 Wood materials

The wood preservation depends highly on the surrounding environment. Wood in the dry ground environment can undergo degradation processes due to various factors such as changes in temperature, humidity, wind... There are many and diverse physical, chemical, or biological factors that can affect the state of these

artifacts. On the contrary, wood in waterlogged environments has fewer factors that affect its decomposition, which slows down this process and allows the wood to survive for a long time³⁴. In this case, we are going to focus on the specific case that concern this PhD that is waterlogged wood.

Waterlogged wood artifacts are generally discovered buried in sediments at the bottom of the sea or buried in moist soil or river/estuarine sediments. Depending on oxygen availability, wood can stay in anoxic (dissolved oxygen is depleted) or in oxic conditions (dissolved oxygen is available). In anoxic conditions or near anoxic waterlogging, the biodegradation of the wood is mainly bacterial.

The bacteria that cause wood degradation are classified according to the degradation pattern they produce into the material: erosion, tunneling and/or cavitation bacteria. The most common form of microbiological attack in anaerobic environments is the so-called erosion bacteria³⁴.

The erosion bacteria (EB) have a spherical shape and colonize the wood from the surface. These bacteria can tolerate low oxygen environments; therefore, they can decompose wooden artifacts despite being buried. Although the decomposition process is faster when oxygen is available. A characteristic feature of the attack of these bacteria is their lack of homogeneity, in fact, the wood is usually more degraded on the outside compared to the inner part that remains intact³⁴.

In the case of tunneling bacteria (TB), they are single-celled bacteria with a spherical or rod-shaped shape. They are usually present in conditions where there is some oxygen and withstand a wide range of temperature and humidity conditions. TB often coexist in nature

with soft rot fungi (which also degrade wood). The mechanism of colonization of these bacteria is from the surface and they pass to inner layers through holes in the wood³⁴.

Cavitation bacteria (CB) are microorganisms which can rarely be found in wood due to the very restricted conditions in which they occur. Unlike EB and TB, the degradation is located in an inner layer of the wood and not on the surface³⁴.

In the specific case of wood in direct contact with seawater, the variables that affect the state of these artifacts are even greater. These types of artifacts can be attacked by the *Teredo Navalis* worm and the woodpecker worm and be degraded by marine sediments. It should be noted that, although the sea salt present in this type of artifact can damage wood or promote corrosion, archaeological wood exposed to saline environments shows few signs of physical and chemical degradation due to the presence of salt which inhibits microbial colonization³⁴.

In anoxic environments it is also possible to find the presence of SRB. They reduce sulfate to sulfur when they metabolize simple organic molecules. Although the activity of these bacteria is dominant in anoxic environments, there are strains that can operate in environments with a higher availability of dissolved oxygen and even in fresh water. These microorganisms are very resistant since they have been found in very extreme conditions such as extreme pH environments (pH 2-10), in volcanoes, mud or in marine sediments. These bacteria in the marine environment compete with other anaerobic bacteria and under conditions of high sulfate concentration, the presence of aerobic bacteria is inhibited. When the presence of iron is also found under these conditions, it reacts with

SRB producing iron sulfides. It is worth mentioning that iron is a common exogenous element in waterlogged wood directly associated to shipwrecks.

Apart from biological colonization, chemical and physical degradation have to be also mentioned. Chemical degradation in waterlogged wood mainly presents losses of the polysaccharide component. The degradation of cellulose in waterlogged wood implies a reduction in relative crystallinity, although the width of the crystal appears to be unaffected. Loss of carboxyl groups associated with glucuronic acid residues in hemicelluloses has been reported, as well as some loss of ester linkages in the lignin-carbohydrate complex (LCC)³⁴.

Regarding physical degradation, it must be said that archaeological waterlogged wood affected by microbiological degradation tends to increase its porosity, and as a result, its maximum water content (MWC) increases, and its residual basic density (RBD) is reduced compared to fresh wood. The MWC or the maximum moisture content is the ratio between the weight of the dry wood and the total weight of the wood, and the water expressed as a percentage. The RBD is the ratio of the density of the archaeological wood compared to a typical value for a fresh wood sample expressed as a percentage. Wood is considered degraded when the MWC value is greater than 150% and severely degraded when MWC exceeds 400% and the RBD is less than 40%³⁴.

Dry environments give rise to completely different degradation pathways on archaeological materials:

1.3.2 Deterioration of the buried cultural heritage

The soil has many different functions which are very useful to the ecosystem. Two of its main functions are the provision of a platform for the built environment and the storage of buried heritage³⁵. There is a wide range of archaeological and Cultural Heritage and buried infrastructure which is preserved in the soil environment. Knowledge about the characteristics of this environment is vital for the management and conservation of buried heritage³⁵. The range of buried objects that can be found are the following: stone, ceramic, bone, metal, wood, plant-based materials, leather, glass, plastic, etc. The distribution of these objects reflects the different past land uses and the possible occupation patterns³⁵.

The estate of conservation of buried objects depends both on the environment of the soil in which they are buried and on the material they are made of, as well as on the nature of their manufacture. However, an important factor not mentioned before must be considered, the time. This factor can directly affect the cultural value of buried objects since over time they can be degraded and even completely destroyed, losing their recognizable morphology and therefore, their cultural value. While some materials such as organic, copper, bronze, and iron are destroyed in the soil, other materials such as ceramic and glass can degrade, but after many years³⁵. To better understand how times affects the degradation process of materials, Arriba-Rodriguez et al. ³⁶ published a study where the degradation time of different materials was evaluated (Figure 5).

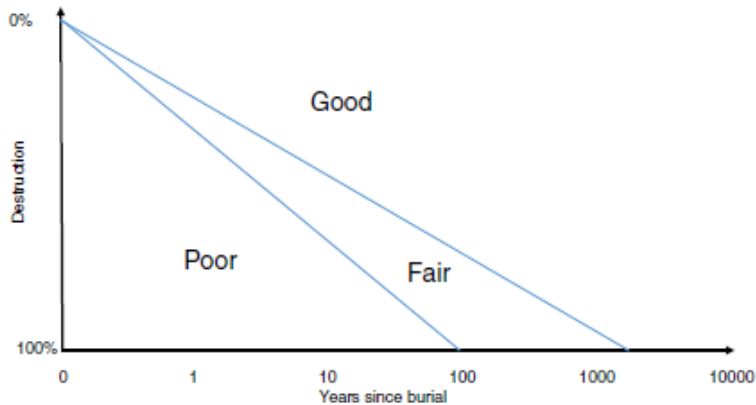


Figure 5 - Preservation of materials buried in soil over time³⁵

To understand the effect that soil has on buried materials, the physical and chemical parameters that characterize soil environment must be previously explained. In this way, the characteristic corrosion processes of different materials in buried environment can be better understood.

1.3.2.1 Physicochemical parameters of the buried environment relevant to the degradation of archaeological pieces

Soil, as marine water and sediments is a very complex and corrosive environment due to its constant changes in underground environment. In 1928, Logan³⁷ determined that the degradation of a buried material depends largely on the characteristics of the soil in which it was buried. For that reason, it is necessary to describe the main factors that influence the degradation of buried pieces. Among them, the most remarkable ones are soil texture, water presence, aeration, redox potential, pH, ion content and bacterial presence.

The soil texture is based on the size distribution of the mineral particles which form the soil. In general terms, a soil is considered to be composed of three main components: clays (diameter < 0.002 mm), silts (diameter $0.002-0.5$ mm) and sand (diameter > 0.5 mm)³⁶. Depending on the percentage in which they are found, the soil classification can be made based on the diagram shown in Figure 6.

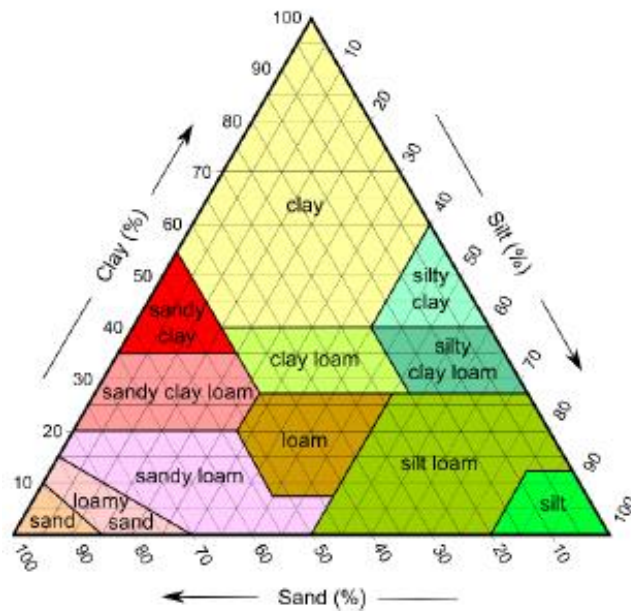


Figure 6 - Diagram for the soil classification³⁶

The soil aeration is a critical parameter for the optimal functioning of the soil. This parameter depends on three different factors: soil porosity, water content and oxygen demand. The lack of oxygen is a serious problem because it affects the soil redox potential, changing the forms of compounds of several important elements (such as Nitrogen, Sulfur and Iron)³⁸.

pH is based on the measurement of the hydrogen ion activity in the soil. The value of pH is directly related to the depth profile. The pH value increases with increasing depth³⁸.

Considering all this, it can be concluded that corrosion process in soil environment is a complex process with many variables involved. The table shown in the Table 1 shows the variables which were described before together with the relationship they have with the degradation process³⁶.

Table 1 – Relationship between soil parameters and degradation phenomena³⁶

| VARIABLE | RELATION |
|-------------------|----------|
| Soil texture | Direct |
| Presence of water | Direct |
| Aeration | Direct |
| pH | Inverse |
| Resistivity | Inverse |
| Redox potential | Direct |
| Ion contents | Direct |
| Bacteria | Direct |

Nevertheless, a medium as complex as this, suggests the simultaneous interaction of all the mentioned variables. Therefore, the degradation pathways that take place in this medium are not the result of just one parameter but, the result obtained due to the interaction of several different parameters (Figure 8)³⁶.

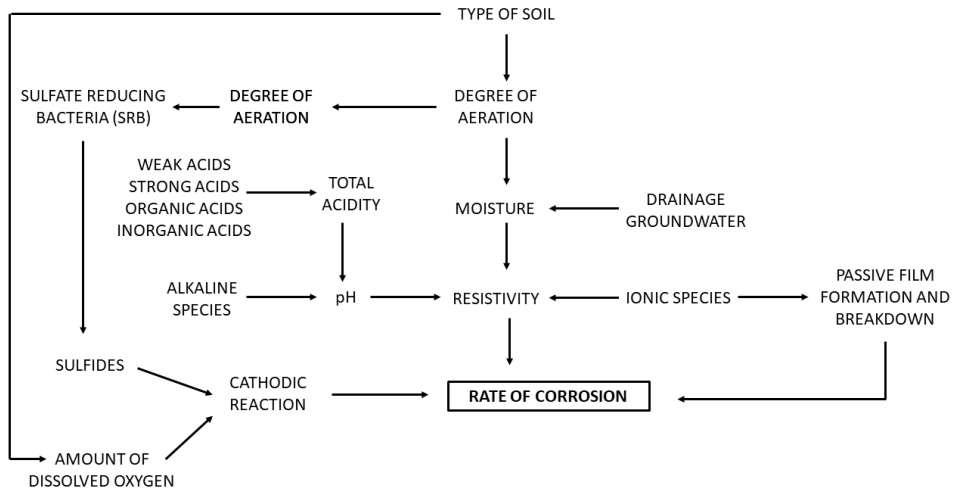


Figure 7 - Behavior of variables in the degradation process³⁶

This study focuses on expanding knowledge about the conservation state of different types of objects buried in soil, how these can be affected by the nature of the material and the type of soil and how information on the distribution of soil can be useful to assess the capacities of preservation of these objects. For this reason, the characteristics of each type of material used in this work will be discussed below.

1.3.2.1.1 Metallic materials

As exposed in the underwater section, the biggest main problem on the metal preservation is the previously mentioned corrosion process that metals can undergo. The effects that it can cause in the metallic structure are the degradation of the material and the structural failures in infrastructures. As in marine environment, underground environment is extremely complex media due to the variability of the local conditions. This environment is characterized by a huge

variability in the local conditions generated by differences on soil chemistry parameters such as conductivity, humidity, etc. Moreover, it is also influenced by external factors such as precipitation and artificial manipulation of the soil. Despite the difficulty to understand this complex environment, it is essential to explain the behavior of metal objects in buried environment³⁶.

The parameters discussed in the previous section have a great influence on the corrosion processes of buried metal pieces.

Regarding the soil texture, the finer particles are considered the worst particles due to the corrosive medium which it forms for buried metal structures. Furthermore, the percentage of clays in the soil composition is decisive due to its great absorbent power which is very effective in the deterioration of metals³⁶.

Regarding the presence of water in metal artifacts, this parameter is of vital importance for the corrosion process to arise in buried environment. In addition to water presence, if the presence of oxygen is also found, the degree of corrosion is increased due to the participation of this element in the oxidation reactions. One of the most common cases of increased oxygen in this type of environment is at the time of archaeological excavations. In addition, these two parameters are directly related to the redox potential, which provides information on the possible presence of microbiological activity. There are some researches from 1979 which demonstrated the correlation between soil moisture and corrosion rates^{39,40}. This is caused because water is the necessary medium for electrochemical corrosion reactions.

Taking into account the pH value, there are studies that provide contradictory information. On the one hand, Oguzie conducted a

study in 2004⁴¹ in which it was concluded that buried metal artifacts were susceptible to corrosion at any pH value. On the other hand, Tibu et al⁴² considered that pH is not dominant factor in the corrosion mechanism when the soils have a pH in the range between 4 and 8.5 (normal pH range in soils). Despite this, research on this field agrees that the more acidic a soil is, the greater degree of corrosion it can cause in the metals in the environment³⁶. It can be concluded that more acidic soils are considered to have a higher risk of corrosion on metal pieces. In contrast, alkaline soils tend to have high concentrations of magnesium and calcium, and these elements form deposits on buried surfaces with protective properties against corrosion.

As in the marine media, the ion content directly affects the stability of metal parts, more specifically in the case of chlorides and sulfates. These elements may be naturally present in soils or may originate from an external source. The presence of this component causes a decrease in soil resistivity. Chloride ions are very harmful since they participate in the anodic dissolution reactions of metals. On the other hand, sulfate ions are less harmful but can become highly corrosive due to bacterial activity. This type of activity can alter the rate of corrosion, either speeding it up or slowing it down. Its degree of acceleration can be caused by the presence of reducing bacteria and the decrease in speed can be caused by the creation of a protective biological patina³⁶.

The concentration of oxygen is another significant parameter which must be taken into account. In neutral or alkaline soils, the concentration of oxygen has a significant effect on the degree of corrosion because of its participation in the cathodic reaction.

Corrosion rate in disturbed soils with high oxygen availability is significantly higher than that in soils that have not been modified. It must be mentioned that excavations can highly increase the degree of soil aeration.

In relation to the presence of oxygen in soil, redox potential must be considered. This parameter is an indicator of the aeration degree in soil. The presence of oxygen and redox potential parameters are directly related and provide information on the possible presence of reducing bacteria in soil.

1.3.2.1.2 Lithic materials

Buried stone artifacts include flint objects, figures, stone hand tools and mortars and building materials. Stones and minerals derived from igneous and metamorphic rocks are considered to be stronger than some sedimentary rock materials, for example sandstones and chalk, especially in humid environments where there are active defrost cycles⁴³. Despite this, this type of stone materials also suffers from chemical, biological and physical degradation issues.

One of the most important factors in the decomposition of stone material along with air pollution are soluble salts. Salts can damage the material in several ways. The most important is the growth of salt crystals within the pores of the material. When water penetrates inside a material, the evaporation or cooling of said water can cause the growth of these crystals (crystallization). This can generate tensions inside the material, which can even break the piece. The origin of this affectation can be very diverse, from air pollution (source of sulfates and nitrates), soil contamination, to the possible use of inappropriate materials⁴⁴.

There are a wide variety of harmful salts for these materials, but one of the best known is sodium sulfate⁴⁵. This salt can have various states of hydration (Ternadite Na_2SO_4 or decahydrated mirabilite $\text{Na}_2\text{SO}_4 \cdot 10\text{H}_2\text{O}$) which makes it a conservation hazard. In the case of Tenardite, it increases in volume up to three times when transforming in mirabilite, causing serious damage to the material. Thanks to advances in research, today the behavior of salts and affected materials can be known, environmental conditions can be predicted thanks to the performance of thermodynamic modeling. In this way, safe ranges of temperature and relative humidity can be predicted to avoid damage by crystallization⁴⁴.

Although to a lesser extent, living organisms also contribute to the decomposition of stone. The role of bacteria has generated great controversy regarding the damage they cause to stone materials. It has been demonstrated that there are biofilms that in certain circumstances can help stabilize stone surfaces or can be an effective natural protection. In other cases, biofilms can also accelerate decomposition and therefore be detrimental to the material. Biofilms have been shown to change the thermal and mechanical behavior of stone, increasing surface wetting and therefore decomposition (and providing a source of organic acids and complexing agents). When it comes to biofilms, the most common organism are lichens and bacteria⁴⁴.

In the case of lichens, they can cause both physical and chemical damage. The physical damage is generated by the penetration of the plant in the material under changes of humidity⁴⁶. The chemical damage that it produces can be observed in 3 different ways, by the secretion of oxalic acid, by the generation of carbonic acid and by the

generation of other acids^{44,47}. In the case of bacteria, they are involved in the chemical breakdown of stone material⁴⁴.

The causes of physical degradation in these materials are mainly caused by differential stress and intrinsic problems. The degradation mechanism known as differential stress is based on the effects of the wet / dry cycle, on the swelling of the clay, on the differential thermal stress and on the stress of the differential expansion rates of the material in the pores versus the stone. That is, anything that causes the surface of the stone to react differently that, on the inside, can result in a crack or detachment of material⁴⁴.

An example of differential hydric stress is found when after a short rain the surface of a stone swells, while the inner part remains dry. An example of stress induced by differential thermal expansion is found when sodium chloride expands five times the speed of calcite at surface temperatures, decomposing limestone by this mechanism⁴⁴.

Moreover, there are also intrinsic degradations due to the material itself, and not to any external factor. There is a great variety of stones that have been used to create different types of heritage that have not been suitable. That is why it is a very important factor that must be studied more deeply⁴⁴.

1.3.2.1.3 Glassy materials

Glassy materials have a good chemical resistance⁴⁸ and are relatively durable materials in buried environment and in many cases, they are discovered intact⁴⁹. The causes affecting their deterioration can be diverse. However, the most important ones are the glass composition⁴⁸ and the environmental conditions⁵⁰. Besides, other

parameters must be taken into account, such as surface morphology, and the different manufacture processes⁵¹. The causes of degradation can be divided into three types: chemical, physical and biological degradation. Next, the three different existing degradations in these materials will be explained more widely.

The main effect of chemical degradations in glassy materials are pits and craters, de-alkalization layers and the formation of dark deposits⁵². The pits and craters are punctual chemical or physical attacks located on the surface of the glass piece and which presents a pseudo-circular morphology. There are several parameters that can trigger this attack, such as the presence of tensions, heterogeneities on the surface and impacts. It is common for most pieces of archaeological origin to present this type of alterations under their superficial corrosion layer and, besides, to present deposits inside the cracks⁵².

With regards to the superficial corrosion layer, these de-alkalization layers are parallel sheets that are found on the surface of the glass and are formed due to the cycles of humidity and dryness that piece undergone. When water comes in contact with the surface of the glass, a hydration layer is generated that modifies the microstructure of the glass. In the dry period, the hydration layer and the piece suffer stresses that can cause the separation of both. If the cycles of humidity and dryness are continuous, a multilayer structure can be formed on the surface, but this structure is very fragile and tends to break when rubbed⁵².

Furthermore, it must be explained that one of the main chemical factors that can affect glass is soil water content⁵³. Apart from the humidity effects already exposed, water can produce hydrolysis of the

glass bonds, favoring the opening of the glass network and the diffusion of water molecules. As a direct consequence of this factor, the formation of a degradation layer called the silica gel layer arises⁵³. This superficial crust is rich in silica and poor in basic ions and it produces a loss in the transparency of the piece. It is at this time when the piece is in a weaker state that it can promote the breaking process⁴⁹.

Regarding dark deposits, these ones are dark colored spots that are generally found on the surface of the sample or between the layers of de-alkalization. Its formation depends on the precipitation of metallic oxides and its growth usually adopts a dendritic behavior. The composition of these deposits is variable, but it is observed mainly in glasses with a high percentage of manganese oxide. In addition, it has been shown how the deposits that are located on the surface of the sample have a higher content of iron oxide than those located between the de-alkalization layers⁵².

In this material, physical degradations can be also observed. These are degradations formed due to mechanical forces such as impacts (falls and shocks), cracks or fractures (pressure on the surface). In the case of impacts, they can occur in the glass material before it is buried, at the time of burial or after, during its excavation. The impacts can have two consequences in these materials depending on the thickness of the piece, the complete breakage (thin thickness) or the formation of a fracture without destroying the piece (thick thickness)⁵².

In the case of cracks or fractures, the reason for their formation may be the stresses produced by changes in the environment or by chemical attacks. A very common example in this case is water, it can

enter in the glass by capillarity through the cracks and can cause a chemical attack resulting in the formation of fractures in the piece and its possible breakage⁵².

In the specific case of glassy material buried in soil, the physical damage produced by the ground can be due to static and dynamic forces. The first increases with depth and the second depend on the movements that take place on the surface and spread through the subsoil. The rigidity of the ground will affect the probability of fracturing the objects. For example, a clay soil is more resistance to deformation and protects better objects from breakage than a moist sandy soil. However, for most solids the dominant factor determining destruction is land use and management rather than soil type⁴⁹. Considering the fragility of the glass, this supposes an important factor in the degradation of the material.

In contrast to other materials, biological colonization is the less aggressive parameter in the degradation of glassy material. Regarding macro-organisms, tree roots or animal burrows can alter materials, displace, and even break them. In the case of micro-organisms, these usually begin to develop in a suitable medium for their growth, such as stone or mortar, and over time, they expand to the closest pieces, such as glass. The most serious effects that micro-organisms can cause is the segregation of chemical compounds that attack the glass.

Despite knowing the possible degradation effects of vitreous materials buried in soil, it is difficult to predict the rate of degradation of these pieces, since it is strongly affected by their composition⁴⁹. However, it is possible to reach several conclusions about what type of soil can aggravate the degradation processes of glassy materials.

For example, under pH=9 conditions, alkali ions leach from the glass matrix, while under more alkaline conditions, hydroxyl ions break silicon-oxygen bonds within the silica structure. In most soils, except in the driest, surface coatings are likely to degrade faster due to their rate of degradation. In contrast, corrosion is expected to be minimal in driest soils. It can be concluded that the more alkaline is the pH, the more likely the laminar surface layer will be formed. For this reason, this type of soil is the most corrosive for these pieces⁴⁹.

Analyzing how these degradations affected pieces involved in an integrated conservation procedure is crucial. In this way, it is important to define first the original material, the employed manufacture procedure and to distinguish all this from the degradation products generated during the burial. Moreover, it is also a key procedure to accurately determine which are the degradation products created on the objects surfaces to define the best restoration and conservation planning to preserve it. In order to obtain all this information on the Cultural Heritage elements study, the possible parameters that affect its deterioration and the conservation processes necessary for each one, it is recommended to appeal to chemical analysis. In this sense, the use of Chemistry knowledge around Archaeology is becoming a standard of the diagnostic practice on archaeological findings.

1.4 CHEMISTRY IN ARCHAEOLOGY

Archaeological chemistry is based on the application of chemical and physical methods to the study of archaeological materials. This science is based mainly on the identification (determination of the original material), authentication (verification the antiquity of an unknown material) and characterization of archaeological materials (determination of chemical composition and alteration compounds). Archaeological chemistry is a very extensive science in which a wide variety of materials are studied, including ceramics, bones, lithic materials, soils, dyes, and organic residues. Its main objective is to expand current knowledge about the human past⁵⁴.

The concept of Archaeological chemistry seems like a new concept, but it is not. To understand the origin of this term, a brief bibliographic review was carried out by Glascock et al., 2016⁵⁵. Years ago, Caley (1951)⁵⁶, Harbottle (1982)⁵⁷ and Pollard and Heron (1996)⁵⁸ already made a description of the works of several famous scientists who pioneered the first compositional studies of archaeological materials. The most prominent mentioned scientists in this field were the following ones: Martin Heinrich Klaproth (1743-1817), Sir Humphry Davy (1778-1829), Michael Faraday (1791-1867), Karl Christian Göbel (1794-1851), Jan Erazim Vöcl (1803-1871), Augustin Alexis Damour (1808-1902), Friedrich Wilhelm Rathgen (1862-1942) and Theodore William Richards (1868-1928)⁵⁵.

One of the most renowned chemists of his time was Martin Heinrich Klaproth who was born in 1743⁵⁹. He began working as an apprentice to an apothecary in 1759. Nine years later, he managed his own apothecary in Berlin. In 1782 he was appointed as a member

of the Prussian medical board thanks to which he travelled all over the world. He also worked as a teacher in positions such as private professor at the Surgical Medical College (1782-1810), at the General War College (1787-1812) and as a professor of Chemistry at the Philosophy Faculty of the University of Berlin (1810-1817). He was a highly recognized chemist due to the discovery of various chemical elements such as zirconium (1789), uranium (1789), titanium (1792), strontium (1793), chromium (1797) and cerium (1803). He also confirmed earlier discovered elements such as tellurium (1798) and beryllium (1798). He was recognized as the father of analytical chemistry for establishing a systematic methodology to perform analytical chemistry. He also pioneered chemistry in archaeology conducting various studies to determine the composition of ancient Greek and Roman coins. These investigations were studied by Caley in 1949⁵⁹. Among many other memberships, in 1795 he was elected as a member of the Royal Society.

Sir Humphry Davy was an English chemist who was born in 1778⁶⁰. He was a known scientist for discovering the alkali and alkaline earth metals⁶¹ such as sodium, potassium, strontium, barium, manganese, and boron. Despite being previously discovered, he identified chlorine and iodine chemical elements. In 1815, he invented the miner's lamp which made the extraction of coal safer. From 1802, Davy was the first professor of chemistry at the Royal Institution, thus acquiring a rapid fame as a scientist and as a popularizer of science. Apart from the studies on chemical elements, Davy's greatest contribution was made in the branch of archaeological chemistry and was based on the characterization of pigment samples from Rome and Pompeii in 1815^{62,63}. In addition to his extensive studies in the field of chemistry, he implemented the so-called practical

demonstrations open to the public, a tradition that continues after more than 200 years.

One of Humphry's laboratory assistants was Michael Faraday. He was born in 1791 into a modest and religious family. During his work as a bookbinder, he was able to read extensively on a wide variety of issues and became a member of the John Tatum City Philosophical Society. He attended Davy's conferences at the Royal Institution and then, he delivered a book of his lecture notes to Davy. Thanks to that, Humphry found work for Faraday at the Royal Institution and later he was chosen as Davy's assistant for a time. Later, in 1825, he was appointed director of the laboratory and in 1833 professor of chemistry. Faraday's research was based on chemistry and on materials science. Despite being a renowned chemist in the field of electromagnetism in his career, Faraday also studied ancient archaeological artifacts, concretely, Romano-British and ancient Egyptian artifacts. Thanks to these studies, he discovered that the glaze used on Roman ceramics was based on lead⁶⁴.

Karl Christian Traugott Friedemann Goebel was a German chemist and pharmacist who was born in 1794⁶⁵. After training as an apothecary, he studied pharmacy at the University of Jena. In 1821 he was appointed as director of the University of Pharmacy and three years later he became a professor at the University of Jena. Unfortunately, there is almost no information about his life and his studies in the field of archaeology. That is why the information mentioned is so brief. However, an important contribution is known in the field of archaeology. This is the article he wrote in 1842 about the study of a collection of bronze artifacts excavated in the Russian

Baltic provinces⁶⁶. In it, he compared the composition of these pieces and found that they were similar to those of Roman Empire.

Jan Erazim Vocel was known as the father of Austrian archaeology⁶⁷. Despite his relevance in history, there is not much information about this scientist⁶⁸. He was born in 1802 in Kutna Hora. He began focusing his studies on education until 1842. Between 1843 and 1850 he was appointed editor of the National Museum Magazine and in it he promoted historical contributions and he introduced archaeology. In 1846 he was elected as a member of the Royal Czech Society of Sciences and three years later he became a director for one year. Vocel's work in the field of archaeology began with the article on the preservation of Czechoslovak antiquities in 1843 and two years later he published his first work. In 1850 one of the author's most important works was published where he discovered that the identification of the sources of raw materials could be made by correlation between the composition of the raw materials and the artifacts⁵⁵. Another of his well-known works was published in 1868 and focused on the archaeological material of Slavic prehistory (prehistory of the Czech Lands). In the last three years of his life, there are several derivative works and lectures devoted to the Stone and Bronze Ages where Vocel pointed out the difference of Siberian bronzes from European ones⁶⁹. He was considered the ancestor of Austrian archaeology for his undeniable contribution to the development of Czech archaeology⁵⁵.

The French mineralogist Damour was born in 1902⁷⁰. After school studies, Damour entered in the Ministry of Foreign Affairs at the age of 18 in the accounting department in 1829. There, he developed his career until reaching the rank of deputy director. In 1853 he decided

to retire and pursue his passion, mineralogy. From then on, his activity focused on the study of rocks⁷¹ and minerals, carrying out chemical analyzes that allowed him to define twenty new mineralogical species. In addition to his mineralogical studies, Damour was a precursor of the collaboration between specialists from other disciplines, such as chemistry, geology, and zoology to achieve broadening the knowledge acquired.

Jhon Percy was a very appreciated metallurgist. He was born in 1817 in Nottingham and did his school studies in the same city. Subsequently, he took a 3-year course at the University of Edinburgh and was graduated in 1839. Then, he moved to Paris to continue his academic studies which put him in contact with some of the leading chemists of his time. With the time, he returned to England and practiced as a physician where he achieved considerable medical fame. Simultaneously with his professional practice, he conducted research in mineralogy and metallurgy. In 1851 he became a professor of metallurgy at the Royal School of Mines for almost 30 years. Between 1861 and 1880, John produced several of his metallurgical works of iron, steel and all other metals. One of his best-known works was a textbook named "Metallurgy: The art of extracting metals from their ores" which he published in 1861 focusing on the branch of archaeological metallurgy⁷². Thanks to his contributions on the production and early use of metals, he was selected in 1885 as President of the Institute of Iron and Steel and as a member of the Royal Society.

Another known scientist in the archaeological chemistry was Friedrich Rathgen⁷³. He was born in 1862 and after his studies, he completed his education presenting his Doctoral Degree in organic chemistry in

1886. During the next year, Rathgen worked as a research assistant to the German Chemist H. H. Landholt. Later, he was hired by the Royal Museums of Berlin to become the first Director of the Chemical Laboratory. It was then when Rathgen was the first to take a scientific approach to the treatment of museum artifacts. Due to that, he was responsible for many of the most important developments in the treatment of archaeological materials and in the application of chemical and physical methods for the conservation of antiquities. This work allowed him to write *The Conservation Antiquities handbook*⁷⁴ published in 1898 and about sixty papers, based on the technology and conservation of archaeological artifacts, were summarized. Prior to his studies in this branch conservation was considered a separate discipline from chemistry and that is the reason why he is regarded as the father of modern archaeological conservation⁷³ (Rathgen 1898)^{55,56,75,76}.

The study carried out by these famous scientists has acquired more importance over time. Thanks to this, nowadays more works in archaeological materials are being carried out by the collaboration of archaeologists, chemists, conservators, corrosion experts, geologists, and statisticians^{56,75-79}.

From the collaboration of different fields such as those mentioned, the previously mentioned term arises, Archaeological Chemistry. This field, known since 19th century, is part of archaeometry science (based on the measurement of the chemical or physical properties of an artifact) which involves the investigation of the inorganic and organic composition of archaeological materials for its proper conservation⁵⁴.

Archaeological Chemistry is based on answering 3 main questions such as “what”, “when” and “where”. The answer to the question

“where”, arises thanks to the investigations in the geographic and geological scope that can be carried out on these materials. On the contrary, the question “what” and “when”, the main concern of archaeology, can be solved thanks to analytical methods and modern instrumentation. These analytical methods offer essential information (composition, provenance, techniques used in their production and age) which help to better understand all the features that surround archaeological materials⁸⁰.

One of the reasons for the success of the application of this science to real and precious archaeological objects relies on the development of non-destructive and portable analytical techniques.

1.5 ANALYTICAL TECHNIQUES

The analysis of art and archaeological objects in different environments is essential for future conservation and restoration processes and for archaeometric studies. But carrying out these analyses on this type of pieces entails certain difficulties: access to the archaeological object or remains, the impossibility of collecting or taking samples, the need for non-invasive or non-destructive techniques, the heterogeneity of the samples and their multicomponent nature. Furthermore, the deterioration of this type of samples can increase the complexity of the analytical procedure by adding more parameters to be determined. For that reason, specific techniques are needed to determine both the composition and distribution of these elements and the alteration products present⁸¹.

In the specific case of Cultural Heritage samples, the analytical task requires special attention on the sampling and on the analyses of these precious ancient artifacts. Actually, there are a large number of archaeological remains that offer potentially valuable information from the past. However, accessing the ruins and therefore such information is not an easy task because a modern technological equipment is necessary for exploration. Roughly there are two ways to access to Cultural Heritage information. On the one hand, if access to the sampling area is not possible, a bibliographical study can be carried out but, unfortunately, sometimes it could be a very limited study. On the other hand, in the case that the sampling area can be accessed, the best option is to perform in situ analysis on the available material with suitable equipment to obtain chemical, geological, and biological data and make a photographic report of the archaeological remains.

With regards to the analysis, on many occasions, these samples are very delicate or they are too big, and they cannot be altered or moved, preventing their transfer to a laboratory for analysis. For these cases, the most used analytical techniques are those known as portable techniques⁸². A portable system can be taken into the emplacement of interest and the analysis can be performed in-situ. In addition, dealing with such precious materials always requires the use of non-destructive or/and non-invasive techniques. These techniques allow performing analysis but without altering or causing damages on the sample. Therefore, the sample remains unaltered for further studies or future museum expositions, for instance. Moreover, when working with this kind of techniques, the pre-treatment of the sample is often not needed, and the analyses are made directly on the sample. This is another reason why they are considered non-destructive because they do not make any changes not physically or chemically into the samples before or after the analysis and no kind of subproducts such as reagents and solvents are generated. In the specific case of chemical studies, by the means of these techniques, elemental, molecular and structural composition of the samples can be ascertained preserving the samples for the future.

Among the non-destructive analytical techniques, in the recent years the most used ones have been the spectroscopic techniques⁸³. These are based on the interaction between electromagnetic radiation and matter where the sample undergoes a process of absorption or emission of light. As a result of this process, an emission or absorption spectrum is obtained, which is the fingerprint of the chemical element detected and can be easily identified. These features make them suitable for characterizing and diagnosing the deterioration mechanism involved in archaeological samples or even

characterizing the raw materials used. In addition, most of the spectroscopic techniques offer the possibility of carrying out measurements in-situ with portable equipment⁸³. All this make them the perfect analytical solution for studying precious and valuable material as Cultural Heritage samples are.

Most of the performance of these techniques is based on the excitation of the sample with different sources. A detector collects the information coming from the excitation of the sample. Then, different kinds of diagrams or graphs are made by the software used for the control of the equipment. These graphs are those analyzed by scientist in order to obtain conclusions.

For the special study of archaeological artifacts several non-destructive techniques have been used in different works along the history⁸³. However, the most employed ones are Raman Spectroscopy^{84,85}, X-Ray Fluorescence (XRF)^{84,86}, Infrared Spectroscopy (IR)^{84,87}, Scanning Electron Microcopy-Electron Dispersive Energy (SEM-EDS)^{84,88}, Laser Induced Breakdown Spectroscopy (LIBS)^{89,90} and X-Ray Diffraction (XRD)^{84,91}.

All these techniques have been used since a long time to define elemental (LIBS, XRF and SEM-EDS), molecular and structural (IR, Raman spectroscopy and XRD) composition of archaeological artifacts and their decay products. With the provided analytical results, valuable information about the remains or about the conservation state of the pieces can be extracted. In this work, all the mentioned techniques have been used except LIBS and IR, they were considered non-suitable for this work case.

X-Ray fluorescence spectroscopy was used to obtain elemental information of Cultural Heritage samples. This technique produces the

irradiation by a primary X-ray beam from an X-Ray tube that collides with the sample and in response, causes the emission of fluorescent X-ray with energies characteristic of the elements present in the sample. The advantages of this technique its multi-elemental capability, the low contamination risk, short term delay obtaining the results and its relatively low investment and operational costs. As disadvantages, it requires specialized training and concern, there are possible matrix effects which can attenuate and enhance signals and there is also the radiation exposure.

Although its first applications were mainly medical for the realization of X-rays of bones of the body⁹², the XRF technique quickly gained importance in the field of metallurgy^{93,94}. Specifically, as it is a rapid and elemental analysis technique, its use in metallurgy and metal pretreatment plants quickly gained great importance, being on the fields in which XRF has greater applicability today. In addition, the XRF analysis methods allows the study of other types of matrixes with different objectives in the Cultural Heritage field, such as the classification of the metallic objects⁹⁵, identification of pigments in paintings⁹⁶ and analysis of glass and pottery⁹⁷.

As mentioned above, another commonly used technique for Cultural Heritage analysis is the SEM-EDS⁸⁴. It is an analytical technique that is used for defining the elemental composition at microscopic resolution. In this case the excitation source is a beam of electrons which interact with the sample. With the response that the sample emits due to the incoming excitation, on the one hand a SEM image is collected. This high-resolution electronic image allows to observe the appearance of the studied sample like size and shapes of the

crystals or the structure of the sample surface at the micrometric scale.

On the other hand, the excitation of the sample also promotes the emission of energy from it. This energy is characteristic of its elemental composition since each element emits a characteristic amount of energy. In this way, the elemental characterization of the sample is performed. Moreover, semi-quantitative analysis of the identified elements can be also performed.

Unfortunately, the technique also presents some drawbacks for samples coming from Cultural Heritage. On the one hand, the sample must be directly deposited in a vacuum chamber, since the analyses are made under vacuum to prevent contamination of the sample and the detector and to maintain a low temperature⁹⁸. This chamber can limit the analysis of some samples by size and can lead to fractionation of them. On the other hand, in order to obtain good images of the sample surface, the sample must be conductive, since obtaining the SEM-EDS image is the result of the interaction of the electrons emitted by the equipment and the sample. If the sample is conductive, no pre-treatment is necessary. In contrast, in the case of non-conductive sample, it must be metallized by means of a device that deposits a layer of a few nanometers of a conductive element, allowing proper images by scanning electron microscopy and an accurate composition determination through EDS⁹⁹. Besides, sample must be translated to the laboratory for the analysis as it is not a portable technique.

Therefore, it could be thought that SEM-EDS could be a useless technique comparing to XRF. Nevertheless, it presents some

advantages at resolution level as providing information about structure of the sample at the micrometric scale.

Besides, it provides the opportunity to relate textures to composition, which could be valuable information for a faster future identification of compounds. Therefore, XRF and SEM-EDS can be considering good collaborative elemental techniques for a complete elemental analysis^{100,101}.

Raman spectroscopy provides molecular information of the studied specimen. In this case, the sample is irradiated with lasers of different wavelength. With the excitation generated by the laser the molecules start vibrating to go back to a basic energy state. This vibration energy is characteristic of each molecule so when it arrives to the detector the signal that it provides is like a fingerprint for each molecule present in the sample. Therefore, once the so-called fingerprint of the compound is collected it is compared with a spectra database to find a match. In this way, the studied sample is molecularly and structurally characterized. Raman analyses is a completely non-destructive technique. Besides being cheap and fast, the number of analyses that can be performed in situ or in the laboratory samples is high enough to guarantee representativity of the detected compounds. As a disadvantage of this technique the most common one is the fluorescence produced by the sample which can affect the obtained spectra. Other common disadvantage of this technique is the low sensitivity and the long acquisition times that need to make imaging by point scanning or mapping¹⁰². In addition, the laser power must be controlled so as not to burn the sample and standard reference will be necessary to compare the results obtained.

This technique has been used in a great variety of studies on different type of materials, especially in cases where the identification on the degradation products is necessary, as is the case of the diagnosis of the conservation state of weathering steel structures^{103,104}, the microbiologically influenced corrosion in archaeological artifacts¹⁰⁵, the study of submerged materials^{106,107}, the studies of ancient pottery¹⁰⁸, characterize biological materials¹⁰⁹ and the investigation of objects in art and archaeology¹¹⁰.

Finally, X-ray diffraction (XRD) is considered one of the most powerful and commonly used characterization techniques for the structural analysis of crystals¹¹¹. Its main characteristics are the consequence of being an electromagnetic probe of matter with a wavelength (λ – 1.5 Å) of a magnitude very similar to the interplanar spacing of solids. Since photons are particles of zero rest mass and free of charge, they interact with a matter in in a way that does not affect its physical state. In addition to this advantage, this technique was widely used in the qualitative identification of different samples and also in the quantitative estimation of mineral components¹¹². The analyses realized with XRD can be obtained quickly and reliably⁹⁹.

The disadvantage of this technique is that the sample must be pulverized and homogenized prior to the analysis. Although is a non-destructive technique, it requires a minimal preparation of the sample. Apart from that, the laser power must be controlled because it can burn the sample. Furthermore, the results obtained by the use of this technique require access to a standard reference data.

Thanks to the advantages in this technique, it has been used to characterize the corrosion products in the rust layer^{113,114}, in the study

of pigments¹¹⁵ and sculptures⁸², in the study of ceramics and archaeological stone analysis¹¹⁵.

Considering the pros and cons of the mentioned techniques, in this work, the XRF and Raman techniques are the techniques that were chosen as the main ones to characterize in an elementary and molecular way the samples. However, when it was required and it was possible, these data were supplemented with data obtained by SEM-EDS and XRD techniques.

All these techniques have been used individually or complementarily for the study of different archaeological pieces in this PhD. Moreover, as it was discussed, most of them can be portable. Therefore, in this PhD, multi-analytical methodology is proposed focused on the use of portable techniques with the combination of laboratory measurements for reaching different aims. The instruments and the methods used are described in the next chapter.

1.6 BIBLIOGRAPHY

The references mentioned in this work are based on the bibliography format described below:

Journals: Estalayo, E. Aramendia, J. Bellot-Gurlet, L. Garcia L. Garcia-Camino, I. Madariaga, J.M. Article title. *Journal abbreviation*, volume, pages (year).

Books: Estalayo, E. Aramendia, J. Bellot-Gurlet, L. Garcia L. Garcia-Camino, I. Madariaga, J.M. *Book title* (year). DOI number.

1. UNESCO. UNESCO official web page. at <<https://whc.unesco.org/en/faq/19>>
2. UNESCO. Records of the General Conference (Seventeenth Session) Paris 1972. *General conference seventeenth session 1*, 135–145 (1972).
3. UNESCO. *Convention concerning the protection of the world cultural and natural heritage. General Conference seventeenth session* (1972).
4. UNESCO. Operational Guidelines for the Implementation of the World Heritage Convention. *World Heritage Center* 1–177 (2019).
5. UNESCO. *Records of the General Conference. Resolutions 1*, (2005).
6. Alonso, G. & Medici, M. in *Indicadores UNESCO de Cultural para el desarrollo. Manual Metodológico* 132–140 (2014).
7. España, M. de C. y Deporte. G. de. UNESCO Patrimonio Mundial. at <<https://www.culturaydeporte.gob.es/cultura/areas/patrimonio/mc/patrimoniomundial/unesco-patrimoniomundial.html>>

8. Sandu, I., Vasilache, V. & Vrînceanu, N. Environmental Technologies in the Field of Scientific Conservation of Cultural Heritage. New Perspectives and Directions of Research. *Present Environment and Sustainable Development* **3**, 97–105 (2009).
9. Europe, C. of. Concerning the Adaptation of Laws and Regulations To the. in *Resolution (76) 28* 1–7 (1976).
10. Convention, E. C., Charter, E., Heritage, A., Assembly, P., No, R. & No, R. Council of Europe: Convention for the Protection of the Architectural Heritage of Europe. *International Legal Materials* **25**, 380–390 (1986).
11. Sablier, M. & Garrigues, P. Cultural heritage and its environment: An issue of interest for Environmental Science and Pollution Research. *Environmental Science and Pollution Research* **21**, 5769–5773 (2014).
12. Dastgerdi, A. S., Sargolini, M. & Pierantoni, I. Climate change challenges to existing cultural heritage policy. *Sustainability Heritage Management* **11**, (2019).
13. Sesana, E., Gagnon, A. S., Ciantelli, C., Cassar, J. A. & Hughes, J. J. Climate change impacts on cultural heritage: A literature review. *Wiley Interdisciplinary Reviews: Climate Change* **12**, 1–29 (2021).
14. UNESCO. Climate change and World Heritage. *Science* **314**, 632–635 (2006).
15. Spiridon, P., Sandu, I. & Stratulat, L. The conscious deterioration and degradation of the cultural heritage. *International Journal of Conservation Science* **8**, 81–88 (2017).

16. School, W. S. How Much Water is There on Earth? (2019). at <https://www.usgs.gov/special-topics/water-science-school/science/how-much-water-there-earth>
17. Little, B. J., Lee, J. S., Briggs, B. R., Ray, R. & Sylvester, A. Examination of archived rusticles from World War II shipwrecks. *International Biodeterioration and Biodegradation* **143**, 1–6 (2019).
18. Chadwick, A. v., Berko, A., Schofield, E. J., Smith, A. D., Mosselmans, J. F. W., Jones, A. M. & Cibin, G. The application of X-ray absorption spectroscopy in archaeological conservation: Example of an artefact from Henry VIII warship, the Mary Rose. *Journal of Non-Crystalline Solids* **451**, 49–55 (2016).
19. Rogerio-Candelera, M. Á. Science, technology and cultural heritage. *Science, Technology and Cultural Heritage* 1–501 (2014). doi:10.1201/b17802
20. Naderi Beni, A., Lahijani, H., Tofighian, H., Guibal, F., Kabiri, K., Gambin, T., Djamali, M., Abaie, H. & Jahani, V. Geoarchaeology of the 18th century Qoroq shipwreck, Caspian Sea, Iran: A tale of sailing in a dynamic environment. *Journal of Archaeological Science: Reports* **34**, (2020).
21. UNESCO. *Convention on the Protection of the Underwater Cultural Heritage*. (2001).
22. Ricca, M. & la Russa, M. F. Challenges for the Protection of Underwater Cultural Heritage (UCH), from Waterlogged and Weathered Stone Materials to Conservation Strategies: An Overview. *Heritage* **3**, 402–411 (2020).

23. Angelini, E., Grassini, S. & Tusa, S. Underwater corrosion of metallic heritage artefacts. *Corrosion and Conservation of Cultural Heritage Metallic Artefacts* 236–259 (2013). doi:10.1533/9781782421573.3.236
24. Florian, M.-L. E. *The underwater environment. Conservation of Marine Archaeological Objects* (Butterworth & Co. (Publishers) Ltd., 1987). doi:10.1016/b978-0-408-10668-9.50007-1
25. Memet, J. B. in *Corrosion of Metallic Heritage Artefacts: Investigation, Conservation and Prediction of Long Term Behaviour* 152–169 (2007). doi:10.1533/9781845693015.152
26. Science, S. Depth sea pH profile. at <<https://skepticalscience.com/print.php?n=918>>
27. Frankel, G. S. Pitting Corrosion of Metals: A Review of the Critical Factors. *Journal of The Electrochemical Society* **145**, 2186–2198 (1998).
28. Engineering, S. of M. S. and. Crevice corrosion. at <<https://www.materials.unsw.edu.au/study-us/high-school-students-and-teachers/online-tutorials/corrosion/types-corrosion/crevice-corrosion>>
29. Loto, C. A. Stress corrosion cracking: characteristics, mechanisms and experimental study. *International Journal of Advanced Manufacturing Technology* **93**, 622–640 (2017).
30. Shehadeh, M., Anany, M., Saqr, K. M. & Hassan, I. Experimental investigation of erosion-corrosion phenomena in a steel fitting due to plain and slurry seawater flow. *International Journal of Mechanical and Materials Engineering* **9**, 1–8 (2014).

31. Yang, L. *Techniques for Corrosion Monitoring*. (2008).
32. Černoušek, T., Ševců, A., Shrestha, R., Steinová, J., Kokinda, J. & Vizelková, K. in *The Microbiology of Nuclear Waste Disposal* 119–136 (2021). doi:10.1016/b978-0-12-818695-4.00006-x
33. Little, B. J., Blackwood, D. J., Hinks, J., Lauro, F. M., Marsili, E., Okamoto, A., Rice, S. A., Wade, S. A. & Flemming, H. C. Microbially influenced corrosion—Any progress? *Corrosion Science* **170**, 108641 (2020).
34. Broda, M. & Hill, C. A. S. Conservation of waterlogged wood—past, present and future perspectives. *Forests* **12**, 1–55 (2021).
35. Kibblewhite, M., Tóth, G. & Hermann, T. Predicting the preservation of cultural artefacts and buried materials in soil. *Science of the Total Environment* **529**, 249–263 (2015).
36. Arriba-Rodriguez, L. de, Villanueva-Balsera, J., Ortega-Fernandez, F. & Rodriguez-Perez, F. Methods to evaluate corrosion in buried steel structures: A review. *Metals* **8**, (2018).
37. Logan, K. H. The Bureau of Standards Soil-Corrosion Investigation. *Journal - American Water Works Association* **21**, 311–316 (1929).
38. Singh, B., Cattle, S. R. & Field, D. J. Edaphic Soil Science, Introduction to. *Encyclopedia of Agriculture and Food Systems* **3**, 35–58 (2014).
39. Ismail, A. I. M. & El-Shamy, A. M. Engineering behaviour of soil materials on the corrosion of mild steel. *Applied Clay Science* **42**, 356–362 (2009).
40. Pereira, R. F. D. C., de Oliveira, E. S. D., Lima, M. A. G. D. A. & Brasil, S. L. D. C. Corrosion of galvanized steel under different soil moisture contents. *Materials Research* **18**, 563–568 (2015).

41. Veleva, L. in *Corrosion Tests and Standards: Application and Interpretation* 882 (2005).
42. Tiba, C. & de Oliveira, E. M. Utilization of cathodic protection for transmission towers through photovoltaic generation. *Renewable Energy* **40**, 150–156 (2012).
43. Kibblewhite, M., Tóth, G. & Hermann, T. Predicting the preservation of cultural artefacts and buried materials in soil. *Science of the Total Environment* **529**, 249–263 (2015).
44. Eric, D. & Price Clifford A. *Research in Conservation. Research in Conservation* (2010).
45. Doehne, E., Selwitz, D., Carson, D. & Selwitz, C. The damage mechanism of sodium sulfate in porous stone. *European research on cultural heritage* **5**, 127–146 (2006).
46. Tokmak, M. & Dal, M. Types of degradation observed in underwater stone artifacts. in *12th International Symposium on Underwater Research* 72–77 (2020).
47. Farooq, M. Mycobial Deterioration of Stone Monuments of Dharmarajika, Taxila. *Journal of Microbiology & Experimentation* **2**, 29–33 (2015).
48. Carmona, N., García-Heras, M., Gil, C. & Villegas, M. A. Chemical degradation of glasses under simulated marine medium. *Materials Chemistry and Physics* **94**, 92–102 (2005).
49. Kibblewhite, M., Tóth, G. & Hermann, T. Predicting the preservation of cultural artefacts and buried materials in soil. *Science of the Total Environment* **529**, 249–263 (2015).

50. Abd-Allah, R. Chemical cleaning of soiled deposits and encrustations on archaeological glass: A diagnostic and practical study. *Journal of Cultural Heritage* **14**, 97–108 (2013).
51. Zacharias, N., Palamara, E., Kordali, R. & Muros, V. Archaeological Glass Corrosion Studies: Composition, Environment and Content. *Scientific Culture* **6**, 53–67 (2020).
52. Palomar Sanz, T. El vidrio arqueológico: Problemas y metodología. in *Actas de las V Jornadas de Investigación del departamento de prehistoria y arqueología de la UAM: Jóvenes investigadores de la Comunidad de Madrid* 79–87 (2016).
53. Palomar, T. & Llorente, I. Decay processes of silicate glasses in river and marine aquatic environments. *Journal of Non-Crystalline Solids* **449**, 20–28 (2016).
54. Zurer, P. S. Archaeological chemistry. *Chemical and Engineering News* **61**, 26–44 (1983).
55. Glascock, M. D. Compositional Analysis in Archaeology History of Compositional Analysis. *Oxford Handbooks Online* 1–25 (2016). doi:10.1093/oxfordhb/9780199935413.013.8
56. Caley, E. R. Early history and literature of archaeological chemistry. *Journal of Chemical Education* **204**, 64–66 (1951).
57. Harbottle, G. *Chemical Characterization in Archaeology. Contexts for Prehistoric Exchange* (Academic Press, Inc., 1982). doi:10.1016/b978-0-12-241580-7.50007-3
58. Pollard, A. M. & Heron, C. *Archaeological Chemistry*. (1996).
59. Caley, E. R. Klaproth as a pioneer in the chemical investigation of antiquities. *Journal of Chemical Education* **26**, (1949).

60. Lamont-Brown, R. *Humphry Davy: Life beyond the lamp*. (Sutton, 2004).
61. Institute, S. H. Humphry Davy. at <https://www.sciencehistory.org/historical-profile/humphry-davy>
62. Humphry Davy. Some experiments and observations on the colours used in painting by the ancients. *Philosophical Transactions of the Royal Society of London* **105**, 97–124 (1815).
63. Davy, H. XXI. Observations upon the Composition of the Colours found on the Walls of the Roman House discovered at Bignor in Sussex. By Sir Humphrey Davy, Knt. F.R.S. in a Letter to Samuel Lysons, Esq. V.P. *Archaeologia* **18**, 222–222 (1817).
64. Moshenska, G. Michael faraday's contributions to archaeological chemistry. *Ambix* **62**, 266–286 (2015).
65. Wikipedia. Karl Christian Traugott Friedemann Goebel. at https://en.wikipedia.org/wiki/Karl_Christian_Traugott_Friedemann_Goebel
66. Göbel, K. C. Über der Einfluss der Chemie auf die Ermittlung der Völker der Vorzeit. (1842).
67. Vélková, L. Jan Erazim Vöcel. (2012). at <https://www.archeologienadosah.cz/o-archeologii/dejiny-oboru/osobnosti-ceske-archeologie/jan-erazim-vocel-1802-1871>
68. Walter, E. Jan Erazim Vöcel (1802-1871): A Pioneer of Czech-Danish Friendship. *Essays on the arts and sciences* 924–927 (2019). doi:10.1515/9783111562575-003
69. Vöcel, J. E. Stein- und Bronzealterthümer. (1869).

70. France, S. G. de. Agustin Alexis Damour. at <https://www.geosoc.fr/propos-html/historique/presidents-de-la-sgf/64-presidents-sgf/441-augustin-alexis-damour.html>
71. Damour, A. Sur la composition des haches en pierre trouvées dans les monuments celtiques et chez les tribus sauvages. *Revue Archéologique* **13**, 190–207 (1866).
72. Percy, J. *Metallurgy: The Art of Extracting Metals from their Ores*. (1861).
73. Gilberg, M. Friedrich Rathgen: The father of modern archaeological conservation. *Journal of the American Institute for Conservation* **26**, 85–104 (1987).
74. Rathgen, F. The Preservation of Antiquities, a Handbook for Curators. *Nature* **73**, 412–412 (1906).
75. Orna, M. v. & Rasmussen, S. C. in *Archaeological Chemistry: A multidisciplinary analysis of the past* 509 (2020). doi:10.2307/504338
76. Oddy, W. A. Chemistry in the conservation of archaeological materials. *Science of the Total Environment, The* **143**, 121–126 (1994).
77. Ullén, I., Nord, A. G., Fjaestad, M., Mattsson, E., Borg, G. C. & Tronner, K. The degradation of archaeological bronzes underground: Evidence from museum collections. *Antiquity* **78**, 380–390 (2004).
78. Lambert, J. B. Archaeological chemistry. *Journal of Chemical Education* **60**, 345–347 (1983).
79. Jakes, K. A. Archaeological chemistry: Materials, methods, and meaning. *ACS Symposium Series* **831**, 1–7 (2002).

80. Goffer, Z. *Archaeological Chemistry*. (2007).
81. Doménech-Carbó, A. & Doménech-Carbó, M. T. Electroanalytical techniques in archaeological and art conservation. *Pure and Applied Chemistry* **90**, 447–461 (2018).
82. Franquelo, M. L., Duran, A., Castaing, J., Arquillo, D. & Perez-Rodriguez, J. L. XRF, μ -XRD and μ -spectroscopic techniques for revealing the composition and structure of paint layers on polychrome sculptures after multiple restorations. *Talanta* **89**, 462–469 (2012).
83. Bitossi, G., Giorgi, R., Mauro, M., Salvadori, B. & Dei, L. Spectroscopic techniques in cultural heritage conservation: A survey. *Applied Spectroscopy Reviews* **40**, 187–228 (2005).
84. de Castro, M. D. L. & Jurado-López, A. The role of analytical chemists in the research on the cultural heritage. *Talanta* **205**, (2019).
85. Committee, A. M. & No, A. Raman spectroscopy in cultural heritage: Background paper. *Analytical Methods* **7**, 4844–4847 (2015).
86. Bezur, A., Lee, L., Loubser, M. & Trentelman, K. *Handheld XRF in Cultural Heritage. A Practical Workbook for Conservators*. (2020).
87. Kendix, E. L., Prati, S., Mazzeo, R., Joseph, E., Sciutto, G. & Fagnano, C. Far Infrared Spectroscopy in the Field of Cultural Heritage. *e-Preservation Science* **7**, 8–13 (2010).
88. van Hoek, C. J. G., de Roo, M., van der Veer, G. & van der Laan, S. R. A SEM-EDS study of cultural heritage objects with interpretation of constituents and their distribution using PARC data analysis. *Microscopy and Microanalysis* **17**, 656–660 (2011).

89. Tereszchuk, K. A., Vadillo, J. M. & Laserna, J. J. Depth profile analysis of layered samples using glow discharge assisted Laser-induced Breakdown Spectrometry (GD-LIBS). *Spectrochimica Acta - Part B Atomic Spectroscopy* **64**, 378–383 (2009).
90. Jiang, L., Sui, M., Fan, Y., Su, H., Xue, Y. & Zhong, S. Micro-gas column assisted laser induced breakdown spectroscopy (MGC-LIBS): A metal elements detection method for bulk water in-situ analysis. *Spectrochimica Acta - Part B Atomic Spectroscopy* **177**, (2021).
91. Gonzalez, V., Cotte, M., Vanmeert, F., de Nolf, W. & Janssens, K. X-ray Diffraction Mapping for Cultural Heritage Science: a Review of Experimental Configurations and Applications. *Chemistry - A European Journal* **26**, 1703–1719 (2020).
92. János, I., Szathmáry, L., Nádas, E., Béni, A., Dinya, Z. & Máthé, E. Evaluation of elemental status of ancient human bone samples from Northeastern Hungary dated to the 10th century AD by XRF. *Nuclear Instruments and Methods in Physics Research, Section B: Beam Interactions with Materials and Atoms* **269**, 2593–2599 (2011).
93. Al-Eshaikh, M. A. & Kadachi, A. Elemental analysis of steel products using X-ray fluorescence (XRF) technique. *Journal of King Saud University - Engineering Sciences* **23**, 75–79 (2011).
94. Vasilescu, A., Constantinescu, B., Stan, D., Radtke, M., Reinholz, U., Buzanich, G. & Ceccato, D. Studies on ancient silver metallurgy using SR XRF and micro-PIXE. *Radiation Physics and Chemistry* **117**, 26–34 (2015).
95. Cruz, J., Manso, M., Corregidor, V., Silva, R. J. C., Figueiredo, E., Carvalho, M. L. & Alves, L. C. Surface analysis of corroded XV–XVI

- century copper coins by μ -XRF and μ -PIXE/ μ -EBS self-consistent analysis. *Materials Characterization* **161**, (2020).
96. Castro, K., Knuutinen, U., Vallejuelo, S. F. O. de, Irazola, M. & Madariaga, J. M. Finnish wallpaper pigments in the 18th-19th century: Presence of $\text{KFe}_3(\text{CrO}_4)_2(\text{OH})_6$ and odd pigment mixtures. *Spectrochimica Acta - Part A: Molecular and Biomolecular Spectroscopy* **106**, 104–109 (2013).
97. Turco, F., Davit, P., Cossio, R., Agostino, A. & Operti, L. Accuracy improvement by means of porosity assessment and standards optimization in SEM-EDS and XRF elemental analyses on archaeological and historical pottery and porcelain. *Journal of Archaeological Science* **12**, 54–65 (2017).
98. Bello, J. F. A. PhD Thesis: Nuevo micro-análisis cuantitativo de metales empleando microscopía electrónica de barrido con dispersión de energías de rayos X. *Universidad Complutense de Madrid* (1999).
99. Wolfgong, W. J. *Chemical analysis techniques for failure analysis: Part 1, common instrumental methods. Handbook of Materials Failure Analysis with Case Studies from the Aerospace and Automotive Industries* (Elsevier Ltd., 2016). doi:10.1016/B978-0-12-800950-5.00014-4
100. Arafat, A., Na'as, M., Kantarelou, V., Haddad, N., Giakoumaki, A., Argyropoulos, V., Anglos, D. & Karydas, A. G. Combined in situ micro-XRF, LIBS and SEM-EDS analysis of base metal and corrosion products for Islamic copper alloyed artefacts from Umm Qais museum, Jordan. *Journal of Cultural Heritage* **14**, 261–269 (2013).
101. Pendleton, M. W., Washburn, D. K., Ellis, E. A. & Pendleton, B. B. Comparing the detection of iron-based pottery pigment on a carbon-

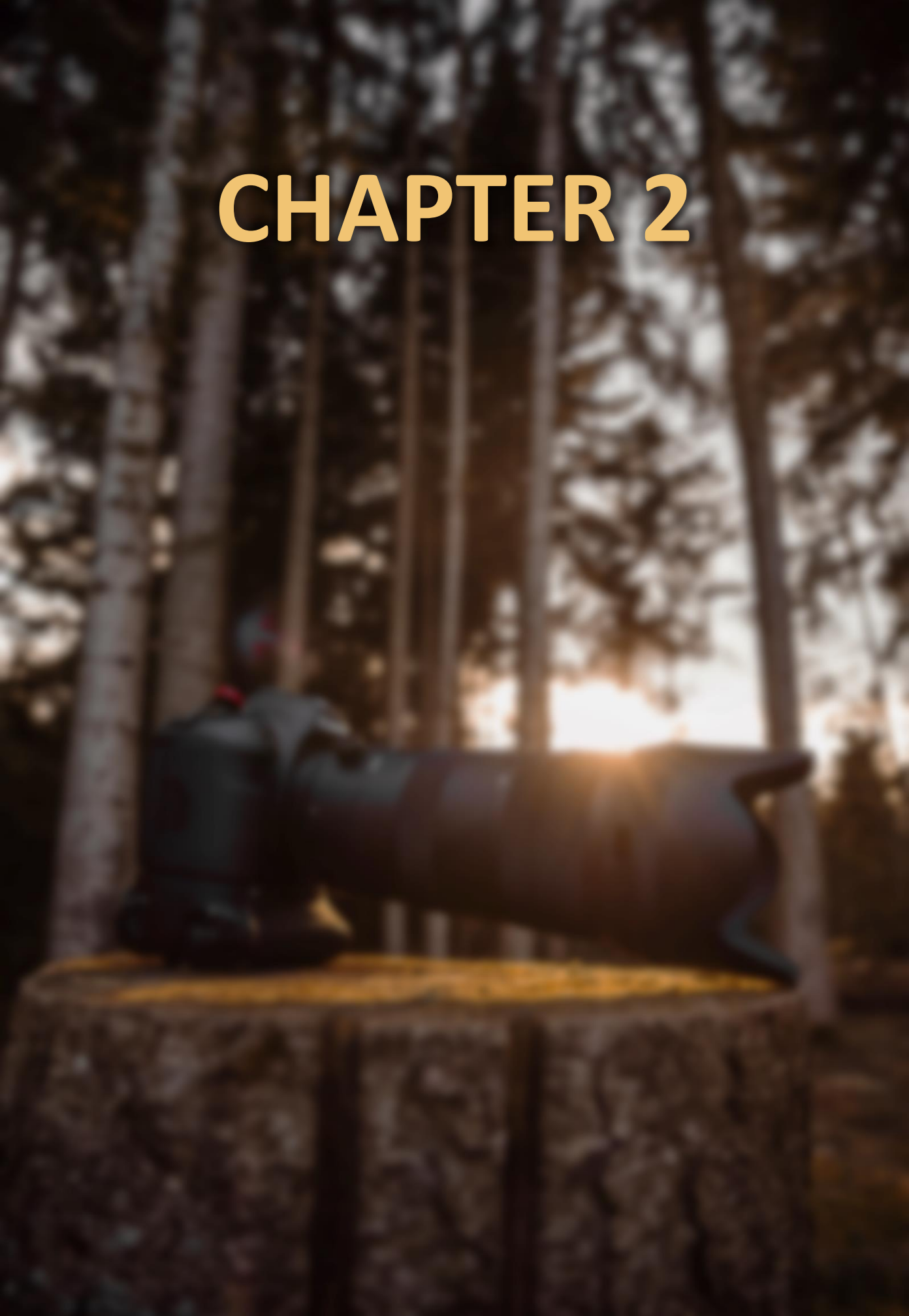
coated Sherd by SEM-EDS and by Micro-XRF-SEM. *Yale Journal of Biology and Medicine* **87**, 15–20 (2014).

102. Eberhardt, K., Stiebing, C., Matthaüs, C., Schmitt, M. & Popp, J. Advantages and limitations of Raman spectroscopy for molecular diagnostics: An update. *Expert Review of Molecular Diagnostics* **15**, 773–787 (2015).
103. Rémazeilles, C., Lévêque, F., Conforto, E. & Refait, P. Long-term alteration processes of iron fasteners extracted from archaeological shipwrecks aged in biologically active waterlogged media. *Corrosion Science* **181**, (2021).
104. Aramendia, J., Gomez-Nubla, L., Bellot-Gurlet, L., Castro, K., Paris, C., Colombar, P. & Madariaga, J. M. Protective ability index measurement through Raman quantification imaging to diagnose the conservation state of weathering steel structures. *Journal of Raman Spectroscopy* **45**, 1076–1084 (2014).
105. Rémazeilles, C., Saheb, M., Neff, D., Guilminot, E., Tran, K., Bourdoiseau, J. A., Sabot, R., Jeannin, M., Matthiesen, H., Dillmann, P. & Refait, P. Microbiologically influenced corrosion of archaeological artefacts: Characterisation of iron(II) sulfides by Raman spectroscopy. *Journal of Raman Spectroscopy* **41**, 1425–1433 (2010).
106. Estalayo, E., Aramendia, J., Matés Luque, J. M. & Madariaga, J. M. Chemical study of degradation processes in ancient metallic materials rescued from underwater medium. *Journal of Raman Spectroscopy* **50**, 289–298 (2019).
107. Kerns, J. G., Buckley, K., Parker, A. W., Birch, H. L., Matousek, P., Hildred, A. & Goodship, A. E. The use of laser spectroscopy to

- investigate bone disease in King Henry VIII's sailors. *Journal of Archaeological Science* **53**, 516–520 (2015).
108. Abdurakhimov, B. A., Kichanov, S. E., Talmaṭchi, C., Kozlenko, D. P., Talmaṭchi, G., Belozerova, N. M., Bălăṣoiu, M. & Belc, M. C. Studies of ancient pottery fragments from Dobrudja region of Romania using neutron diffraction, tomography and Raman spectroscopy. *Journal of Archaeological Science* **35**, (2021).
109. Butler, H. J., Ashton, L., Bird, B., Cinque, G., Curtis, K., Dorney, J., Esmonde-White, K., Fullwood, N. J., Gardner, B., Martin-Hirsch, P. L., Walsh, M. J., McAinsh, M. R., Stone, N. & Martin, F. L. Using Raman spectroscopy to characterize biological materials. *Nature Protocols* **11**, 664–687 (2016).
110. Vandenabeele, P. Raman spectroscopy in art and archaeology. *Journal of Raman Spectroscopy* **35**, 607–609 (2004).
111. Rajiv, K. & Mittal, K. L. in *Developments in Surface Contamination and Cleaning* **12**, 23–105 (2019).
112. Engler, P. & Iyengar, S. S. Analysis of mineral samples using combined instrument (XRD, TGA, ICP) procedures for phase quantification. *American Mineralogist* **72**, 832–838 (1987).
113. Aramendia, J. PhD Thesis: Analytical diagnosis of the conservation state of weathering steel exposed to urban atmospheres. *Universidad del Pais Vasco (UPV/EHU)* (2013).
114. Kamimura, T., Nasu, S., Tazaki, T., Kuzushita, K. & Morimoto, S. Mössbauer spectroscopic study of rust formed on a weathering steel and a mild steel exposed for a long term in an industrial environment. *Materials Transactions* **43**, 694–703 (2002).

115. Castro, K. PhD Thesis: Pigment characterisation on paper-based artworks by vibrational spectroscopic techniques. *Universidad del País Vasco (UPV/EHU)* (2004).

CHAPTER 2



2. OBJECTIVES

“The world suffers a lot. Not because the violence of bad people. But because of the silence of the good people” – “El mundo sufre mucho, no por la violencia de las malas personas sino por el silencio de las buenas personas” – Napoleón Bonaparte

World Heritage is the set of cultural and natural assets that have been inherited from our ancestors, and which allow us to understand and know more about the history, customs and way of life so far today. World Heritage is the base on which humanity builds its collective memory and identity, it is what makes us identify with a culture, with a language and, with a specific way of life.

As described in the introduction of this PhD, a large part of the Cultural Heritage existing today has suffered, suffers, or will suffer different degradation processes due to different factors, depending on their particular situation. These degradation problems can be of diverse nature and must be studied carefully not to lose their heritage value.

In this sense, the main objective of this PhD thesis was to identify the problem present in different type of archaeological pieces exposed to different environments, manufactured in different materials and subjected to different conservation procedures. In this way, identifying the main reason for their current conservation state was also an aim.

For this purpose, in this work we selected two shipwrecks, Urbieta and the Bakio shipwrecks, in order to better understand the problems that may be present under buried marine conditions. These two shipwrecks were sunk in locations subjected to very disparate conditions but from both, several metallic and wooden pieces were extracted. On the other hand, three types of buried archaeological samples were also selected. In this case, different origin materials exposed to similar burial conditions in soil were analyzed: glass beads from Vaccaei Culture, some silex tools and some archaeological iron slags.

In order to achieve the mentioned general objective, some operational objectives were designed to facilitate its fulfillment:

1. To carry out elemental and molecular characterization of the different archaeological pieces through the use of non-destructive techniques using portable or laboratory equipment.
2. To define the raw materials.
3. To study the conservation state of the pieces defining possible degradation mechanisms characteristic of each burial environment.
4. To compare between the portable and laboratory equipment, establishing a complete analytical methodology for the study and conservation of archaeological pieces.
5. To analytically assess conventional chemical treatments applied by curators for archaeological pieces preservation, studying their efficiency.

CHAPTER 3

A blurred background image of a person using a microscope in a laboratory setting. The person's hands are visible, adjusting the microscope. The microscope is a compound light microscope with a black body and silver objective lenses. The background is out of focus, showing a white wall and a black surface.

3. MATERIALS AND METHODS

*“The important thing in science is not so much to obtain new facts as to discover new ways of thinking about them” – “Lo importante en la ciencia no es tanto obtener nuevos hechos como descubrir nuevas formas de pensar sobre ellos” –
William Lawrence Bragg*

The analytical study of the Cultural Heritage requires special attention on the sampling and on the analyses of precious ancient artifacts. There are a large number of archaeological remains that offer potentially valuable information from the past. However, accessing the ruins and artefacts preserved in collections to perform their scientific analysis to extract as much information as possible is not an easy task because a modern technological equipment is necessary for exploration. Roughly there are two ways to access to Cultural Heritage information. On the one hand, if access to the sampling area or artefacts is not possible, a bibliographical study can be carried out but, unfortunately, sometimes it could be a very limited study. On the other hand, in the case that the sampling area or artefacts can be accessed, the best option is to perform in situ analysis on the available material with suitable equipment to obtain chemical, geological, and biological data and make a photographic report of the archaeological remains.

With regards to the analysis, on many occasions, these samples are very delicate or they are too big, and they cannot be moved, preventing their transfer to a laboratory for analysis.

For these cases, the most used analytical techniques are those known as portable techniques. A portable system can be taken into the emplacement of interest and the analysis can be performed in-situ. In addition, dealing with such precious materials always requires the use of non-destructive or/and non-invasive techniques. These techniques allow performing analysis but without altering or causing damages on the sample. Therefore, the sample remains unaltered for further studies, conservation actions or future museum expositions, for instance. Moreover, when working with this kind of techniques, the pre-treatment of the sample is not needed, and the analyses are made directly on the sample. This is another reason why they are considered non-destructive because they do not make any changes not physically or chemically into the samples before or after the analysis and no kind of subproducts such as reagents and solvents are generated.

In the specific case of chemical studies, by the means of these techniques, elemental, molecular and structural composition of the samples can be ascertained preserving the preservation of samples for the future.

Among the non-destructive analytical techniques, in the recent years the most used ones have been the spectroscopic techniques¹. These are based on the interaction between electromagnetic radiation and matter where the sample undergoes a process of absorption or emission of light. As a result of this process, an emission or absorption spectrum is obtained, which is the fingerprint of the chemical element detected and can be easily identified. These features make them suitable for characterizing and diagnosing the deterioration mechanism involved in archaeological samples or even characterizing the raw materials used. In addition, most of the

spectroscopic techniques offer the possibility of carrying out measurements in-situ with portable equipments². All this make them the perfect analytical solution for studying precious and valuable material as Cultural Heritage samples are.

Most of the performance of these techniques is based on the excitation of the sample with different sources. A detector collects the information coming from the excitation of the sample. Then, different kinds of diagrams or graphs are made by the software used for the control of the equipment. These graphs are those analyzed by scientist in order to obtain conclusions.

For the special study of archaeological artifacts several non-destructive techniques have been used in different works along the history¹. However, the most employed ones are Raman Spectroscopy^{3,4}, X-Ray Fluorescence (XRF)^{3,5}, Infrared Spectroscopy (IR)^{3,6}, Scanning Electron Microcopy-Electron Dispersive Energy (SEM-EDS)^{3,7}, Laser Induced Breakdown Spectroscopy (LIBS)^{8,9} and X-Ray Diffraction (XRD)^{3,10}.

All these techniques have been used since a long time to define elemental (LIBS, XRF and SEM-EDS), molecular and structural (IR, Raman spectroscopy and XRD) composition of archaeological artifacts and their decay products. With the provided analytical results, valuable information about the remains or about the conservation state of the pieces can be extracted. In this work, all the mentioned techniques have been used except LIBS and IR).

X-Ray fluorescence spectroscopy was used to obtain elemental information of the selected Cultural Heritage samples. This technique uses the irradiation of a primary X-ray beam from an X-Ray tube that collides with the sample and in response, causes the emission of

fluorescent X-ray with energies characteristic of the elements present in the sample. The advantages of this technique are its multi-elemental capability, the low contamination risk, short term delay obtaining the results and its relatively low investment and operational costs. As disadvantages, it requires specialized training and concern, there are important matrix effects which can attenuate and enhance signals and there is also the radiation exposure.

Although its first applications were mainly medical for the analysis of bones of the body¹¹, the XRF technique quickly gained importance in the field of metallurgy^{12,13}. Specifically, as it is a rapid and elemental analysis technique, its use in metallurgy and metal pretreatment plants quickly gained great importance, being on the fields in which XRF has greater applicability today. In addition, the XRF analysis methods allows the study of other types of matrixes with different objectives in the Cultural Heritage field, such as the classification of the metallic objects¹⁴, identification of pigments in paintings¹⁵ and analysis of glass and pottery¹⁶.

As mentioned above, another commonly used technique for Cultural Heritage analysis is SEM-EDS³. It is an analytical technique to define the elemental composition at microscopic resolution. In this case, the excitation source is a beam of electrons which interact with the sample. With the response that the sample emits due to the incoming excitation, on the one hand a SEM image is collected. This high-resolution electronic image allows to observe the appearance of the studied sample like size and shapes of the crystals or the structure of the sample surface at the micrometric scale. On the other hand, that excitation also promotes the emission of energy from it. This energy is characteristic of its elemental composition since each element emits

a characteristic amount of energy. In this way, the elemental characterization of the sample is performed. Moreover, semi-quantitative analysis of the identified elements can be also performed. A limitation of the technique is the unavailability to detect light elements, Cl, C, O, N, etc., elements that are important in samples of Cultural Heritage.

Unfortunately, the technique presents also some drawbacks for samples coming from Cultural Heritage. First, the sample must be directly deposited in a vacuum chamber, since the analyses are made under vacuum to prevent the absorption of electrons by atmospheric molecules, allowing to detect all the electrons moving from the sample¹⁷. This chamber can limit the analysis of some samples by size and can lead to fractionation of them. Moreover, to obtain good images of the sample surface, the sample must be conductive. If the sample is conductive, no pre-treatment is necessary. In contrast, in the case of non-conductive samples, a layer of a few micrometers of a conductive element must be deposited on the surface to obtain good images by scanning electron microscopy and an accurate composition determination through EDS¹⁸. Besides, the sample must be translated to the laboratory for the analysis as currently it is not a portable technique.

Therefore, it could be thought that SEM-EDS could be a useless technique comparing to XRF. Nevertheless, it presents some advantages at resolution level as providing information about the composition of the sample at the micrometric scale. Also, the light elements can be detected.

Besides, it provides the opportunity to relate textures to composition, which could be valuable information for a faster future identification

of compounds. Therefore, XRF and SEM-EDS can be considered good collaborative elemental techniques for a complete elemental characterization^{19,20}.

Raman spectroscopy provides molecular information of the studied specimen. In this case, the sample is irradiated with lasers of different wavelength. With the excitation generated by the laser, the molecules start vibrating to go back to a basic energy state. This vibration energy is characteristic of each molecule so when it arrives to the detector the signal that it provides is like a fingerprint for each molecule present in the sample. Therefore, once the so-called fingerprint (the Raman spectra) of the compound is collected it is compared with a spectra database to find a match. In this way, the studied sample is molecularly characterized. Moreover, Raman spectroscopy also provides structural information as polymorphs of the same compound have different Raman responses, as well as the same compound with different number of crystalline waters. Another important advantage of this technique is the sensitivity to detect amorphous compounds, compounds that are mostly present in the patinas of the Cultural Heritage artefacts or assets.

Raman spectroscopy is a completely non-destructive technique. Besides being cheap and fast, the number of analyses that can be performed in situ or in the laboratory samples is high enough to guarantee representativity of the detected compounds in a short time. As a disadvantage of this technique the most common one is the fluorescence produced by the sample which can affect the quality of the obtained spectra. Other common disadvantage of this technique is the low sensitivity and the long acquisition times that need to make imaging by point scanning or mapping²¹. In addition, the laser power

must be controlled so as not to burn the sample and standard reference will be necessary to compare the results obtained.

This technique has been used in a great variety of studies on different type of materials, especially in cases where the identification on the degradation products is necessary, as is the case of the diagnosis of the conservation state of weathering steel structures^{22,23}, the microbiologically influenced corrosion in archaeological artifacts²⁴, the study of submerged materials²⁵, the studies of ancient pottery²⁶, characterize biological materials²⁷ and the investigation of objects in art and archaeology²⁸.

Finally, X-ray diffraction (XRD) is considered one of the most powerful and commonly used characterization techniques for the structural analysis of crystals²⁹. Its main characteristics are the consequence of being an electromagnetic probe of matter with a wavelength ($\lambda - 1.5 \text{ \AA}$) of a magnitude very similar to the interplanar spacing of solids. Since photons are particles of zero rest mass and free of charge, they interact with a matter in in a way that does not affect its physical state. In addition to this advantage, this technique was widely used in the qualitative identification of different samples and also in the quantitative estimation of mineral components³⁰. The analyses realized with XRD can be obtained quickly and reliably¹⁸.

The disadvantage of this technique is that the sample must be pulverized and homogenized prior to the analysis. Thus, it is a micro-destructive technique, although, it requires a minimal amount (few milligrams) of the sample. Moreover, amorphous compounds cannot be detected by XRD, an important drawback in the field of Cultural Heritage diagnosis.

Thanks to the advantages in this technique, it has been used to characterize the corrosion products in the rust layer^{31,32}, in the study of pigments³³ and sculptures³⁴, in the study of ceramics and archaeological stone analysis³³.

Considering the pros and cons of the mentioned techniques, in this work, the XRF and Raman techniques were selected as the techniques to characterize the elemental, molecular and structural composition of the samples. However, when it was required and it was possible, these data were supplemented with data obtained by SEM-EDS and XRD techniques.

All these techniques have been used individually or complementarily for the study of different archaeological pieces in this PhD. Moreover, as it was discussed, most of them can be portable. Therefore, in this PhD, multi-analytical methodology is proposed focused on the use of portable techniques with the combination of laboratory measurements for reaching different aims. The instruments and the methods used are described below.

3.1 SPECTROSCOPIC INSTRUMENTS FOR IN-SITU ANALYSIS

3.1.1 Portable Raman Spectroscopy

For the determination of the molecular (and structural) composition of the pieces in-situ, the measurements were performed using two different handheld InnoRam spectrometers (BWTEK_{INC.}, USA). One was provided with 785 and the other with 532 nm excitation lasers, a fixed 1200-line/mm grating and a charge-coupled device (CCD) detector were used in both cases (Figure 1). These systems were equipped with a probe which can be used in two different ways; on the one hand, it can be used handling it by the user. On the other

hand, it can be placed in a microscope with a manual X-Y-Z stage that was connected to a micro-video camera to acquire images focusing on the area of interest in which the spectrum was collected, performing in this way microscopic analysis (see Figure 1). In this work, both modes were employed depending on the size and morphology of the sample. The spectrometers worked in a spectral range from 100 to around 3500 cm^{-1} (depending on the system) with a mean resolution of 4 cm^{-1} . The software used for instrument control and data collection was the BWSpec (B&WTEK_{INC}, Newark, USA).

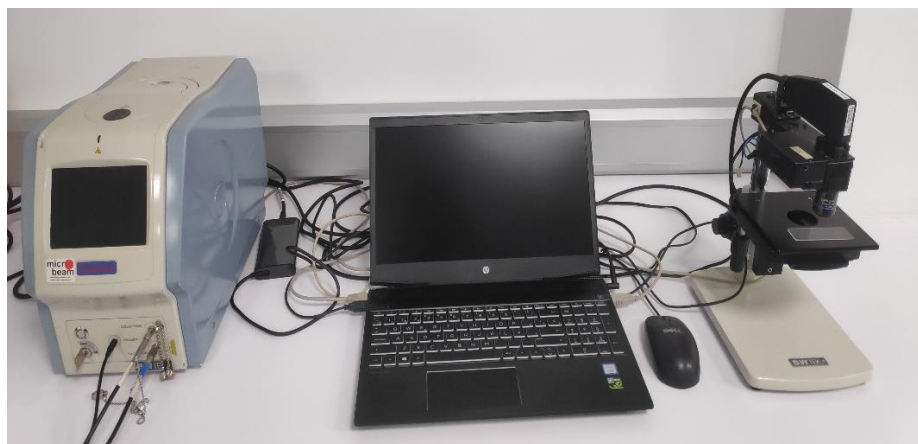


Figure 8 - Raman portable equipment

3.1.2 Handheld Energy Dispersive X-Ray Fluorescence (EDXRF)

In-situ EDXRF measurements were performed using the XMET5100 EDXRF analyzer (Oxford Instruments, UK) (Figure 2). The instrument was used for the determination of the elemental composition of the pieces. It was equipped with a Rhodium X-Ray tube working at a maximum voltage and current of 45 kV and 50 mA respectively, and the size of the emitted X-Ray beam was 9 mm. The analyzer included a Peltier cooled silicon drift detector (SDD) of high resolution that is

able to provide an energetic resolution of 150 eV (FWHM value of the Mn $K\alpha$ line). The equipment contains a PDA to control de spectrometer parameters and to save all the obtained data. All the information obtained was transferred from the PDA to a computer to be transformed later into binary .txt files, where the x-axis shows Energy in keV and the y-axis shows Intensity in counts. This equipment can provide semi-quantitative information as it contains different methods based on Fundamental Parameters (FP). The semi-quantitative values are presented only as approximate value to justify which element is in greater proportion (majority element) or less proportion (minor element) in the samples under study. All the results obtained were analyzed using ezData (ChemiLab, USA) software.



Figure 9 - Handheld XRF equipment fully operational

3.2 SPECTROSCOPIC INSTRUMENTS FOR LABORATORY ANALYSIS

When in situ analyses required to be completed or when sample sizes allowed transporting them to the laboratory, benchtop equipment were also employed. Laboratory devices normally provide a better accuracy, higher sensitivity, and imagery options. Therefore, when

possible or when in situ analyses were not conclusive, artifacts or micro-samples were taken to the laboratory for further analyses.

Mentioned samples were taken by the traditional sampling mode. Using a scalpel and a brush, micro samples were taken and preserved in zip bags, previously identified, and properly labeled. The amount of sample collected was appropriate to ensure the representativeness of each study and to ensure that the planned analyses were carried out without damaging the sampled object.

This step was of great importance to ensure that the sampling did not alter the appearance or the state of the pieces which is a must when working with Cultural Heritage elements.

3.2.1 Laboratory Raman Spectroscopy

At the laboratory, Raman analyses were carried out with two different instruments. On the one hand, an InVia Renishaw Raman micro spectrometer was used (Figure 3), coupled to a DMLM Leica microscope with 5x, 20x and 50x magnification objectives and equipped with a 532 and 785 nm excitation lasers. The grating of the 532 nm laser is 1800 l/mm and the grating of the 785 nm laser is 1200 l/mm. It is provided with a CCD detector (Peltier cooled). The mean spectral resolution is around 1 cm^{-1} and the spectra were obtained in a range of 100-3200 cm^{-1} .

All the point-by-point measurements done with this equipment were taken with the following acquisition parameters: an exposure time between 2-10 seconds and between 3-100 accumulations. Whenever it was needed, in order to improve the quality of the spectrum, the measurements were set up modifying these parameters within the commented range. The data collection software was the Wire 4.2.



Figure 10 - Renishaw InVia equipment

On the other hand, a LabRam HR800 (Horiba Jobin Yvon company) spectrometer was employed at the MONARIS lab (Paris, France). This equipment is characterized by a focal length of 800 mm, equipped by a Peltier cooled CCD detector and coupled to an ionized argon Laser from Coherent. Analyses were performed using the 514.5 nm laser and the Rayleigh filtering was achieved using Ultra Low Frequencies (ULF) BraggGrateNotch Filter. Using a 600 lines/mm grating (allowing the recording in one acquisition of the whole spectral range of our interest) the spectral resolution of the equipment was around 3 cm^{-1} . The measurements were performed with the 50x and 100x objectives of an Olympus microscope BX41 (Tokyo, Japan) coupled to the spectrometer providing analysis diameters of about $3 \mu\text{m}$ and $1 \mu\text{m}$ respectively. LabSpec was the software used for instrument control and data collection.

With both Raman benchtop devices, Raman imaging was also performed to obtain a large set of representative Raman data and to

get information about the spatial distribution of the compounds in the sample.

For the Raman analyses (including in-situ measurements) the laser power was modulated in order to avoid thermo-decomposition and chemical or mineralogical transformations. The power applied was set at the source at a maximum of 50 mW, while on the sample was always less than 20 μ W. To obtain good results, all the spectrometers were daily calibrated, prior to any analysis, with the 520.5 cm^{-1} Raman band with the use of a silicon chip. The interpretation of the acquired results was carried out by the comparison of the obtained Raman spectra with pure standards found in bibliography, in our databases³⁵ and in the RRUFF online database³⁶. A final consideration regarding Raman measurements done indoor is that care must be taken because the artificial light photons can reach the spectrometer detector, whose signal can be confused with the Raman signal from the sample. In consequence, Raman spectroscopic analyses are done in darkness.

3.2.2 Micro-Energy Dispersive X-Ray Fluorescence Spectroscopy (μ -ED-XRF)

For the characterization of the elemental distribution of the samples at millimeter scale and to obtain the elemental composition, the M4 TORNADO (Bruker Nano GmbH, Berlin, Germany) energy dispersive X-Ray Fluorescence spectrometer was used (Figure 4). The instrument is equipped with a micro-focus side window, Rh X-Ray tube powered by a low power HV generator and is cooled by air. The Rhodium X-Ray tube can work at a maximum voltage of 50 kV and at maximum current of 700 μ A that the X-Ray source allows. This instrument was set using polycapillar lenses at a spatial/lateral resolution down to 25 μ m for this work. It incorporates an X-Flash silicon drift detector with

30-mm² sensitive areas and energy resolution lower than 129 eV for Mn K α to detect the fluorescence radiation emitted by the sample. In order to improve the detection of the lightest elements ($Z > 11$), measurements were carried out under vacuum (20 mbar) with the use of a diaphragm pump MV 10 N VARIO-B to perform the analysis of light elements. In addition, the instrument is equipped with two video-microscopes which were used to focus the interested area, one of them used for the exploration of the sample with a low magnification (1 cm² areas) and the other one used for final focusing (1 mm² area)³⁷.

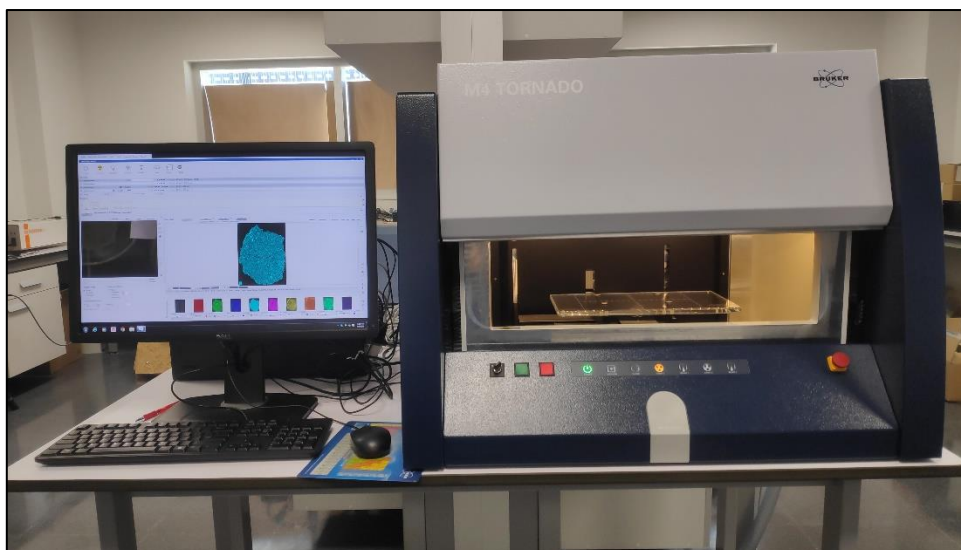


Figure 11 - M4 Tornado micro-EDXRF equipment

Thanks to the motor-driven X-Y-Z positioning stage that this XRF equipment includes, different types of measurements can be carried out. For instance, point measurement, line scans, multi-point and mapping (measurement of an area already marked) can be made. On the one hand, the punctual measurement is an adequate measurement for homogeneous and small samples, giving very fast

analysis. On the other hand, the mappings are very suitable for heterogeneous samples. In this work, the distribution of major, minor and trace elements was evaluated using the mapping option. This mode provides, on the one hand, a sum XRF spectrum of all the points measured in the map, providing information of the elements detected in the whole image. On the other hand, a color image of each element distribution is also provided. There each color is assigned to a specific element and the intensity of said color is given by the concentration of each element. In addition to these results, the equipment can perform a semi-quantitative analysis of the samples based on an estimation of mass balance (%).³⁸ The elemental maps were obtained using 25 μm of lateral resolution and the time of each mapping depended on the area analyzed and the distance between point and point. In order to obtain these maps, the $K\alpha$ line of each element (in most of the cases) was used after a previous elemental assignation and the spectral data acquisition and treatment was performed using the M4 TORNADO software.

3.2.3 Scanning Electron Microscope – Energy Dispersive X-Ray Spectroscopy (SEM-EDS)

To deepen the aforementioned studies, analyses were carried out with the SEM-EDS (Figure 5). An EVO®40 Scanning Electron Microscope (Carl Zeiss NTS GmbH, Germany) coupled to an X-Max Energy dispersive X-Ray spectroscopy system (Oxford Instruments, UK) was used for electron image acquisitions and elemental composition determinations of the sample. SEM images were acquired at high vacuum employing an acceleration voltage of 20 KV. It was reached up to 1000x using a secondary electron detector. The elemental mapping analysis (EDS, on the right of the Figure 5) was performed

using an 8.5 mm working distance, a 35° take-off angle and an acceleration voltage of 20 KV³¹.



Figure 12 - On the left, SEM-EDS system with and EDS detail on the right

3.2.4 X-Ray diffraction (XRD)

These analyses were carried out in the SGIker analytical service of the UPV/EHU. The measurements were performed with a powder diffractometer PANalytical Xpert PRO, equipped with a copper tube ($\lambda\text{CuK}_{\alpha_{\text{media}}} = 1.5418 \text{ \AA}$, $\lambda\text{CuK}_{\alpha_1} = 1.54060 \text{ \AA}$, $\lambda\text{CuK}_{\alpha_2} = 1.54439 \text{ \AA}$), vertical goniometer (Bragg-Brentano geometry), programmable divergence aperture, automatic interchange of samples, secondary monochromator and PixCel detector (Figure 6). The measurement conditions were 40 KV and 40 mA, with an angular range (2θ) scanned between 5 and 80°. For the data treatment of the diffractograms and the identification of the mineral phases, the specific software PANalytical Xpert HighScore in combination with the specific powder diffraction file database (International Centre for Diffraction Data – ICDD, Pennsylvania, USA) was used.



Figure 13 - PANalytical Xpert PRO Powder X-Ray diffractometer

3.3 BIBLIOGRAPHY

The references mentioned in this work are based on the bibliography format described below:

Journals: Estalayo, E. Aramendia, J. Bellot-Gurlet, L. Garcia L. Garcia-Camino, I. Madariaga, J.M. Article title. *Journal abbreviation*, volume, pages (year).

Books: Estalayo, E. Aramendia, J. Bellot-Gurlet, L. Garcia L. Garcia-Camino, I. Madariaga, J.M. *Book title* (year). DOI number.

1. Bitossi, G., Giorgi, R., Mauro, M., Salvadori, B. & Dei, L. Spectroscopic techniques in cultural heritage conservation: A survey. *Applied Spectroscopy Reviews* **40**, 187–228 (2005).
2. Winkler, E. M. *Stone in Architecture*. *Stone in Architecture* (1997). doi:10.1007/978-3-662-10070-7
3. de Castro, M. D. L. & Jurado-López, A. The role of analytical chemists in the research on the cultural heritage. *Talanta* **205**, (2019).
4. Committee, A. M. & No, A. Raman spectroscopy in cultural heritage: Background paper. *Analytical Methods* **7**, 4844–4847 (2015).
5. Bezur, A., Lee, L., Loubser, M. & Trentelman, K. *Handheld XRF in Cultural Heritage. A Practical Workbook for Conservators*. (2020).
6. Kendix, E. L., Prati, S., Mazzeo, R., Joseph, E., Sciutto, G. & Fagnano, C. Far Infrared Spectroscopy in the Field of Cultural Heritage. *e-Preservation Science* **7**, 8–13 (2010).

7. van Hoek, C. J. G., de Roo, M., van der Veer, G. & van der Laan, S. R. A SEM-EDS study of cultural heritage objects with interpretation of constituents and their distribution using PARC data analysis. *Microscopy and Microanalysis* **17**, 656–660 (2011).
8. Tereszchuk, K. A., Vadillo, J. M. & Laserna, J. J. Depth profile analysis of layered samples using glow discharge assisted Laser-induced Breakdown Spectrometry (GD-LIBS). *Spectrochimica Acta - Part B Atomic Spectroscopy* **64**, 378–383 (2009).
9. Jiang, L., Sui, M., Fan, Y., Su, H., Xue, Y. & Zhong, S. Micro-gas column assisted laser induced breakdown spectroscopy (MGC-LIBS): A metal elements detection method for bulk water in-situ analysis. *Spectrochimica Acta - Part B Atomic Spectroscopy* **177**, (2021).
10. Gonzalez, V., Cotte, M., Vanmeert, F., de Nolf, W. & Janssens, K. X-ray Diffraction Mapping for Cultural Heritage Science: a Review of Experimental Configurations and Applications. *Chemistry - A European Journal* **26**, 1703–1719 (2020).
11. János, I., Szathmáry, L., Nádas, E., Béni, A., Dinya, Z. & Máthé, E. Evaluation of elemental status of ancient human bone samples from Northeastern Hungary dated to the 10th century AD by XRF. *Nuclear Instruments and Methods in Physics Research, Section B: Beam Interactions with Materials and Atoms* **269**, 2593–2599 (2011).
12. Al-Eshaikh, M. A. & Kadachi, A. Elemental analysis of steel products using X-ray fluorescence (XRF) technique. *Journal of King Saud University - Engineering Sciences* **23**, 75–79 (2011).
13. Vasilescu, A., Constantinescu, B., Stan, D., Radtke, M., Reinholz, U., Buzanich, G. & Ceccato, D. Studies on ancient silver metallurgy using

- SR XRF and micro-PIXE. *Radiation Physics and Chemistry* **117**, 26–34 (2015).
14. Cruz, J., Manso, M., Corregidor, V., Silva, R. J. C., Figueiredo, E., Carvalho, M. L. & Alves, L. C. Surface analysis of corroded XV–XVI century copper coins by μ -XRF and μ -PIXE/ μ -EBS self-consistent analysis. *Materials Characterization* **161**, (2020).
 15. Castro, K., Knuutinen, U., Vallejuelo, S. F. O. de, Irazola, M. & Madariaga, J. M. Finnish wallpaper pigments in the 18th-19th century: Presence of $\text{KFe}_3(\text{CrO}_4)_2(\text{OH})_6$ and odd pigment mixtures. *Spectrochimica Acta - Part A: Molecular and Biomolecular Spectroscopy* **106**, 104–109 (2013).
 16. Turco, F., Davit, P., Cossio, R., Agostino, A. & Operti, L. Accuracy improvement by means of porosity assessment and standards optimization in SEM-EDS and XRF elemental analyses on archaeological and historical pottery and porcelain. *Journal of Archaeological Science* **12**, 54–65 (2017).
 17. Bello, J. F. A. PhD Thesis: Nuevo micro-análisis cuantitativo de metales empleando microscopía electrónica de barrido con dispersión de energías de rayos X. *Universidad Complutense de Madrid* (1999).
 18. Wolfgang, W. J. *Chemical analysis techniques for failure analysis: Part 1, common instrumental methods. Handbook of Materials Failure Analysis with Case Studies from the Aerospace and Automotive Industries* (Elsevier Ltd., 2016). doi:10.1016/B978-0-12-800950-5.00014-4
 19. Arafat, A., Na'ees, M., Kantarelou, V., Haddad, N., Giakoumaki, A., Argyropoulos, V., Anglos, D. & Karydas, A. G. Combined in situ micro-XRF, LIBS and SEM-EDS analysis of base metal and corrosion

- products for Islamic copper alloyed artefacts from Umm Qais museum, Jordan. *Journal of Cultural Heritage* **14**, 261–269 (2013).
20. Pendleton, M. W., Washburn, D. K., Ellis, E. A. & Pendleton, B. B. Comparing the detection of iron-based pottery pigment on a carbon-coated Sherd by SEM-EDS and by Micro-XRF-SEM. *Yale Journal of Biology and Medicine* **87**, 15–20 (2014).
 21. Eberhardt, K., Stiebing, C., Matthaüs, C., Schmitt, M. & Popp, J. Advantages and limitations of Raman spectroscopy for molecular diagnostics: An update. *Expert Review of Molecular Diagnostics* **15**, 773–787 (2015).
 22. Rémazeilles, C., Lévêque, F., Conforto, E. & Refait, P. Long-term alteration processes of iron fasteners extracted from archaeological shipwrecks aged in biologically active waterlogged media. *Corrosion Science* **181**, (2021).
 23. Aramendia, J., Gomez-Nubla, L., Bellot-Gurlet, L., Castro, K., Paris, C., Colomban, P. & Madariaga, J. M. Protective ability index measurement through Raman quantification imaging to diagnose the conservation state of weathering steel structures. *Journal of Raman Spectroscopy* **45**, 1076–1084 (2014).
 24. Rémazeilles, C., Saheb, M., Neff, D., Guilminot, E., Tran, K., Bourdoiseau, J. A., Sabot, R., Jeannin, M., Matthiesen, H., Dillmann, P. & Refait, P. Microbiologically influenced corrosion of archaeological artefacts: Characterisation of iron(II) sulfides by Raman spectroscopy. *Journal of Raman Spectroscopy* **41**, 1425–1433 (2010).
 25. Kerns, J. G., Buckley, K., Parker, A. W., Birch, H. L., Matousek, P., Hildred, A. & Goodship, A. E. The use of laser spectroscopy to

- investigate bone disease in King Henry VIII's sailors. *Journal of Archaeological Science* **53**, 516–520 (2015).
26. Abdurakhimov, B. A., Kichanov, S. E., Talmaṭchi, C., Kozlenko, D. P., Talmaṭchi, G., Belozerova, N. M., Bălăṣoiu, M. & Belc, M. C. Studies of ancient pottery fragments from Dobrudja region of Romania using neutron diffraction, tomography and Raman spectroscopy. *Journal of Archaeological Science* **35**, (2021).
 27. Butler, H. J., Ashton, L., Bird, B., Cinque, G., Curtis, K., Dorney, J., Esmonde-White, K., Fullwood, N. J., Gardner, B., Martin-Hirsch, P. L., Walsh, M. J., McAinsh, M. R., Stone, N. & Martin, F. L. Using Raman spectroscopy to characterize biological materials. *Nature Protocols* **11**, 664–687 (2016).
 28. Vandenaabeele, P. Raman spectroscopy in art and archaeology. *Journal of Raman Spectroscopy* **35**, 607–609 (2004).
 29. Rajiv, K. & Mittal, K. L. in *Developments in Surface Contamination and Cleaning* **12**, 23–105 (2019).
 30. Engler, P. & Iyengar, S. S. Analysis of mineral samples using combined instrument (XRD, TGA, ICP) procedures for phase quantification. *American Mineralogist* **72**, 832–838 (1987).
 31. Gutierrez, J. A. PhD Thesis: Analytical diagnosis of the conservation state of weathering steel exposed to urban atmospheres. *Universidad del Pais Vasco (UPV/EHU)* (2013).
 32. Kamimura, T., Nasu, S., Tazaki, T., Kuzushita, K. & Morimoto, S. Mössbauer spectroscopic study of rust formed on a weathering steel and a mild steel exposed for a long term in an industrial environment. *Materials Transactions* **43**, 694–703 (2002).

33. Castro, K. PhD Thesis: Pigment characterisation on paper-based artworks by vibrational spectroscopic techniques. *Universidad del País Vasco (UPV/EHU)* (2004).
34. Franquelo, M. L., Duran, A., Castaing, J., Arquillo, D. & Perez-Rodriguez, J. L. XRF, μ -XRD and μ -spectroscopic techniques for revealing the composition and structure of paint layers on polychrome sculptures after multiple restorations. *Talanta* **89**, 462–469 (2012).
35. Castro, K., Pérez-Alonso, M., Rodríguez-Laso, M. D., Fernández, L. A. & Madariaga, J. M. On-line FT-Raman and dispersive Raman spectra database of artists' materials (e-VISART database). *Analytical and Bioanalytical Chemistry* **382**, 248–258 (2005).
36. Lafuente, B., Downs, R. T., Yang, H. & Stone, N. in *Highlights in Mineralogical Crystallography* 1–30 (2016). doi:10.1515/9783110417104-003
37. Morillas, H., Maguregui, M., Huallparimachi, G., Marcaida, I., García-Florentino, C., Lumbreras, L., Astete, F. & Madariaga, J. M. Multianalytical approach to evaluate deterioration products on cement used as consolidant on lithic material: The case of Tello Obelisk, Lima (Peru). *Microchemical Journal* **139**, 42–49 (2018).
38. Aramendia, J., Gomez-Nubla, L., Castro, K., Fdez-Ortiz de Vallejuelo, S., Arana, G., Maguregui, M., Baonza, V. G., Medina, J., Rull, F. & Madariaga, J. M. Overview of the techniques used for the study of non-terrestrial bodies: Proposition of novel non-destructive methodology. *Trends in Analytical Chemistry* **98**, 36–46 (2018).

CHAPTER 4

The background of the page is a repeating pattern of white circles. Each circle contains a different abstract, colorful design. Some circles have dark backgrounds with bright, multi-colored speckles (purple, blue, green, yellow). Others have solid dark backgrounds with lighter, multi-colored shapes. The overall effect is a vibrant, textured background.

4. SAMPLES AND EMPLACEMENTS

“No great discovery was ever made without a bold guess” – “Ningún gran descubrimiento se hizo nunca sin una conjetura audaz” – Isaac Newton

In this study, artifacts of different origin, type and composition have been analyzed. For clarity, in this chapter they will be classified based on their origin: objects buried in marine environment (wet or waterlogged conditions) and pieces buried in soil environment (damp conditions). The following is a more detailed characterization of the mentioned samples.

4.1 SAMPLES BURIED IN MARINE OR ESTUARINE SEDIMENTS

Regarding marine environment artifacts, we have focused on those linked to two shipwrecks, Urbietta and Bakio. The different materials found on the shipwreck are, nowadays in different state of conservation.

4.1.1 Urbietta shipwreck

4.1.1.1 Historical context

The Gernika estuary (Basque Country, Northern Spain) was one of the oldest and most important penetration river routes on the Basque coast. Although its mouth has been historically hampered by fluctuating sand bars, the Izaola island and the estuary protected by

Cabo Matxitxako have always been a nautical attraction for penetrating the inner lands as its depth has made it navigable up to the town of Gernika. The most important records of the ancient navigation through this estuary were identified in the settlements of the Roman era¹.

In 1998, some channeling works on the Oka River began near the village of Gernika concretely, in the places called “Urbieta” and “Portuzarra” which meaning in Basque language are “places with two canals” and “old port”, respectively. In July same year, at 4 meters deep, at the confluence of the Golako stream (Urdaibai estuary), the backhoe that was building a breakwater partially discovered a shipwreck of the second half of the 15th century that became the only medieval ship existing to date in the Basque Country. This received the name of the location: Urbieta (Figure 1)¹.



Figure 14 - The discovery of the Urbieta shipwreck

Since the area was not subjected to any preventive archaeological protection, no archaeological action was considered in the projected works. Furthermore, the archaeological impact created by the channeling works lead to almost the total destruction of the shipwreck. Therefore, an archaeologist who worked in the region, alerted the city council about the dangerous situation of the shipwreck. Thanks to this, the city council proceeded to an archaeological control of the works. By this means, a global procedure for the excavation, research and recovery was planned in order to promote the conservation of the shipwreck¹.

The shipwreck was resting on the bank of the river with a gentle slope that pointed towards the current course of the water. It was surrounded by a sequence of layers of eroded gravel and of iron ore alternated with other layers of sand and mud that covered the shipwreck. The presence of iron ore promoted the theory that the vessel could be engaged in an important activity of transferring or transporting this mineral in area¹.

After the excavation, it was observed that even though the vessel was stranded, it kept all its strakes from the keel to the rail. The central part of the shipwreck and a third of its length was destroyed by the backhoe that discovered it. The most solid pieces could be recovered but most of the construction details were lost, such as the cockpit and the mas seating system¹.

The extraction of the shipwreck was a process of a great difficulty² due to the large number and excellent consistency of the nails that secured the hull of the shipwreck. Cutting mentioned nails involved excessive archaeological aggression. Therefore, it was decided to extract the shipwreck by block despite its difficulty, the high operation

cost, its subsequent consolidation, and the final restitution of forms¹. In this way, the contour of the shipwreck was excavated to a depth of 1.6 meters, then a sequence of tubes was placed which form a horizontal cut-off plane. In addition, due to the inconsistency of the field, a perimeter belt of the block (60 cm) was built, made with simple boards and metallic structure. This base was reinforced with metallic structure, and it served to create the base on which the ship rested. Finally, a high-powered crane extracted it to a temporary warehouse near the extraction area.

Once the shipwreck was extracted, the foreign matter (sludge, sands and consolidation structures) was removed from the shipwreck. Then, the shipwreck was introduced in a metal cage and the assembly was placed in a barrel subjected to a conservation treatment based on immersion on polyethylene glycol PEG 4000 (at 75% of PEG and at 60 °C) where it remained for two years¹. Once the treatment was finished, the excess of PEG was removed, and the shipwreck was transported to a shipyard for the restitution of the hull. For the total restitution of the original forms, it was necessary to develop hypothetical plans of the boat from the excavation drawing of the remains and laboratory drawings of each of the pieces. All of them served to obtain the templates of the original boat shape¹.

After a visual and bibliographic analysis of the ship, it has been considered that the general morphology of the ship corresponds to a clinker-built architecture. The clinker is a constructive form used until the middle of the XVI century that implies the previous construction of the hull before the structure¹. Regarding the use that was given to the ship, the most accepted theory about the use of this shipwreck is that this ship focused its last years on the transport of iron^{1,3}. This

theory is supported by documents³ that reference the commercial route that the boats made to Gernika and its surroundings. In addition, it is supported by the existence of several ports in the vicinity of Gernika the presence of ironworks in the area⁴ and the presence of iron ore in the site.

Since the wreck was not completely recovered, different type of works were carried out to symbolically complete the rest of the boat and to exhibit it as close as possible to its original appearance. Finally, the ship was delivered to the maritime museum of Bilbao on January 9, 2006, where it was exhibited for two years¹. Nowadays, both the shipwreck and the extracted pieces are conserved and preserved in the Archaeological Museum of Bilbao¹.

The Urbieta shipwreck constitutes a key discovery because it is the only ship of this era and typology located to date in the Cantabric coast. This circumstance allows specialists in the field studying the relationships and evolutionary lines between their constructive form and the different traditions of the architecture of the North Atlantic. Among this group of specialists, it is worth mentioning the Canadian research group of Parks Canada Agency⁵, which is focused on the study of the Basque whaler of the 16th century called, San Juan. According to them, the Urbieta shipwreck constitutes the only testimony of naval architecture of Basque origin prior the aforementioned whaler, which gives it extraordinary value and a cultural dimension not only locally but at international scale¹.

Hereunder, the characteristics of the area surrounding the shipwreck will be described, in order to better understand the geochemical and environmental conditions that surrounded it for a long time.

4.1.1.2 Emplacement

After explaining the historical context, the characteristics of the area where the shipwreck was found will be described below. This area is constituted by the Oka River and its estuary, located in Gernika (Basque Country, Northern Spain)⁶.

Thanks to some studies carried out in the Gernika area, it has been possible to provide a general overview of the environmental conditions in this area. The Oka River has a drainage area of 149 km² and covers a distance of 25 km with an average depth of 3.5 meters⁷. Due to the special ecological conditions of this area, in 1984 it was declared as National Biosphere Reserve (UNESCO). The Gernika area is a rural site and industrial activity⁸ is concentrated in the town of Gernika, in the upper area of the river. There, most of companies are dedicated to metal work and this fact constitutes a potential source of contamination by the dumping of heavy metals to the river. In fact, Irabien et al⁹, demonstrated that the concentration of various metals such as Zn, Pb, Cu, Cr and Ni have high values in the lower area of the river as a result of a moderate anthropogenic influence coming from upstream. Both the river and the surrounding area are mainly composed of sedimentary rocks from the Cretaceous and to a lesser extend basaltic rocks⁶. It should be said that the shipwreck is located in the upper area of the river.

Most of the estuary area is dominated by seawater at high tide, causing high salinity in the outer half (pH 8¹⁰). On the contrary, in the headwater area, freshwater contributions are received from the Oka River. In addition, the upper reaches of the estuary present large

amounts of nutrients and organic matter due to an old primary wastewater treatment plant¹¹.

4.1.1.3 Description of the analyzed samples

For this work, four selected iron nails extracted from Urbieta shipwreck were studied (Figure 2). The aim of these analysis was, on the one hand, to provide archaeologists with more information about the original composition, raw material and production of the metallic pieces. On the other hand, it was also an aim to understand how the different conservation procedures affected the state of the pieces. The samples were covered by a compact rust layer with sediment remains on the surface.

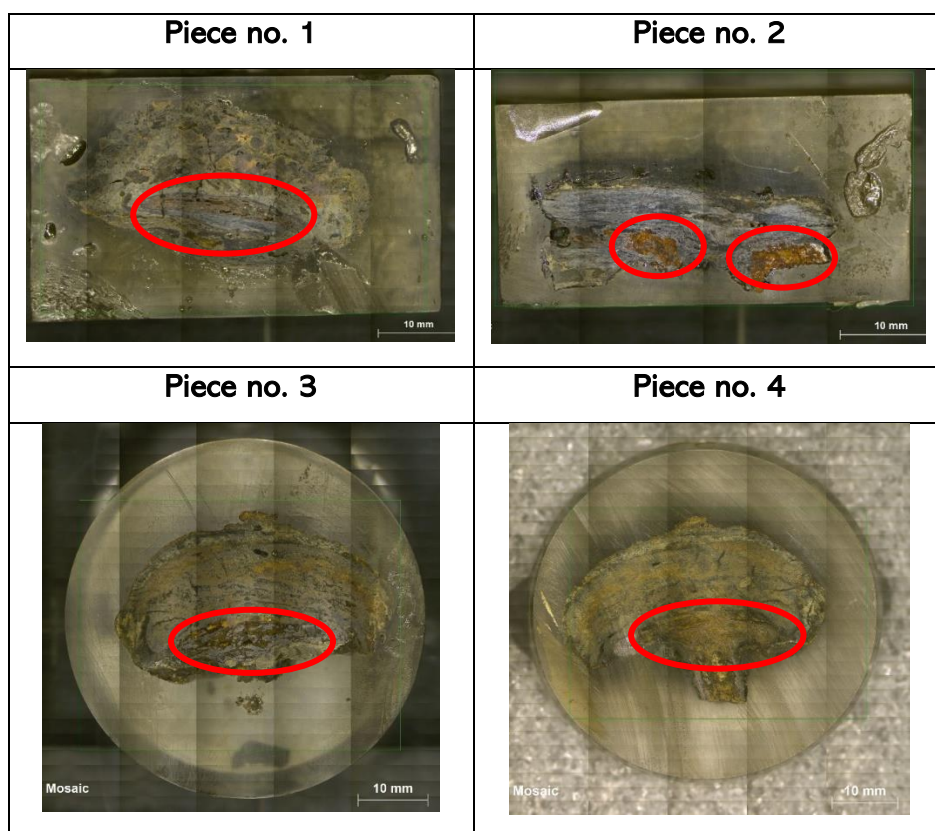


Figure 15 - Four analyzed iron nails from Urbieta shipwreck

In Figure 2, the core of the samples is marked with a red ellipse. It must be said that the samples 1, 3, and 4 lost already any metallic core, and only sample 2 conserved a small metallic core. At first glance, in Figure 3, it can be distinguished two areas, the inner part of the samples no. 2 and the no. 3 and the external part of them.



Figure 16 – The inner part of two iron nails. On the left, iron nail no. 2. On the right, iron nail no. 3.

4.1.1.4 Conservation state and restauration treatments

As an experiment to define the most adequate conservation treatment, four samples were subjected to different restoration and conservation treatments. The selected 4 nails were extracted in 2008 at the Archaeological Museum of Bilbao. It should be mentioned that after a preliminary examination, the museum specialists confirmed that within the 4 analyzed pieces, piece 2, probably underwent a mechanical cleaning treatment (removal of corrosion layers) before arriving at the museum, between 1998-2000. Unfortunately, this was not documented. There is also no documentation about possible previous chemical stabilization treatment in any of the four selected pieces. However, these pieces were then correctly treated in the Archaeology Museum of Bilbao. First, the four of them underwent a desalination process immersing them in a series of baths in tap water. After this, sample labeled as number on did not receive any treatment,

sample 2 was treated with tannic acid, sample 3 was immersed together with the surrounding wood pieces in polyethyleneglycol (PEG) and sample 4 was separated from the wood and treated also with PEG. After that, cross sections of the four selected pieces were prepared in epoxy resin, as can be observed in the previous Figure 2.

4.1.2 Bakio shipwreck

4.1.2.1 Historical context

In 1984, a rescue group discovered some cannons at the bottom of the cove of Areaga, Bakio's beach¹² (Basque Country, Northern Spain) (Figure 4) at a depth of about 6 meters (depending on the tide)¹³ and at around 150 meters from the coast. This finding was reported to the Archaeological Museum and later to the Provincial Council of Bizkaia. Since then, the find has been known as the Bakio shipwreck¹².



Figure 17 - On the left, Bakio's beach at low tide. On the right, the approximate location of the shipwreck

In 1999, a group of residents of Bakio began to sack various materials from the shipwreck. The list of the extracted pieces is the following one: an iron anchor, a swivel gun, 84-pounder guns, a lead ingot, 54-pounder rounds shots, a hook shaped iron item, three bar

shots of two different models, two hammock cranes, two lead sheeting, two flintlock muskets of two different models with bullets, five handspikes, a candlestick, and a cork¹².

In 2004, the archaeologist Jose Manuel Matés Luque and his team carried out the cataloging of the extracted materials and the underwater prospecting of the extraction area. The objective of this study was to characterize the extracted material, as well as the material that may still remain in-situ and to determine the nature and situation of the archaeological site. The archaeological pieces for study were a total of 33¹².

Thanks to the archaeological investigations carried out on the pieces that present some type of inscription, the vessel was dated between the middle of the 18th to the middle of the 19th century. The hypothesis put forward by archaeologists is that it was a British military ship, considering the presence of cannons, bullets, crowbars, and others with a length of between 20 and 30 meters¹². Besides, there are other hypothesis suggesting¹² that it was a merchant vessel where cannons were also present. The presence of the cannon in this case fulfilled other purposes such as, for instance, ballast. Finally, according to the research carried out by Mr. Sabin de Uriarte¹², it was suggested that Bakio shipwreck was an English sloop that sought refuge on Bakio's beach and sank around the 1850s. Unfortunately, no document has been found that confirms or reject mentioned hypothesis¹².

In addition, for the cataloging and characterization of the pieces, a study of the movement of the sea was carried out to understand the impact of the waves on the shipwreck. Thanks to this, the constant activity of the seabed was verified, even when the sea was calm. This

seabed activity can have two different consequences on the conservation of the shipwreck. On the one hand, it will cover it by sand creating a kind of natural shelter for the structure. On the other hand, the same sand that protects the shipwreck can act as an eroding agent if the shipwreck is close to the surface or even if at some point is exposed, being at the mercy of physical-chemical and mechanical actions that alter them¹².

In 2005, between the end of May and the beginning of June, a team of two divers together with a boat and its crew, carried out a non-invasive survey in 40x30 meters area using an underwater metal detector. Thanks to this study, it was possible to estimate the number of metallic pieces that were submerged in the shipwreck¹⁴. Despite the results obtained, the study was not conclusive since non-metallic pieces, such as glass, ceramic or wood, cannot not be detected with the employed device. These materials could still be buried in the prospecting area and the metal detector cannot identify them¹⁵.

In 2012, another control dive was carried out on the shipwreck to observe if any material, remains of the vessel or equipment could be visible. This attempt was unsuccessful because the site was still covered by a thick layer of sand (Figure 5). The fact that the shipwreck has been covered for years does not mean that it will always remain covered. The sea is a very dynamic ecosystem, and it is not possible to know when the movements of the bottom sand can expose the shipwreck. For this, it is necessary to continue carrying out explorations and control dives¹⁶.



Figure 18 - Sand layer observed in the shipwreck in the 2012 immersion

In order to better understand the importance of the sea and its effects on the Bakio's shipwreck, the characteristics of the beach and the sea in this area will be described below.

4.1.2.2 Emplacement

Bakio's beach is 356 meters long, has a low tide area of 75.497 m² and a high tide area of 34.137 m². This beach is partially protected from the sea and the prevailing winds by the dam in the bay of Plentzia¹⁷.

The littoral dynamics in Bakio's bathing waters is fundamentally coastal. This beach is oriented to the open sea and is frequently subjected to strong waves, predominantly northwesterly winds. The dispersion in these waters will be mainly due to the action of the waves and the currents are due to the wind and tides. Regarding to wave conditions, Bakio's beach has a strong swell. In fact, according to the average estimate of the annual energy flow average estimate on the Basque coast, this beach can be classified as having a high average degree of exposure to waves. Due to the fact that it is an

open beach, it has been considered that the water renewal time is equal to or less than 7 days¹⁷.

This beach has a main source of contamination which is the discharge from the EDAR (Industrial Water Treatment). However, in the last three years the annual qualification of the bathing waters of this beach has been adequate and it is considered that currently it does not present a risk of contamination in the short term¹⁷.

4.1.2.3 Description of the analyzed samples

Even if a big effort was put on trying to recover more materials from the shipwreck, only 33 are nowadays catalogued. From these 33, we have access to few ones for this study. On the one hand, a bullet and an iron concretion which covered the bullet (Figure 6.1 and 6.2), and a musket and a metallic fallen part of the musket (Figure 6.3 and 6.4) which are currently stored in the Archaeological Museum of Bilbao were analyzed.



Figure 19 – Four analyzed pieces from Bakio's shipwreck in Archaeological Museum of Bilbao

The bullet was composed probably by lead as a main element, with an iron concretion surrounding it. The musket was composed mainly by iron and wood and the decorations were composed mainly by

copper, according to visual analysis. The detached part was mainly composed by iron according to visual analysis

On the other hand, a swivel gun, seven eight-pounder guns and an iron anchor were also analyzed. The swivel gun and the iron anchor are exhibited in the Bakio's Town Hall (Figure 7). The eight-pounder guns are in a warehouse managed by the city of Bakio (Figure 8) and stored on top of each other in a poor state of preservation.

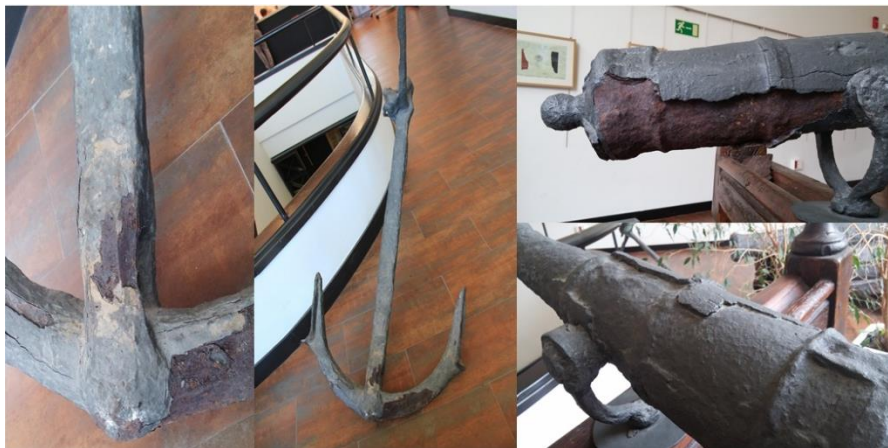


Figure 20 - On the left, two images of the iron anchor. On the right, two images of the swivel gun



Figure 21 – Seven eight-pounder guns analyzed

Some detached pieces from the anchor and the swivel-gun were also considered for this work. Considering the size of the artifacts they could not be transported to the laboratory. In this way, these small flakes provided the possibility to perform further analysis of the surfaces in the laboratory. In the case of the iron anchor, four detached pieces were collected and are shown in Figure 9.

Figure 10 shows the six pieces detached from the swivel gun's surface and collected for analysis. The outer face was that, exposed to the council atmosphere, and the second one is the inner face that was in contact with the bulk of the anchor. As it can be observed in Figures 9 and 10, the outer face of all the pieces has a grey color, due to the treatment applied to the artifacts and the inner face has a red color. Information about the treatments applied to the pieces will be expanded in the following section.









| | OUTER FACE | INNER FACE |
|-------------|---|--|
| Piece no. 1 |  |  |
| Piece no. 2 |  |  |
| Piece no. 3 |  |  |
| Piece no. 4 |  |  |

Figure 22 - Four detached samples from the iron anchor













| | OUTER FACE | INNER FACE |
|-------------|---|--|
| Piece no. 1 |  |  |
| Piece no. 2 |  |  |
| Piece no. 3 |  |  |
| Piece no. 4 |  |  |
| Piece no. 5 |  |  |
| Piece no. 6 |  |  |

Figure 23 - Six detached samples from the swivel gun

Apart from these pieces mentioned, a dust sample was taken from the inner of one of the eight-pounder guns, and a dust sample from the inner and the external of a piece of a swivel gun and a sample from the inner and external part of the anchor.

4.1.2.4 Conservation state and restauration treatments

As in the previous section, the treatments that these samples of different groups underwent will be described. All the information that is given in this section was provided by the curator of the Archaeological Museum of Bilbao, who treated the pieces of this shipwreck storage in the Museum, and the archaeologist Jose Manuel Matés Luque who was the PI in the research of this shipwreck. Unfortunately, prior to cataloguing of the samples, some non-referenced treatments were applied to the samples.

The samples were subjected to different restauration procedures along the time. This is why they are presentig different conservation states. In the case of the group of samples stored at the Archaeological Museum of Bilbao, the bullet and the musket, were treated by the museum curator. In 2012, when these samples arrived to the museum, the curator treated them following different methodologies, depending on the type of material to stabilize degradation processes and maintain an adequate state of conservation.

First and foremost, a visual examination of the pieces was performed to confirm the treatments that they underwent previously. In this way it was seen that the pieces suffered an intervention focused on the removal of the concretions created in the seabed. Regarding the musket, these concretions covered the original surface causing the exposure of the wood core. They seemed to be removed in order to

appreciate the original appearance of the object. Moreover, during these non-documented interventions some previously detached parts were added using a material similar to a bluetack (only in the musket). Finally, it is thought that the musket wood suffered a possible application of a varnish on its surface¹⁸.

After first preliminary examination, the next step was to visually analyze the state of conservation of the musket and the result was that the piece was very deteriorated and in a precarious state of conservation. The original wood was dehydrated, splintered and fragmented after the uncontrolled cleaning carried out before (Figure 11). Moreover, it was noticed that there was not a barrel. The metallic iron parts shown a very advanced corrosion state. In contrast, the copper parts shown a lower degree of corrosion. The bullet was well preserved as the iron concretion created around protected it.



Figure 24 – Details of the musket where the state of conservation can be appreciated

After this extensive study, the curator of the museum proceeded in 2013 and 2016 with the following treatments: First, the removal of non-original additives was done manually. Then, the softening of the corrosion on metallic parts (iron details in the musket and bullet) was

done with EDTA (Ethylenediaminetetraacetic Acid) for cleaning and removing the most resistant areas without damaging corrosion patina. The consolidation of the wood was done by the injection and impregnation of Paraloid B72. The stabilization of the iron metallic patina (in the musket) was done using tannic acid. After that, the trigger and formal musket decorations were added using Acril 33 at 75% mixed with sawdust. After total removal of surface chlorides by mechanic cleaning, samples were submerged into an alcohol bath for 2 hours. Then, the application of tannic acid with a brush and the application of Paraloid B72 was performed on the metal of the plate to protect it. Finally, the adherence of the fragmented pieces was performed by means of Paraloid B72 and then, samples were preserved with non-dry silica gel¹⁸.

In the case of the rest of the samples (iron anchor, eight-pounder gun and a swivel gun) Bakio's council sent them in 2005 to a company that performed the following external treatment: blast mechanical cleaning grade Sa2 ½ of ISO 8501-1: 1988¹⁹. This ISO was based in the preparation of the steel materials before the application of paints and related products. The mechanical cleaning grade means a very thorough blast-cleaning. The rust and the foreign matter shall be removed and finally the surface is cleaned with a vacuum cleaner, with a clean brush or with clean and dry compressed air. Finished the surface treatment according to ISO standard, the application of a zinc phosphate polyamide epoxy primer coat (with an average dry film thickness of 50 µm), application of two coats of thick coat epoxy paint (with an average dry film thickness per coat of 75µm) for a better preservation of the pieces was performed. Unfortunately, and despite these chemical treatments, most of the extracted pieces are in a very poor conservation state. In contrast to museum pieces which are

conserved under controlled conditions, these samples are not. As mentioned before, the anchor and the swivel-gun are exposed in the town's city hall. In the case of eight-pounder guns, they are conserved in a warehouse property of the town hall. They are located on the damp floor on the warehouse, along with some flowerpots, bags of soil, shovels and several large, opened bags of salt, throwing salt in some of the cannon.

As mentioned before, the poor condition in which these samples are conserved caused a high degradation level in all the pieces and an extensive alteration on the surfaces. All this is causing the detachment of parts of the artifacts surfaces.

4.2 SAMPLES BURIED IN SOIL

As mentioned above, in addition to samples in marine sediments, samples subjected to rather different chemical/physical conditions have been analyzed. Concretely, we have focused on three types of pieces of different composition and origin such as glass beads, tools, and archaeological slags buried in different kind of soils.

4.2.1 Glass beads of Vaccaei culture

4.2.1.1 Historical context

The archaeological world is an example that something small and insignificant can be something of great historical relevance or importance. Something as small as glass in the form of beads were of great prestige during Iberian protohistory. In fact, they can provide information on possible relationships between Iberian Peninsula and other Mediterranean cultures since, at that time, these were precious imported pieces to the Iberian Peninsula²⁰ from the rest of the Mediterranean regions.

The city of Pintia (Padilla del Duero, Valladolid, Northern Spain) is of great archaeological interest site. It is the most important one in the inner of the Iberian Peninsula in terms of glass beads due to the great collection of them that have been collected, about more than 1000 by 2018. This extensive collection of pieces has allowed to shed light on the Vaccaei people whose origin is attributed to the local substrate of the “Soto the Medinilla” culture²⁰.

The city of Pintia has an associated necropolis that is known as “Las Ruedas” (Figure 12) and it is the only crematorium cemetery that has been excavated and studied from the Vaccaei culture. This necropolis,

about six hectares size, is located about three hundred meters south of Las Quintanas (the nearby ancient city)²¹.



Figure 25 – The necrópolis “Las Ruedas” in the city of Pintia

Thanks to the studies carried out since 1979 on more than 300 excavated tombs, it has been possible to gain knowledge about funeral rituals in this society. In this way, it has been known that from the 4th to the 1st centuries BC, their main funerary rite was focused on the cremation of the corpse, which was accompanied with elements characteristic of its social condition, age or gender. During the excavations carried out between 2000 and 2017, new pieces were found, increasing the amount of discovered glass beads in Las Ruedas necropolis²⁰.

These last excavations suggested as well that the activity of this cemetery was continued for more than half a millennium, between the end of the 5th century BC and the beginning of the 2nd AD. Besides, by the research of a nearby crematorium it was discovered that the belongings together with the remains of the corps were collected in

an urn and transferred to the cemetery. There, a large accumulation of ashy sediments was found that confirms the close relationship of this site with the cremation activity of the necropolis over twenty or thirty generations²¹.

Nowadays, there are few studies in relation to this type of pieces^{20,22} in the Iberian Peninsula. Important information has been extracted for this research works but there is still much work to carry out. In fact, this is the reason why complete characterization of these pieces is necessary, from their structure and morphology to their elemental and molecular composition. In this way, valuable information about this unknown civilization will be available.

4.2.1.2 Emplacement

This Vacceo settlement was located in a complex landscape where sandy environment, limestones plateaus and other type of different environments coexists. This was a strategic site because of the protection offered by different landforms being the most characteristic feature the sedimentary plains in the inner of the Duero Basin²³.

The sediments that fill the basin are sandy, mostly siliceous, but other tertiary marls and limestone can also be found. The climate in this area is continental-mediterranean type, with very hard winters and approximately three months of summer drought. The annual mean temperature and rainfall are 11.9°C and 420 mm, respectively²³.

The forests in this area were subjected to intensive and traditional logging since the mid-19th century. The human activity that took place during the last millennia (mainly the cultivation of cereals and vineyards) left scattered remains of the original forests in the vicinity

of the archeological site. In sites with more humid soils, a small representation of deciduous forest is detected²³.

4.2.1.3 Description of the analyzed samples

This work was focused on the study of 14 objects (Figure 13) which came from Pintia site. Concretely, they came from the necropolis of “Las Ruedas” and were recovered in the 2000 and 2017 campaigns. It is considered that they correspond to a period between the IV and I centuries BC and where selected as representative sample of the most common shapes, colors, and degradation states within the complete collection of recovered glass beads. It should be mentioned that blue samples predominate over the colors and that samples with thermal alterations have not been included in order to carry out a precise study on the original composition, structure and possible degradation processes^{20,22}.

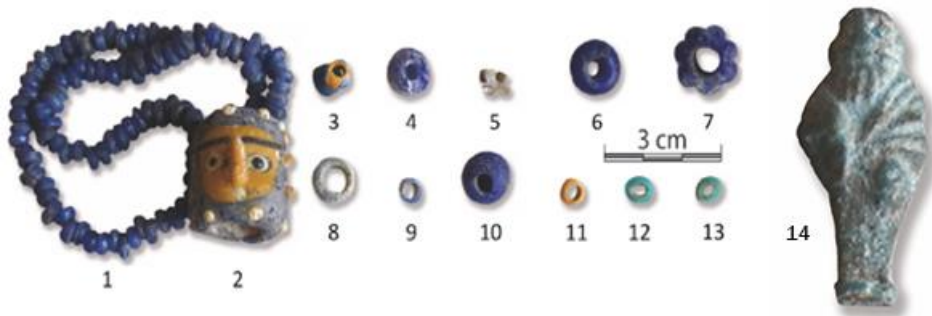


Figure 26 – Studied Vaccaei glass beads on the left, and a togado's figure on the right

Hereunder, a brief description of the studied pieces was made. Regarding item number 1, it is a necklace of blue beads that presents a homogeneous color. Piece number 2 is the most unique piece of

the entire series. This polychrome piece represents two different human faces in opposite arrangement as shown in Figure 14.

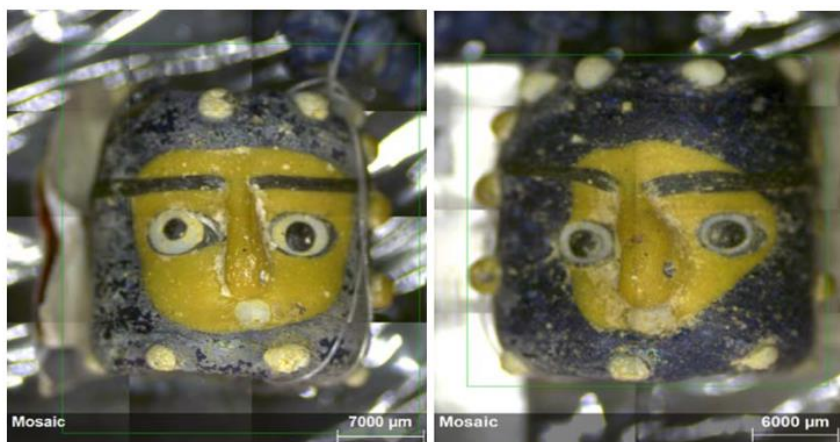


Figure 27 – Piece no. 2. On the left, face A. On the right, face B

The rest of the pieces are necklace beads of different shapes, colors, sizes and states of conservation that were manufactured from vitreous pastes. About piece number 3, it is a piece where yellow, blue and white colors predominate. Piece number 4 is a blue sample with white streaks. In the case of sample number 5, it is a whitish piece that is broken into several pieces. Samples number 6 and 7 are blue with gray stripes whose only difference is the size and its shape. In the case of sample number 8, it has a homogeneous gray color around the entire sample. In sample number 9, the blue color predominates along with white and gray stripes. Sample 10 is the biggest sample (together with samples 6 and 7) compared to previously mentioned one that presents a homogeneous blue color. Sample number 11 has a homogeneous yellow color around the entire sample. And finally, samples number 12 and 13 are two pieces of very similar color and size. Finally, piece number 14, the togado's

figure, may have been a pendant, it is from a later period and was found out of context.

4.2.1.4 Conservation state and restauration treatments

There was no technical information about possible conservation or restoration treatments on these pieces so, they were not chemically treated. For that reason, the 14 pieces were visually evaluated to be able to identify the state of conservation of each one of them.

Pieces number 5, 8, 9, 12 and 13 are preserved in a poor state of conservation and will be discussed one by one below. For instance, piece number 5 was a fragile sample and because of this, it was broken into several parts. The surface of piece number 8 showed high degree of porosity. Piece number 9 shows a decolored blue color in most of the surface (darkened and discolored sample) and white-grey depositions. These depositions may be the result of the beginning of a degradation process. The beginning of the degradation together with the losing color gives the pieces a fragile appearance. Piece number 12 and 13 are very similar pieces and both present a high porosity. Finally, piece number 14, the togado's figure, presented a decolored blue color in most of the surface.

In contrast, pieces number 1, 2, 3, 4, 10 and 11 are conserved in a better state. All of them present a well-preserved color, a low porosity degree and no degradation patterns were observed on the surfaces.

4.2.2 Lithic tools

4.2.2.1 Historical context

Since its discovery in 1980, the Nahal Hermar cave (Figure 15) has been interpreted as a place of worship where ceremonies were held as indicated by the object found in it. This cave is a small chamber (7x8 m²) with an entrance on the right bank of a homonymous dry river in the southern Judean desert, 11 km from the city of Arad. After being discovered, the cave was looted and later in 1983 was excavated by Bar-Yosef and by Alon in 1988. Thanks to these excavations, some objects dated to the middle of the second half of the eight millennium BC were found. Several objects such as a decorated skull, human figurines made of bones, fragments of sculptures which have an obvious ritual worship character and presented well-preserved organic remains were found. Along with them, lithic tools were also found. In this last group, it is worthy to highlight a complete sickle with flint blades inserted in a wooden handle²⁴.

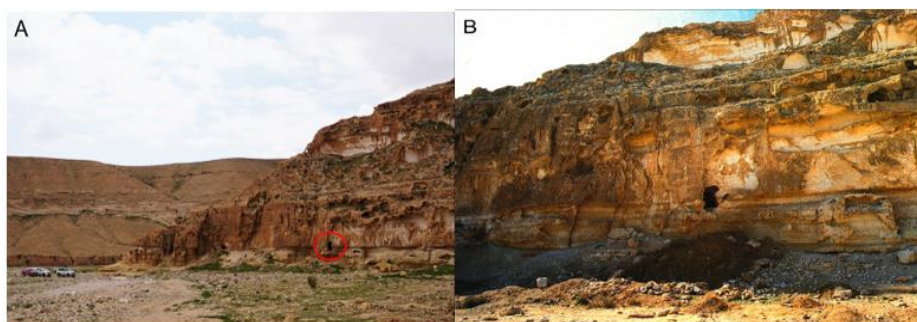


Figure 28 – Different views of the Nahal Hermar Cave

In order to ascertain the use of lithic tools recovered in Nahal Hermar cave, 6 tools were studied, from their elemental and molecular

composition to the identification of the residue present in some of the selected samples. This study can provide us an idea of the materials that were employed at the time and the set of functions for which they were produced.

4.2.2.2 Emplacement

There is not much information about the environmental conditions of this cave. However, near this cave it is located (Figure 16) the Christmas cave (and Qumran cave as well). Given that the two caves are connected by the Dead Sea, about 100 km away, it can be considered that the environmental information obtained for the second cave may be valid and similar to the Nahal Hemar Cave. Both caves are very close to the Dead Sea, Nahal Hemar cave concretely, is 8 km away from the Dead Sea).



Figure 29 – Location of Nahal Hemar Cave

The average of annual temperature in this area is 21°C, the average of annual precipitation is 100 mm (average of 1960-1990 period) and the climate is arid, which involves hot and dry summers and moderate winters. Christmas cave does not have a permanent source of water available nearby, although easily accessible ephemeral ponds can be found alongside the Kidron stream. It should be mentioned that the environmental conditions on the surface of the cave are very similar to other refuge cave in the Judean Desert. That is why this formation is very useful and comparable to the Nahal Hemar cave²⁵.

Christmas cave is a karst-type cave that, in its formation, was filled with water. Currently, the cave is dry and does not host significant karst processes. Topographic data indicates that this cave was formed within the Judean desert aquifer, along planes of tectonic weakness. This general description is shared by most of the great caves of the Judean Desert²⁵.

4.2.2.3 Description of the analyzed samples

This work was focused on the lithic material found in the Nahal Hemar cave. From the 21 lithic samples which are stored in the Israel Museum (Jerusalem), 6 different pieces were selected for its analytical study. The selected pieces are showed in the Figure 17.

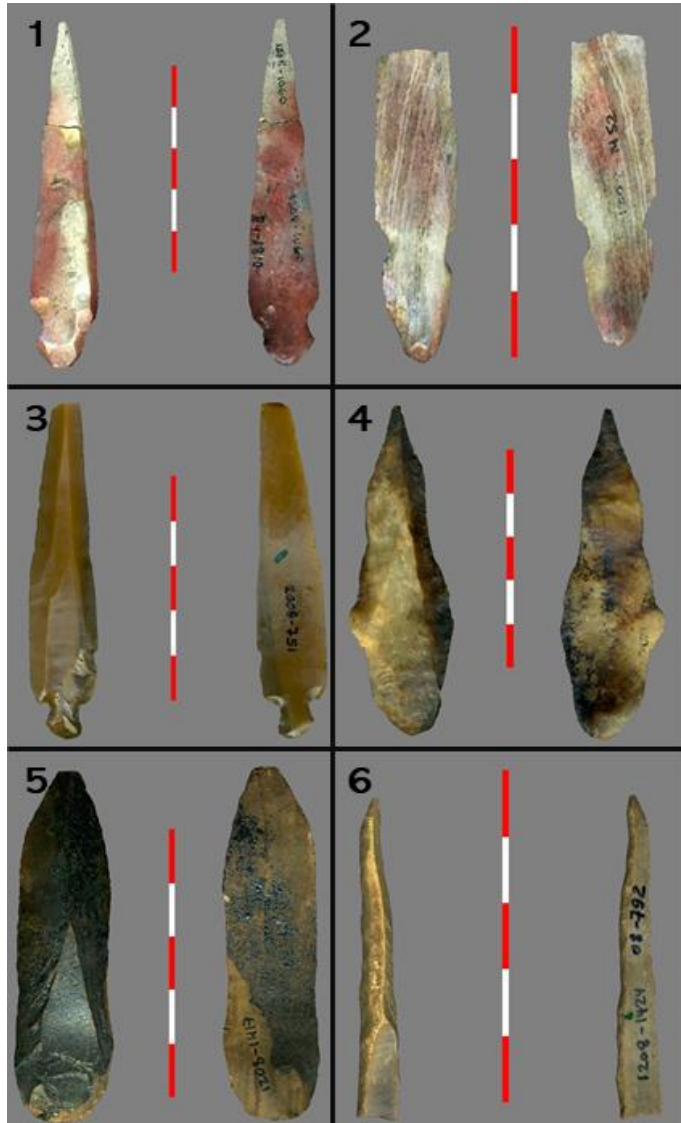


Figure 30 – The six analyzed tools

After a preliminary visual examination and the information provided by the archaeologist Dr. Juan José Ibañez, the following preliminary characterization of each sample could be detailed. Piece number 1 seems to have undergone a consolidation treatment²⁶. In general, it looks very burned, and the heel is very abraded. The edges are sharp

and are not retouched. The following sample, number 2, also appears to have suffered a consolidation treatment and looks very burned which its heel scorched. Piece number 3 does not have traces of burning. A brown-black residue can be observed specially on the right side and its heel is not abraded. In piece number 4, there is still evidence of some residue. The edge is polished, but it seems chipped or eroded, it is not known if voluntarily. This sample may be used for butcher aims. The piece number 5 shows a layer of black color like bitumen residue. Sample number 6 is a sickle piece which present mastic residues. It appears to have suffered an invasive polishing in the middle area. That is why its domestic use can be deduced. Piece number 7 again shows an eroded heel. It is very sharp piece in some areas so it can be thought that it has been used by butchers. Furthermore, there are also possible residues on the right and on the distal side. The edge of this piece is somewhat different from the rest, but it is still eroded. Piece number 8 seems to have been used for mechanical drilling such as mineral drilling due to its regular marks. And finally, piece number 9 appears somewhat affected by fire and shows a brown-black residue in the surface. In addition, the heel showed abraded²⁶.

4.2.2.4 Conservation state and restauration treatments

These six samples have not undergone any type of treatment after their excavation. They are kept as they were collected from Nahal Hemar cave. The only process is a simple cleaning to be able to remove all the concretions or sediments adhered. In addition, some of the analyzed pieces (pieces 1 and 2) seems to have undergone a consolidation treatment thanks to the information provided by the archaeologist Juan Ibañez²⁶.

4.2.3 Iron archaeological slags

4.2.3.1 Historical context

Finally, some archaeological iron slags were analyzed for this PhD. The iron has been a valuable item since BC centuries. However, it acquired its maximum value in the Iron Age²⁷. The extraction and transformation of the mineral was an essential activity in different regions of Europe, including the Basque Country²⁸. During history, this element has been used in a wide variety of fields. One of its first uses was in the manufacture of war weapons, as it guaranteed victory and protection from other civilizations. Then, advances in the use of this metal were observed in agriculture, where iron was used for the manufacture of plow tips that allowed man to work the land and crops in a better way. The perfect knowledge about the use of this material allowed its use for the elaboration of jewels, crafts and fabrics. Even nowadays, iron is the most used metal in the industry due to its hardness, especially in construction²⁷.

In archaeological research, the remains of iron pieces are of great value because they provide a valuable information about the production and consumption of this element in ancient times. A key requirement for obtaining this information is the development of new means to track iron objects to their production origins. Among them you can find the chemical analysis of the slags. Slags are waste material from mining or smelting sites and varies due to the process and the additives used to produce melted iron²⁹. Therefore, the analysis of these wastes can provide information about the raw material and the production procedure. This is the reason why old

ironworks, where archaeological slags are often found, are of great historical relevance.

In the Basque Country iron has been a mineral of great importance²⁸. The existence of abundant iron deposits has been continuous from the Second Iron Age to recent times. In this way, the fundamental economic activity of Bizkaia has been centered on the extraction and transformation of ore³⁰ for a long time. Thanks to the good quality of the iron produced in this area, the Basque iron and ironworks became internationally recognized³¹. To better understand the operation of these ironworks³² and the differences among them, first it is necessary to carry out a brief classification. In general, there are two types of ironworks. Depending on the use of hydraulic energy there are mountain ironworks and hydraulic ironworks. The mountain ironworks or better known as “haizeolak” in Basque, are designated to the primitive ironworks or furnaces to produce iron that were located on the heights of the mountains and operated by force of arms³³. In the case of hydraulic ironworks, the force of water was used to produce the process of obtaining iron³³. This PhD focuses on a mountain forge of great historical relevance such as the Pobal forge, the last forge that has been active in the Basque Country³⁴. Unfortunately, there are many lacks in the knowledge about the production of iron in mountain forges. In this sense, analytical studies of the remains of these forges can provide valuable information about the technology and procedure employed.

4.2.3.2 Emplacement

The iron archeological slags which were studied in this work come from the “El Pobal” (Muskiz, Bizkaia, Spain) ironwork (Figure 18). El Pobal forge was originally an emplacement chosen by the Salazar

family to replace another old forge in the El Vado area. Thanks to the documentation that exists today^{34,35}, it can be deduced that this ironwork was built at the beginning of the 16th century. At that time, the ironwork was a mountain ironwork or “haizeola” which used a traditional system to obtain the metallic iron³⁶.



Figure 31 – On the left, location of the “El Pobal” ironwork. On the right, the ironwork

Throughout the second half of the 15th century and the first of the 16th and with the advancement of technology, hydraulic ironworks emerged. The appearance of this system did not mean the definitive abandonment of the old one, since in small communities such as the one in El Pobal, there was not enough economic disposition to build the facilities that required a hydraulic system. In 1575 Juan de Salazar made several repairs to the ironwork that were repeated between the 17th-18th centuries. It is suspected that at this time the mountain ironworks such as El Pobal underwent significant changes in their mechanisms, becoming hydraulic ironworks. In the case of El Pobal, there were changes in the workshop and the entire hydraulic infrastructure (dam, channel, hydraulic tunnel) was rebuilt. It is in the 19th century when the traditional Basque steel industry suffered a

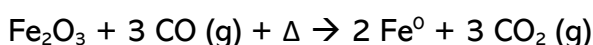
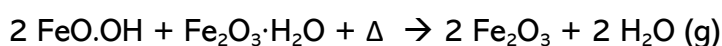
serious decline with the result of a complete mechanical intervention. It was then when El Pobal ironwork completely improved the machinery and constructions of the forge (the coal bunkers, the bellows, the hammer, or the anvil)^{34,35}.

In summary, the El Pobal forge has undergone extensive evolution over time. The investigations^{34,35} carried out in this enclave got a more complete information of this foundry. However, apart from the historical changes that this ironwork suffered, and the information extracted from the study of documents and observation of the remains, chemical characterization of the obtained minerals and wastes will provide more valuable data.

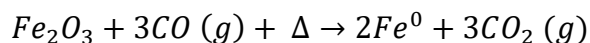
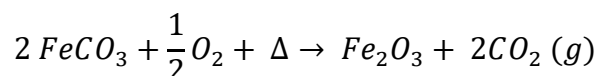
The mineralogic composition of the iron ores near El Pobal hydraulic forge are siderite (FeCO_3), goethite ($\text{FeO}\cdot\text{OH}$) and limonite ($\text{Fe}_2\text{O}_3\cdot\text{H}_2\text{O}$)³⁷. It is known that the chemical reduction of the iron ore to obtain metallic iron is the use of a two-step treatment with carbon. Probably this carbon had vegetal origin the XIV-XVIII centuries due to the absence of mineral carbon (anthracite) in the area and the abundance of oak and beech trees.

In the mentioned iron reduction procedure, the first step is the partial oxidation of carbon to CO, in the absence of air. The oxygen required to form the CO is extracted from the mineral when heating the carbon in absence of air. The second step is the chemical reduction of the iron ore. Depending on the original minerals, there are two possible reduction reactions pathways:

1 – Starting from goethite ($\text{FeO}\cdot\text{OH}$) and limonite ($\text{Fe}_2\text{O}_3\cdot\text{H}_2\text{O}$):



2 – Starting from siderite (FeCO_3):



In those times, the temperature reached in the ovens of reduction was not high enough as to guarantee the 100% conversion of the iron ore into metallic iron. Thus, in the slags matrix remains of the original mineral used to perform the metal work should be found. This makes the analysis of slags very useful for obtaining information about previous procedures and ores.

4.2.3.3 Description of the analyzed samples

The selected samples from the “El Pobal” ironwork can be observed in the Figure 19. The size of the pieces was very different, finding pieces about 10 centimeters to pieces of 2 centimeters. Dark colors similar to goethite are the most common but the hues varied from sample to sample.

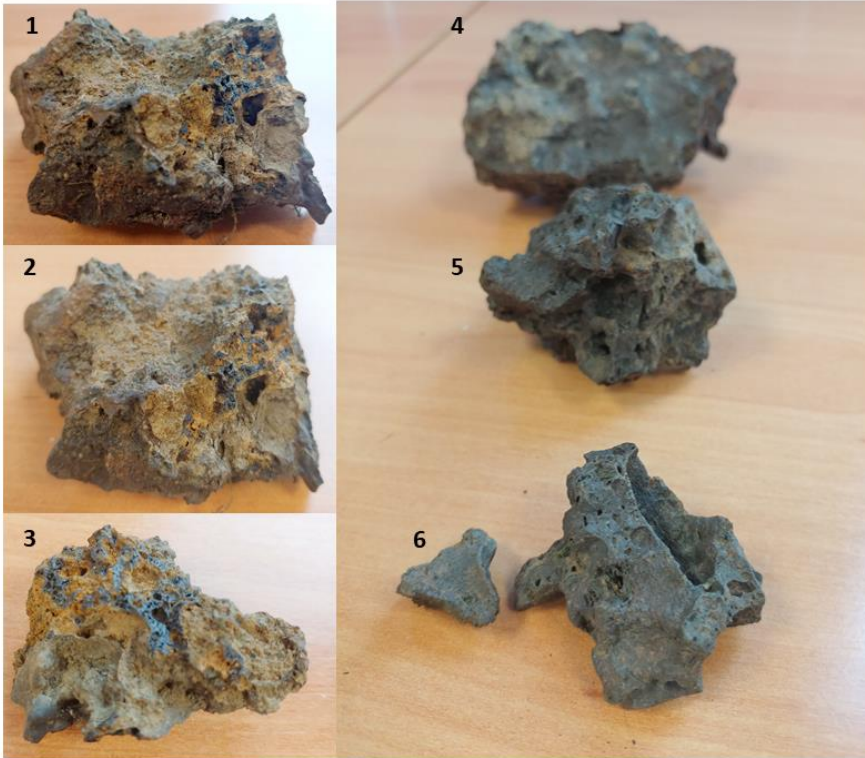


Figure 32 – Samples analyzed from “El Pobal” ironwork

4.2.3.4 Conservation state and restoration treatments

The studied pieces did not go through any restoration process or at least they were not documented. The conservation of these samples since they were discovered was not the most suitable one, after all these pieces have been together with other sediments and wastes exposed outdoors to meteorological agents (rain, wind, erosion...).

4.3 BIBLIOGRAPHY

The references mentioned in this work are based on the bibliography format described below:

Journals: Estalayo, E. Aramendia, J. Bellot-Gurlet, L. Garcia L. Garcia-Camino, I. Madariaga, J.M. Article title. *Journal abbreviation*, volume, pages (year).

Books: Estalayo, E. Aramendia, J. Bellot-Gurlet, L. Garcia L. Garcia-Camino, I. Madariaga, J.M. *Book title*, (year). DOI number.

1. Izaguirre, M. El Pecio de Urbieta (Gernika) País Vasco. *Heritage at Risk. Underwater cultural heritage at risk: managing natural and human impact*. 90–92 (1998).
2. Bilbao, M. M. Memoria de actividades. *Cuadernos de Relaciones Laborales* **33**, 477–481
3. Izaguirre, M. & Valdés, L. Avance de excavación del pecio del siglo XV de Urbieta (Gernika). *Itsas Memoria. Revista de Estudios Marítimos del País Vasco* **2**, 35–41 (1998).
4. Unsain, J. M. *La memoria sumergida. Arqueología y patrimonio subacuático vasco. Untzi Museoa - Museo Naval* (2004).
5. Loewen, B. The Red Bay vessel. An example of a 16th-century Biscayan ship. *Itsas Memoria. Revista de Estudios Marítimos del País Vasco* **168**, 193–199 (1998).
6. Irabien, M. J. & Velasco, F. Heavy metals in Oka river sediments (Urdaibai National Biosphere Reserve, northern Spain): Lithogenic and anthropogenic effects. *Environmental Geology* **37**, 54–63 (1999).

7. Madariaga, J. Modelización del estuario de Gernika (Urdaibai). *Kobie Serie Ciencias Naturales XX*, (1991).
8. Mijangos, L., Ziarrusta, H., Ros, O., Kortazar, L., Fernández, L. A., Olivares, M., Zuloaga, O., Prieto, A. & Etxebarria, N. Occurrence of emerging pollutants in estuaries of the Basque Country: Analysis of sources and distribution, and assessment of the environmental risk. *Water Research* **147**, 152–163 (2018).
9. Irabien, M. J. PhD Thesis: Mineralogía y geoquímica de los sedimentos actuales de los ríos Nervión-Ibaizabal, Butrón, Oka y Nieve. Índices de gestión ambiental. *Universidad del País Vasco (UPV/EHU)* (1993).
10. Solaun, O., Rodríguez, J. G., Menchaca, I., López-García, E., Martínez, E., Zonja, B., Postigo, C., López de Alda, M., Barceló, D., Borja, Á., Manzanos, A. & Larreta, J. Contaminants of emerging concern in the Basque coast (N Spain): Occurrence and risk assessment for a better monitoring and management decisions. *Science of the Total Environment* **765**, (2021).
11. Villate, F., Iriarte, A., Uriarte, I. & Sanchez, I. Seasonal and interannual variability of mesozooplankton in two contrasting estuaries of the Bay of Biscay: Relationship to environmental factors. *Journal of Sea Research* **130**, 189–203 (2017).
12. Luque, J. M. M. Pecio de Bakio. *Arkeoikuska: Investigación Arqueológica* 370–373 (2004).
13. Arqueología, M. N. de. Arqueología subacuática en Bizkaia. El pecio de Bakio, investigación y puesta en valor. in *Actas de las Jornadas de ARQUA 2011* (ed. Ministerior de Educación, C. y D.) 131–138 (2011).

14. Luque, J. M. M. in *Actas de las V Jornadas de Jóvenes en Investigación Arqueológica. Arqueología para el siglo XXI* 250–255 (2012).
15. Luque, J. M. M. Pecio de Bakio. *Arkeoikuska: Investigación Arqueológica* 95–99 (2005).
16. Luque, J. M. M. Pecio de Bakio. *Arkeoikuska: Investigación Arqueológica* 145–156 (2012).
17. Solaun, O., Garmendia, J. M., del Campo, A., González, M., Revilla, M. & Franco, J. *Perfiles de las aguas de baño de la zona litoral de la Comunidad Autónoma del País Vasco. URA* (2016).
18. García, L. *Information provided by the archaeologist*.
19. I.S.O. Preparation of steel substrates before application of paints and related products - Visual assessment of surface cleanliness. *International Organization for Standardization* (1988). at <<https://www.iso.org/standard/15711.html>>
20. Pinto, J., Prieto, A. C., Coria-Noguera, J. C., Sanz-Minguez, C. & Souto, J. Investigating glass beads and the funerary rituals of ancient Vaccae culture (S. IV-I BC) by Raman spectroscopy. *Journal of Raman Spectroscopy* **52**, 170–185 (2021).
21. Valladolid, U. de. La Necropolis de Las Ruedas: Estelas y tumbas. at <<https://pintia vaccea.es/seccion/la-necropolis-de-las-ruedas-estelas-y-tumbas>>
22. Sanz, C. & Coria, J. C. in *Novedades arqueológicas en cuatro ciudades vacceas: Dessobriga, Intercatia, Pintia y Cauca* 129–156 (2018).
23. Hernández, L., Rubiales, J. M., Morales-Molino, C., Romero, F., Sanz, C. & Gómez Manzanque, F. Reconstructing forest history from archaeological data: A case study in the Duero basin assessing the

- origin of controversial forests and the loss of tree populations of great biogeographical interest. *Forest Ecology and Management* **261**, 1178–1187 (2011).
24. Borrell, F., Ibáñez, J. J. & Bar-Yosef, O. Cult paraphernalia or everyday items? Assessing the status and use of the flint artefacts from Nahal Hemar Cave (Middle PPNB, Judean Desert). *Quaternary International* **569–570**, 150–167 (2020).
 25. Porat, R., Davidovich, U. & Frumkin, A. in *Outdoor Qumran and the Dead Sea. Proceedings of the Hebrew University - COST Cultural Heritage Workshop* (2012).
 26. Ibáñez, J. J. *Information provided by the archaeologist*.
 27. Blakelock, E., Martínón-Torres, M., Veldhuijzen, H. A. & Young, T. Slag inclusions in iron objects and the quest for provenance: an experiment and a case study. *Journal of Archaeological Science* **36**, 1745–1757 (2009).
 28. Franco Pérez, F. J. & Gener Moret, M. Early ironwork in Biscay: Survey, excavation, experimentation and materials characterization. An integral study of the mountainside ironworks (ferrerías de monte or “haizeolak”). *Materials and Manufacturing Processes* **32**, 876–884 (2017).
 29. Ettler, V., Johan, Z., Zavřel, J., Selmi Wallisová, M., Mihaljevič, M. & Šebek, O. Slag remains from the Na Slupi site (Prague, Czech Republic): Evidence for early medieval non-ferrous metal smelting. *Journal of Archaeological Science* **53**, 72–83 (2015).

30. Franco, J. Haizeolak en Bizkaia: Una investigación de largo recorrido sobre la arqueología de la producción del hierro. *Kobie Serie Anejo* **13**, 21–37 (2014).
31. Orueta, E. PhD Thesis: Análisis de los materiales de las ferrerías de Bengola (Munitibar) y Urtubiaga (Ea). *Universidad del País Vasco (UPV/EHU)* (2018).
32. Franco Pérez, F. J., Etxezarragaortuondo, I. & Lonbide, X. A. The origins of iron technology in the Basque Country: mountainside ironworks or haizeolak. *Kobie Serie Paleoantropología* **34**, 267–282 (2015).
33. Álvarez, J. L. I. Las ferrerías de monte: una revisión bibliográfica. *Kobie Serie Paleoantropología* **18**, 207–214 (1989).
34. Uriarte, R. Gestión y cambio técnico en una empresa siderúrgica tradicional: la ferrería El Pobal (s. XVI-XX). *Revista Internacional de los Estudios Vascos* **54**, 411–463 (2009).
35. Torrecilla, M. J. La ferrería de “El Pobal” (Muskiz, Bizkaia). *Kobie Serie Paleoantropología* **26**, 245–272 (2000).
36. Franco, J. PhD Thesis: Arqueología y paleosiderurgia prehidráulica en Bizkaia (siglos III-XIII) Tras las huellas de los antiguos ferrones. *Universidad del País Vasco (UPV/EHU)* (2017).
37. Pereda, I. La metalurgia prehidráulica del hierro en Bizkaia: el caso de los alrededores del pantano de Oriola (Trapagaran, Bizkaia). *Kobie Serie Paleoantropología* **XX**, 109–122 (1993).

CHAPTER 5



5. RESULTS FROM THE SAMPLES BURIED IN MARINE SEDIMENTS

"From birth, man carries the weight of gravity on his shoulders. He is bolted to earth. But man has only to sink beneath the Surface of the sea and he is free" –

"Desde su Nacimiento, el hombre lleva el peso de la gravedad sobre sus hombros. Está atornillado a la tierra. Pero el hombre no tiene más que hundirse bajo la superficie del agua y ser libre" – Jacques-Yves Cousteau

The protection of visible at the eye materials and elements (paintings, building, museum objects, archaeological sites, etc.) of Cultural Heritage has worried the population for years. Unfortunately, the same cannot be said for Underwater Cultural Heritage, probably because it cannot be appreciated directly by the citizens. Underwater Archaeology is focused on the study of the protection and conservation of sub-aquatic materials. There are a large number of archaeological remains underwater which offer potentially valuable information from the past, e.g. Vasa warship¹ or the Mary Rose². However, accessing the wrecks or underwater ruins and sites, and therefore getting such information is not an easy task because modern technological equipment for exploration is necessary. In addition, few people have access to this type of equipment because of its high cost. Hence, the underwater archaeological pieces tend to

be extracted. The extraction or recovery of underwater materials as such is not the most suitable option for the conservation of these kind of materials but regrettably, is the most common practice. According to UNESCO International Convention in 2001³, the in-situ preservation of Underwater Cultural Heritage is considered as the first option before allowing or engaging in any activities directed at this heritage. In-situ conservation is not a simple process, but it ensures the conservation of the pieces. On the contrary, their extraction supposes a physic-chemical alteration because the conditions of their surrounding vary drastically, from the marine environment (high salinity, anoxic conditions, etc) to a terrestrial environment (highly oxidant atmosphere)⁴.

Regarding chemical alteration, one of the most important problems that affect these pieces is sulfur accumulation. This process is very common on marine archaeological wood preserved under anoxic conditions in seawater. This sulfur reduced compounds could affect to other materials which are in contact with that wood (metal, textile, etc)². Moreover, when the reduced sulfur compounds present in the extracted material brought into contact with oxygen during extraction procedure, sulfuric acid could be produced by an oxidation process, which cause serious problems to the extracted pieces⁵. These problems are related to the presence of cracks in the parts, making objects brittle, thus losing the mechanical properties of the material⁶. Apart from sulfur, there are other elements that can cause damage to this type of pieces experimenting degradation processes without any solution, losing their heritage or cultural value. Such as the case of iron, which in contact with wood, caused serious problems⁷.

In order to study different shipwreck situations, such as shipwrecks submerged in estuary sediments and shipwrecks extracted from marine environment (sandy sediments), we designed this work on some remains from two different shipwrecks located in the Basque Country (Northern Spain). On the one hand, the Urbieta shipwreck, a shipwreck extracted in 1998 from Gernika estuary and preserved in Archaeological Museum of Bilbao was studied. On the other hand, the Bakio beach shipwreck, a still submerged shipwreck from which several pieces were extracted in 1999, and some of them were analyzed.

Considering the fragility of these materials, the main objective of this work is to ascertain which degradation processes are generating the decaying process by the use of non-destructive techniques. For this aim, it was crucial to define the raw materials used in the manufacture process of the pieces and to assess the performance of the applied treatments, exposed in Chapter 4. In some cases, the employed methodologies were complemented with destructive analysis combining in-situ and laboratory approaches.

In this chapter, all the results obtained from the analysis of the samples described in the Chapter 4 as buried in marine sediments (Urbieta shipwreck and Bakio shipwreck) are commented and discussed. The results are divided into two parts, according to localization of the pieces, the chemical treatment of each one and the exposure to different environments.

5.1 THE URBIETA SHIPWRECK

The analysis of the Urbieta shipwreck samples was possible thanks to the collaboration and participation of the Archaeological Museum of Bilbao. They provided us with the access to the iron nails of this shipwreck for their chemical analysis and diagnosis. As a first approach, samples were analyzed in-situ at the Archaeological Museum of Bilbao with portable equipment to carry out elemental and molecular analyzes without the need to move the pieces to the laboratory.

First of all, samples were analyzed in the Museum by means of ED-XRF. Among others, the presence of zinc was observed in the nails (Figure 1). The presence of zinc caused serious doubts among Museum's archaeologists and curators about its origin. In order to explain its origin two hypothesis were proposed by them: on the one hand the origin of the zinc could be inherent to the alloy. However, an iron alloy containing Zn on that period was never reported before. On the other hand, Zn could come from an external source. Nevertheless, such an important amount of Zn in all the analyzed pieces resulted suspicious. Considering this, it deemed necessary to investigate further on the origin of this element. For that reason, some destructive procedures and more detailed laboratory analyses were planned. For this aim, the pertinent permits to translate the pieces to the laboratory and to carry out more exhaustive analysis were requested.

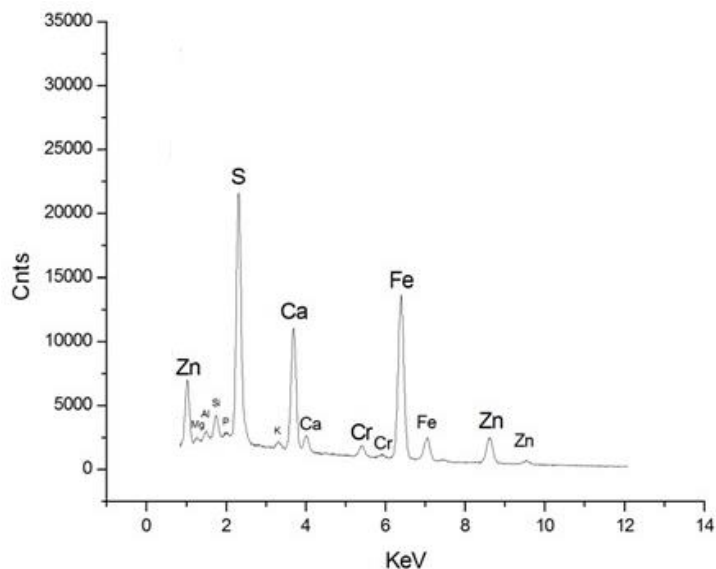


Figure 33 – Elemental results obtained by portable ED-XRF in Urbieta iron nails

Once in the laboratory, first of all, cross-sections of four different nails were prepared. Then, SEM-EDS and ED-XRF imaging techniques were used to accept/reject the hypothesis exposed above. SEM-EDS and ED-XRF imaging analyses were performed to obtain the elemental distribution maps (spectroscopic images) of the elements detected, especially the distribution of zinc.

The distribution of Zn in the four analyzed nails (Figure 2, 3, 4 and 5) revealed that it was always concentrated on the surface of the pieces in all of the analyzed samples. This fact indicated that the source of Zn was probably exogenous. In order to accept definitively this hypothesis, several pieces of Urbieta shipwreck wood were also analyzed using SEM-EDS. If the wood contained Zn, it would indicate that its origin was clearly exogenous and that it did not belong to the alloy. The results revealed that the wood had also a high presence of

zinc. This fact allowed us to accept the hypothesis that pointed Zn as an external factor, rejecting the hypothesis of the Fe/Zn alloy.

Thinking about the possible origin of this Zn, the working hypothesis was centered on the possible presence of this metal in the sediments where the shipwreck was discovered. The literature search revealed that some research studies⁸, focused on heavy metals quantification in the Oka River sediments, detected high presence of zinc. This river has long suffered during the XX century the waste dumping of liquids and solids containing important amounts of Zn, which promoted an increase of the presence of zinc in the sediments⁸. In this way, it could be said that the zinc (pollution) from the sediments was migrated and deposited to the surface of the nails.

Besides, in order to assess the effectiveness of different preservation treatments, nails treated following different procedures such as PEG or tannic acid were also considered for the study. Regarding the relative amount of Zn in the nails, differences among these differently treated samples were observed. The relative presence of this element was 6.7 % in non-treated nail, 1.2 % in tannic acid nail and 3.5 % in PEG nail. This fact revealed that such preservation treatments achieved detaching part of the deposited Zn, being the most remarkable one the tannic acid treatment. In fact, Figures 2, 3, 4 and 5 show qualitative differences in the presence and distribution of Zn depending on the treatment.

Regarding other elements, differences in their distribution were also observed by ED-XRF imaging, as seen in the same Figures.

The ED-XRF images showing the distribution of elements in the nail sample no. 1, which has not any treatment, is shown in the Figure 2.

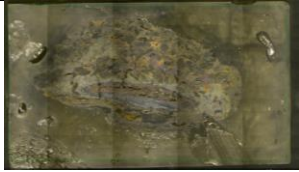
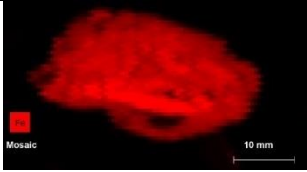
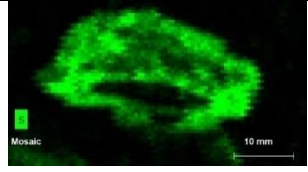
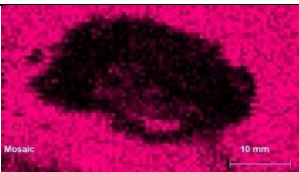
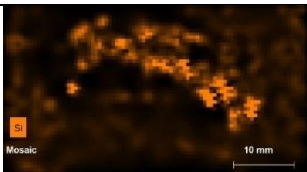
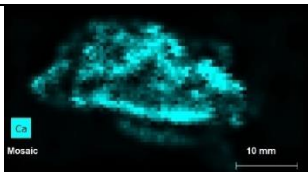
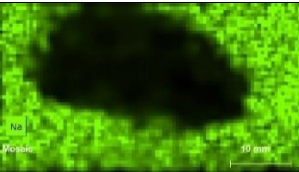
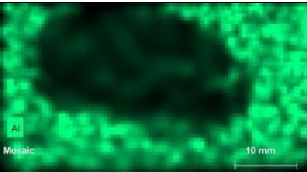
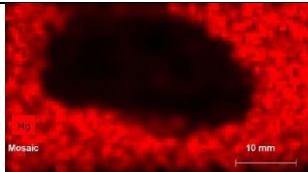
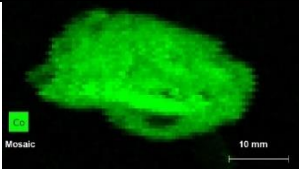
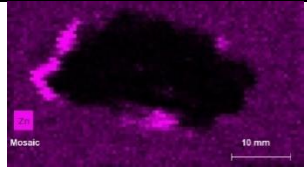
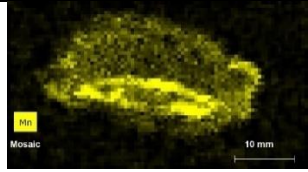
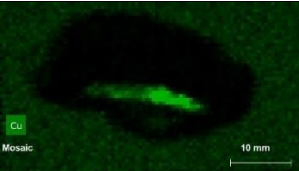
| | | |
|---|---|--|
| Piece no. 1 | Iron | Sulfur |
|  |  |  |
| Chlorine | Silicon | Calcium |
|  |  |  |
| Sodium | Aluminum | Magnesium |
|  |  |  |
| Cobalt | Zinc | Manganese |
|  |  |  |
| Copper | | |
|  | | |

Figure 34 – Elemental image of the nail no. 1 by ED-XRF

As expected, iron was the main element in this sample since its distribution occupies the entire area of the nail. However, the spectroscopic image has allowed us to observe a metallic core in

central part of the piece that was not visible to the naked eye (as commented in the Chapter 4). This core was detected because iron and other minor elements of the metal such as copper, manganese and cobalt were more concentrated in the center of the piece, although their distribution is not uniform. In the case of cobalt, its distribution showed that it was present in all around the sample, being more concentrated in the metal core. Manganese and copper were detected in the inner part of the sample, just in the metal core. However, in the case of manganese, its presence is also observed in lower relative amounts in the entire sample. This distribution gave us information about the nature of the iron alloy used to manufacture the nails, containing detectable amounts of Cu, Mn and Co associated to iron.

Regarding other elements, sulfur was detected in the whole piece but not in the center where the remains of the core metal alloy are ascertained. Therefore, it could be said that its presence must be related to the corrosion of the external parts of the nail in the presence of materials rich in sulfur, being part of the bulk preserved from that corrosion process related to the content of sulfur. Moreover, it is worthy to mention that its spatial distribution is not homogeneous along the corroded nail. This is a clear indication that this element does not belong to the original composition of the alloy.

The presence of silicon was visible only in the upper part of the sample. In contrast, calcium was present in the inner part of the pieces, including in the core of the metal that remained. Finally, chlorine, sodium, aluminum and magnesium were detected in a very low presence inside the piece. All these elements are part of marine sediments and its presence in the nails must be explained as a natural

process of element migration from the sediments and a further trapping in the layers of the corroded nails.

Apart from the element distribution maps, the semi-quantitative composition of the sample was also analyzed by ED-XRF. The elemental analysis of this corroded and bib-treated sample is shown below. The values were computed as the normalized percentage of the elements present, ordered from highest to lowest using the software for alloy's quantification provided by the manufacture of the ED-XRF instruments: Fe (75.0 %), S (15.7 %), Cl (4.1 %), Si (1.6 %), Ca (0.9 %), Na (0.8 %), Al (0.6 %), Mg (0.4 %), Co (0.3 %), Zn (0.3 %), Mn (0.2 %), Cu (0.1 %). Other elements detected at the trace level (normalized percentages less than 0.1%) by the ED-XRF equipment were not considered since they do not present significant data for the diagnosis.

These percentages of the major and minor elements should not be considered accurate because the contribution of the particular background (this is not an alloy alone, but an altered iron material with exogenous elements due to the corrosion process and uptake of elements from the sediments) was not considered in the theoretical calibration used by the manufacturer. However, considering that the obtained data was relative, they can only be used for comparison within the same sample and between samples since the background was the same (or nearly the same) for all of them.

The comparison of the relative amount of exogenous elements with regard to the original elements in the alloy of the nails (Fe, Co, Mn and Cu amount for the 75.6%), reveals a very important impact of the corrosion process in the particular burial sediments of where the Urbietta shipwreck was discovered.

The uptake of sulfur is very remarkable (15.7% of the total amount of elements). As its relative amount is much larger than the other uptaken elements, we considered the important influence of the wood where the nails were used, as the source of the sulfur content in the corroded iron nails.

The second most dangerous element for iron preservation is chlorine (it amounts for the 4.6% of the total elements in the nail sample). Its presence must be considered in the designing of the preservation procedure, especially the amount of chlorine the most dangerous element due to its reactivity with metallic iron.

Other elements coming from their natural presence in estuarine sediments (Na, Mg and K from seawaters and Si, Al, Na, Ca and Mg from the clays of the rivers sediments) have been uptaken in remarkable amounts (4.3% of the total), Thus their removal during the preservation treatment should also be considered because they do not form part of iron alloys (elements in their metallic form) being trapped inside the nails as cations bounded to negative sites.

For the sample no. 2, which has been intended to be preserved by the tannic acid treatment, the ED-XRF distribution map is shown in the Figure 3.


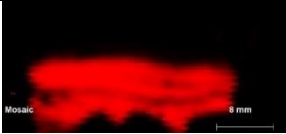
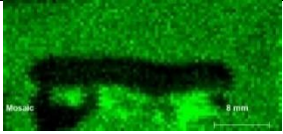
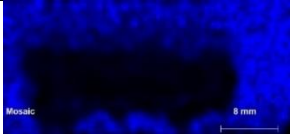
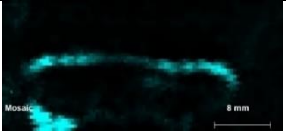
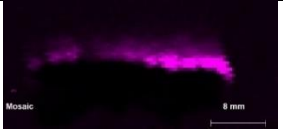
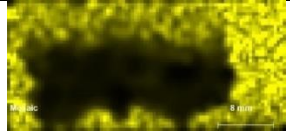

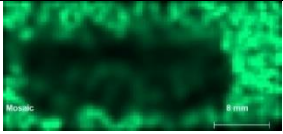
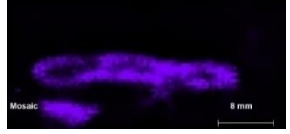
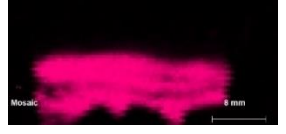
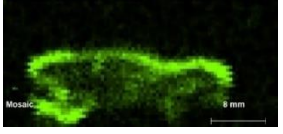
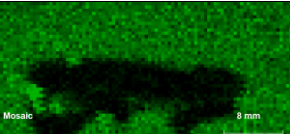
| Piece no. 2 | Iron | Chlorine |
|---|--|---|
|  |  |  |
| Sodium | Sulfur | Zinc |
|  |  |  |
| Magnesium | Silicon | Aluminum |
|  |  |  |
| Calcium | Cobalt | Manganese |
|  |  |  |
| Copper | | |
|  | | |

Figure 35 – Elemental image of the nail no. 2 by ED-XRF

In this sample, the distribution of iron was the same than that of the sample no.1, all along the piece, but with a higher central core that contains a detectable hole. The presence of that hole may suggest a remarkable corrosion in a layered distribution. Cobalt is again present in the entire analyzed sample although it is concentrated in the central core, as manganese did in part.

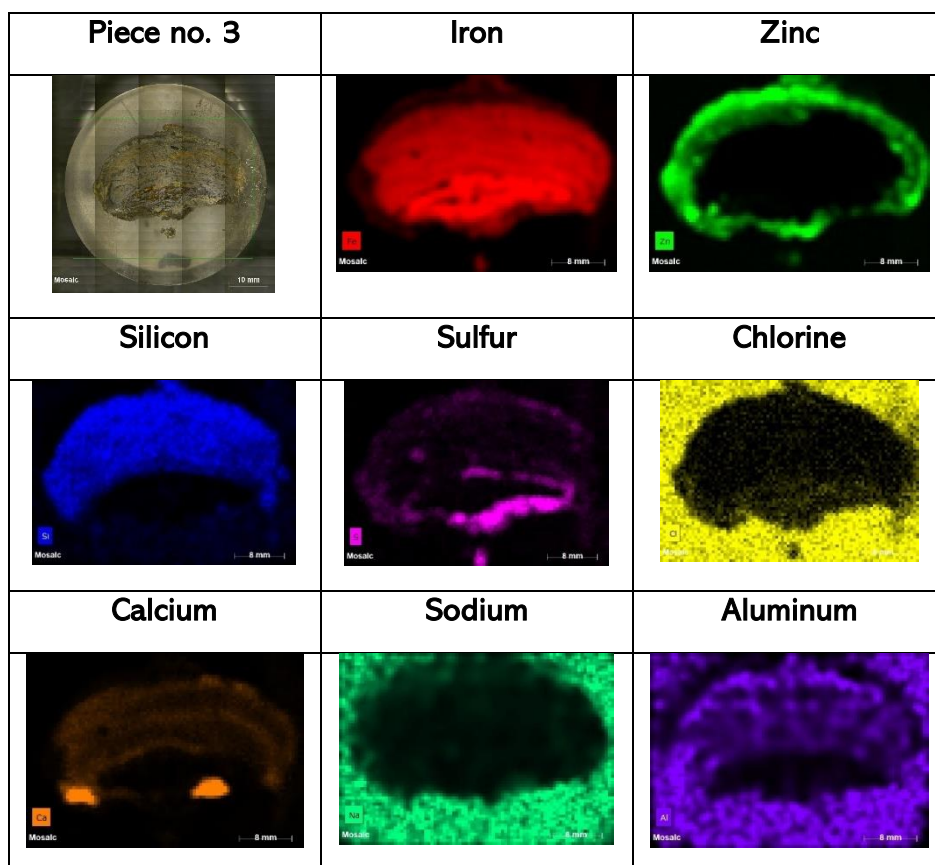
For this sample, the presence of copper was detected in a small area on the left side of the sample, suggesting that the presence of this element could not be related as being part the original alloy but as an input form the polluted sediments that have also important amounts of this metal⁸. Thus, for this sample, Co and Mn should be considered as part of the original iron alloy used to manufacture the nail.

Chlorine was present in the lower part of the piece, concretely down the area where the metallic core was preserved. This lower part of the sample looks the one with the higher presence of corroded products. In the case of sodium, magnesium, and aluminum, the presence of these elements in the sample seemed to be very low, once again less than the background. Sulfur, zinc, and silicon were only detected in the external part of the sample. In the case of sulfur, it was detected just in the perimeter of the sample, being not so extended than in the case of nail no. 1. Finally, calcium was detected just above the core of the piece.

Apart from ED-XRF map distribution, the elemental analysis of this sample is shown below using the normalized percentage of the elements present ordered from highest to lowest: Fe (85.1 %), Cl (4.6 %), Na (2.7 %), S (2.0 %), Zn (1.8 %), Mg (1.0 %), Si (0.9 %), Al (0.7 %), Ca (0.6 %), Co (0.3 %), Mn (0.2 %), Cu (0.1 %). According to these results and comparing with the previous ones, it must be said that this sample is the only sample that preserves better the original material. Considering cobalt and manganese as part of the original alloy, the 85.6% of the original elements are present in this nail sample treated with the tannic preservation process.

The lower presence of sulfur, in comparison to sample No. 1 is remarkable. However, the amount of chlorine is comparable to nail No. 1. This is indicative that the tannic preservation treatment removes some of the corrosion elements although one of the most dangerous one (chloride) is not effectively removed. This data suggested the development of an alternative treatment to effectively remove chlorine from iron artefacts with chlorine concentrations around 5%, that is now in progress in the research group where this PhD was developed.

The ED-XRF distribution map of elements for the sample no. 3, which was subjected to the PEG treatment together with wood, is shown in the Figure 4.



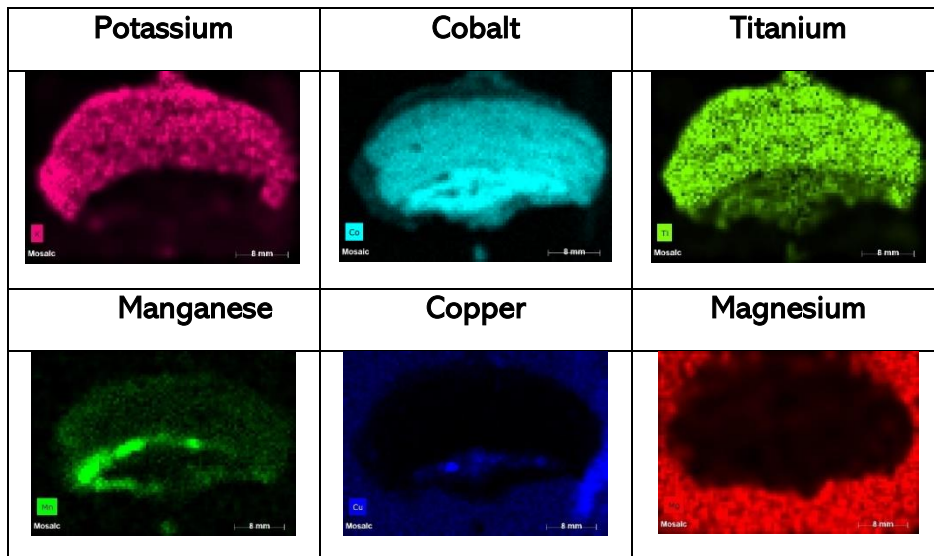


Figure 36 - Elemental image of the nail no. 3 by ED-XRF

As expected, iron was detected as the main element, and its distribution occupied the entire sample. In addition, as in the previous samples, thanks to this analysis it was possible to observe remains of the metal core of the piece not detectable at naked eye. In this core the presence of iron, cobalt, manganese and copper were distinguished, suggesting their presence as minor elements of the iron alloy used to manufacture the nail.

Zinc showed almost the same distribution as shown in the sample than described before. Its presence was detected in all the perimeter of the sample, only in the external areas. In the case of silicon, this element appeared only in the upper part of the piece, as observed for aluminum, potassium, and titanium. These elements were detected from the center of the piece to the external area. In contrast, sulfur was only detected in the lower part of the sample, surrounding part of the metal core of the sample. Calcium was an element only detected in two distinguished areas in the lower area of the sample.

Apart from element map distribution, the semi-quantitative analysis of this sample was performed using the normalized percentage of the elements method implemented in the software of the manufacturer. The results ordered from highest to lowest were: Fe (70.2 %), Zn (9.0 %), Si (8.1 %), S (4.3 %), Cl (1.9 %), Ca (1.9 %), Na (1.8 %), Al (1.6 %), K (0.4 %), Co (0.3 %), Ti (0.2 %), Mn (0.1 %), Cu (0.1 %), Mg (0.1 %). According to these results and comparing with the previous ones, it must be said that in this sample the presence of sulfur is still remarkable while that of chlorine is much lower.

However, the amount of zinc is surprisingly high, being the total amount of exogenous elements close to 30%, indicating a highly impacted sample although it was subjected to the PEG preservation treatment. Maybe, the PEG treatment is not so effective when other transition element, not belonging to the original alloy like zinc, are present in the metallic pieces to be preserved.

The presence of the element belonging to the natural sediments is like in other samples, being in this case titanium in minor amounts, not at trace levels.

For the sample no. 4, which was subjected to the PEG treatment, the ED-XRF map distribution is shown in the Figure 5. The sample has been analyzed in other orientation to see the head and body of the nail.


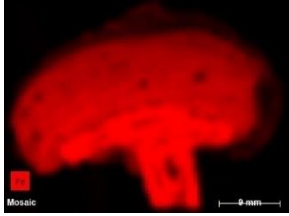

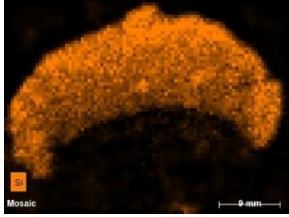
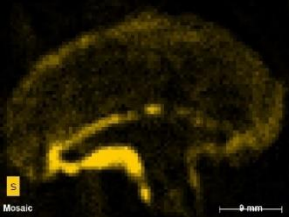
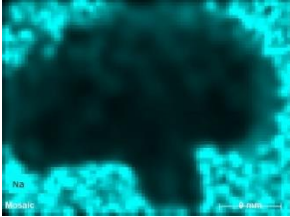
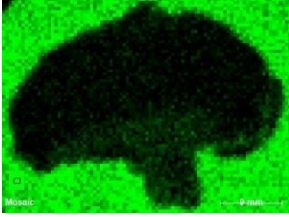
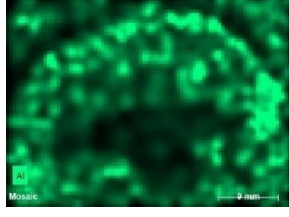
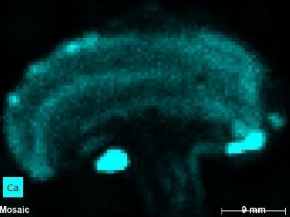
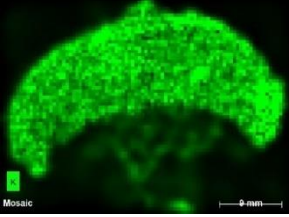
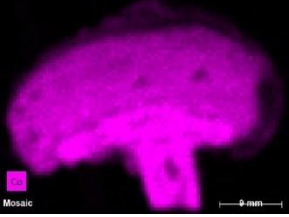
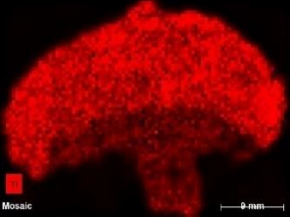
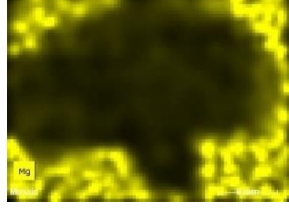
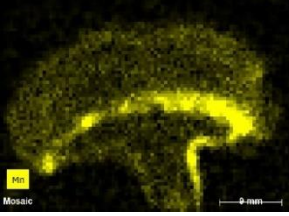
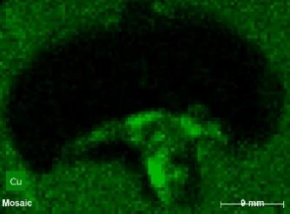
| | | |
|---|---|--|
| <p>Piece no. 4</p> | <p>Iron</p> | <p>Zinc</p> |
|  |  |  |
| <p>Silicon</p> | <p>Sulfur</p> | <p>Sodium</p> |
|  |  |  |
| <p>Chlorine</p> | <p>Aluminum</p> | <p>Calcium</p> |
|  |  |  |
| <p>Potassium</p> | <p>Cobalt</p> | <p>Titanium</p> |
|  |  |  |
| <p>Magnesium</p> | <p>Manganese</p> | <p>Copper</p> |
|  |  |  |

Figure 37 - Elemental image of the nail no. 4 by ED-XRF

Probably this is the best view of the nail, with the clear central apparently non-altered body showing the presence of cobalt, manganese and copper as the elements accompanying to iron, i.e. the minor elements of the iron alloy used to manufacture the nail. However, manganese and copper were detected in the inner part of the sample, but with different distribution. In the case of manganese, it was concentrated surrounding the metal core. And in the case of copper, it was detected in the central part of the sample, in the metal core. In the case of cobalt, this element was located in the entire sample, including the metal core.

The presence of zinc was distributed throughout the perimeter of the sample, and it did not penetrate into the metal core. Silicon was present on the outer face of the piece; it was only detected in the corrosion area. Potassium and titanium have similar distribution as silicon. In the case of sulfur, its presence was only detected in the lower area, surrounding the metal core of the sample. Aluminum was detected around all the sample except in the metal core. Calcium was only detected in some specific areas of the sample located in the lower part.

Apart from element map distribution, the elemental analysis of this sample is shown below using the normalized percentage of the elements present ordered from highest to lowest: Fe (71.9 %), Zn (8.3 %), Si (7.6 %), S (3.7 %), Na (2.1 %), Cl (1.8 %), Al (1.8 %), Ca (1.5 %), K (0.5 %), Co (0.3 %), Ti (0.2 %), Mg (0.1 %), Mn (0.1 %), Cu (0.1 %). It must be said that XRF equipment has detected more elements than the exposed in this work, but it was decided not to mention elements with a normalized percentage less than 0.1% since

they are present at trace levels. According to these results and comparing with the previous ones, it must be said that this sample presented similar results as the ones obtained from the samples no. 1 and no. 3.

In summary, all the obtained elemental information helped us to understand the current state of the pieces and to be able to make the following statements:

SEM-EDS and ED-XRF imaging helped us to reject the hypothesis that the presence of zinc was due to the manufacture process. Furthermore, the ED-XRF imaging showed how the distribution of zinc was related to the external part of the samples, thus confirming external contamination.

Regarding the elements detected in the samples, it can be concluded that there was a series of elements that were typical of the samples (endogenous) and another series of elements whose origin was exogenous. Within the group of endogenous elements were iron, copper, cobalt, and manganese, which are supposed to be part of the alloy. Within the group of exogenous elements were chlorine, sodium, magnesium, zinc, sulfur, aluminum, silicon, titanium, and potassium. It should be highlighted that all the analyzed samples presented the same exogenous elements.

However, it was observed that the distribution of aluminum was different in the studied samples. This element showed a different distribution pattern in the samples no. 3 and no. 4. Its presence was detected in most of the area of the sample, except in the core area.

In the case of sulfur, it was found that the distribution varied depending on the treatment used. In the case of piece no. 1, 3 and

4, the sulfur was present in the entire area of the sample except in the core. In the case of piece no. 2, sulfur was present just in the surface area. Therefore, it can be said that PEG treatment was not effective in terms of removing sulfur from these pieces or avoiding its penetration as the distribution detected in the pieces treated with PEG was similar to the non-treated one. In contrast, tannic treatment revealed that it acts as a good barrier against sulfur attack.

In the case of silicon, all samples except no. 2 showed the same pattern, it was detected in all three cases in the area that occupies just above the metallic core up the surface, the area corresponding to the concretion zone. On the contrary, in the sample no. 2, silicon was only detected in specific areas on the outside. Therefore, it can be concluded that the treatment with tannic acid was the most efficient treatment to reduce a higher contribution from exogenous materials.

Calcium was detected inside the pieces in the case of pieces no. 1 and no. 2 but in the other pieces, calcium was detected in the outer area closest to the core of the piece. This difference in the pieces leads to the hypothesis that treatment with PEG was treatment which more efficiently avoided the penetration of exogenous materials in the inner of the samples.

In the case of zinc, this element was detected in the surface area of the pieces, although in some cases it has penetrated more than in others, such as in pieces no. 3 and no. 4. In these pieces, the presence of zinc was observed in the external surface area of the piece, forming a thick layer. In contrast, in the case of pieces no. 1 and no. 2, it was detected in a specific surface area and in a smaller extent. Therefore, it can be said that the treatment with tannic acid or the procedure

that involves the treatment seems to be more suitable for the cleaning procedure of this element taking into account that tannic acid is a very used acid-based corrosion inhibitor in ferrous materials⁹. This complex avoided the corrosion process so that fewer elements were observed along the corrosion layer (since the corrosion layer is less advanced and smaller).

In the case of manganese, it was possible to observe how this element was detected in the four cases surrounding the core, in the internal part. Except for piece no. 2, where it was found that manganese was present in the external zone of the sample. The same was happened in the case of cobalt and copper. These two elements were detected in the core of the four samples. Except for piece no. 2, where its presence was not detected in this area. These differences could be related to the conservation state of the metallic core. In the case of the piece no. 2, the metallic core seemed to be in a well conservation state. However, in the rest of the samples the presence of manganese, copper, and cobalt revealed an incipient state of corrosion of the metallic core of the pieces. So, the piece no. 2 presented a best maintained core possibly this difference was due to the treatment undergone.

Potassium and titanium were elements detected only in pieces no. 3 and no. 4, so its presence could be related to the PEG treatment that these samples have undergone as if they were coming from the burial, it would have been detected in all samples. In both, these two elements were present in the concretion area of the piece, without reaching the metal core.

Regarding the treatments carried out in the pieces, significant differences can be observed between them. In the piece without any

type of treatment, it was possible to observe how the zinc had barely penetrated the sample. However, sulfur, silicon, and calcium have reached the innermost layers of the samples.

On the contrary, in the treated samples it can be observed how the tannic acid treatment prevented the penetration of exogenous materials along the corrosion layer, except chlorine. On the other hand, the treatment with PEG was not that effective since it was observed how elements such as silicon, potassium, titanium, and zinc have formed a deeper layer than in the sample without treatment.

Therefore, it can be concluded that, among the proposed treatments, it was considered that the tannic acid treatment was the most appropriate due to the conservation of higher part of the metallic nucleus and due to the shallower depth at which they were found the exogenous materials, although chlorine is not effectively removed.

5.1.1 Mineral phases detected in the nails

To better understand the possible penetration mechanism of the exogenous elements, and to clarify the possible corrosion pathways, Raman spectroscopy was used to identify the mineral phases present in the analyzed nails.

By means of Raman spectroscopy, it was found that all the surface of the analyzed pieces were formed mainly by goethite (α -FeO(OH)) and lepidocrocite (γ -FeO(OH)) (Figure 6). In this Figure it can be observed how Raman bands of goethite at 248 cm^{-1} , 300 cm^{-1} , 385 cm^{-1} , 548 cm^{-1} and 685 cm^{-1} overlaps the bands at 251 cm^{-1} , 303 cm^{-1} and 375 cm^{-1} , 525 cm^{-1} and 650 cm^{-1} of lepidocrocite. However, the identification of both compounds was possible depending on their relative amounts at the spot size levels.

Goethite is the most stable and common iron phase in buried artifacts, so its presence was expected¹⁰. Lepidocrocite is an active iron phase and it is one of the most characterized in iron metal pieces that have suffered corrosion after being buried in the moist sediments and in the presence of dissolved oxygen¹¹. With time, lepidocrocite tends to transform into goethite in a corrosion passivation procedure¹². Considering this, the presence of these iron oxyhydroxides gives information about the conservation state of the iron nails analyzed, concretely, the presence of lepidocrocite indicates that the material is not thermodynamically passivated yet¹³. Furthermore, ferroxihite (δ -FeOOH) was also found (Figure 10). This compound is another iron oxy-hydroxide polymorph such as goethite and lepidocrocite which indicates again the formation of Fe^{3+} species¹⁴. This iron form is considered unstable because it tends to transform into more stable phases such as lepidocrocite first and then as goethite (α -FeOOH)¹⁵.

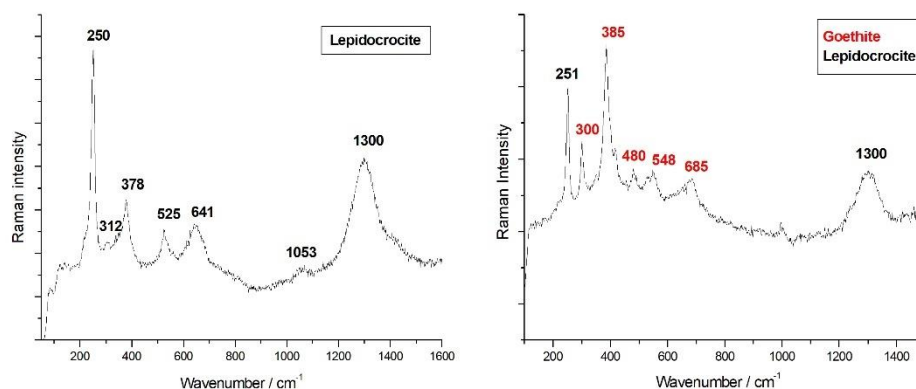


Figure 38 - Raman spectra obtained from the inner face of the iron nails. On the left, lepidocrocite and on the right, goethite and lepidocrocite

Besides, other iron oxides such as magnetite were found (Figure 7). Magnetite, with Raman bands at 350 cm^{-1} and 670 cm^{-1} , occurs as a

thin, stable, and homogeneous iron oxide, which protects the iron surface against further corrosion¹⁶. This compound appears in environments with lacking oxygen conditions, such as buried materials where its formation is favored¹⁷.

Apart from iron phases, some mineral phases that may come from the sediment and were trapped in the corrosion layer¹⁸ were detected. In this way, amorphous carbon (1350 cm^{-1} and 1600 cm^{-1} Raman bands), calcite (CaCO_3 , Raman bands at 155 cm^{-1} , 281 cm^{-1} , 712 cm^{-1} , 1086 cm^{-1}) and gypsum ($\text{CaSO}_4 \cdot 2\text{H}_2\text{O}$, main Raman band at 1006 cm^{-1}) were identified by means of Raman spectroscopy. The Raman spectrum of calcite can be observed in Figure 7.

Moreover, in the spectra showed on the left of Figure 7 a sharp medium intensity peak at 155 cm^{-1} which can be related to the presence of elemental sulfur^{19,20} can be appreciated. The presence of different sulfur compounds (such as elemental sulfur and different sulfides and sulfates) confirms the action of the sulfate-reducing bacteria²¹. This confirmation can be made since a micro-biological study²² considered the SRB responsible for the formation of FeS ²². This fact aggravated the state of conservation of the pieces since the presence of sulfides and sulfates caused both chemical and physical deterioration.

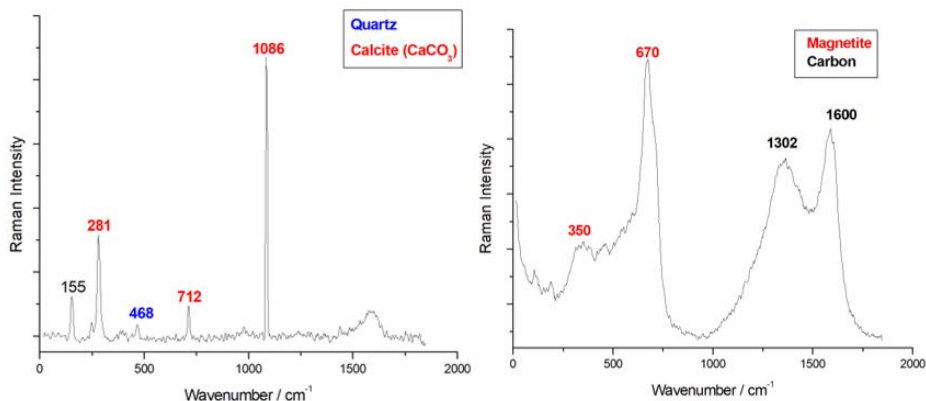


Figure 39 - Raman spectra obtained from the inner face of the iron nails. On the left, calcite and quartz and on the right, magnetite and amorphous carbon

In this way, pyrite (FeS_2) was found indicating as mentioned before, the action of the SRB in the Urbieta shipwreck (Figure 8). The Raman bands of pyrite were found at 341 cm^{-1} , 377 cm^{-1} and 427 cm^{-1} . Huisman et al.²³ reported the presence of this compound in several wooden samples extracted from different waterlogged sites, marine or terrestrial. Rémazeilles et al.²⁴ as well reported the heterogeneous presence of this compound on the extracted nails from the shipwreck. Considering the burial context of the shipwreck and the anoxic conditions that it involves, pyrite may have formed in situ over time by anoxic formation of makinawite promoted by sulfide produced by the microbial activity. However, makinawite was not detected in these samples because it was more likely completely transformed into pyrite²⁵ via greigite²⁴.

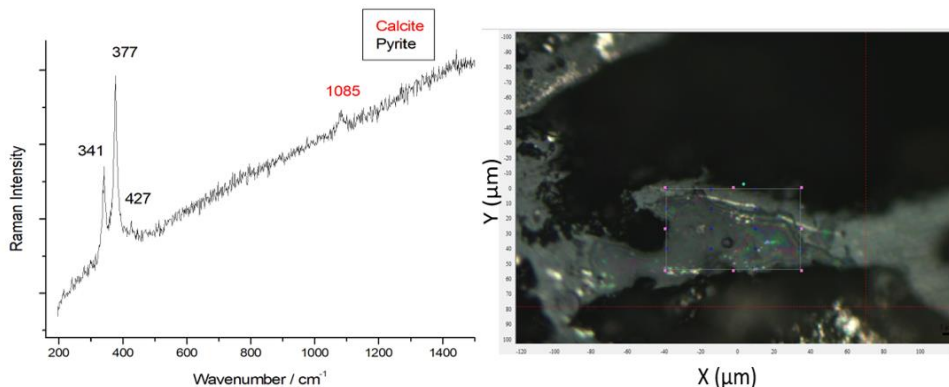


Figure 40 - Raman spectra showing calcite and pyrite on the left, and the analysis area (external region)

Apart from the mentioned compounds, some different sulfides and other sulfur related compounds were also found in the samples as can be observed in the Figure 9. In the case of marcasite (FeS_2), the iron sulfide shows the possible microbial activity just like pyrite. Marcasite Raman bands were detected at 322 cm^{-1} and 385 cm^{-1} . The presence of marcasite could be related to the acidity of the medium and can be formed as a result from the oxidation of mackinawite²⁶, as described in Figure 11. Moreover, it is worthy to point out that zinc sulfide called sphalerite was also found (ZnS) in some areas of the nails, suggesting that microbial activity responsible of the sulfide formation, can transform the dissolved zinc arriving from the sediments in stable zinc sulfide deposited on the surface of the nails.

Regarding the distribution of the iron sulfides it can be said that the presence of pyrite was found in a massive way in the whole area of the nails. In contrast, marcasite was detected only in the more superficial layers of the corrosion bulk.

Oxidized sulfur compounds were also detected. The presence of rozenite ($\text{FeSO}_4 \cdot \text{H}_2\text{O}$, Figure 9) was detected in these samples and its

presence was taken as proof that oxidation of pyrite was occurred⁷. The detection of this compound was possible thanks to its characteristic Raman band at 990 cm^{-1} ²⁷.

In addition, zinc sulfates were also detected. Zinc sulfate forms different type of compounds depending on the numbers of hydrates²⁸. In this case, on the one hand, goslarite ($\text{ZnSO}_4 \cdot 7\text{H}_2\text{O}$) was found by its Raman bands at 984 cm^{-1} and 997 cm^{-1} (Figure 9). On the other hand, a zinc sulfate with a single molecule of water was also detected, gunningite²⁹ ³⁰ ($\text{ZnSO}_4 \cdot \text{H}_2\text{O}$) showed in the Figure 10. The main Raman bands of gunningite was detected at 1022 cm^{-1} .

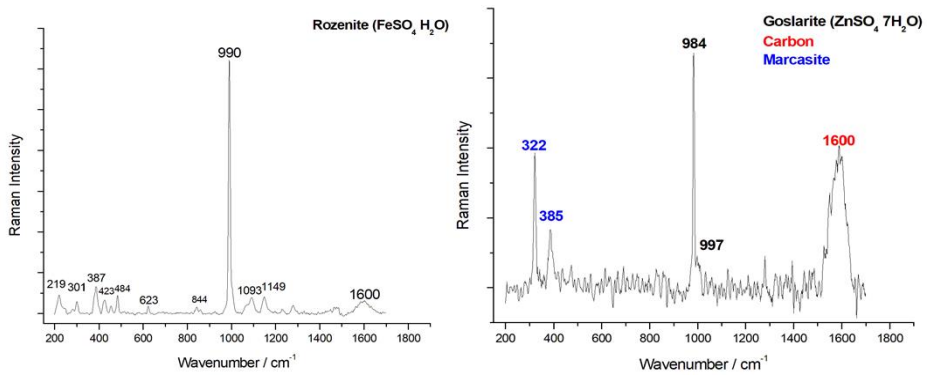


Figure 41 - Raman spectra obtained from the external face of the iron nails showing rozenite on the left and goslarite, marcasite, and carbon on the right.

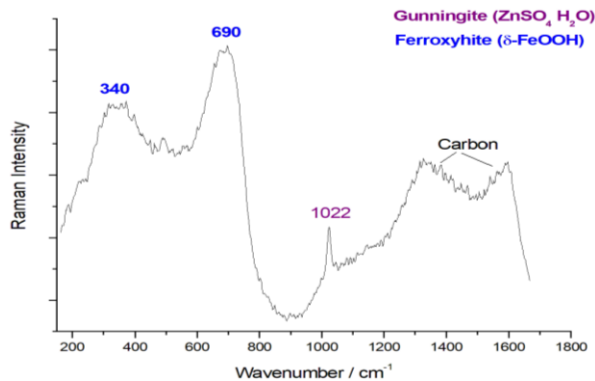


Figure 42 - Raman spectra of gunningite and ferroxihite

To better understand the formation processes of these iron sulfides and sulfates, the oxidation processes of mackinawite can be observed in Figure 11. In this image it can be observed how in anoxic conditions pyrite could be formed and then, under aeration conditions such as those produced after the extraction of a shipwreck, iron oxyhydroxides and iron sulfates could be formed.

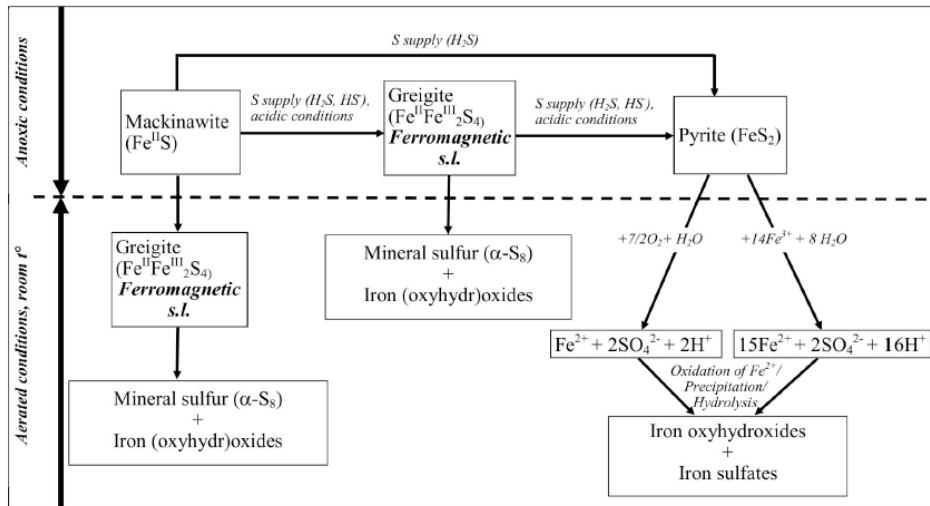


Figure 43 – Oxidation process of mackinawite³¹

Observing Figure 11, the chemical mechanism for the detection of pyrite and mackinawite and the non-detection of greigite could be hypothesized. Mackinawite is the result of sulfide-assisted corrosion of iron³¹. Under anoxic conditions and with a continuous sulfide source, as in the case of the presence and activity of SRB, mackinawite can be oxidized into greigite. Subsequently, greigite can be oxidized into pyrite. The anoxic oxidation of mackinawite to pyrite via greigite involves the progressive assimilation of sulfide species. In this way, the overdose of sulfides that are capable of preventing the

development of SRB is never reached. As no greigite has been found in this case, it can be considered that the microbiological activity has not been very intense, but something punctual.

Greigite was an intermediate compound in the oxidation process of mackinawite into pyrite or in the oxidation of mackinawite into mineral sulfur and iron oxyhydroxide³¹. Its detection is very important for understanding iron sulfides evolution and the effects of MIC. However, the detection of this compound is particularly difficult with micro-analysis methods so magnetic measurement techniques must be used³¹.

Regarding Zn presence in the nails, observing the molecular results, other hypothesis for the origin of the Zn presence arose. Zinc sulphate compound was most frequently used in a great variety of applications, being one of them wood preservative³². The reason why the presence of this compound was found may be due to the use of zinc sulfate in the wood of the shipwreck for its preservation. With the passage of time and due to contact with sediments, the possible presence of the reducing sulfate bacteria (SRB) in these environments has been able to cause the deterioration of zinc sulfate into zinc sulfide (sphalerite) in the wood and due to the contact of the wood with the nails³³. This possibility was confirmed by the fact that zinc was found by means of XRF in the outer area of nails and wood and that both zinc sulfides and sulfates were found by Raman spectroscopy in the same area.

However, the other possible source of zinc, the presence of zinc in sediments around the wreck, cannot be rejected. Zinc sulfides could be formed by SRB and then the sulfates could be generated by later oxidation of sulfides after extraction of the pieces. Both possibilities

must be taken into account since the results obtained do not allow any of them to be ruled out and there is not written data about the treatment of the wood in the past.

Finally, siderite (FeCO_3) was also detected at the inner part of the corrosion bulk, that closer to the metal core. This compound is normally formed in buried iron archaeological pieces where anoxic environment prevail³⁴.

Considering the overall results, some chemical and thermodynamic modelizations by the MEDUSA software were performed to understand better the processes which were taking place. The chemical conditions used for the modeling were the following ones. On the X axis the variation of the redox potential was represented and on the Y axis the logarithmic concentration of the formed products in solution. The original species, as the original compounds state was unknown, were introduced as cations of Ca^{2+} , Zn^{2+} and Fe^{2+} and the HS^- anion. The concentration for these selected cations was 0,02 M for zinc and calcium and 0,01 M for iron³⁵. This difference is based on the fact that calcium and zinc are more soluble than iron, so their concentration would be higher in dissolution. The pH selected for this study was set at 7,5. This value was extracted from a scientific work performed on the estuary to study the physic-chemical parameters³⁶.

$[\text{Ca}^{2+}]_{\text{TOT}} = 20.00 \text{ mM}$
 $[\text{HS}^-]_{\text{TOT}} = 40.00 \text{ mM}$
 $\text{pH} = 7.50$

$[\text{Zn}^{2+}]_{\text{TOT}} = 20.00 \text{ mM}$
 $[\text{Fe}^{2+}]_{\text{TOT}} = 10.00 \text{ mM}$

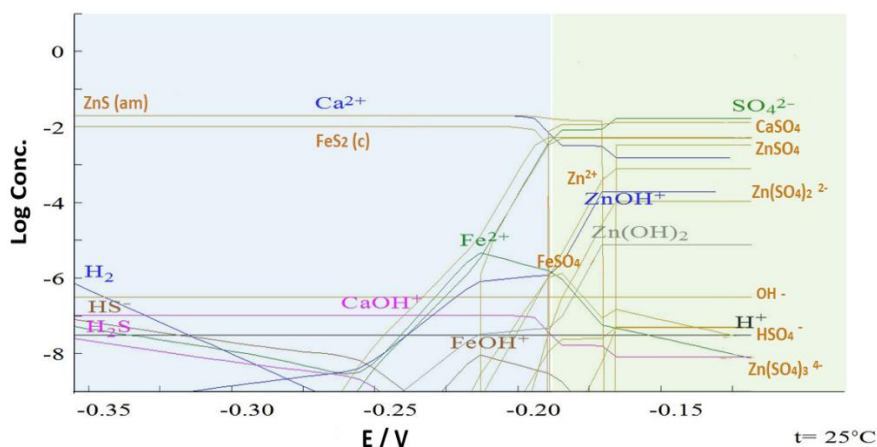


Figure 44 – Logarithmic diagram for the formation of different compounds from metallic iron at different redox potentials, being present also Ca, Zn and sulfides

As it can be observed in the Figure 12, the Medusa diagram shows all the species that can be formed in the conditions specified before. In the diagram, two clearly zones can be observed. The first one where sulfides are present, from -0.35 V to -0.20 (blue color) and the second one where sulfates dominate, from -0.20 V to -0.15 V (green color). Due to the presence of the elements shown in both zones, it was concluded that the analyzed nails have passed from left side to the right one of the X axis, varying the potential from pre to post burial of the pieces as oxidation proceeds.

The resulting diagram predicted most of the detected compounds by Raman spectroscopy, demonstrating the analyzed pieces suffered the two explained oxidation phases. Taking into account the spectroscopic results, no hypothesis for the formation of these compounds could be proposed because it does not allow us to decide on the order of formation of the sulfur and iron compounds.

Moreover, observing the diagram and the Raman results it was concluded that the presence of zinc and calcium affects the balance of iron sulfate and therefore, it affects the piece since there is a competition among the available cations (Fe^{2+} , Ca^{2+} , Zn^{2+}) for the HS^- anion. Therefore, it is clearly seen that a different thermodynamic equilibrium is created depending on the surrounding exogenous species and conditions.

5.1.2 Discussion of Urbieta shipwreck analyses

After these results, it can be said that the chemical characterization of these iron nails has been meaningful in order to have more complete information about their molecular and elemental compositions. This work proved that the proposed methodology, based on the combination of Raman spectroscopy and ED-XRF, both non-destructive techniques are suitable for evaluating the conservation state of archaeological samples and to get information about the raw material at the same time.

The distribution of the elements has allowed knowing which elements present in the samples could be of interest for different interpretations. On the other side, Raman spectroscopy has helped to understand the possible degradation processes that these pieces may have suffered and helped us to determine the degree of degradation of these pieces (providing information on the compounds that have been formed).

Regarding to the type of instrumentation employed, it should be mentioned that portable equipment was widely used providing useful data, in similar cases, in which a museum must be accessed, and pieces should be analyzed in-situ. In this case, in-situ results were a

suitable first approach. However, they presented also a considering disadvantage, such as the fact that it was not possible to know the distribution of the elements and compounds and/or the depth where they were detected. Considering, the valuable information that this kind of data has provided in this study, it is considered crucial to complement the information obtained by portable equipment with laboratory equipment just when specific questions need to be answered (as the origin of Zn).

In addition, it is important to mention the importance of carrying out some destructive procedure for specific purposes as it is the preparation of cross sections for the same aim exposed before. This procedure cannot always be carried out on Cultural Heritage samples, and it is critical to assess in which situations they are worthy. In this case, there were a large number of extracted nails from the shipwreck (> 100), so the option of cutting several nails could be considered. Using cross-sections gives us information about how the composition of the inner to the outer layer of the pieces varies. Unfortunately, the destruction of unique pieces of Cultural Heritage is unfeasible and not advisable in most of the cases.

In this way, the analytical results showed how the conservation state of these iron nails was not the same, depending on the treatment they had undergone. In the case of the piece no.1, without any treatment, it was concluded how this was the piece in which the sulfur has penetrated the most. Due to this, sulfur in contact with the metal core of the piece can cause oxidation of said core. In addition, direct contact with marine archaeological wood, as in the case of iron nails, can cause acidity by oxidation of sulfur compounds. For this reason,

this piece was considered the worst preserved piece of the four nails analyzed.

For the three treated nails, significant differences were observed in the results. Comparing PEG treated nails with tannic acid treated nail. In the case of the two nails treated with PEG in different ways, it can be observed how the results obtained were very similar to each other. Elements such as silicon, titanium and potassium have penetrated to the area where the core was located. Contrary, zinc was also detected in the surrounding area of the nail.

However, in the case of the sample no. 2, treated with tannic acid, none of these elements mentioned have penetrated to the area where the core was located. This means that the treatment applied in the piece no. 2 did not allow exogenous elements to penetrate into the piece, avoiding corrosion and deterioration of the metallic core. Therefore, in broad terms, it can be elucidated that the treatment based on the application of tannic acid³⁷ for the piece was the most appropriate regarding its conservation. A studied performed by T. Perez³⁸ demonstrated the protective effects of the tannic acid treatments with respect to corrosion as it blocks the action of oxygen and humidity.

Moreover, regarding conservation treatments, it can be also concluded that the study of any archaeological sample extracted from the marine environment is necessary for its subsequent treatment which allows the piece to be conserved and preserved over time.

In relation to the degradation state of these pieces, we can also conclude which factors were able to promote the degradation of these pieces. As previously mentioned, the main degradation factor in these nails was the sediment conditions. This shipwreck was submerged in

river water for many years, which seriously aggravated the condition of the ship and its structure. The presence of zinc in the sediments and in the river water and another series of exogenous elements found in the nails could cause serious problems ever since. Zinc contamination in these nails was playing a very important role at the chemical level. This element was very reactive and competes with iron to generate sulfides and sulfates, which led to an alteration of the chemical equilibrium of the piece as a whole. In this way, sulfur played a fundamental role as another important factor in the degradation process. Once the shipwreck was extracted, another degradation factor was oxygen. The presence of this element in environmental conditions aggravated the formation of sulfides and sulfates, worsening the conservation state of the archaeological pieces.

Therefore, it can be said that the degradation factor of these pieces were factors such as the presence of sulfur and zinc, coming from sulfate-reducing bacteria and coming from sediment and from uncontrolled discharges, and the presence of oxygen in the pieces, which caused a very drastic change in the environmental conditions of the samples.

Among the degradation factors that may have affected these pieces, one of the most important at an archaeological level was the presence of sulfur. This element has caused several damages to other shipwrecks, such as the *Vasa*^{1,5} or the *Mary Rose*³⁹. The presence of sulfur compounds in archaeological materials buried in marine sediment is very common⁵. When a material remains submerged for a long time in a marine environment, in contact with submerged archaeological wood, iron and in contact with sediments, it can be attacked by SRB. This bacteria form a biofilm on the metal piece

causing electrochemical reactions and causing local corrosion of the samples⁴⁰. In addition, its presence in the metal piece can locally alter the physical-chemical parameters of the metal surface, such as pH and dissolved oxygen concentration (resulting in the decrease of both⁴⁰).

Many studies were performed on the effects of sulfur compounds in submerged or buried pieces, as is the case of C. Rémazeilles et al.^{6,22,31}, Y. Fors et al.^{5,7,41,42}, C. Björdal et al.⁴³, C. Gjelstrup et al.⁴⁴, M. Sandstrom et al.¹. All of them had studied the presence of this compound and its possible formation process in wood and in buried pieces concluding that the effects of these compounds are detrimental to the state of preservation of archaeological pieces.

5.2 THE BAKIO SHIPWRECK

As mentioned in Chapter 4, for this PhD project several pieces belonging to this shipwreck were analyzed. In this 5.2 section the results obtained for each group of samples are exposed.

5.2.1 Musket and bullet analysis

The pieces extracted from the Bakio's shipwreck, such as the musket and the bullet, were analyzed in-situ in at the Archaeological Museum of Bilbao, to prevent their translation to the laboratory, with elemental and molecular portable analytical techniques. The bullet (piece no. 1) was surrounded by a concretion (piece no. 2) that completely covered it. Piece no. 2 was detached from piece no. 1 providing access to the bullet indeed. The musket (piece no. 4) was made up of a wooden part, a metallic part, and a decorative part. In this case, the metallic part of the musket was also detached (piece no. 3). All the pieces were analyzed independently, and the results of each piece are shown below.

For the elemental characterization by ED-XRF, unfortunately, only three pieces were available for this analysis (Sample 1, 2 and 4 from Figure 5 in Chapter 4). The metal part of the musket, piece no. 3, was not available because it was being processed by the archaeologists of the museum.

First, the center of the bullet and the concretion areas were analyzed (pieces no. 1 and no. 2) and the results were compared in the Figure 13. The ED-XRF analysis performed in the center of the bullet (on the left of Figure 13), showed that it was composed mainly by lead and in minor extent by sulfur, chlorine, calcium, iron and copper. The results obtained for the concretion area surrounding the bullet (on the right of Figure 13) revealed that it was composed mainly of iron,

with a lower presence of other elements such as sodium, sulfur, chlorine, calcium, titanium, copper and lead. Most of the elements detected may have a marine origin, as in the case of calcium, sulfur, chlorine and sodium. The detection of copper may be due to the composition of the bullet.

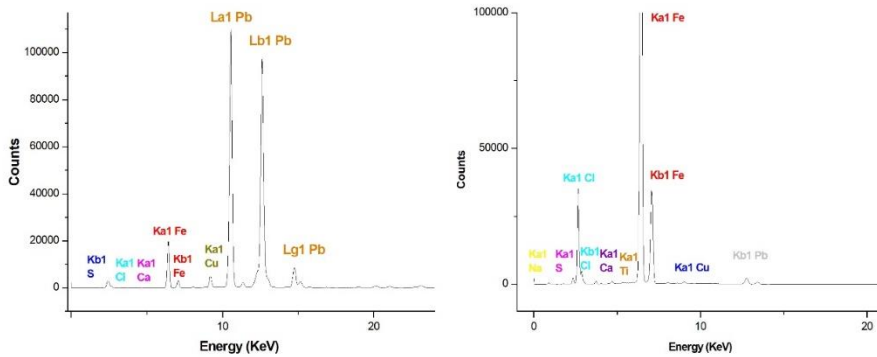


Figure 45 - Portable ED-XRF results for the bullet on the left, and for the iron concrete on the right

These results made us consider a hypothesis about the formation of the concretion. Lead is a more stable element, so it does not corrode so easily, but iron is a very reactive element, which under marine environmental conditions could react by forming a concretion around the bullet. Then, when the environmental conditions change drastically in the extraction of the pieces, the iron rust layer was detached.



Figure 46 - Portable ED-XRF for the should stock of the musket

In the should stock of the musket, the part of the gun that provided structural support, elemental analysis revealed the detection of calcium, iron, and strontium (Figure 14). This may mean that with the effect of the waves and the contact with the sediments and sand, a layer of small depositions may have formed in this area, covering part of the sample.



Figure 47 - Portable ED-XRF results for the wood area of the musket

In the wood areas, the high presence of iron together with other elements, such as sulfur, chlorine, calcium and lead was detected

(Figure 15). Most of these elements such as chlorine, calcium and sulfur were characteristic of seawater ions, so their origin could be related to its sinking. The presence of sulfur indicates the microbiological activity. In the case of lead and iron, their origin may come from the corrosion due to the contact of waterlogged wood with metal pieces. The presence of lead and sulfur in wood was also observed in other shipwrecks such as the Vasa⁷, the Mary Rose⁷, Mandirac³¹ or Lyon Saint-Georges wreck n°4(LSG4)³¹.

The contact of the oxygen present in the atmosphere with the subaquatic archaeological pieces could have caused an acid state due to the oxidation of sulfur compounds, especially in the presence of iron ions, as in the case of Vasa⁷.

In the decorative parts of the musket, the elemental results obtained are shown in Figure 16. It can be concluded that the decorative parts of the musket were composed mainly of copper and zinc (brass alloy) and to a lesser extent of other minor elements such as sulfur, chlorine, calcium and iron.



Figure 48 - Portable ED-XRF results for the decorations of the musket

The trigger area appeared to be similar or the same as the decorative areas of the musket to the naked eye. However, in this case, two different spectra were obtained which are showed in Figure 17.

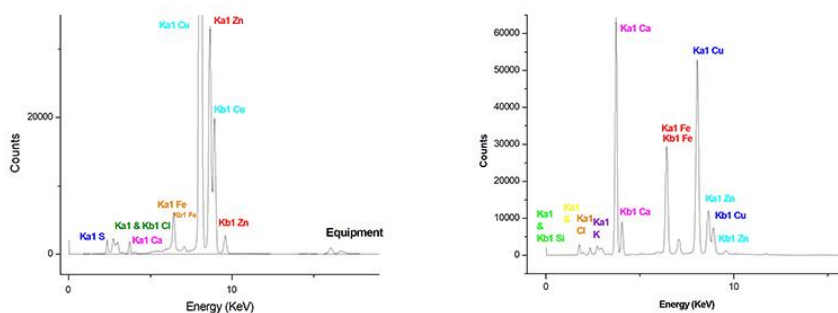
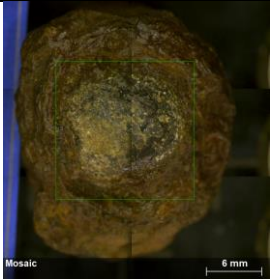
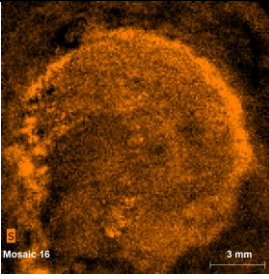
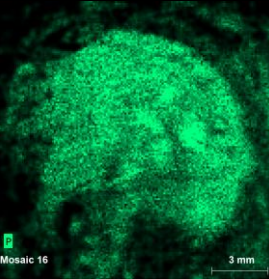
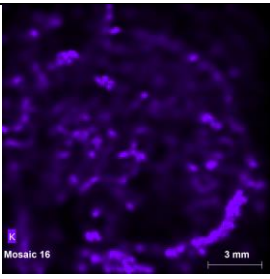
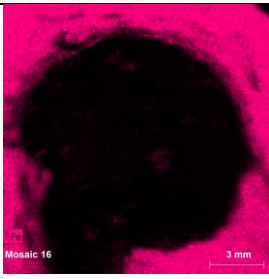
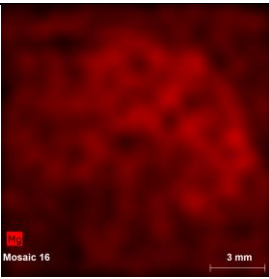
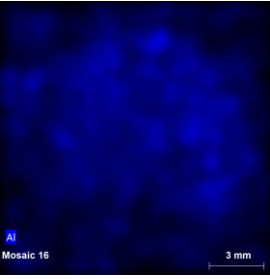
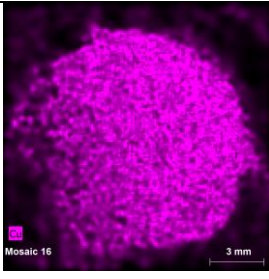
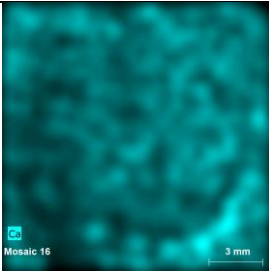


Figure 49 - Portable ED-XRF results for the trigger of the musket

The two different spectra obtained for this area showed little differences, such as the presence of silicon and potassium and the different intensity of calcium, iron, copper and zinc signals. Despite these differences, the elemental composition of this area was very similar to the one obtained in the musket decorations.

In order to get more detailed information, the pertinent permits were requested to transport the bullet (piece no. 1) to the laboratory and

to carry out more exhaustive analyses. Unfortunately, it was not possible to perform this with the rest of the pieces because of their state of conservation and its size.

| Piece no. 1 | Sulfur | Phosphorus |
|---|---|--|
|  |  |  |
| Potassium | Iron | Magnesium |
|  |  |  |
| Aluminum | Copper | Calcium |
|  |  |  |

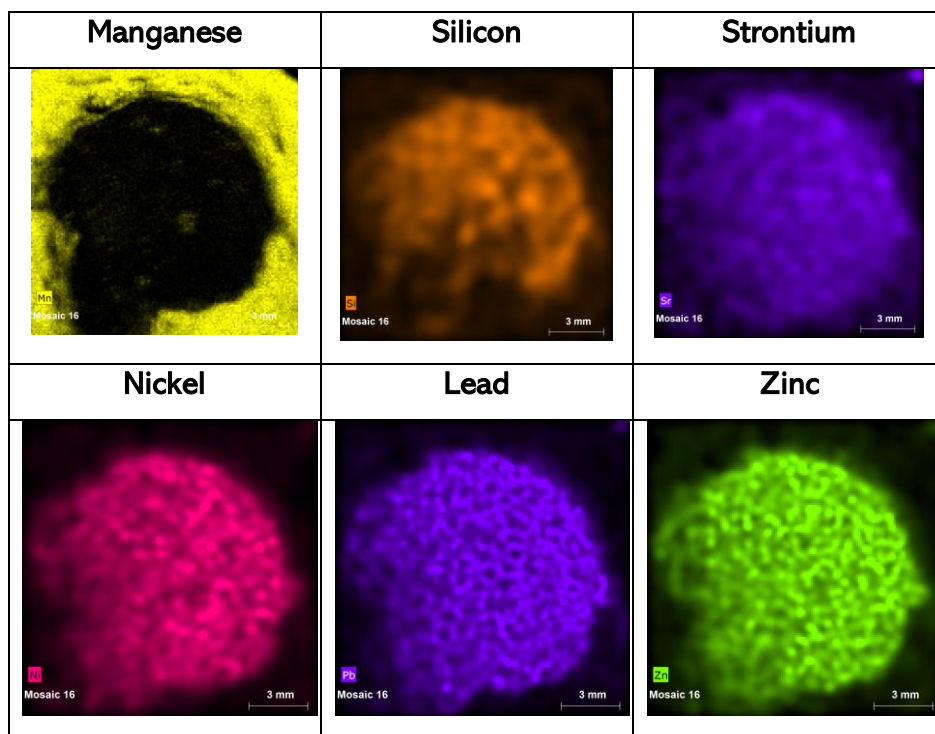


Figure 50 - Elemental image of the piece no. 1 by ED-XRF

In the laboratory, ED-XRF image analyses were performed in order to get information about the distribution of the elements. In this way, some elements such as sulfur, phosphorus, copper, silicon, strontium, nickel lead and zinc were only detected in the bullet (Figure 18). The distribution map of these elements was the same except for the case of sulfur, phosphorus, and silicon. These ones showed a different distribution pattern from each other. On the other hand, iron and manganese were found surrounding the area of the bullet, in the concretion.

As previously mentioned, the bullet was composed mostly by lead. Iron was only detected surrounding the bullet and lead was only detected in the bullet. In the Figure 19 the elemental distribution map

of both elements where the presence of each on in the sample was clearly observed.

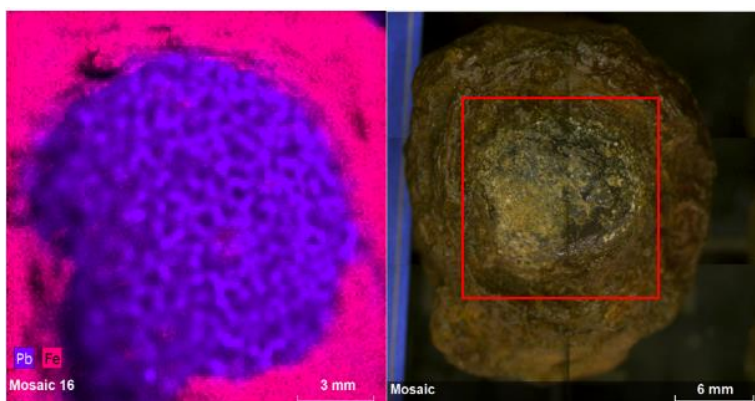


Figure 51 - Elemental image of iron and lead in the piece no. 1 by ED-XRF

The elemental mapping performed on the back of the bullet did not provide new information regarding the distribution of the elements detected.

Regarding the molecular characterization by portable Raman spectroscopy, the results obtained were divided into four parts, one for each piece as follows:

The results obtained for the bullet (piece no. 1) showed the presence of goethite and elemental sulfur (Figure 20). The presence of these two compounds was detected around all the pieces of this shipwreck. Goethite confirmed that despite the deterioration of the metal piece, its state of conservation may be relatively stable since it is the most stable iron corrosion compound. The detection of elemental sulfur was a sign of the biological activity that the piece may have undergone underwater. Sulfate-reducing bacteria, in anoxic environments, reduced the sulfur compounds present in seawater (sulfate ions) for the degradation of organic compounds to form

hydrogen sulfide. Then sulfide can be oxidized to different less reduced sulfur compounds, such as elemental sulfur when the pieces are extracted and get in contact with the atmospheric environment²¹.

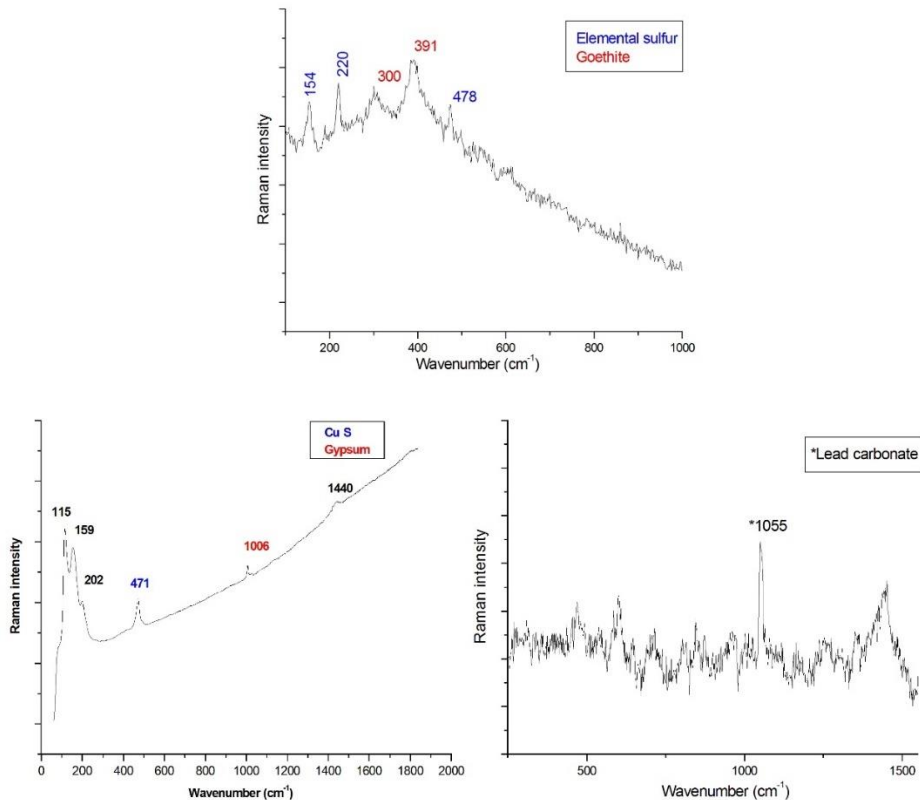


Figure 52 - Portable Raman results obtained from the piece no. 1

Apart from these compounds, others compounds such as CuS, gypsum ($\text{CaSO}_4 \cdot 2\text{H}_2\text{O}$) and lead carbonate (PbCO_3) were also detected. As discussed above, the detection of different sulfur compounds such as sulfides and sulfates confirm the presence and activity of SRB. In this case, a copper sulfide was detected thanks to the band observed at 471 cm^{-1} , characteristic of the sulfur-sulfur

bond⁴⁵. As for the band characteristic of the Cu-S bond, it should be observed at 270 cm^{-1} but it is likely to be indistinguishable because it is much weaker band than the S-S bond⁴⁶.

Gypsum was also detected based on its characteristic Raman band of the sulfate vibration at 1006 cm^{-1} and the presence of lead carbonate was confirmed thanks to the 1055 cm^{-1} Raman band of carbonate bounded to lead. The presence of gypsum in the samples involves the transformation from reduced sulfur compound to this sulfate salt and this formation often involves a large volume expansion resulting in the alteration of the conservation state of the sample⁷.

In the analysis performed on the piece no. 2, the iron concrete layer, the results obtained showed the presence of two iron oxides, lepidocrocite and goethite. Apart from them, quartz (SiO_2) was detected thanks to the recognition of its main Raman band at 465 cm^{-1} .

The molecular analysis performed by portable equipment on the sample no. 3 showed the presence of different iron oxides such as lepidocrocite and goethite, together with the presence of elemental sulfur and erdite ($\text{NaFeS}_2 \cdot 2(\text{H}_2\text{O})$), as can be seen in Figure 22. The presence of erdite⁴⁷, with main Raman bands at 218 cm^{-1} , 281 cm^{-1} , 393 cm^{-1} , 484 cm^{-1} and 593 cm^{-1} , demonstrated the activity of sulfate-reducing bacteria which in turn react with the iron present in the sample to give a hydrated sodium iron sulfide.

From a total of 100 point-by-point measurements performed on the piece, it was observed that lepidocrocite was the iron specie most frequently detected. As it is already known, goethite is the most stable and common iron phase in buried artifacts⁴⁸. This oxide tends to form a homogeneous corrosion layer that protects the metallic

sample. Lepidocrocite, in contrast, is a thermodynamically more active phase, which not to have protective properties and it trends to transform into goethite. Furthermore, lepidocrocite formation generates a higher mechanical stress and a volume expansion than in the case of goethite⁴⁹. Therefore, it can be concluded that the presence of lepidocrocite in this piece has led to the formation of cracks on the surface of the sample, getting worse its state of conservation⁵⁰.

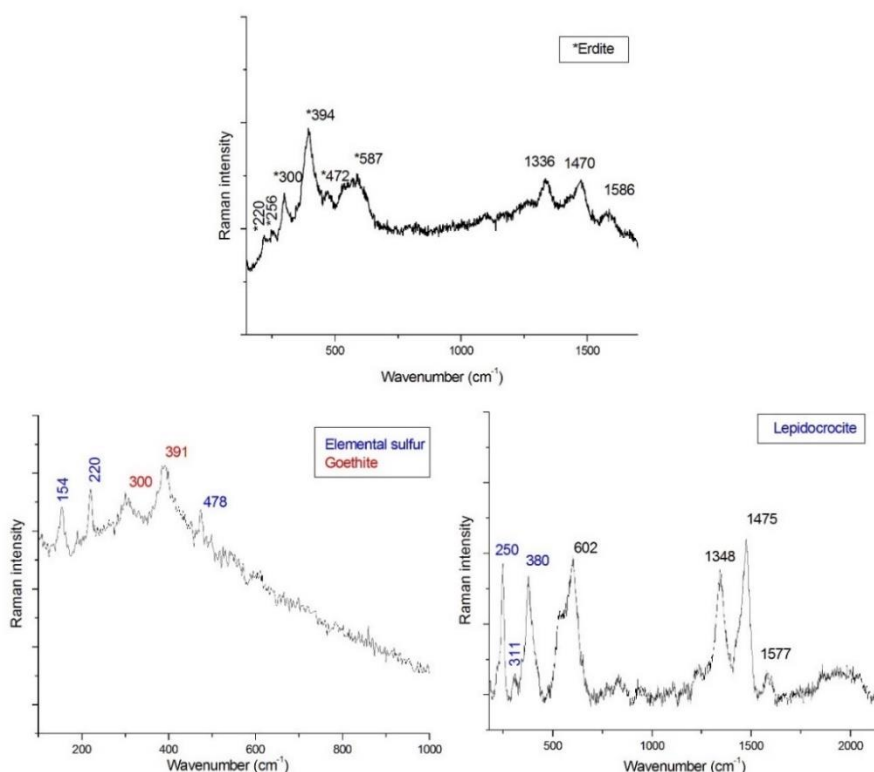


Figure 21 - Portable Raman results obtained from the piece no. 3

In addition to the compounds described above, in Figure 21, in the spectrum where erdite was found, bands of unrecognized compounds were also observed. Kostadinovska et al.⁵¹ performed Raman analysis

of iron gall ink where its characteristic Raman bands are at 1333 cm^{-1} , 1481 cm^{-1} and 1587 cm^{-1} . Given that the Raman bands found in piece no. 3 were in a similar position to that described by Kostadinovska et al.⁵¹, the possibility has been raised that the bands found in that were due to the presence of iron gall ink. This component is an iron pyrogallate which has a plant origin. It was employed as black ink for more than 18 centuries⁵¹.

The Raman analyses performed on the musket only detected throughout the piece elemental sulfur (Figure 22), once again confirming the SRB activity.

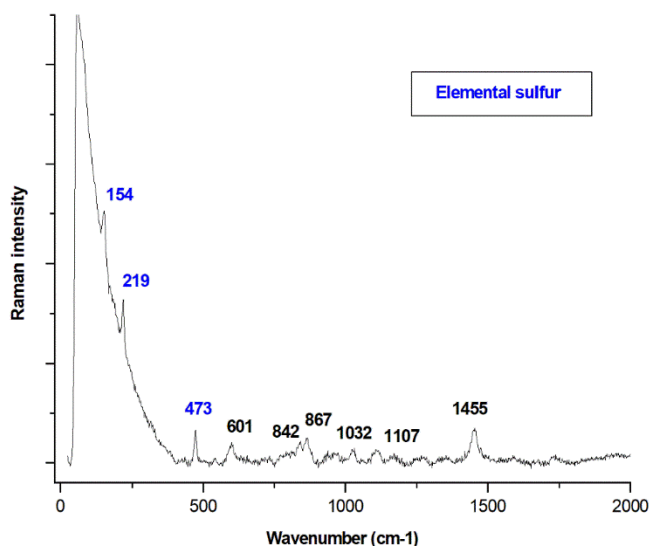


Figure 22 - Portable Raman results from the musket

With the idea of obtaining more molecular information, only the smallest pieces, the bullet and the iron concretion (pieces no. 1 and no. 2), were transferred to the laboratory.

Molecular analysis of the bullet with laboratory Raman equipment revealed the presence of litharge (PbO) and laurionite (PbOHCl), both

shown in Figure 23. The presence of lead (II) oxide was detected by the characteristic Raman band at 146 cm^{-1} . Its origin may be related to the formation of a protective layer of corrosion products formed during burial or due to a long exposure to the external environment⁵² forming a chemical reaction between the oxygen in contact with the lead of the bullet⁴. Once exposed to the atmospheric environment, they are quite stable compounds.

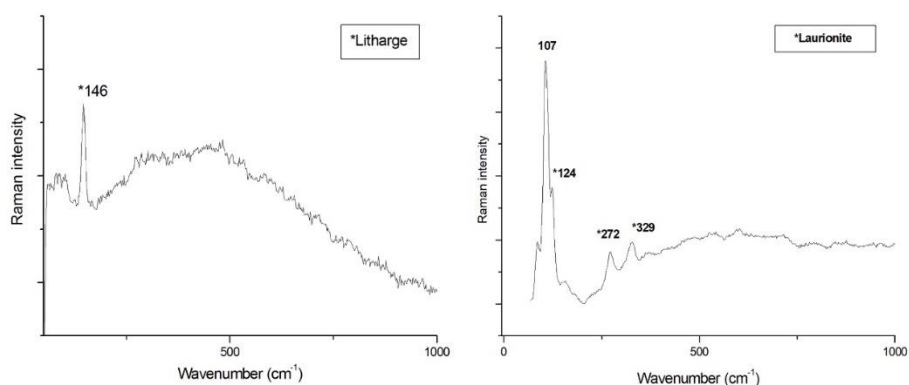


Figure 23 - Raman spectroscopy laboratory results obtained from the bullet

In the case of laurionite⁵³, this mineral was identified by the detection of three characteristic Raman bands, the principal one located at 124 cm^{-1} and other two at 272 cm^{-1} and 329 cm^{-1} . Lead chloride minerals concretely laurionite and paralaurionite are mixed anionic species which are thermodynamically stable. These minerals are of archaeological significance and are mainly found among the leaching products of slag dumps⁵⁴. Unfortunately, there is not much information of Raman spectroscopy analysis on this type of minerals.

The analysis performed on the iron concretion (piece no. 2), showed the presence of a mixture of iron oxides as can be observed in the

Figure 24, together with the three characteristic bands of iron-gallate like complexes.

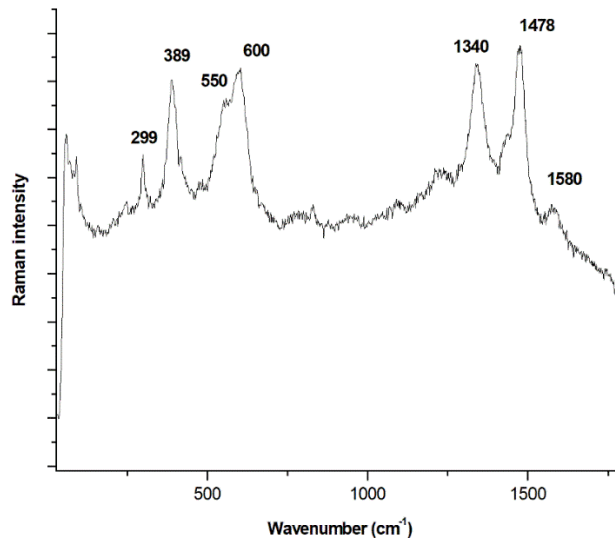


Figure 24 - Raman spectroscopy laboratory results from the iron concrete

In this case, iron oxides such as goethite, hematite and akaganeite were detected. Together with the characteristic Raman bands of goethite, 299 cm^{-1} , 389 cm^{-1} , 550 cm^{-1} , 600 cm^{-1} , traces of hematite (293 cm^{-1}) and akaganeite (300 cm^{-1}) were also detected. The presence of these compounds is due to the result of the corrosion processes inherent to iron.

Apart from iron oxides, the presence of a compound with characteristic Raman bands between 1300 cm^{-1} and 1600 cm^{-1} was again detected. Its characteristic Raman bands coincide with the main Raman band of iron gall ink⁵¹.

5.2.2 Detached pieces from the iron anchor and the swivel gun

As commented in Chapter 4, two pieces exposed on the Bakio's town hall were analyzed, an anchor and a swivel gun. The poor state of conservation of the pieces and their location did not allow us to carry out in-situ analysis of the samples. Due to the detaching process that they were suffering, some corrosion chips detached from the anchor and from the swivel gun were collected and transferred to the laboratory for their analysis. Since the objective of these pieces was to know the possible differences in growth of the corrosion layer, both sides of the selected pieces were analyzed.

The results obtained in the characterization of the raw materials employed in the manufacture of Bakio's extracted pieces will be shown and discussed next. From the elemental point of view, the semi-quantitative results obtained by ED-XRF for the external face of the iron anchor were Fe (87.9 %), Al (5.6 %), Ca (3.3 %), Si (1.9 %), K (0.6 %), Ti (0.2 %), S (0.2 %), Cl (0.2 %), Mn (0.1 %). Besides, the semi-quantitative results obtained for the internal face of the iron anchor were Fe (97.5 %), Cl (1.6 %), Al (0.3 %), Si (0.2 %), Na (0.1 %), S (0.1 %), Ca (0.1 %), Pb (0.1 %).

In the case of the swivel gun, the semi-quantitative results obtained for the external face were Fe (82.7 %), Al (10.2 %), Ca (2.7 %), Si (1.7 %), Pb (0.9 %), Co (0.4 %), Na (0.3 %), Cl (0.3 %), Mn (0.2 %), P (0.1 %), Ti (0.1 %), S (0.1 %), K (0.1 %), Mg (0.1 %), Zn (0.1 %). In addition, semi-quantitative results obtained for the inner face were Fe (87.4 %), Al (7.1 %), Ca (2.7 %), Si (1.0 %), P (0.6 %), Pb (0.6 %), Co (0.3 %), Ti (0.2 %), Mn (0.1 %). This semi-quantitative data was calculated from the analysis of the whole surface of the mentioned chips.

The detection of various elements in both pieces suggested the use of cast-iron in the manufacture since the XV century⁵⁵ as the raw material for the pieces^{56,57}. Cast-iron is an alloy mainly composed of iron, carbon (1.5-4%), and silicon (1-3%) with other minor elements such as traces of aluminum, sulfur, manganese, chromium or phosphorus⁵⁶⁻⁵⁹. Unfortunately, carbon cannot be detected by ED-XRF. Considering the results, raw material of the pieces was a cast-iron low in silicon; the low silicon concentration represents that carbon cannot be converted in graphite, avoiding the formation of softer iron due to the presence of graphite^{60,61}.

In both pieces analyzed, the relative presence of silicon was higher in the external parts than in the inner parts. Considering that epoxy resin applied during restoration works conducted in 2005 was epoxy polyamide zinc phosphate, some elements detected in the samples such as silicon and phosphorous may come from the epoxy resin⁶². This fact can explain how the application of epoxy resin is another possible source of contribution (apart from the source of cast-iron) for the presence of silicon and phosphorous in the samples.

Aluminum was also detected in both pieces in a high relatively presence. Its detection could be directly related to the manufacture process. Aluminum is one of the basic alloying elements added to cast-iron for increasing the fire resistance of the material⁶³. Its origin could also be related to sediments.

The presence of calcium in both pieces must be considered as a contamination due to its low concentration and should be related with compounds present in the seawater and/or sediments where the anchor was settled. The same applies for chloride and potassium, which are elements present in the marine sediments and seawater.

Here, sulfur merits a double consideration because it can be part of the cast-iron but also can have a biological origin from the microbial activity around the burial.

As discussed above, the raw material of the pieces seems to be a cast-iron low in silicon. The low concentration of this element represents that carbon cannot be converted in graphite, avoiding the formation of softer iron due to the presence of that graphite. However, if carbon is not converted to graphite during melting, it could react with iron to form iron carbide. To avoid this problem, manganese is added because manganese carbide is most easily formed than iron carbide; moreover, manganese carbide promoted the hardness of cast-iron, and this was known since XIV century. However, the source of this element could also come from the iron ore or from the alloying elements present in cast-iron⁶⁰. Therefore, with the information obtained, the source of manganese is not clear.

Another element that requires special attention is lead. This element appears in the outer and in the inner face of the samples analyzed. At first, the presence of this element in these samples seems difficult to explain. Lead is not an element belonging to the cast-iron typical alloy, so this origin is excluded. Therefore, its origin must be related to an external contribution. The only possibility of finding lead around the pieces is in the composition of other pieces analyzed of the same shipwreck as in cannonballs and shotgun bullets in one musket that were found together with the analyzed samples. These pieces are composed mainly by lead. Taking this into account and considering that the reactivity of oxidized lead (II) with chloride promotes the formation of PbCl_4^{2-} in seawater environments, it could be said that

this species could migrate from the lead objects to the iron ones, being trapped on the iron surfaces¹⁹.

In the case of titanium, it was present in the outer face of the anchor but not in the inner one. If the titanium was part of the manufacturing process of the pieces, it would be present both inside and outside, but that is not the case. Therefore, its presence in the outer face of the sample must be due to the use of titanium oxide in the paints applied in 2005 during the restoration work of the artifact.

If a comparison is made between the results obtained from the different faces for the different parts, the major elements detected in the external face showed the same results. Maybe these results are the same because (a) both pieces are manufactured with cast-iron and (b) were subjected to the same chemical treatment and exposed to the same environment. In contrast, the results obtained from the inner face of the pieces showed the presence of the different elements such as chlorine, sodium, sulfur, phosphorus, cobalt, titanium and manganese. This suggested that the bulk of the cast-iron in the cannon is different from the one used for the anchor due to differences in elements and its relative presence as observed in the XRF measurements. Therefore, it can be deduced from these results that the anchor and the swivel gun were from different eras. This hypothesis would be supported by the archaeologist Jose Manuel Matés Luque, whose studies also affirm that the anchor did not belong to the same period as the rest of the shipwreck's materials.

In general terms, the raw materials employed on the manufacture process according to the use of cast-iron were iron, carbon, silicon, aluminum, manganese and phosphorous. However, silicon and aluminum can be detected both as part of the raw materials and as

contribution from sediment/seawater. The rest of elements detected could be exogenous compounds such as chlorine, potassium, calcium, lead, sodium, cobalt, magnesium, titanium and zinc. All of them were not part of the raw material, they were detected in the samples due to external contamination.

Regarding Raman spectroscopy, first the results obtained from the analysis of the iron anchor are exposed. It was found that the external face of these pieces was formed mainly by lepidocrocite ($\gamma\text{-FeO(OH)}$) and akaganeite ($\beta\text{-Fe}_2(\text{OH})_3\text{Cl}$; Figure 25). Lepidocrocite is one of the most reported results in metal pieces that have suffered corrosion after being buried in the moist sediments and in the presence of dissolved oxygen⁶⁴. However, the composition of the corrosion layer could vary depending on the burying condition (pH, concentration of oxygen, and presence of salts). This iron phase is a thermodynamically active and unstable phase because it trends to transform into goethite⁵⁰. Its presence and the absence of goethite in the sample shows the instability of the corrosion layer.

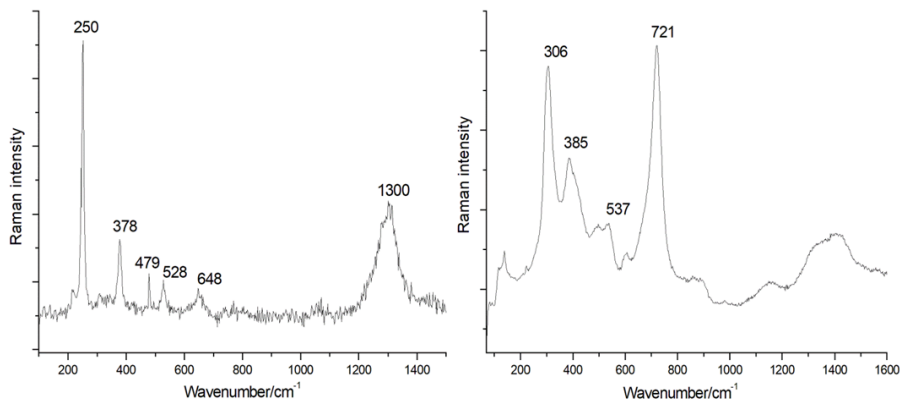


Figure 53 - Raman spectrum of the outer face of the iron anchor showing the bands of lepidocrocite (left) and akaganeite (right)

Akaganeite, with the three characteristic Raman bands at 306 cm^{-1} , 385 cm^{-1} and 721 cm^{-1} , is an oxy-hydroxide that is formed when the artifacts are in contact with chloride-rich environments⁶⁵; the Raman spectrum of akaganeite shown in Figure 15 is almost identical to one reported by Neff et al.⁶⁶. It is known that chlorides are the most harmful stressor for archaeological irons^{67,68} and must be removed as soon as the pieces are extracted from the burial⁶⁹.

The presence of these iron oxyhydroxide, lepidocrocite, and akaganeite gives information about the conservation state of the analyzed pieces. In this case, it is confirmed that the conservation treatment applied some years ago was not effective because chlorides were not removed, as evidenced by the presence of akaganeite, and the presence of lepidocrocite indicates that the material is not thermodynamically passivated yet.

In contrast, in the inner face of the pieces analyzed from the iron anchor, a greater number of iron oxides than in the outer face were detected, particularly, goethite, maghemite, as well as lepidocrocite (Figure 26). As in the previous case, the inner face of these pieces is composed mainly by lepidocrocite but not akaganeite. The presence of goethite ($\alpha\text{-FeOOH}$), the most stable and common iron phase in buried artifacts⁶⁶, was scarcely found reduced to some specific areas. Therefore, it could be said that the same problem was found in the inner part. The transition of lepidocrocite to goethite⁶⁴ can be seen in the inner face of these samples, like Figure 26 shows. Maghemite ($\gamma\text{-Fe}_2\text{O}_3$) is a compound that appears commonly in the rust layer of the buried archaeological pieces. Apart from the iron phases, some degradation products that may come from the sediment or from airborne particulate matter¹⁸ and have been trapped in the corrosion

layer were also detected. For instance, gypsum and calcite, were found (Figure 26).

Moreover, compounds belonging to the reaction of the epoxy resin with the metal were detected, such as rutile (TiO_2), suggesting again the use of this filler in the paints of the past restoration treatment performed in 2005. This could mean that the treatment has not reacted properly with the material of the archaeological piece or the loss of the applied protector layer, probably due to the incompatibility between materials. Anyway, it is demonstrated that the best treatment for an iron buried tool exposed to the atmosphere is that which accelerates the transformation of lepidocrocite/akaganeite into goethite^{68,70}.

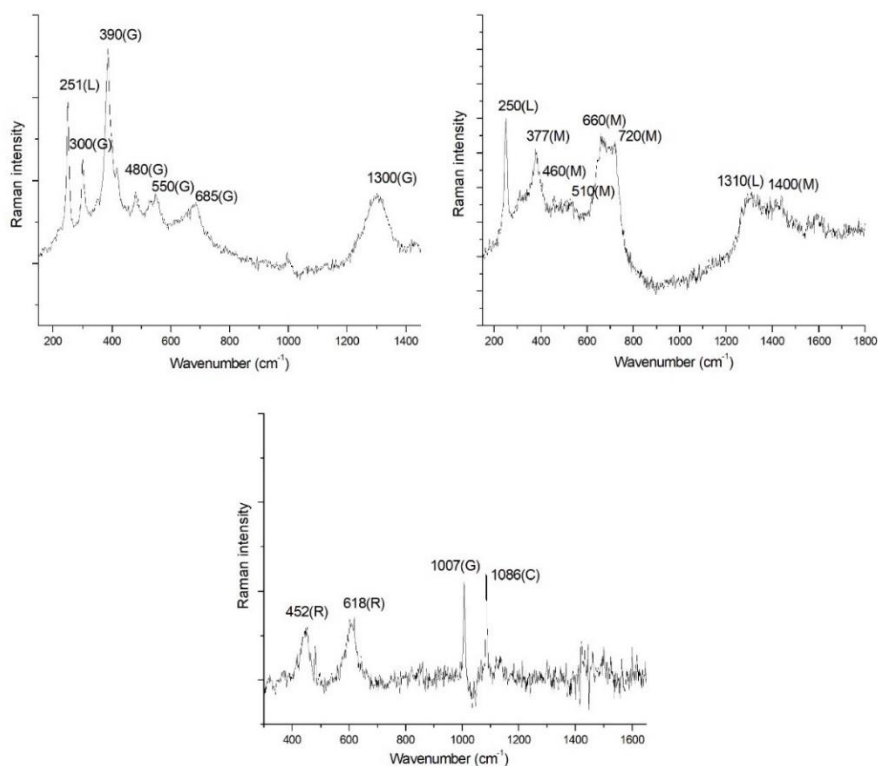


Figure 2654 - Raman spectra obtained on different spots of the inner face of the anchor

Summarizing, it can be said that in the analyzed pieces, the predominant compound was lepidocrocite, which means that the pieces are still evolving from lepidocrocite to goethite maybe because they were extracted from the sea and have not reached equilibrium. The massive presence of lepidocrocite is attached to the cracking process of the rust layer, which is dangerous for the good preservation of iron pieces⁶⁴ because this crack allows the oxygen to enter through the corrosion layer corroding the metal core. If this process continues with time, the pieces will be converted to dusty material and therefore lost.

In the case of the analysis of the outer face of the extracted pieces from the swivel gun, hematite ($\alpha\text{-Fe}_2\text{O}_3$) and lepidocrocite were detected (Figure 27). Hematite is a red iron oxide that can be formed when other oxyhydroxides of iron are heated over 250°C. This compound is not usually formed as a corrosion product in underground conditions, but even so, its presence can be detected in archaeological iron. Considering that the laser during the Raman analysis was modulated to avoid any transformation of iron oxyhydroxide to hematite, the formation of the latter by means of the analysis is rejected. Therefore, the presence of this compound can be related to the fact that this object was exposed to high temperatures, during the shots, before burial⁵⁰. When studying iron oxides, it is crucial to start very low laser power to avoid misunderstanding caused by thermal alterations.

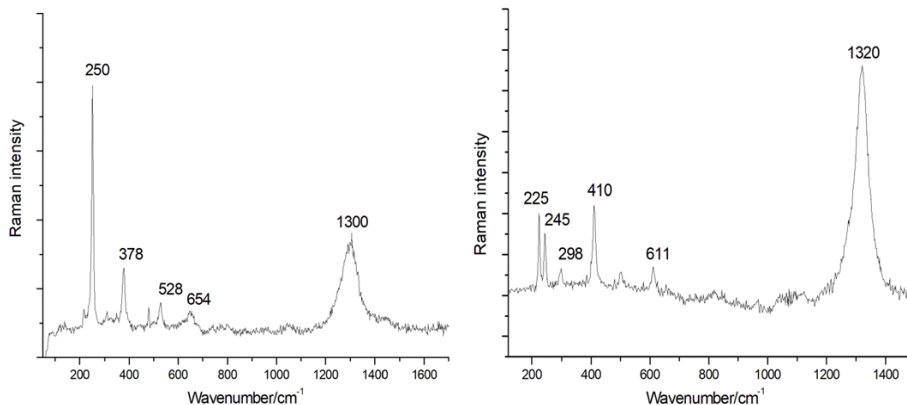


Figure 55 - The two iron compounds systematically detected in the outer face of the swivel gun. On the left, lepidocrocite and on the right, hematite

In contrast to the outer face, the analysis of the inner face of the analyzed pieces from the swivel gun, revealed the same scenario as in the case of the inner face of the iron anchor was found. A greater number of iron oxides than in the outer face of the sample were detected (Figure 28). More concretely, maghemite, goethite, akageneite, and also lepidocrocite were detected.

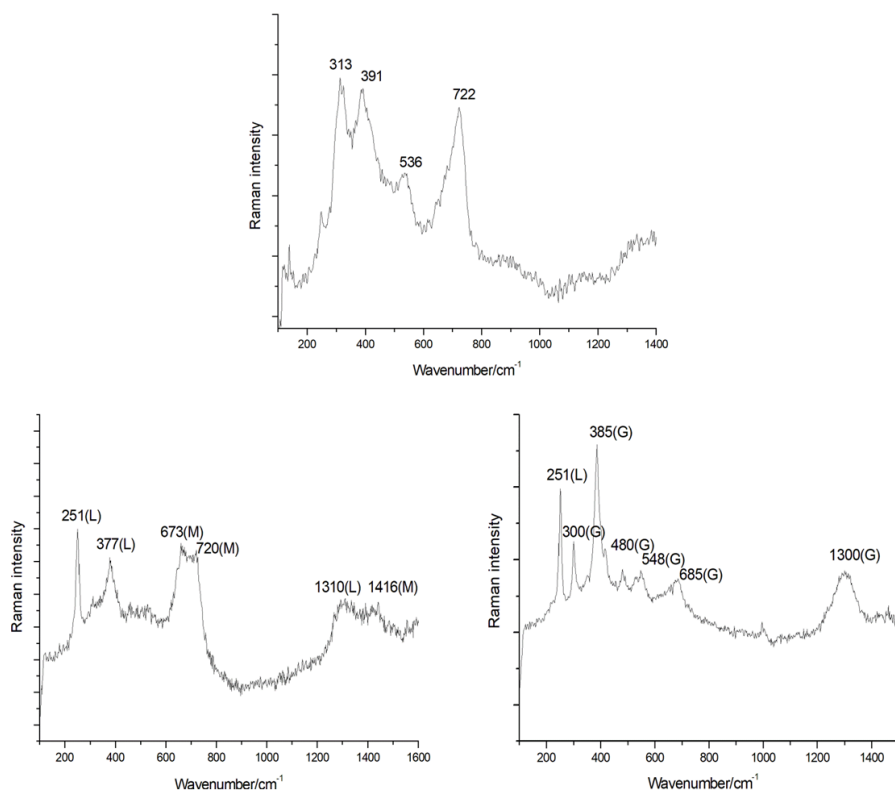


Figure 28 – Raman results obtained from the inner face of the swivel gun. On the top, akageneite; on the left, bands of maghemite (M) and lepidocrocite (L); and on the right, bands of goethite (G) and lepidocrocite (L)

Although goethite, akageneite, and maghemite were detected only in specific areas of the samples, lepidocrocite was identified all over the entire sample. Furthermore, some exogenous compounds were detected such as gypsum and calcite, but not rutile, as in the outer faces of the anchor samples (Figure 29). This could mean that the epoxy resin applied reacted with the metallic part of the samples resulting on the detection of these exogenous compounds.

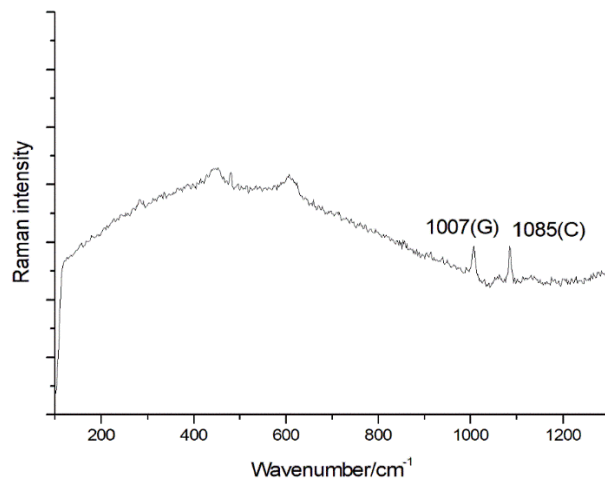


Figure 29 - Raman results obtained from the inner face of the swivel gun showing bands of gypsum and calcite

In general terms, the comparison of the results obtained from the two pieces allowed us to confirm that the differences observed were the presence of akaganeite, hematite and rutile. Akaganeite was detected in the external face of the anchor but not in the external face of the swivel gun. Hematite was detected in the external face of the swivel gun but not in the same face of the anchor. And rutile was detected in the inner face of the anchor but not on the inner face of the swivel gun.

In order to confirm the conclusions obtained from Raman and XRF analysis, the possibility of using destructive analysis was considered. In this PhD, XRD is considered destructive because it requires grinding the sample for its analysis. However, as the sample is homogenized, more representative results are obtained. The results obtained for the internal and the external face of the iron anchor are shown in the Figure 30.

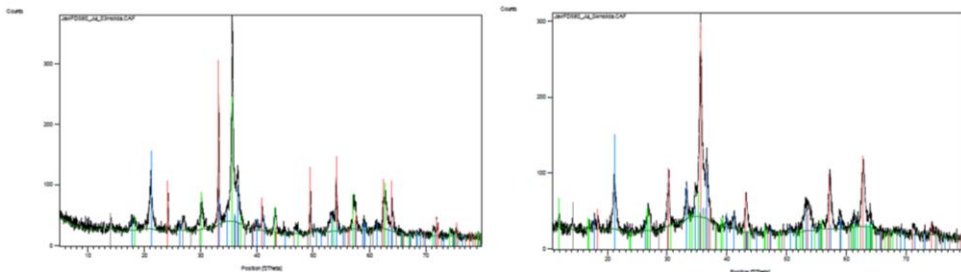


Figure 30 - On the left, XRD results from the external part of the iron anchor. On the right, the XRD results from the internal part of the iron anchor.

In the spectra shown in the Figure 30, various compounds were identified. In the case of the external part of the iron anchor, hematite (Fe_2O_3) was identified and indicated in red color, goethite ($\alpha\text{-FeO(OH)}$) was identified and indicated in blue color, magnetite (Fe_3O_4) was identified in green color, and a low presence of lepidocrocite ($\gamma\text{-FeO(OH)}$) was identified and indicated in gray color. In addition to these compounds, it should be mentioned that little presence of halite (NaCl) was also identified. In the case of the internal part of the iron anchor, magnetite (Fe_3O_4) was identified indicated in red color, low presence of goethite was identified in blue color, low presence of akageneite was identified in green color, and low presence of lepidocrocite was identified in gray color. These results again demonstrate that the conservation state of the pieces was not adequate for archaeological pieces.

Regarding XRD analyses for the internal and the external face of the swivel gun, the results obtained are showed in Figure 31.

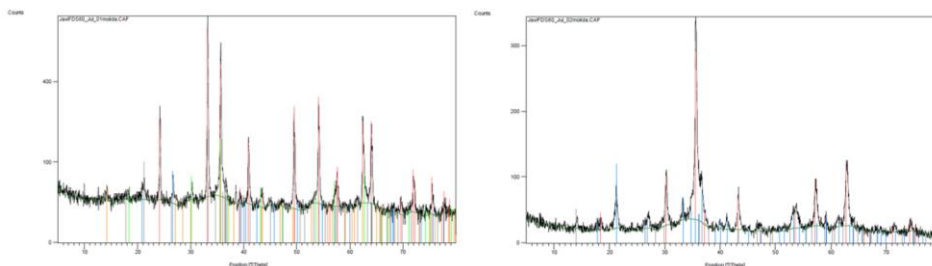


Figure 31 – On the left, XRD results from the external part of the swivel gun. On the right, the XRD results from the internal part of the swivel gun.

In the spectra shown in the Figure 31, various compounds were identified. In the case of the external part of the swivel gun, hematite (Fe_2O_3) was identified in red color as dominant phase, magnetite (Fe_3O_4) was identified in green color, a low presence of quartz (SiO_2) was identified in blue color and low presence of goethite ($\alpha\text{-FeO(OH)}$) and lepidocrocite ($\gamma\text{-FeO(OH)}$) were detected in gray and in orange color respectively. Apart from these phases, once again halite (NaCl) was probably detected. In the case of the internal part of the swivel gun, magnetite (Fe_3O_4) was identified in red color as a dominant phase, goethite ($\alpha\text{-FeO(OH)}$) was identified in blue color, and a small presence of lepidocrocite ($\gamma\text{-FeO(OH)}$) was identified in gray color.

The results obtained using XRD for the two samples were similar to the ones obtained with the Raman spectroscopy, but not the same, and the comparison of both techniques can be observed in Table 1 and 2. By means of this technique, more iron phases were detected in the sample, as for the external as for the inner face. In addition, the main phase identified by Raman did not coincide with those identified by XRD. It can be concluded that, despite the partial destruction of the sample collected, the XRD results have allowed us to obtain more complete information on the iron oxides present in these pieces.

Table 2 – Compounds detected by Raman spectroscopy in the different analyzed samples

| IRON ANCHOR | SWIVEL GUN |
|--|--|
| External face | |
| Lepidocrocite, Akaganeite | Lepidocrocite, Hematite |
| Inner face | |
| Goethite, Maghemite, Lepidocrocite Gypsum, Calcite, Rutile | Goethite, Maghemite, Lepidocrocite, Akaganeite Gypsum, Calcite |

Table 3 - Compounds detected by XRD in the different analyzed samples

| IRON ANCHOR | SWIVEL GUN |
|---|---|
| External face | |
| Goethite, Hematite, Magnetite, Lepidocrocite Halite | Goethite, Hematite, Magnetite, Lepidocrocite Quartz, Halite |
| Inner face | |
| Goethite, Magnetite, Lepidocrocite, Akaganeite | Goethite, Magnetite, Lepidocrocite |

However, the same could not be said for the exogenous compound detected by Raman as gypsum, calcite and rutile. XRD technique did not detect the presence of this compound on the pieces. This is related to the spatial resolution of each technique. Raman spectroscopy was performed using a microscope. Considering the small size of the exogenous particles present in the samples, a macroscopic technique fails in their detection. Therefore, in the

specific case of exogenous compounds, the XRD technique was somewhat limited compared to Raman spectroscopy.

5.2.3 Eight-pounder guns

As explained before, several eight-pounder guns from Bakio's shipwreck were analyzed. Concretely the 7 cannons kept in the town hall warehouse. In this case they were analyzed with portable equipment of X-ray fluorescence and Raman spectroscopy, due to the size of the pieces that did not allow to transferring them to the laboratory.

Regarding the elemental results obtained with the portable ED-XRF equipment, Figure 32 shows the elemental composition of the eight-pounder guns.

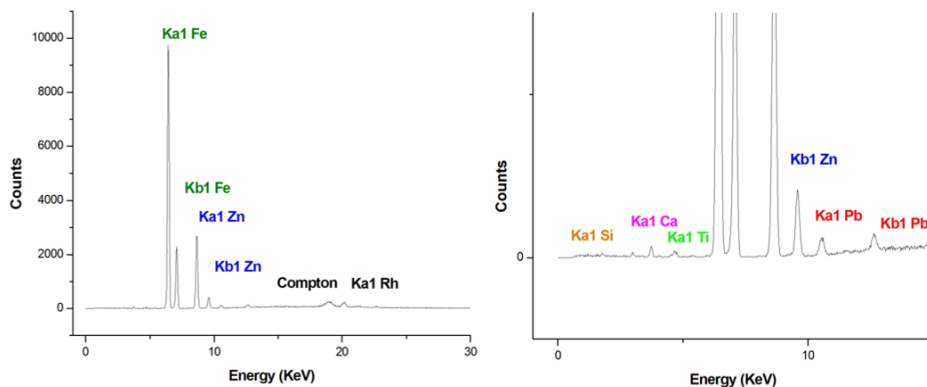


Figure 32 – On the left, Elemental characterization of metallic the eight-pounder guns by the use of X-Ray fluorescence and zoom of the spectrum to observe the minor elements, on the right

In Figure 32, all the elements detected in the eight-pounder guns can be observed. It can be concluded how these pieces were composed mostly by iron, with a lower presence of other elements such as zinc, lead, calcium, titanium, and silicon. The presence of silicon confirms

the possible use of cast-iron in the manufacturing process of the eight-pounder guns.

Regarding the results obtained by Raman spectroscopy, all the eight-pounder guns showed the presence of a characteristic iron oxide, akaganeite (Figure 33). As explained before, akaganeite is an oxy-hydroxide that is formed in chloride-rich environments⁶⁵ and it was detected thanks to its main Raman bands at 306 cm^{-1} and 385 cm^{-1} .

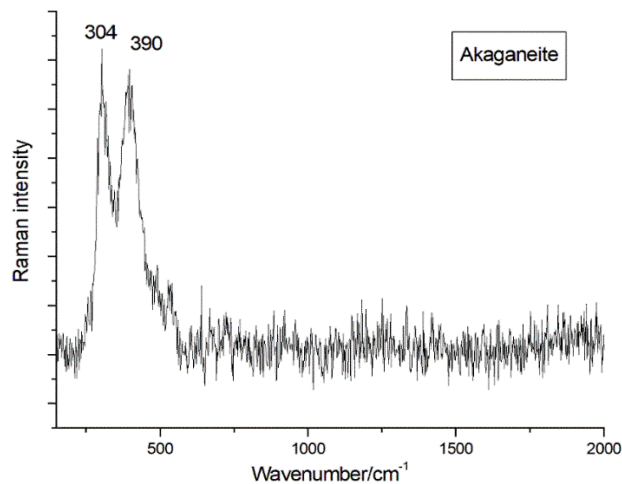


Figure 33 - Raman spectrum of akaganeite

The presence of this iron oxide may be due to the poor conservation of the eight-pounder guns. Once extracted from the sea, the seven eight-pounder guns were kept in the town hall warehouse without any type of treatment for many years. These inadequate storage conditions of the archaeological material may be the reason for its deterioration and oxidation for years.

Apart from this iron oxide, the presence of amorphous carbon was detected in many of the eight-pounder guns (Figure 34). The

presence of this element may be due to soot deposited in the samples or may be due to exogenous contamination.

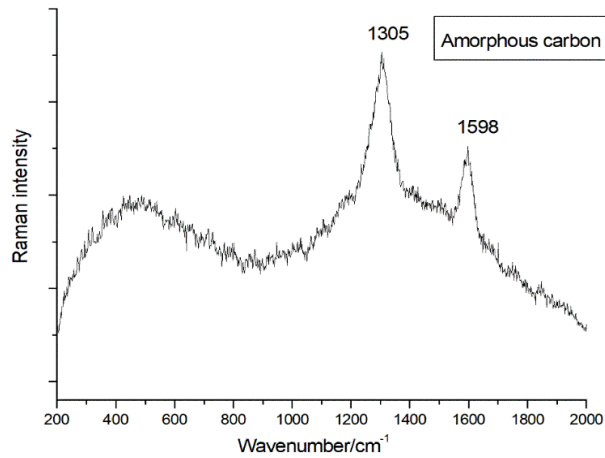


Figure 34 - Raman spectrum of amorphous carbon

In addition to XRF and Raman analyses, a dust sample was taken from inside the mouth of one of the eight-pounder guns for subsequent analysis. It should be mentioned that the analyzed sample was mainly formed by sand/dust adhered to the inner part of the eight-pounder gun.

This sample was analyzed by X-ray diffraction (XRD) and the results are shown below in the Figure 35.

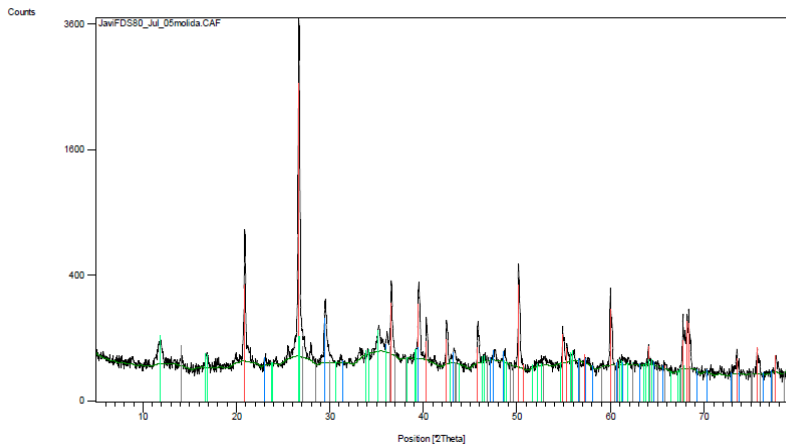


Figure 35 – EDX spectrum of the eight-pounder gun analyzed

In the spectrum shown in the Figure 35, various compounds were identified. Quartz (SiO₂) is identified in red color, calcite (CaCO₃) is identified in blue color, a small presence of akageneite in green color, and lepidocrocite in gray color.

These results showed the presence of iron oxides such as akageneite and lepidocrocite that were directly related to the deterioration of these pieces to the point of producing the detaching of small pieces in the form of dust and adhered to the metal piece. Quartz and calcite were related to the presence of exogenous matter.

5.2.4 Discussion of Bakio shipwreck analyses

Considering the different nature of the samples analyzed in this shipwreck (different raw material, different conservation state, different conservation treatments, different storage conditions...) the discussion of the results will be performed by sample set.

In general terms it can be said that, after these results, the chemical characterization of Bakio's extracted pieces has been meaningful in order to have a deeper knowledge of the manufacture procedure of these pieces and the degradation processes that they have suffered. This work probed again that the proposed methodology, based on the combination of Raman spectroscopy and ED-XRF non-destructive techniques, are enough for assessing the conservation state of iron archaeological pieces.

5.2.4.1 Musket and bullet analysis

In conclusion, non-destructive techniques, especially Raman spectroscopy, are very suitable tools for the diagnosis of the degradation processes of underwater materials. Despite the good condition of these pieces, the presence of lepidocrocite, elemental sulfur and lead oxide (litharge) can aggravate the condition of the pieces over time, increasing the cracks already present. However, the most corrosive species is the elemental sulfur that, when in contact with atmospheric oxygen can be oxidized with time to sulfuric acid causing further deterioration of the pieces.

5.2.4.2 Detached pieces from the iron anchor and the swivel gun

The analytical results showed the poor conservation state of the fallen pieces due to the high presence of lepidocrocite in their surfaces as well as the presence of akageneite in the outer parts of the samples. That is why, we considered that the conservation procedure applied in 2005 to both pieces, the anchor and the swivel gun, was not able to prevent the degradation processes. A correct process of restoration or preservation of iron materials should focus on preventing the formation of lepidocrocite and akageneite or on

stabilizing the existing lepidocrocite in the form of goethite. In this sense, the protection of underwater iron artifacts with a double layer of organic coating has been recently proposed as an effective treatment to preserve such archaeological iron artifacts⁷¹.

5.2.4.3 Eight-pounder guns

These samples underwent the same conservation treatment. However, once extracted, they were storage without any type of control or care.

As a direct result of the non-suitable storage conditions, seven eight-pounder guns were found in a deteriorated state of conservation. Upon preliminary inspection, a thick layer of dust and advanced corrosion was observed in the muzzle area of the eight-pounder guns. In all of them the presence of akageneite was detected and several of them showed the presence of amorphous carbon.

As a direct consequence of what has been said so far, the eight-pounder guns have never been valued, nor have they been appreciated for their Heritage value. Their conservation state has been deteriorating over time and due to the conditions in which they have been preserved. Due to all this, it is considered that in the case of not treating this type of pieces adequately, the best option is the option of conservation and preservation of the Underwater Cultural Heritage in-situ, as recommended by UNESCO.

5.3 CONCLUSIONS OF SAMPLES BURIED IN MARINE/ESTUARINE SEDIMENTS

In general terms, it can be said that the planned non-destructive methodology for the different aims of samples buried in marine sediments has been very successful. In all the analyzed samples, it has been possible to attain the proposed aims without the need to carry out any type of destructive analysis.

It is assumed that in the cases in which it has been possible, destructive analysis have been carried out in order to complete the information provided by the non-destructive techniques. In the case of the Urbieta shipwreck, a large number of iron nails were extracted and that is why the archeologist of the Archaeological Museum of Bilbao considered the option of preparing cross sections of the selected nails to be able to carry out much more exhaustive analysis on which to obtain more information. Moreover, it should be said that the cross-sections were analyzed by means of non-destructive techniques, so the pieces remain preserved for future analysis. In the case of Bakio, the destructive analysis of some pieces was performed because analyses were being carried out on small fallen parts of the swivel gun and the iron anchor. Therefore, this type of analysis can be considered depending on the conditions of the analyzed archaeological pieces.

Regarding the conservation of these pieces, the collaboration of experts from different fields is required. In this way, a specially adapted and long-lasting conservation can be designed for such complex materials. The tasks that must be carried out in the future are focused on finding, testing and designing new and more appropriate methods to ensure the conservation of the materials and

to advise which treatment should be applied in each case. For this, it will be necessary to know the distribution and location of compounds that directly affect its state, such as sulfates and sulfides.

The two cases treated for samples buried in marine sediments have several aspects in common, but also many differences between them were pointed out. It could be said that both samples, Urbieta and Bakio, are samples buried in marine environments, but there is a difference. Urbieta was a shipwreck found buried in sediments near the Golako stream (Urdaibai estuary), that is, in an estuary. On the contrary, the Bakio's shipwreck is a wreck that is still submerged in sea water, covered by a large layer of sand and very close to the coast.

The conditions that affect both shipwrecks may be similar in certain cases, but not the same. The Urbieta shipwreck is directly affected by the river water and the sediments. In this case, sediments contain a non-expected contribution of heavy metals due to the discharges placed in it. On the contrary, the influence of the tides, salinity, and marine sediments directly affect the Bakio's shipwreck. This is why the problems we find in these shipwrecks are totally different. In the case of Urbieta we find some nails with a high concentration of zinc and sulfur. On the contrary, in Bakio we find serious degradation problem that arises from pieces extracted without control and not treated properly.

Apart from these differences, the samples also present certain similarities that must be mentioned, being the clearest one the sulfur cycle generated by SRB and the presence of metal in contact with wood.

Regarding the similarities in the conservation state, in the case of Bakio's samples, the pieces that have not been treated by specialists have suffered a higher deterioration than the rest, as is the case of the Bakio's eight-pounder guns, the anchor and the swivel gun. This situation leads us to consider the creation of a new methodology for the conservation and preservation of archaeological pieces. This methodology is based on the request of a previous examination by a specialist and on the realization of specific stabilization treatments for this type of materials. This new methodology would prevent the archaeological samples from being treated by specialists from other fields and would avoid industrial treatment which are not suitable for them.

5.4 BIBLIOGRAPHY

The references mentioned in this work are based on the bibliography format described below:

Journals: Estalayo, E. Aramendia, J. Bellot-Gurlet, L. Garcia L. Garcia-Camino, I. Madariaga, J.M. Article title. *Journal abbreviation*, volume, pages (year).

Books: Estalayo, E. Aramendia, J. Bellot-Gurlet, L. Garcia L. Garcia-Camino, I. Madariaga, J.M. *Book title*, (year). DOI number.

1. Sandstrom, M., Jalilehvand, F., Persson, I., Gelius, U., Frank, P. & Hall-Roth, I. Deterioration of the seventeenth century warship Vasa by internal formation of sulphuric acid. *Nature* **415**, 893–897 (2002).
2. Fors, Y. & Sandström, M. Sulfur and iron in shipwrecks cause conservation concerns. *Chemical Society Reviews* **35**, 399 (2006).
3. UNESCO. *Convention on the protection of the Underwater Cultural Heritage Unesco*. (2001).
4. Dillmann, P., Watkinson, D., Angelini, E. & Adriaens, A. *Corrosion and conservation of cultural heritage metallic artefacts. Corrosion and Conservation of Cultural Heritage Metallic Artefacts* (Woodhead Publishing Limited, 2013). doi:10.1533/9781782421573
5. Fors, Yvonne. PhD Thesis: Sulfur-related conservation concerns for marine archaeological wood: The Origin, Speciation and Distribution of Accumulated Sulfur with Some Remedies for the Vasa. (2008).
6. Rémazeilles, C., Saheb, M., Neff, D., Guilminot, E., Tran, K., Bourdoiseau, J. A., Sabot, R., Jeannin, M., Matthiesen, H., Dillmann, P.

- & Refait, P. Microbiologically influenced corrosion of archaeological artefacts: Characterisation of iron(II) sulfides by Raman spectroscopy. *Journal of Raman Spectroscopy* **41**, 1425–1433 (2010).
7. Fors, Y. & Sandström, M. Sulfur and iron in shipwrecks cause conservation concerns. *Chemical Society Reviews* **35**, 399–415 (2006).
 8. Irabien, M. J. Vertido de escorias en el Rio Oka (Reserva Natural de la Biosfera de Urdaibai Vizcaya): Aspectos mineralógicos y geoquímicos. *Geogaceta* **25**, 111,113 (1999).
 9. Carlin, W. & Keith, D. H. An improved tannin-based corrosion inhibitor-coating system for ferrous artefacts. *International Journal of Nautical Archaeology* **25**, 38–45 (1996).
 10. Neff, D., Dillmann, P., Descostes, M. & Beranger, G. Corrosion of iron archaeological artefacts in soil: Estimation of the average corrosion rates involving analytical techniques and thermodynamic calculations. *Corrosion Science* **48**, 2947–2970 (2006).
 11. Selwyn, L. in *Proceedings of Metal 2004, National Museum of Australia Canberra ACT* 294–306 (2004).
 12. Schwertmann, U. & Taylor, R. M. The influence of silicate on the transformation of lepidocrocite to goethite. *Clays and Clay Minerals* **20**, 151–158 (1972).
 13. Hanesch, M. Raman spectroscopy of iron oxides and (oxy)hydroxides at low laser power and possible applications in environmental magnetic studies. *Geophysical Journal International* **177**, 941–948 (2009).

14. Mielczarski, J. A., Atenas, G. M. & Mielczarski, E. Role of iron surface oxidation layers in decomposition of azo-dye water pollutants in weak acidic solutions. *Applied Catalysis B: Environmental* **56**, 289–303 (2005).
15. Gutierrez, J. A. PhD Thesis: Analytical diagnosis of the conservation state of weathering steel exposed to urban atmospheres. *Universidad del Pais Vasco (UPV/EHU)* (2013).
16. Bajt Leban, M. & Kosec, T. Characterization of corrosion products formed on mild steel in deoxygenated water by Raman spectroscopy and energy dispersive X-ray spectrometry. *Engineering Failure Analysis* **79**, 940–950 (2017).
17. Schlegel, M. L., Bataillon, C., Brucker, F., Blanc, C., Prêt, D., Foy, E. & Chorro, M. Corrosion of metal iron in contact with anoxic clay at 90°C: Characterization of the corrosion products after two years of interaction. *Applied Geochemistry* **51**, 1–14 (2014).
18. Aramendia, J., Gomez-Nubla, L., Castro, K. & Madariaga, J. M. Structural and chemical analyzer system for the analysis of deposited airborne particles and degradation compounds present on the surface of outdoor weathering steel objects. *Microchemical Journal* **123**, 267–275 (2015).
19. Estalayo, E., Aramendia, J., Castro, K., Madariaga, J. M., Garcia, L. & Garcia-Camino, I. in *Conserving Cultural Heritage* 319–321 (2018). doi:10.1201/9781315158648-80
20. Nims, C., Cron, B., Wetherington, M., Macalady, J. & Cosmidis, J. Low frequency Raman Spectroscopy for micron-scale and in vivo characterization of elemental sulfur in microbial samples. *Scientific Reports* **9**, 1–12 (2019).

21. Muyzer, G. & Stams, A. J. M. The ecology and biotechnology of sulphate-reducing bacteria. *Nature Reviews Microbiology* **6**, 441–454 (2008).
22. Rémazeilles, C., Neff, D., Bourdoiseau, J. A., Sabot, R., Jeannin, M. & Refait, P. Role of previously formed corrosion product layers on sulfide-assisted corrosion of iron archaeological artefacts in soil. *Corrosion Science* **129**, 169–178 (2017).
23. Huisman, D. J., Manders, M. R., Kretschmar, E. I., Klaassen, R. K. W. M. & Lamersdorf, N. Burial conditions and wood degradation at archaeological sites in the Netherlands. *International Biodeterioration and Biodegradation* **61**, 33–44 (2008).
24. Rémazeilles, C., Lévêque, F., Conforto, E. & Refait, P. Long-term alteration processes of iron fasteners extracted from archaeological shipwrecks aged in biologically active waterlogged media. *Corrosion Science* **181**, (2021).
25. Rémazeilles, C., Lévêque, F., Conforto, E., Meunier, L. & Refait, P. Contribution of magnetic measurement methods to the analysis of iron sulfides in archaeological waterlogged wood-iron assemblies. *Microchemical Journal* **148**, 10–20 (2019).
26. Rémazeilles, C., Tran, K., Guilminot, E., Conforto, E. & Refait, P. Study of Fe(II) sulphides in waterlogged archaeological wood. *Studies in Conservation* **58**, 297–307 (2013).
27. Aramendia, J., Gómez-Nubla, L., Castro, K. & Madariaga, J. M. Spectroscopic speciation and thermodynamic modeling to explain the degradation of weathering steel surfaces in SO₂ rich urban atmospheres. *Microchemical Journal* **115**, 138–145 (2014).

28. Höffler, F., Müller, I. & Steiger, M. Thermodynamic properties of ZnSO₄(aq) and phase equilibria in the ZnSO₄–H₂O system from 268 K to 373 K. *Journal of Chemical Thermodynamics* **116**, 279–288 (2018).
29. Falgayrac, G., Sobanska, S. & Brémard, C. Raman diagnostic of the reactivity between ZnSO₄ and CaCO₃ particles in humid air relevant to heterogeneous zinc chemistry in atmosphere. *Atmospheric Environment* **85**, 83–91 (2014).
30. Rudolph, W. W., Brooker, M. H. & Tremaine, P. R. Raman spectroscopy of aqueous ZnSO₄ solutions under hydrothermal conditions: Solubility, hydrolysis, and sulfate ion pairing. *Journal of Solution Chemistry* **28**, 621–630 (1999).
31. Rémazeilles, C., Lévêque, F., Conforto, E., Meunier, L. & Refait, P. Contribution of magnetic measurement methods to the analysis of iron sulfides in archaeological waterlogged wood-iron assemblies. *Microchemical Journal* **148**, 10–20 (2019).
32. Höffler, F., Müller, I. & Steiger, M. Thermodynamic properties of ZnSO₄(aq) and phase equilibria in the ZnSO₄–H₂O system from 268 K to 373 K. *Journal of Chemical Thermodynamics* **116**, 279–288 (2018).
33. Labrenz, M., Druschel, G. K., Thomsen-Ebert, T., Gilbert, B., Welch, S. A., Kemner, K. M., Logan, G. A., Summons, R. E., de Stasio, G., Bond, P. L., Lai, B., Kelly, S. D. & Banfield, J. F. Formation of sphalerite (ZnS) deposits in natural biofilms of sulfate-reducing bacteria. *Science* **290**, 1744–1747 (2000).
34. Neff, D., Reguer, S., Bellot-Gurlet, L., Dillmann, P. & Bertholon, R. Structural characterization of corrosion products on archaeological

- iron: an integrated analytical approach to establish corrosion forms. *Journal of Raman Spectroscopy* **35**, 739–745 (2004).
35. Aramendia, J., Gómez-Nubla, L., Castro, K. & Madariaga, J. M. Spectroscopic speciation and thermodynamic modeling to explain the degradation of weathering steel surfaces in SO₂ rich urban atmospheres. *Microchemical Journal* **115**, 138–145 (2014).
 36. Rodriguez-Iruretagoiena, A., Elejoste, N., Gredilla, A., Fdez-Ortiz de Vallejuelo, S., Arana, G., Madariaga, J. M. & de Diego, A. Occurrence and geographical distribution of metals and metalloids in sediments of the Nerbioi-Ibaizabal estuary (Bilbao, Basque Country). *Marine Chemistry* **185**, 82–90 (2016).
 37. Carlin, W. & Keith, D. H. An improved tannin-based corrosion inhibitor-coating system for ferrous artefacts. *International Journal of Nautical Archaeology* **25**, 38–45 (1996).
 38. Pérez, T. Estudio de la efectividad del ácido tánico sobre piezas de hierro arqueológico. (2017).
 39. Chadwick, A. v., Berko, A., Schofield, E. J., Smith, A. D., Mosselmans, J. F. W., Jones, A. M. & Cibin, G. The application of X-ray absorption spectroscopy in archaeological conservation: Example of an artefact from Henry VIII warship, the Mary Rose. *Journal of Non-Crystalline Solids* **451**, 49–55 (2016).
 40. Memet, J. B. in *Corrosion of Metallic Heritage Artefacts: Investigation, Conservation and Prediction of Long Term Behaviour* 152–169 (2007). doi:10.1533/9781845693015.152
 41. Fors, Y., Grudd, H., Rindby, A., Jalilehvand, F., Sandström, M., Cato, I. & Bornmalm, L. Sulfur and iron accumulation in three marine-

- archaeological shipwrecks in the Baltic Sea: The Ghost, the Crown and the Sword. *Scientific Reports* **4**, (2014).
42. Fors, Y., Jalilehvand, F., Damian, E., Björdal, C., Phillips, E. & Sandström, M. Sulfur and iron analyses of marine archaeological wood in shipwrecks from the Baltic Sea and Scandinavian waters. *Journal of Archaeological Science* **39**, 2521–2532 (2012).
43. Björdal, C. G. & Fors, Y. Correlation between sulfur accumulation and microbial wood degradation on shipwreck timbers. *International Biodeterioration and Biodegradation* **140**, 37–42 (2019).
44. Gjelstrup, C. & Fors, Y. International Biodeterioration & Biodegradation Correlation between sulfur accumulation and microbial wood degradation on shipwreck timbers. *International Biodeterioration and Biodegradation* **140**, 37–42 (2019).
45. Jana, A., Jana, S. K., Sarkar, D., Ahuja, T., Basuri, P., Mondal, B., Bose, S., Ghosh, J. & Pradeep, T. Electro spray deposition-induced ambient phase transition in copper sulphide nanostructures. *Journal of Materials Chemistry A* **7**, 6387–6394 (2019).
46. Milekhin, A. G., Yeryukov, N. A., Sveshnikova, L. L., Duda, T. A., Rodyakina, E. E., Gridchin, V. A., Sheremet, E. S. & Zahn, D. R. T. Combination of surface- and interference-enhanced Raman scattering by CuS nanocrystals on nanopatterned Au structures. *Beilstein Journal of Nanotechnology* **6**, 749–754 (2015).
47. Lafuente, B., Downs, R. T., Yang, H. & Stone, N. in *Highlights in Mineralogical Crystallography* 1–30 (2016).
doi:10.1515/9783110417104-003

48. Jegdić, B., Polić-Radovanović, S., Ristić, S. & Alil, A. Corrosion stability of corrosion products on an archaeological iron artefact. *International Journal of Conservation Science* **3**, 241–248 (2012).
49. Bastidas, D. M., Röss, J., Martin, U., Bosch, J., la Iglesia, A. & Bastidas, J. M. Crystallization pressure and volume variation during rust development in marine and urban-continental environments: Critical factors influencing exfoliation. *Revista de Metalurgia* **56**, 1–15 (2020).
50. Jegdić, B., Polić-Radovanović, S., Ristić, S. & Alil, a. Corrosion Stability of Corrosion Products on an Archaeological Iron Artefact. *International journal of conservation science* **3**, 241–248 (2012).
51. Kostadinovska, M., Jakovleska Spirovska, Z. & Minčeva-Šukarova, B. A spectroscopic study of inks from a rare Old Slavic manuscript: Liturgical Collection of chronicles , scriptures , etc. 311–316 (2013). doi:10.13140/RG.2.2.11773.56808
52. Degriigny, C. & le Gall, R. Conservation of ancient lead artifacts corroded in organic acid environments: Electrolytic stabilization/consolidation. *Studies in Conservation* **44**, 157–169 (1999).
53. Florentino, C. G. PhD Thesis: Development of innovative analytical methodologies, mainly focused on X-ray fluorescence spectrometry, to characterise building materials and their degradation processes based on the study performed in the historical building Punta Begoña Gall. *Journal of Chemical Information and Modeling* **53**, 1689–1699 (2019).
54. Frost, R. L., Martens, W., Klopogge, J. T. & Ding, Z. Raman spectroscopy of selected lead minerals of environmental significance.

Spectrochimica Acta - Part A: Molecular and Biomolecular Spectroscopy **59**, 2705–2711 (2003).

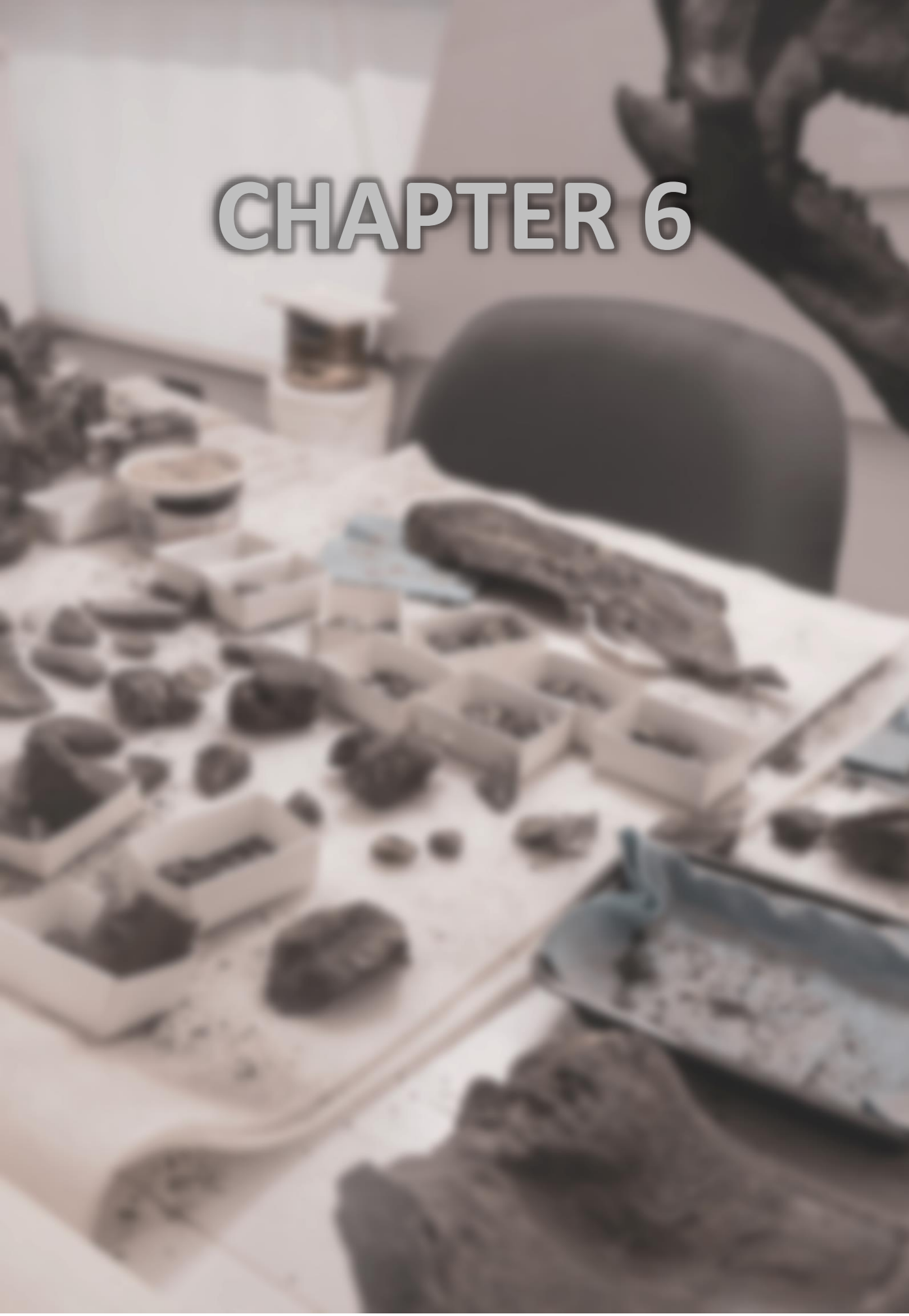
55. Krause, K. *Arms and the State: Patterns of Military Production and Trade*. (Cambridge University Press, 1996).
56. Ciarlo, N. C., López, A. N., de Rosa, H. M. & Pianetti, M. Naval Crossfire: A Comparative Analysis of Iron Projectiles from Mid-18th to Early 19th Centuries European Warships. *Procedia Materials Science* **8**, 712–721 (2015).
57. Cvikel, D., Ashkenazi, D., Stern, A. & Kahanov, Y. Characterization of a 12-pdr wrought-iron cannonball from the Akko 1 shipwreck. *Materials Characterization* **83**, 198–211 (2013).
58. Tylecote, R. F. *A History of Metallurgy*. (1976).
59. Stefanescu, D. M. Classification and Basic Metallurgy of Cast Iron. *Properties and Selection: Irons, Steels, and High-Performance Alloys* **1**, 3–11 (2018).
60. Singh, R. in *Applied Welding Engineering* 65–81 (2016). doi:10.1016/B978-0-12-804176-5.00007-4
61. Akil, C. & Geveci, A. Optimization of conditions to produce manganese and iron carbides from Denizli-Tavas manganese ore by solid state reduction. *Turkish Journal of Engineering and Environmental Sciences* **32**, 125–131 (2008).
62. Duraisamy, R., Pownsamy, K. & Asgedom, G. Chemical Degradation of Epoxy-Polyamide Primer by Electrochemical Impedance Spectroscopy. *ISRN Corrosion* **2012**, 10 (2012).

63. Soiński, M. S., Jakubus, A., Kordas, P. & Skurka, K. The effect of aluminium on graphitization of cast iron treated with cerium mixture. *Archives of Foundry Engineering* **14**, 95–100 (2014).
64. Selwyn, L. Overview of archaeological iron: the corrosion problem, key factors affecting treatment, and gaps in current knowledge. *Proceedings of Metal 2004, National Museum of Australia Canberra ACT* 294–306 (2004).
65. Réguer, S., Dillmann, P. & Mirambet, F. Buried iron archaeological artefacts: Corrosion mechanisms related to the presence of Cl-containing phases. *Corrosion Science* **49**, 2726–2744 (2007).
66. Neff, D., Dillmann, P., Bellot-Gurlet, L. & Beranger, G. Corrosion of iron archaeological artefacts in soil: Characterisation of the corrosion system. *Corrosion Science* **47**, 515–535 (2005).
67. Rémazeilles, C., Neff, D., Kergourlay, F., Foy, E., Conforto, E., Guilminot, E., Reguer, S., Refait, P. & Dillmann, P. Mechanisms of long-term anaerobic corrosion of iron archaeological artefacts in seawater. *Corrosion Science* **51**, 2932–2941 (2009).
68. Veneranda, M., Aramendia, J., Gomez, O., Fdez-Ortiz de Vallejuelo, S., Garcia, L., Garcia-Camino, I., Castro, K., Azkarate, A. & Madariaga, J. M. Characterization of archaeometallurgical artefacts by means of portable Raman systems: corrosion mechanisms influenced by marine aerosol. *Journal of Raman Spectroscopy* **48**, 258–266 (2017).
69. Kergourlay, F., Guilminot, E., Neff, D., Remazeilles, C., Reguer, S., Refait, P., Mirambet, F., Foy, E. & Dillmann, P. Influence of corrosion products nature on dechlorination treatment: case of wrought iron archaeological ingots stored 2 years in air before NaOH treatment.

Corrosion Engineering, Science and Technology **45**, 407–413 (2010).

70. Veneranda, M., Costantini, I., de Vallejuelo, S. F.-O., Garcia, L., García, I., Castro, K., Azkarate, A. & Madariaga, J. M. Study of corrosion in archaeological gilded irons by Raman imaging and a coupled scanning electron microscope–Raman system. *Philosophical Transactions of the Royal Society of London A: Mathematical, Physical and Engineering Sciences* **374**, (2016).
71. Ashkenazi, D., Nusbaum, I., Shacham-Diamand, Y., Cvikel, D., Kahanov, Y. & Inberg, A. A method of conserving ancient iron artefacts retrieved from shipwrecks using a combination of silane self-assembled monolayers and wax coating. *Corrosion Science* **123**, 88–102 (2017).

CHAPTER 6



6. RESULTS FROM THE SAMPLES BURIED IN SOIL

“There is no fundamental difference between man and animals in their ability to feel pleasure and pain, happiness, and misery” – “No hay ninguna diferencia fundamental entre el hombre y los animales en su capacidad de sentir placer y dolor, felicidad y miseria” – Charles Darwin

In this chapter, the analytical results obtained from the Vaccaei glass beads, lithic tools from the Nahal Hemar cave and iron archaeological slags from El Pobal are exposed and discussed.

6.1 GLASS BEADS OF VACCAEI CULTURE

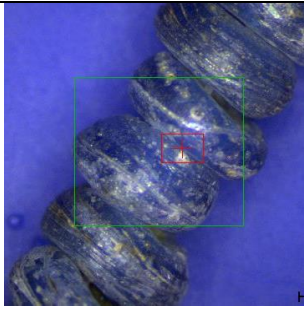

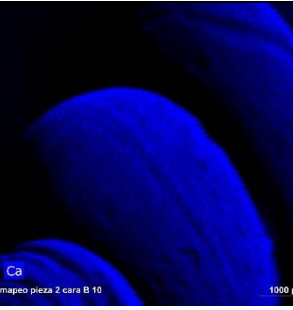
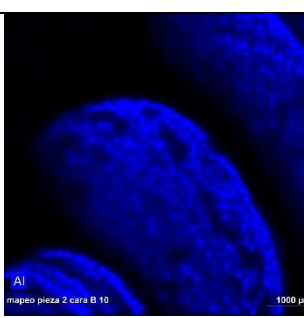
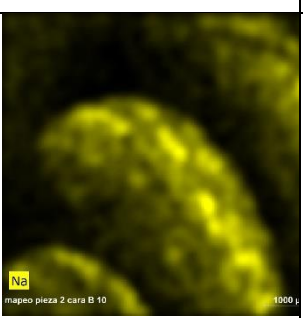
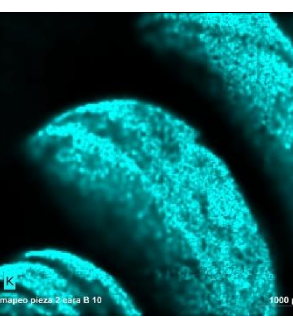
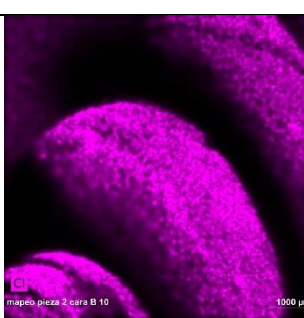
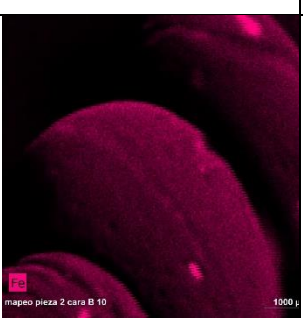
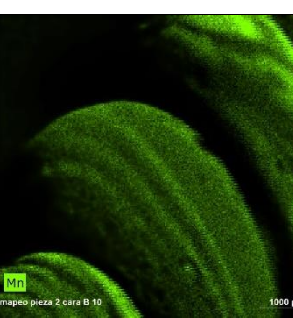
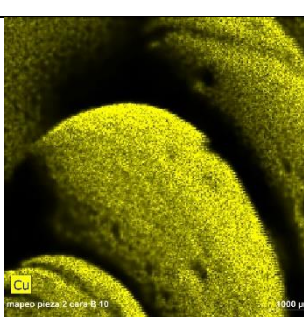
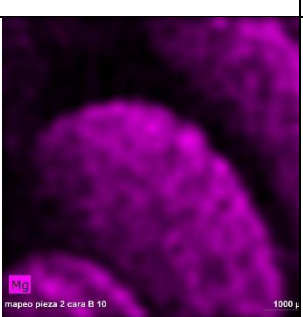
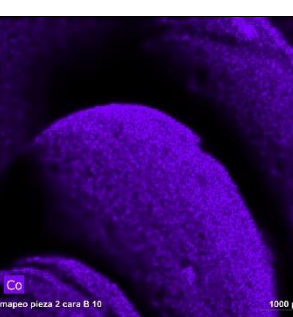
The analysis of the glass beads was possible thanks to the collaboration and participation of the Department of Física de la Materia Condensada, Cristalografía y Mineralogía of Valladolid University (UVa).

The main aim of the analysis was to know the composition and distribution of the elements present in the samples without altering them. Therefore, the analyses were carried out using the ED-XRF laboratory equipment to perform point-by-point and elemental distribution image analysis.

All the glass beads exposed in Chapter 4 were analyzed by performing elemental distribution mapping and various punctual measurements.

The aim of the different methodologies was to get knowledge about the distribution of the elements present in the samples and to relate the presence of the elements with the colors employed in the pieces. Moreover, by the information provided by point-by-point analysis, accurate data about degraded and not degraded areas was obtained in order to define the degradation patterns. Next, the results obtained for the elemental analysis of the 14 glass beads already described in Chapter 4 of Samples and Emplacements are going to be shown. The results exposed are ordered from highest to lowest abundances regarding to normalized percentage.

At first, the blue necklace (piece no. 1) was analyzed, and its elemental distribution is shown in Figure 1.

| | | |
|---|---|--|
| <p>Piece no. 1</p> | <p>Silicon</p> | <p>Calcium</p> |
|  |  |  |
| <p>Aluminum</p> | <p>Sodium</p> | <p>Potassium</p> |
|  |  |  |
| <p>Chloride</p> | <p>Iron</p> | <p>Manganese</p> |
|  |  |  |
| <p>Copper</p> | <p>Magnesium</p> | <p>Cobalt</p> |
|  |  |  |

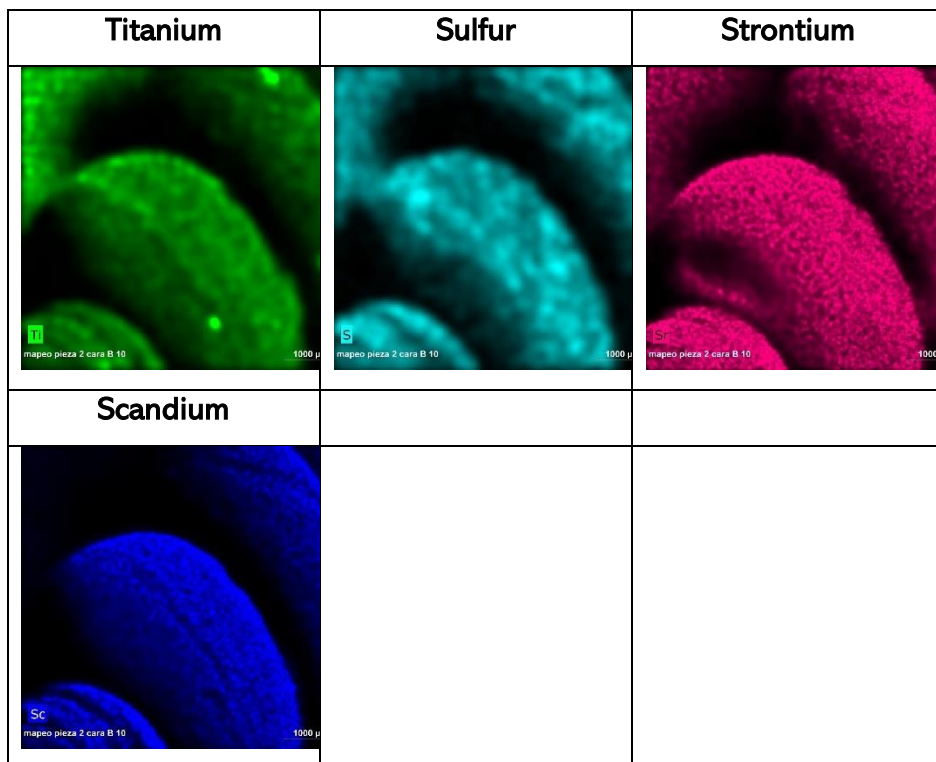


Figure 56 – Elemental image of the glass beads no. 1 by ED-XRF

In these results it can be observed how calcium and silicon were the two main elements that showed a homogeneous distribution all along the pieces. Aluminum was also distributed in all the piece surfaces but not as homogeneously as the previous elements. Actually, aluminum seemed to be less concentrated on the whitish stripes present in the beads. At the same time, these areas where the presence of aluminum was not found, the presence of sodium seemed to be detected, since their maps were totally complementary.

Potassium and chloride were also present throughout the piece and were correlated since they showed the same distribution map. In the case of iron and manganese, although they were present throughout the piece, they seemed to have a higher presence in the areas

mentioned degradation areas. Scandium resembles the distribution of these two elements, except that its presence was not detected in the white areas. In the case of copper, magnesium and cobalt, the three present a very similar distribution maps except form some specific differences. Copper seemed to be present in a lower relative presence in the white areas of the piece. On the contrary, in those areas there seemed to be higher presence of cobalt. In the case of magnesium, its presence was observed homogeneously throughout the piece.

With regard to elements such as titanium, sulfur and strontium, although the three were present in the entire piece, they have different distributions and do not correlate each other. However, it should be mentioned that, in this particular case, the background seems to have the presence of these elements. That is why these results have to be compared with those obtained from specific measurements to find out if they are elements present in very low relative concentration.

In order to corroborate the results obtained through the map distribution, point-by-point measurements were made, and the most significant results are shown below (Figure 2).

The point-by-point analysis performed in the degraded area observed in the Figure 2 showed the following semi-quantitative composition of the sample using normalized percentage of the elements present ordered from highest to lowest:

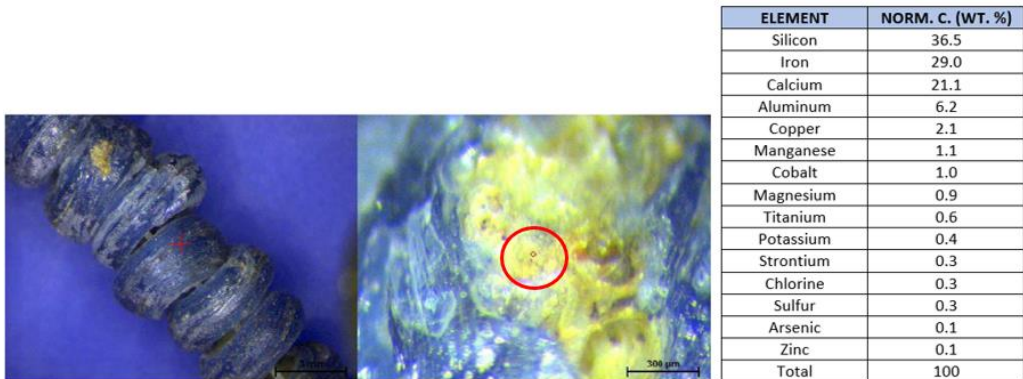


Figure 57 - Punctual analysis of the degraded area in piece no. 1

The semi-quantitative results of this deteriorated area, with yellow color, demonstrate how calcium, iron and aluminum are three elements present in a high relative percentage. To find out if these two elements are characteristic of the deteriorated areas, they were compared with a measurement taken from a non-deteriorated area (at naked eye) that can be seen in Figure 3.

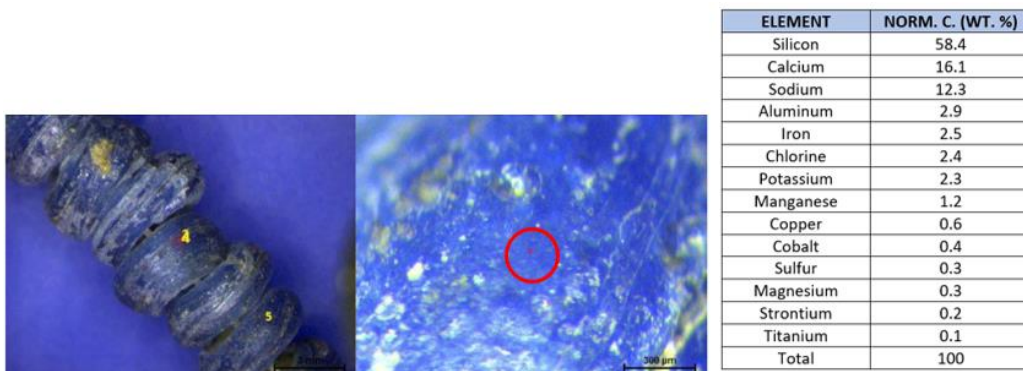


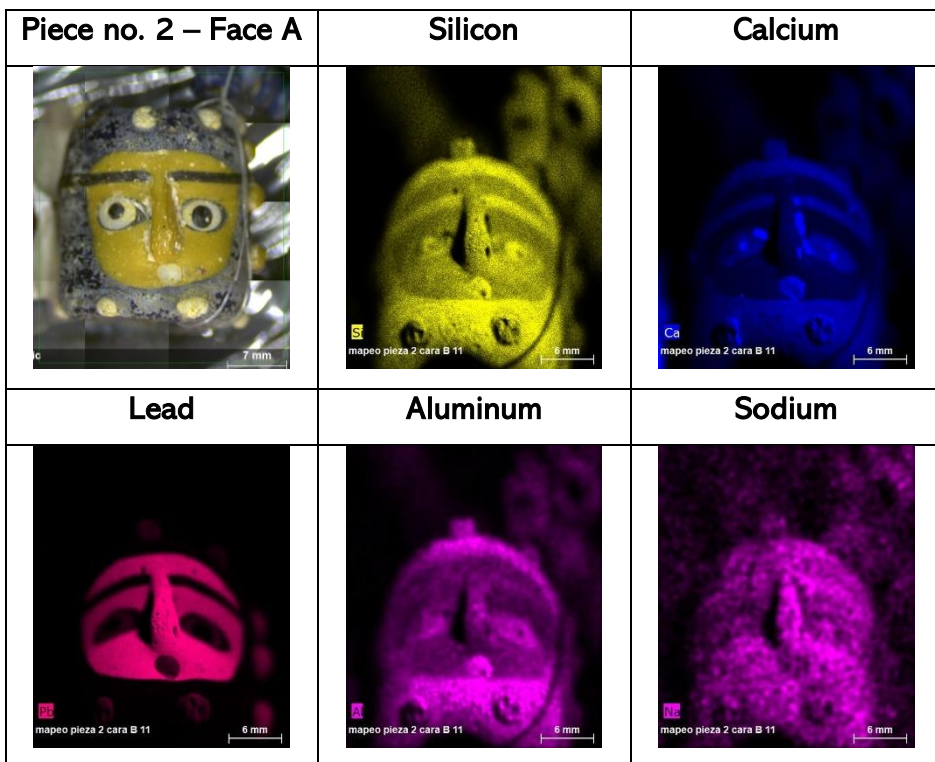
Figure 58 – Punctual analysis of the blue area of the piece no. 1

These results show that the relative presence of calcium is not related to its presence in degraded areas, since in both areas its normalized

percentage is high. On the contrary, the presence of iron and aluminum increases considerably when it comes to a degraded area such as the one show in Figure 2.

Moreover, a clear difference in sodium can be observed. This element is not detected in the altered zone, on the contrary, in the unaltered zone (blue area), a high relative percentage of sodium is detected. Something similar happens with chlorine, its presence is minimal in the altered area, but its presence increases when the unaltered area was analyzed.

The elemental distribution map obtained from the face A of the two faces sample (piece no. 2) is shown in Figure 4.



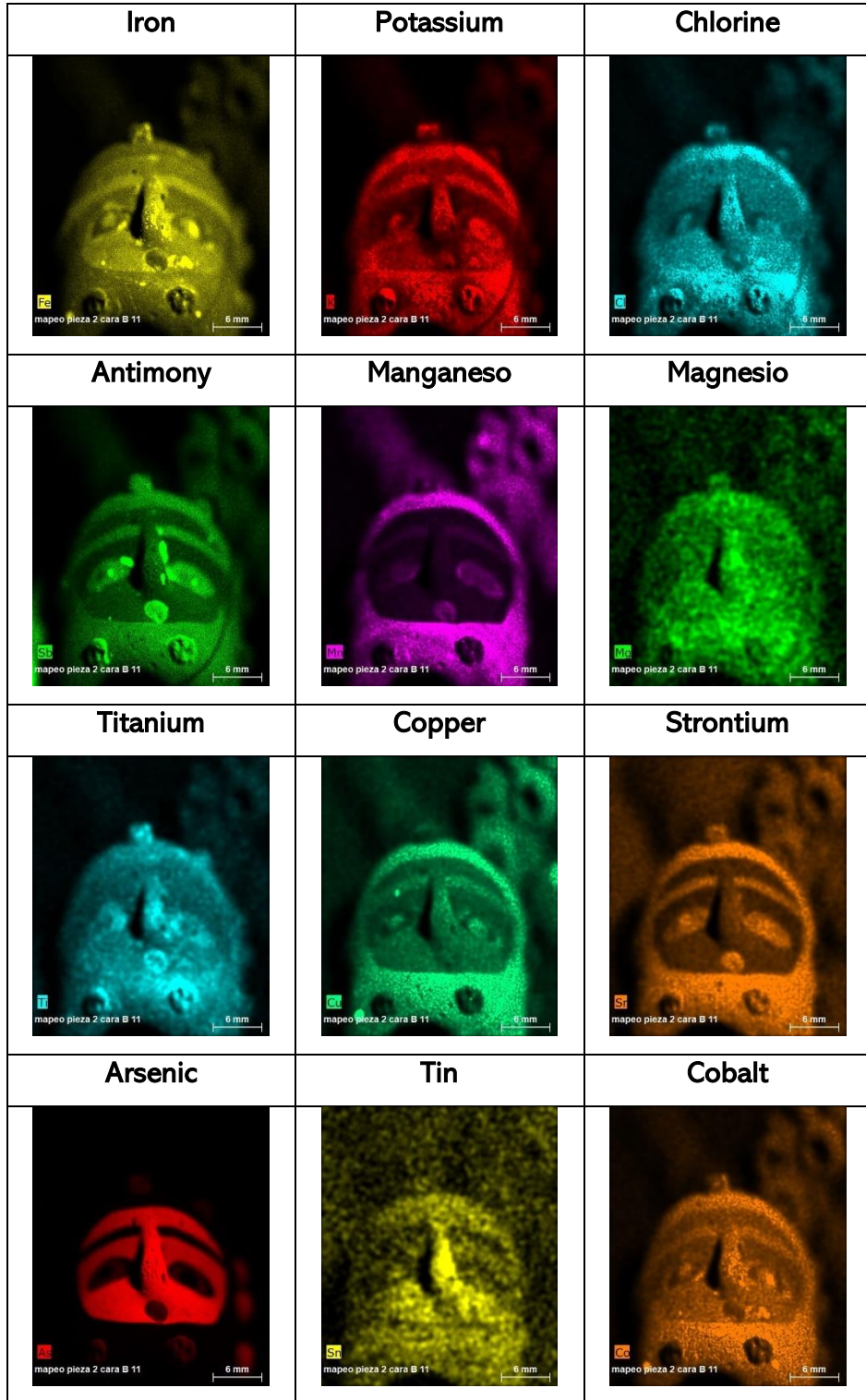


Figure 59 - Elemental image of the face A in the glass beads no. 2 by ED-XRF

In this piece, correlations between colors and elemental composition can be observed, for instance, yellow, white, gray and black. Regarding the results obtained, it can be observed that silicon, chlorine and potassium show a very similar distribution. Both are present throughout the piece in a homogeneous way. Although they seem to give a greater signal in the whitish regions present on the external blue area.

There are two elements that seem to be present in two colors in particular, calcium and antimony, which are present in the gray and white colors of the face. Aluminum shows a similar distribution to these two elements, with one exception, aluminum does not appear to be present in the eyebrows, and calcium and antimony do.

Lead and arsenic show a very clear distribution. It is only present in the yellow areas (inner part) of the piece. Quite the opposite of what happens with manganese, which is only present in the gray zone of the sample (outer zone). On the other hand, Cu and Sr seem to have a very similar distribution to magnesium, although with some significant differences. Strontium was present in some areas where copper was not detected, such as the white points of the face, the eyebrows, and the sclerotic area of the eye.

In the case of sodium and magnesium, their distribution is very similar, they are two elements present throughout the entire piece and do not seem to be related to any particular color. Iron, despite being present throughout the piece, seems to show up again in the most deteriorated areas of the sample, in the white areas that surround the nose. Titanium and cobalt are present in the entire sample, although they seem to have a greater presence in the white area of the nose and in the gray area (external part). In the case of

tin, is an element that does not resemble any other in its distribution. Its presence seems to be majority in the internal area of the face, especially in the nose area.

To corroborate the correlations between the detected elements and the observed colors, several specific measurements were made, and the most significant ones are shown below.

The point-by-point analysis performed in the yellow area of the inner face is observed in the Figure 5. The semi-quantitative composition of this point using normalized percentage of the elements present ordered from the highest abundances to the lowest one is the following one:

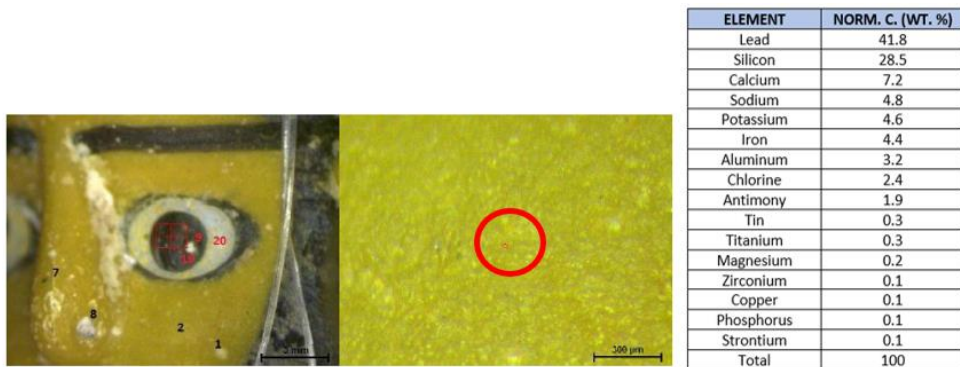


Figure 60 - Punctual analysis of the yellow area of the piece no. 2 in the face A

It can be observed that lead is the main element in this yellow area. Another point-by-point analysis was made in the white points which were located in the gray area (external part) of the sample. This area can be observed in the Figure 6. Semi-quantitative results obtained for this point in normalized percentage are the following ones:



Figure 61 – Punctual analysis of the white points of the piece no.2 in the face A

Apparently, if the results of the white point and the yellow area are compared, it can be seen how the results obtained are very similar to each other. There are no significant differences between the different zones.

To corroborate the elemental composition of the original gray area and the deteriorated gray area, the point-by-point results were compared in Figure 7.

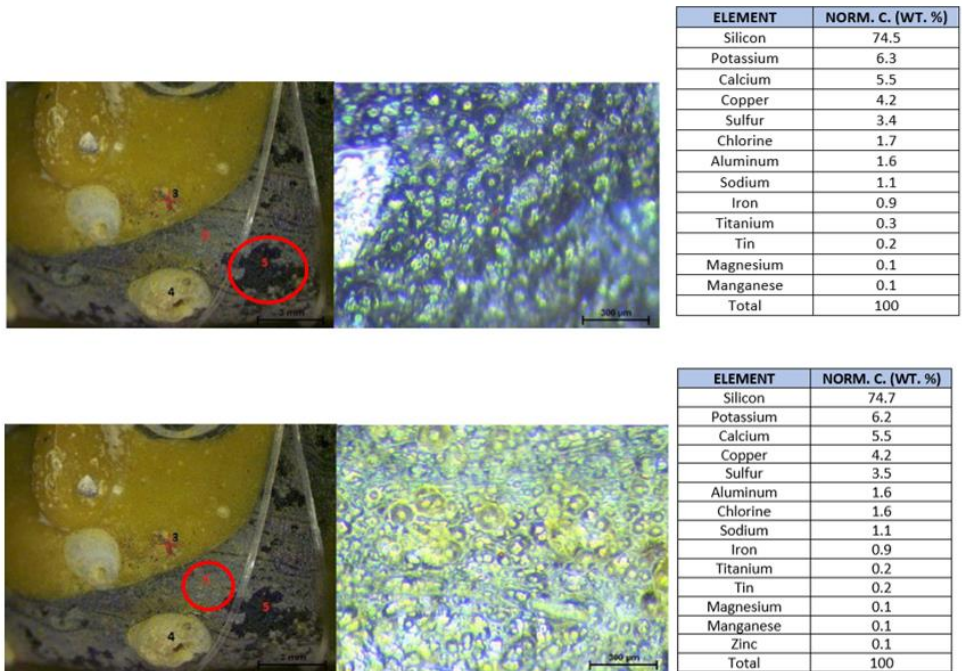


Figure 62 - Punctual analysis of the original gray area (at the top) and punctual analysis of the degraded gray area (below) of the piece no.2 in the face A

Despite the visual differences in the color of these zones, the mapping results agree with the semi-quantitative results since the elemental composition does not vary from one zone to another despite the observed color loss.

The results obtained by punctual analysis performed on white area near the nose of the face are showed in the Figure 8.

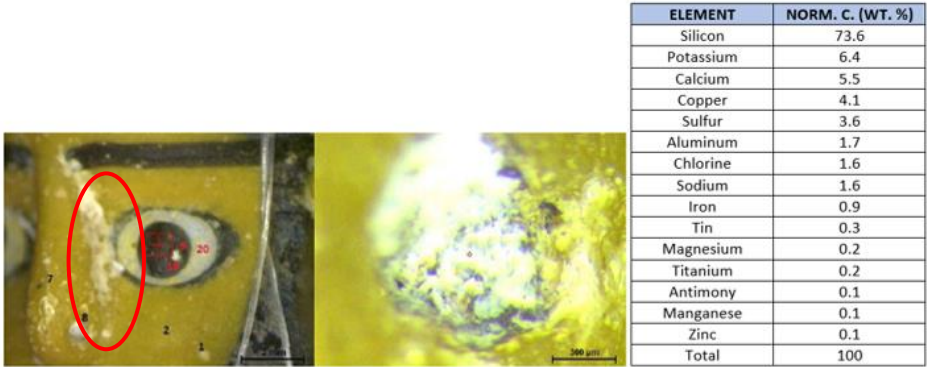


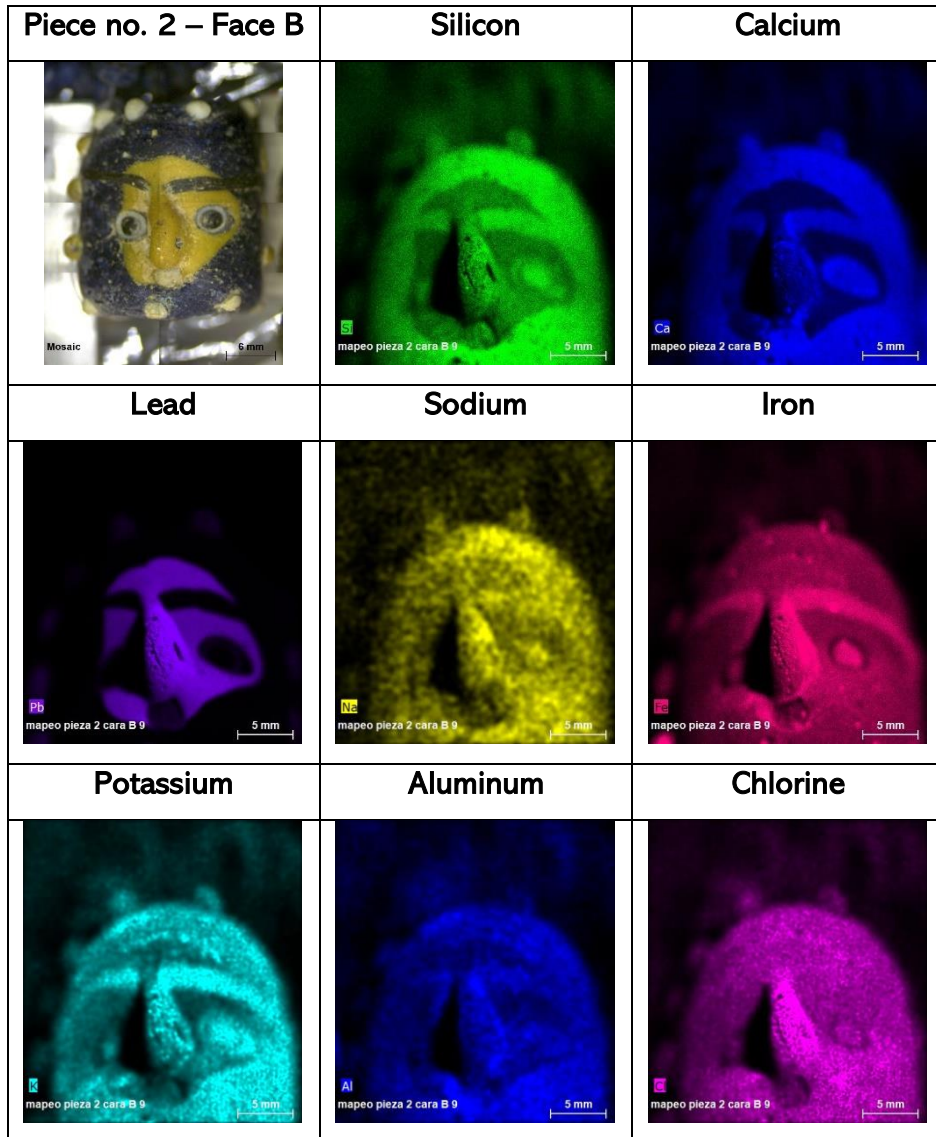
Figure 63 - Punctual analysis performed in white points of the face A in the piece no.2

This white point was compared with another white points of the face such as the white point of the eye and the results obtained were very similar.

This comparison was also made in the black areas of the face (eyebrow, pupil and all the external part of the sample) and all of them showed a very similar elemental composition. The semi-quantitative values obtained show that the main elements for the analyzed areas ordered from highest to lowest were silicon, calcium, sodium and iron, with little differences in the values between each analyzed point.

To sum up, the presence of some elements can be related to some colors used in the piece. This is the case of the yellow zone, which can be directly related to the presence of lead and arsenic. The gray area can be related to the presence of copper and manganese and in a lower presence, iron and cobalt. Black areas can be related to iron. Finally, white areas were related with the presence of calcium and antimony.

Elemental map distribution obtained from the piece no.2, concretely, from the face B is showed in the Figure 9.



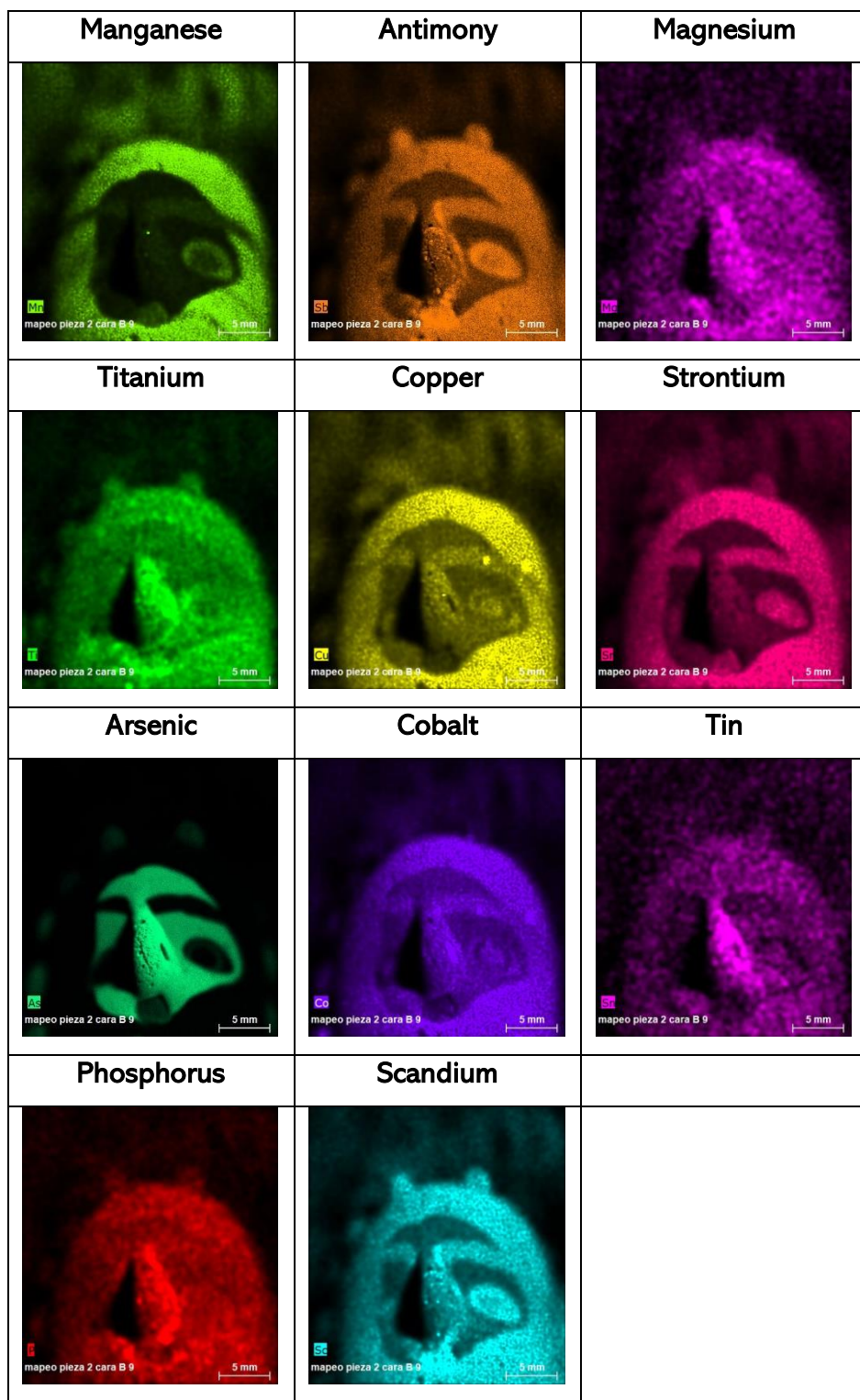


Figure 64 - Elemental image of the face B in the glass beads no. 2 by ED-XRF

Face B of this piece is different from piece A but similar in general appearance, both are surrounded by a gray color in the external area, and both show small white/yellow bumps on the gray area of the face. The face is yellow, and the eye and nose are similar to the other face.

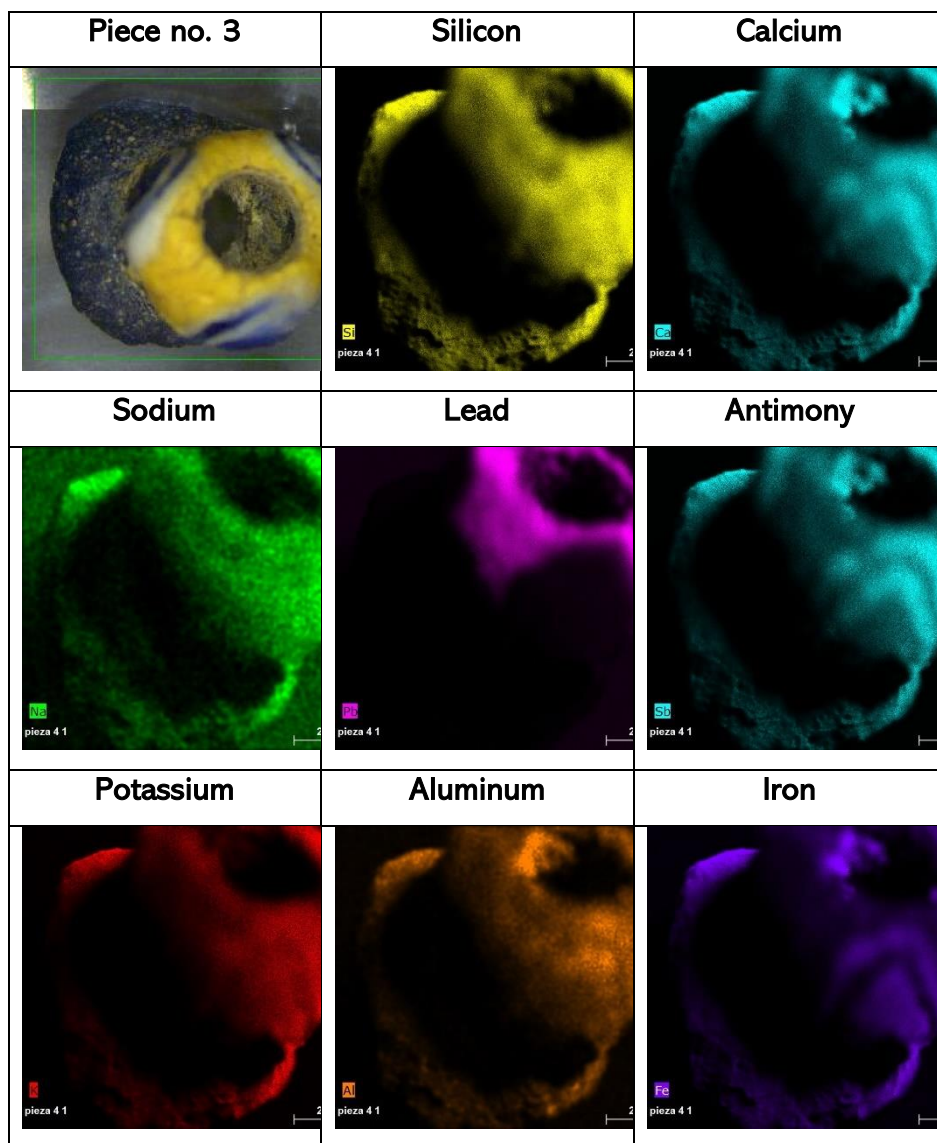
Silicon, calcium, potassium, antimony, strontium and scandium have a nearly identical distribution. All of them are detected throughout the gray area that surrounds the face, in the eyebrows, part of the nose and in the eyes. The distribution of copper and cobalt closely resembles these groups but has little differences. Copper and cobalt were not detected in the eyebrows, nor in the eyes or in the nose. On the contrary, iron was present in the internal zone of the face, but not in the gray (external) zone.

In the case of sodium, aluminum, chlorine, magnesium, titanium, tin and phosphorus, its distribution was found throughout the entire piece, especially in the area of the nose.

Lead and arsenic return to the same previous pattern commented, their presence was only visible on the inside of the face, except for the eye and eyebrows.

The point-by-point results obtained for the different points of this face were very similar to the previously commented results of face A. They did not present any variation regarding the order of the detected elements. There was a little variation regarding the semi-quantitative values obtained.

The elemental distribution map obtained from the piece no.3 is shown in Figure 10.



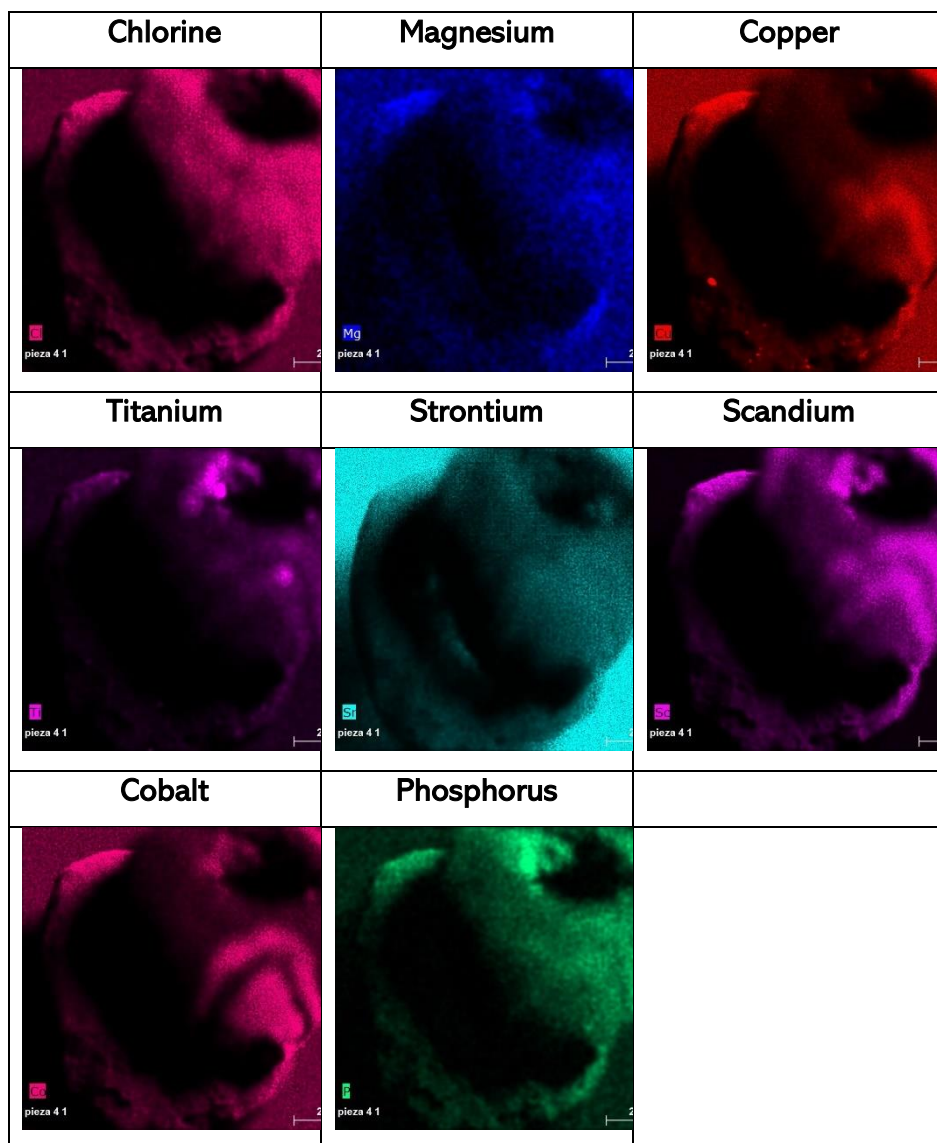


Figure 65 - Elemental image of the glass beads no. 3 by ED-XRF

As it can be seen in this figure above, the appearance of this piece is quite particular, since it seems to be the superposition of two beads, a blue one below, and a yellow one with blue motifs on top.

By means of ED-XRF, it can be also observed how silicon, sodium potassium, chlorine and phosphorus have the same elemental

distribution in the piece; they are present around the entire piece, without being characteristic of any particular color. It is worth to mention that potassium seems to show a higher presence on the right side of the upper piece. On the contrary, in the case of calcium, antimony, iron, copper, scandium, and cobalt their distributions indicate that their presence is detected in the blue areas of the piece, that is, in the lower piece and in the decorations of the upper piece. Aluminum has a similar distribution to this group of elements but not the entirely identical. Its presence is not observed in the blue decorations as in the previous case, but it is observed in the internal part of the piece and in the lower piece.

Lead is again present only in the yellow areas, as in the case of the upper piece, which seems to indicate that this element was part of the composition of this color. Magnesium, like strontium, seems to be present throughout the entire sample, but its presence is also detected in the spectral background, so its presence is not completely clear. Titanium seems to be present only in the internal area of the upper piece and in some specific areas of the sample, so it does not seem to be directly related to any color.

Apart from the distribution map, punctual analysis performed in the yellow area of the upper piece is observed on the left in the Figure 11. On the right, the semi-quantitative composition of this point using normalized percentage of the elements present ordered from highest to lowest is observed.



Figure 66 - Punctual analysis of the yellow area of the piece no.3

In this case, silicon was the main element of the sample, in contrast to the previous cases where lead was the main element in yellow areas. Within the aim of comparing degraded and non-degraded areas, punctual analyses were made in the inner part of the piece also in the yellow area (Figure 12).



Figure 67 – Punctual analysis of the inner yellow area of the piece no. 3

The results obtained from the inner part of the upper piece showed the decrease in the percentage of lead found in the internal zona compared to the external zone. The reason may be the deterioration of this inner part or the different paint composition of this part.

Different blue areas were also analyzed and compared each others to observe if they were little differences. The results obtained reveal that semi-quantitative results were very similar in most of the blue areas analyzed for all elements except for potassium. This element shows a higher presence in the blue decoration that was on the right side of the upper piece, as it was commented in the map distribution.

A white little area observed in the upper piece was also analyzed and compared with blue area to know if there were differences between both zones and it was possible to confirm that the semi-quantitative composition of both zones was very similar.

It can be concluded that the blue color of this piece has the main presence of silicon, calcium and sodium. In addition, this area contains also copper, iron, cobalt, potassium, and antimony as minor elements. The yellow area of the sample present lead as the main element. Finally, the white area showed silicon, calcium and sodium as the main elements, like in the blue one.

In the case of the sample no. 4, the elemental distribution obtained from ED-XRF is shown in the Figure 13.

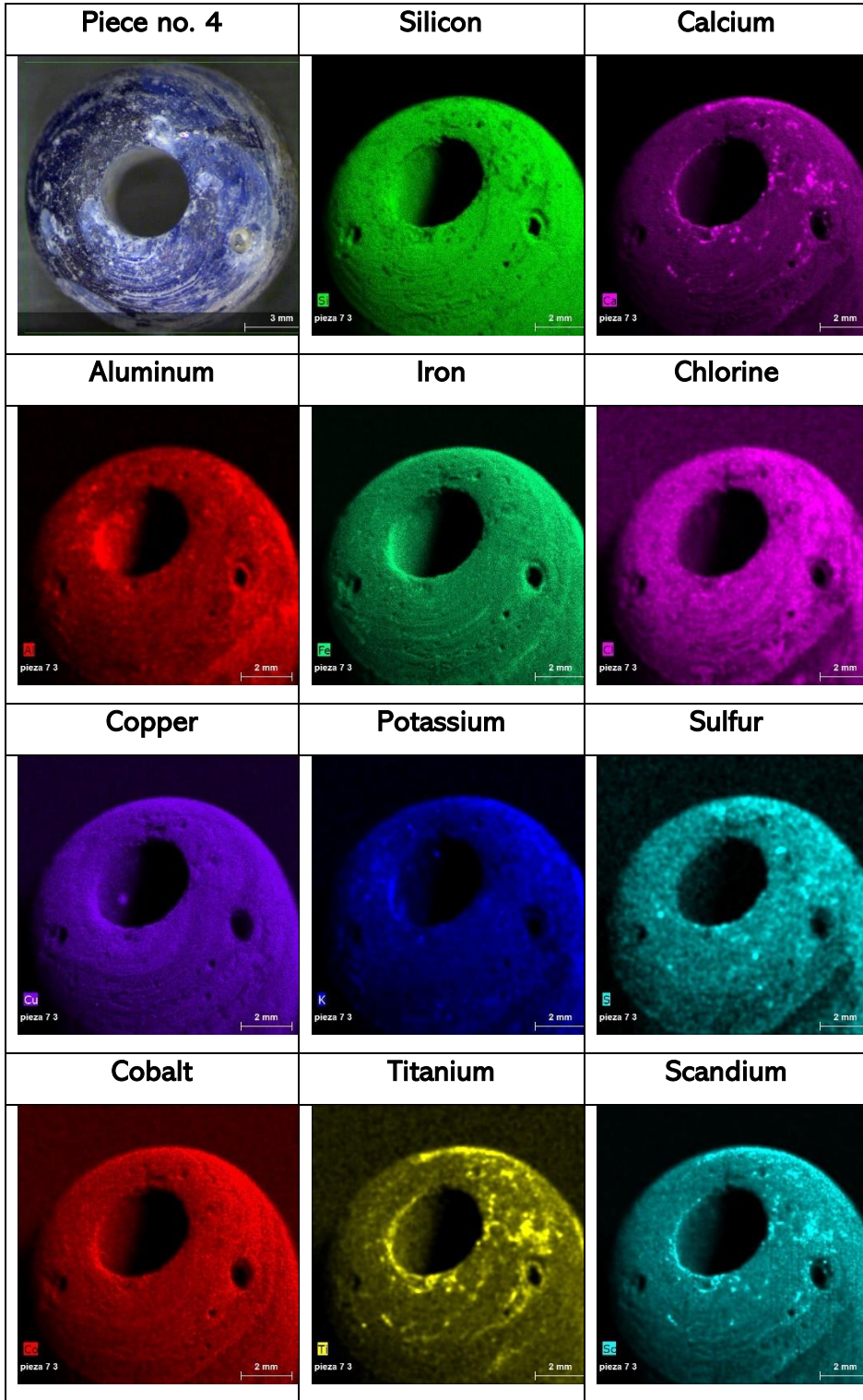


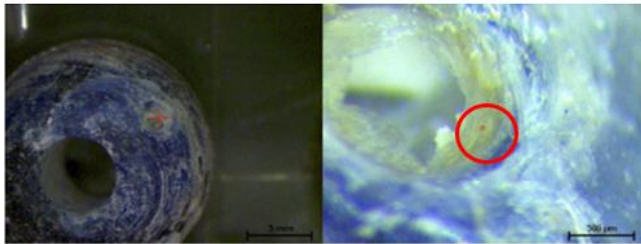
Figure 68 - Elemental image of the glass beads no. 4 by ED-XRF

As it can be observed, this sample has a blue color all along the sample, but its deterioration has caused a loss of color in several areas, showing a whitish or brownish hue.

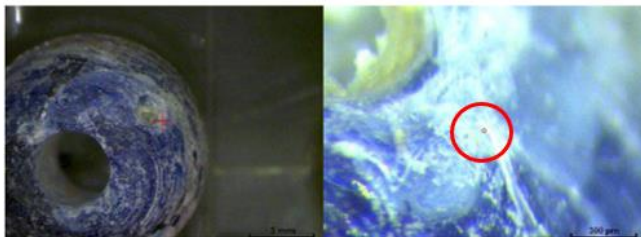
In this sample, silicon, aluminum, iron, chlorine, copper, potassium, and cobalt show a very similar distribution among themselves. They are homogeneously distributed all along the surface area of the sample. It should be mentioned that aluminum and potassium also show a higher presence in the inner area of the piece and in the upper right area.

In the case of calcium, despite being present throughout the entire sample, there is a greater presence in specific areas that do not match with blue color. These areas may be whitish areas. This hypothesis can be demonstrated later with the point-by-point analysis of the different zones. Finally, sulfur, titanium, and scandium are also present in the entire area of the sample, but its presence is higher in specific areas. These areas may be the most deteriorated ones.

To verify the presence of various elements in areas of possible deterioration, point-by-point analyses were carried out. In the Figure 14, a brown deteriorated area was observed on the top, and a white deteriorated area on the bottom and its semi-quantitative analysis can be observed on the right side of each one.



| ELEMENT | NORM. C. (WT. %) |
|-----------|------------------|
| Silicon | 81.7 |
| Calcium | 6.9 |
| Magnesium | 3.6 |
| Aluminum | 3.3 |
| Iron | 2.8 |
| Potassium | 0.5 |
| Titanium | 0.4 |
| Chlorine | 0.3 |
| Copper | 0.3 |
| Sulfur | 0.1 |
| Cobalt | 0.1 |
| Total | 100 |



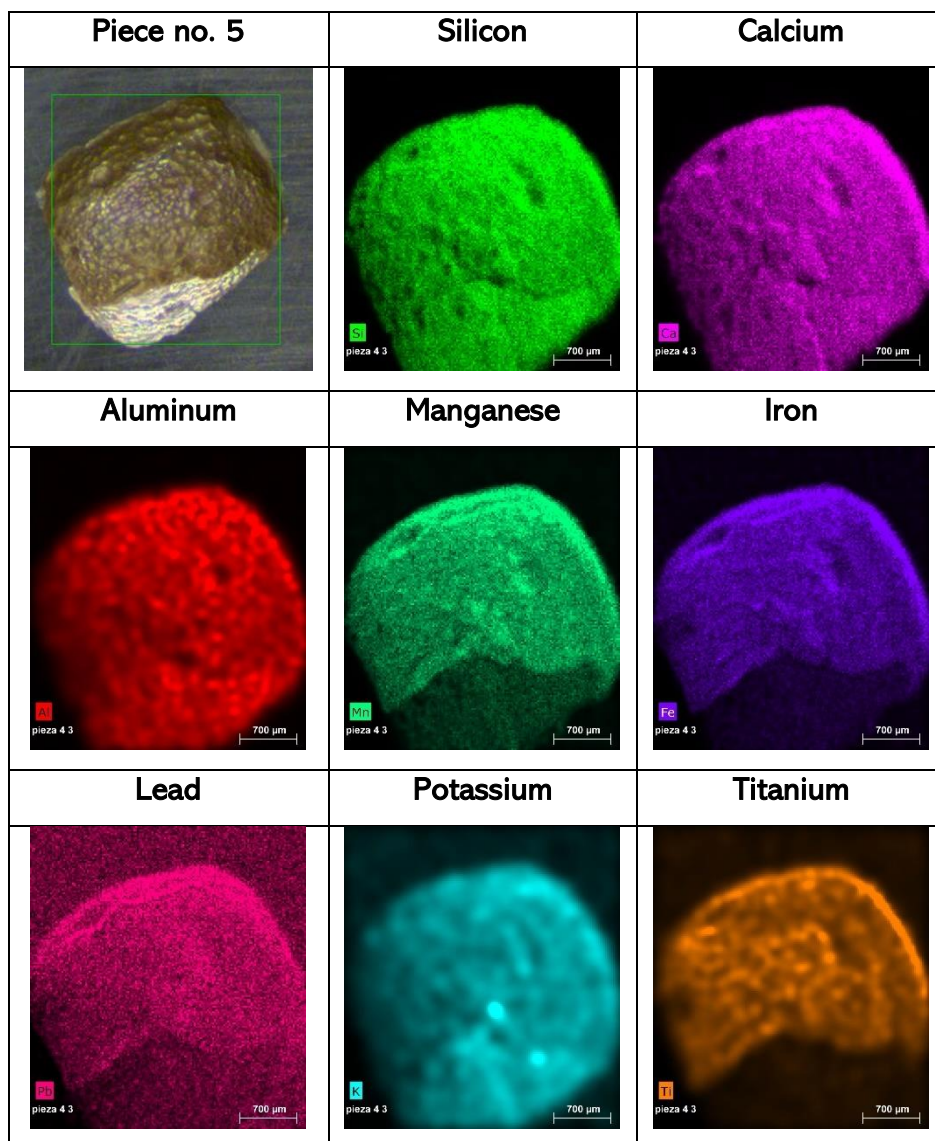
| ELEMENT | NORM. C. (WT. %) |
|-----------|------------------|
| Silicon | 74.0 |
| Calcium | 15.1 |
| Aluminum | 3.7 |
| Iron | 2.4 |
| Chlorine | 1.3 |
| Copper | 1.0 |
| Potassium | 0.5 |
| Sodium | 0.4 |
| Magnesium | 0.3 |
| Sulfur | 0.3 |
| Titanium | 0.3 |
| Cobalt | 0.3 |
| Strontium | 0.2 |
| Scandium | 0.1 |
| Manganese | 0.1 |
| Total | 100 |

Figure 69 – Punctual analysis of the brown (upper image) and white (bottom image) areas in the piece no.4

It can be observed that the three main elements detected in the different areas were not the same. In the brown area the presence of magnesium is higher than in the white area. On the contrary, in the white area, the presence of calcium is higher than in the brown area. Regarding the remaining elements, significant differences can be seen, but since their values are less than 1 % (wt %), they were not considered crucial for these deteriorated areas.

In the case of the blue areas, point-by-point analysis demonstrated very similar values to the ones obtained in the white area analyzed in the Figure 14. So, it could be hypothesized that the blue area may have lost its original blue color and acquired a whitish color but without altering its elemental composition.

In the case of the sample no. 5, the elemental distribution obtained from ED-XRF is shown in the Figure 15.



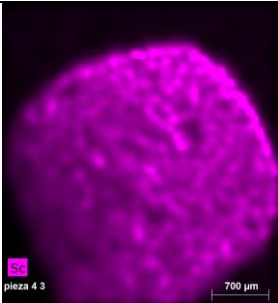
| Scandium | | |
|---|--|--|
|  | | |

Figure 70 - Elemental image of the glass beads no. 5 by ED-XRF


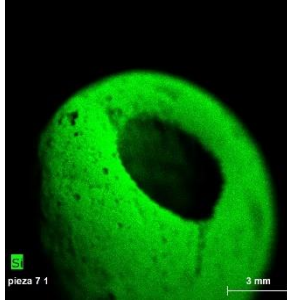
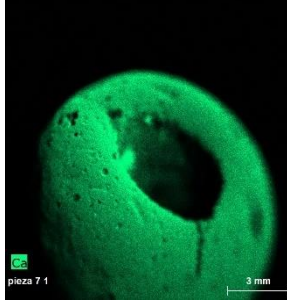
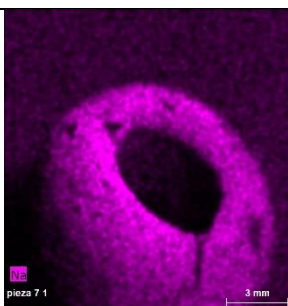
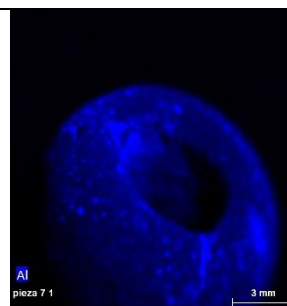
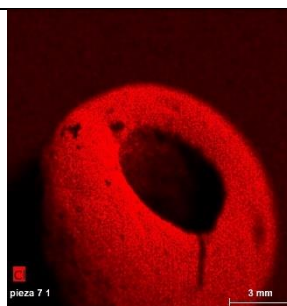
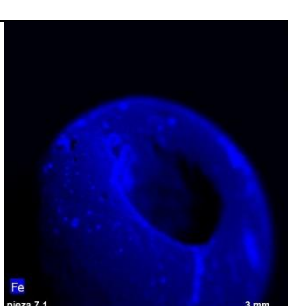
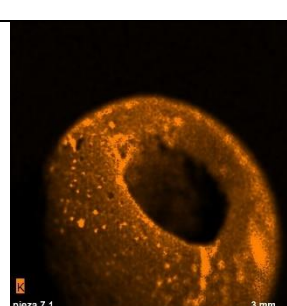
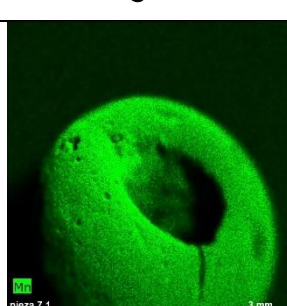
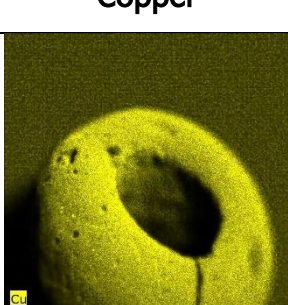
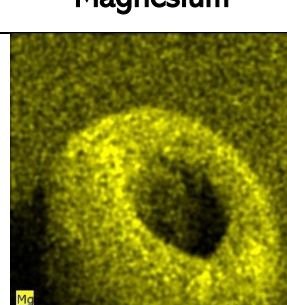
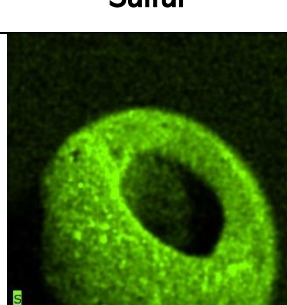
This sample shows a new different color compared with the previous ones, brown color.

The element distribution in this sample shows similar distribution in the case of silicon, calcium, aluminum, potassium and scandium. They were present in the entire area of the sample. In addition, manganese, iron, lead and titanium were also detected throughout all the sample but with a lower detection on the bottom.

Apart from elemental map distribution, point-by-point analyses were performed to obtain more accurate information than that already obtained by mapping. The results obtained from the different points analyzed have shown very similar semi-quantitative values, where the main elements ordered from highest to lowest were silicon, calcium, aluminum, manganese, iron and lead.

It can be concluded that in this particular case, the specific measurements have not yielded new information on the information already obtained by means of elemental ED-XRF mapping.

The analysis performed by ED-XRF in the sample no. 6, showed the elemental distribution which can be observed in Figure 16.

| | | |
|---|---|--|
| <p>Piece no. 6</p> | <p>Silicon</p> | <p>Calcium</p> |
|  |  |  |
| <p>Sodium</p> | <p>Aluminum</p> | <p>Chlorine</p> |
|  |  |  |
| <p>Iron</p> | <p>Potassium</p> | <p>Manganese</p> |
|  |  |  |
| <p>Copper</p> | <p>Magnesium</p> | <p>Sulfur</p> |
|  |  |  |

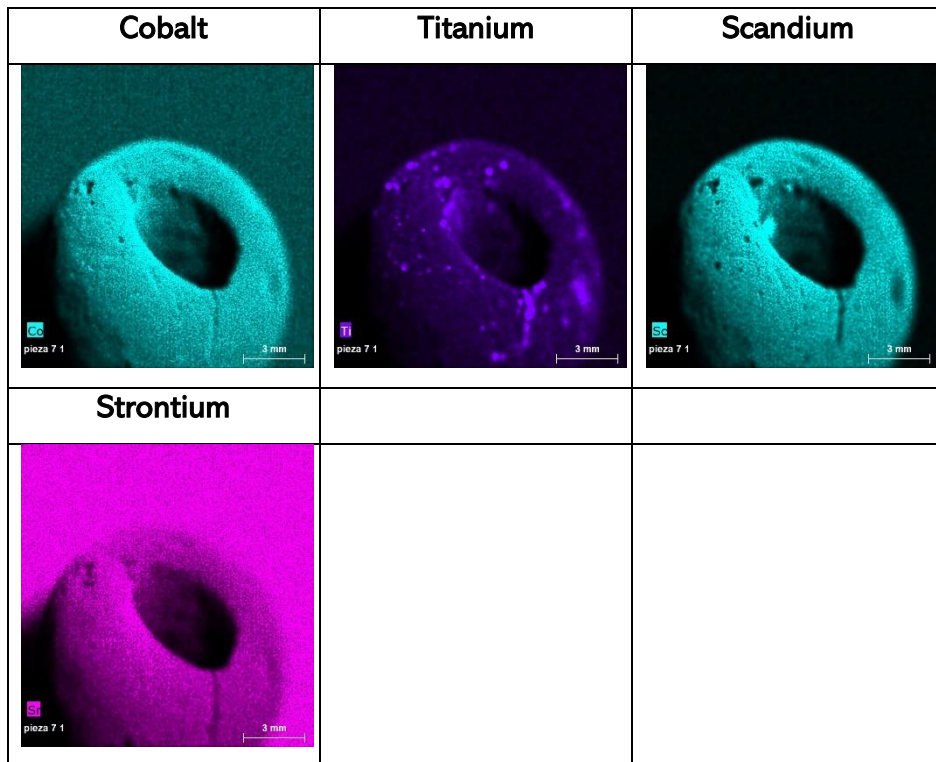


Figure 71 - Elemental image of the glass beads no. 6 by ED-XRF

This sample, like in the piece no. 4, has a blue color but it has also little white and brown areas which seems to be degraded areas.

The elemental distribution of the sample no. 6 showed how silicon, calcium, sodium, chlorine, manganese, copper, cobalt, scandium, and strontium have the same distribution. They are detected homogeneously distributed in all the entire area of the sample.

In contrast, aluminum, iron, sulfur, potassium, and titanium present another elemental distribution where the higher presence is detected in some specific areas, the more degraded areas of the sample. For that reason, it could be possible that the presence of these elements would be related to surface alterations. As commented in other samples, some elements such as magnesium, cobalt, strontium, and

sodium seemed to be detected more intensely in the background than in the piece.

To corroborate the presence of some elements in degraded areas, point-by-point measurements were made. The most interesting areas to analyze were the brown and white ones and its semi-quantitative values were exposed near the point analyzed in the Figure 17.

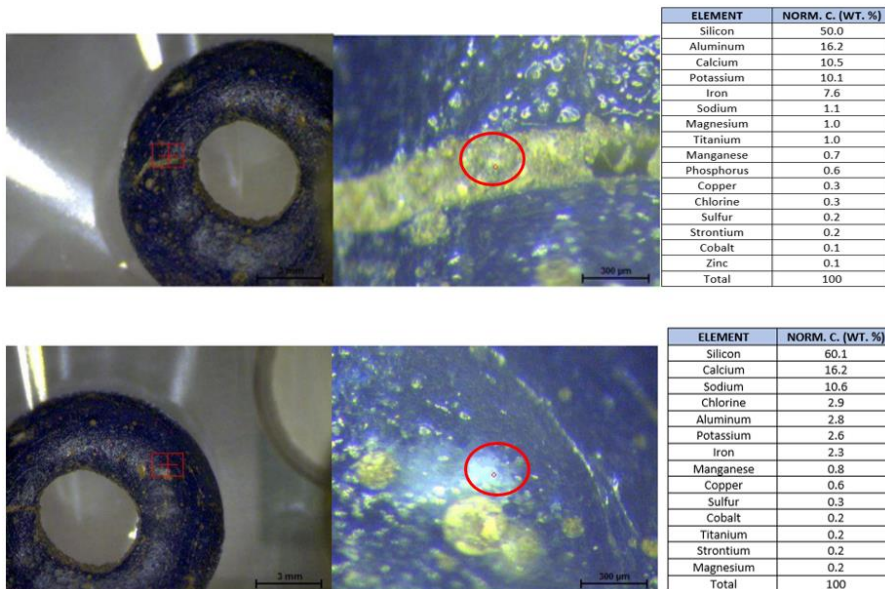


Figure 72 – Punctual analysis of the brown area (upper image) and white area (below image) of the piece no.6

Regarding the semi-quantitative results, there it can be observed how aluminum, potassium, iron and magnesium have significant differences in their values. These ones are higher in the brown area than in the white area. On the contrary, chlorine and sodium values are higher in white areas.

In the case of the original blue areas analyzed, their semi-quantitative values are exposed in the Figure 18.

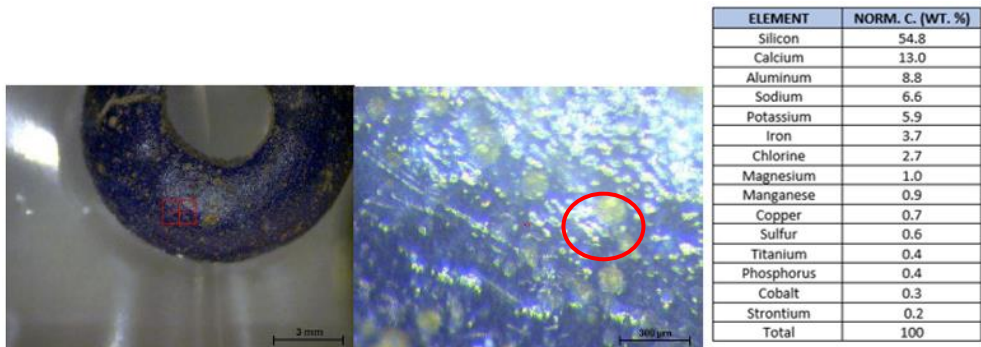
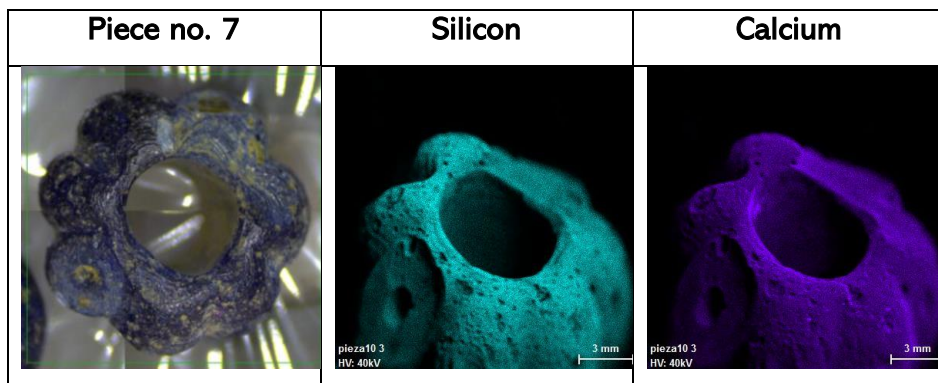


Figure 73 – Punctual analysis of the blue area of the piece no.6

There, its similar semi-quantitative values to those explained before can be observed, with some differences. As in the case of original blue analyzed in the blue beads, the main elements detected were again silicon and calcium.

In the case of the sample no. 7, the elemental distribution obtained from ED-XRF is shown in the Figure 19.



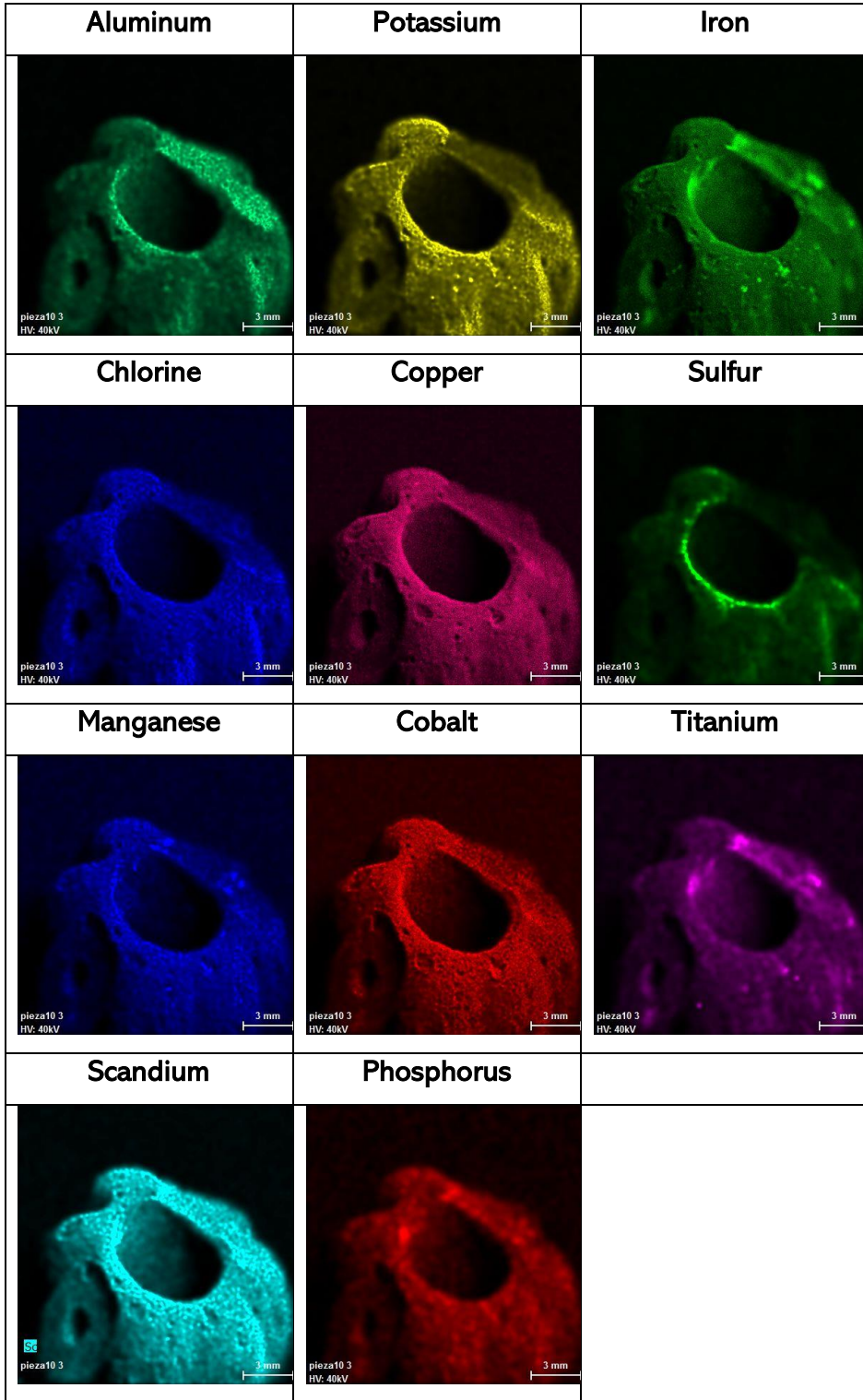


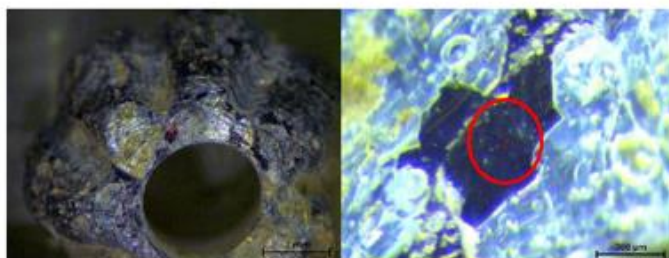
Figure 74 - Elemental image of the glass beads no. 7 by ED-XRF

These sample, as the piece no. 6 described before, has a blue color all around the sample. As observed in piece no. 6, it has white and brown areas that appear to be areas of degradation. Unlike the previous one, this one has curved shapes on the outside of the sample.

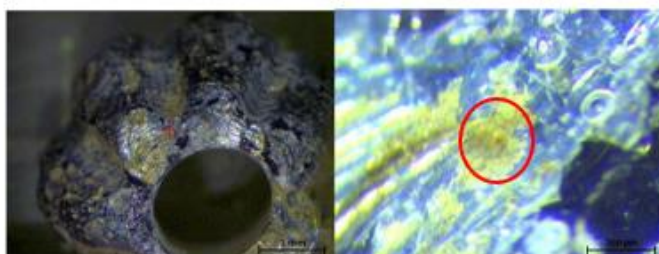
These results showed in Figure 17 presented similar distribution for silicon, calcium, chlorine, copper, cobalt, and scandium. The presence of these elements is homogeneous around the entire sample.

In addition, potassium and sulfur are detected in the inner part of the sample, but with different distribution. Sulfur is only located in the inner part of the sample. In contrast, potassium is present in the inner part of the sample and in other specific areas which seems to be white areas. Iron, manganese, titanium and phosphorus are detected in the inner part of the sample, in some specific areas which may be brown areas. Aluminum showed a different distribution to the rest of the elements because its presence is higher in the right part of the sample and in the inner side.

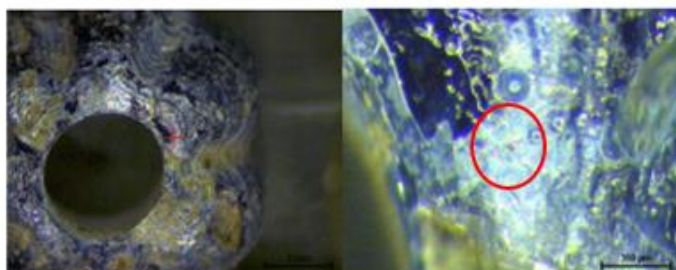
Different colored areas were tested by point-by-point analysis and the obtained semi-quantitative results for white, brown, and original blue areas are shown in Figure 20.



| ELEMENT | NORM. C. (WT. %) |
|-----------|------------------|
| Silicon | 67.8 |
| Calcium | 14.2 |
| Sodium | 7.6 |
| Chlorine | 2.4 |
| Potassium | 2.0 |
| Aluminum | 1.8 |
| Iron | 1.6 |
| Copper | 0.8 |
| Sulfur | 0.5 |
| Manganese | 0.3 |
| Cobalt | 0.3 |
| Magnesium | 0.3 |
| Titanium | 0.1 |
| Strontium | 0.1 |
| Scandium | 0.1 |
| Total | 100 |



| ELEMENT | NORM. C. (WT. %) |
|------------|------------------|
| Silicon | 50.6 |
| Calcium | 19.7 |
| Iron | 10.8 |
| Aluminum | 7.8 |
| Chlorine | 2.5 |
| Titanium | 2.0 |
| Potassium | 1.4 |
| Copper | 1.4 |
| Manganese | 0.9 |
| Sodium | 0.7 |
| Sulfur | 0.7 |
| Phosphorus | 0.6 |
| Cobalt | 0.4 |
| Strontium | 0.2 |
| Scandium | 0.1 |
| Lead | 0.1 |
| Zinc | 0.1 |
| Total | 100 |



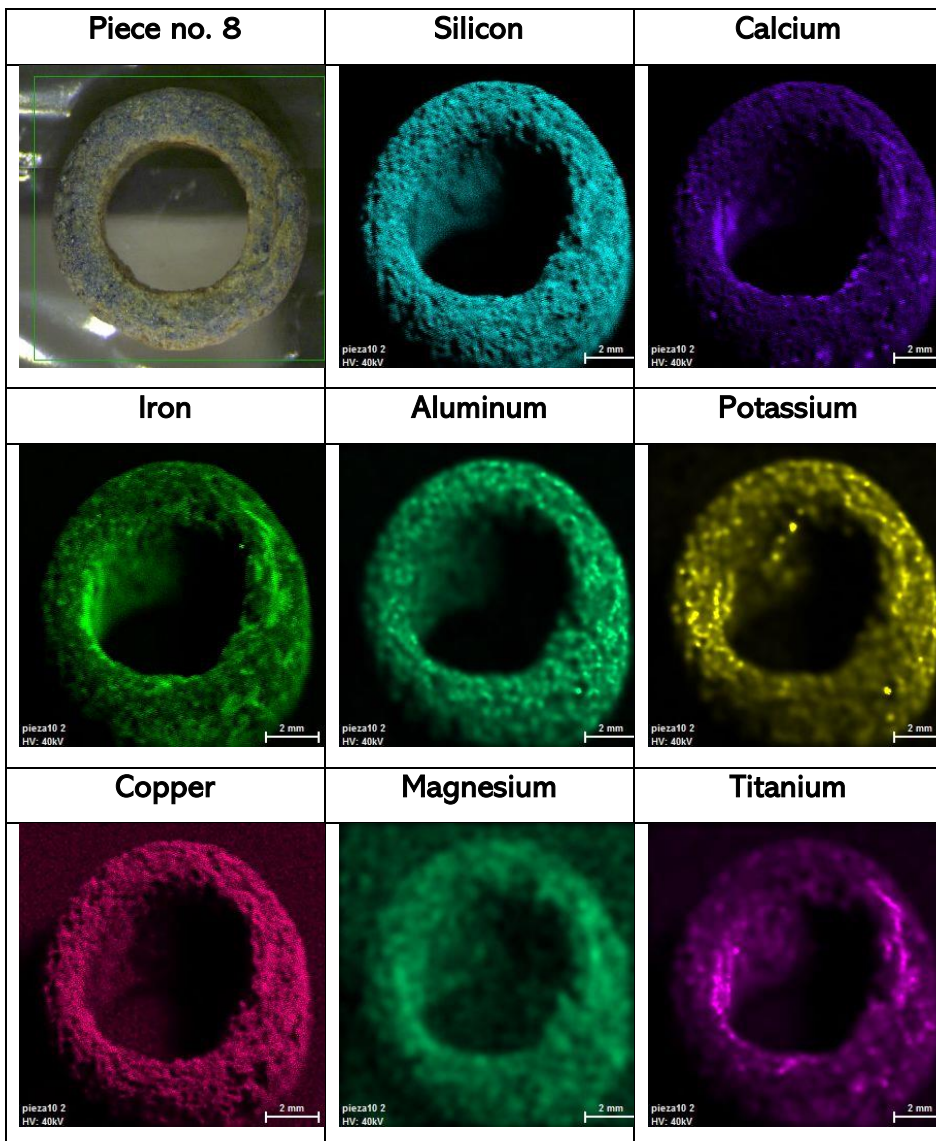
| ELEMENT | NORM. C. (WT. %) |
|-----------|------------------|
| Silicon | 64.0 |
| Calcium | 14.1 |
| Aluminum | 10.5 |
| Potassium | 3.1 |
| Sodium | 2.3 |
| Chlorine | 1.9 |
| Iron | 1.8 |
| Copper | 0.8 |
| Sulfur | 0.3 |
| Cobalt | 0.3 |
| Manganese | 0.3 |
| Magnesium | 0.2 |
| Titanium | 0.2 |
| Strontium | 0.2 |
| Total | 100 |

Figure 75 - Punctual analysis performed in the blue (up), yellow (medium), and white (down) areas of the piece no.7

Surprisingly, Figure 20 how the distribution of the elements detected in this sample was not the same as the commented for the previous sample. In this case, sodium semi-quantitative values increase in blue

areas, aluminum values increase in degraded zones such as white and brown colored ones and iron was present in yellow areas with a higher value. Brown areas are specific areas where blue color was degraded, and a mixture of yellow and brown color could be observed.

In the case of the sample no. 8, the elemental distribution obtained from ED-XRF is shown in the Figure 21.



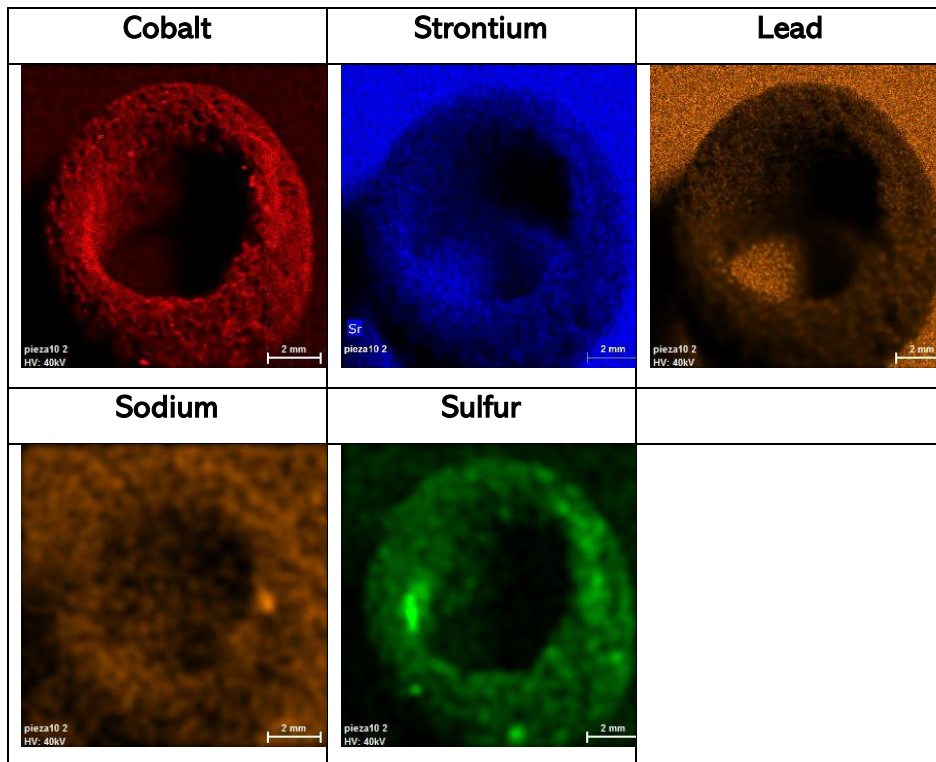


Figure 76 - Elemental image of the glass beads no. 8 by ED-XRF

At first glance, it can be appreciated how the color of this piece was almost completely lost. It was covered by a brown color throughout the entire piece and the original color was barely preserved.

In this sample, elements such as silicon, aluminum, and copper are distributed all around the sample. In the case of elements like calcium, iron, potassium, titanium, and cobalt, they showed a similar distribution located in the inner part of the sample and in the right zone. Probably, its presence was higher in more degraded areas of the sample. Sulfur has a similar distribution to these elements, but its presence seems to be higher in the background. Finally, the presence of magnesium, strontium, lead, and sodium was detected in the background of the sample.

Apart from the distribution map, specific measurements were made in different areas to observe possible elemental changes depending on the color. The semi-quantitative results were very similar in blue, white and brown areas, but not in yellow ones.

In the Figure 22 the semi-quantitative results of the analyzed yellow and blue areas are showed together with their respective semi-quantitative results.

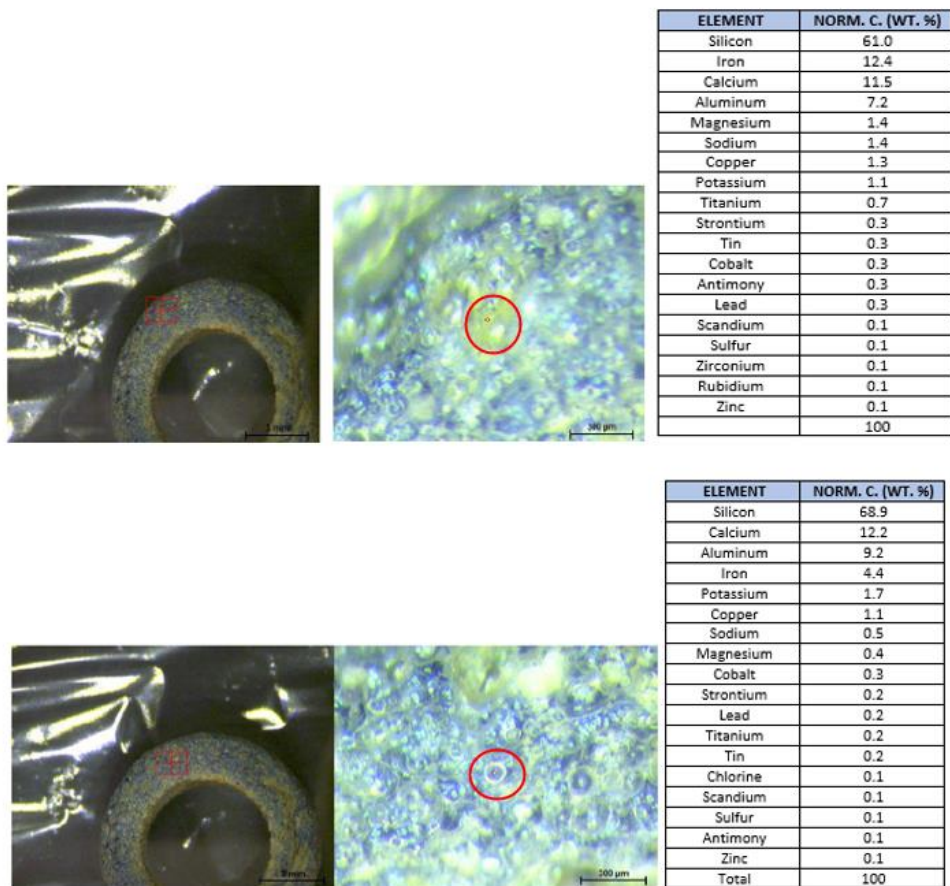
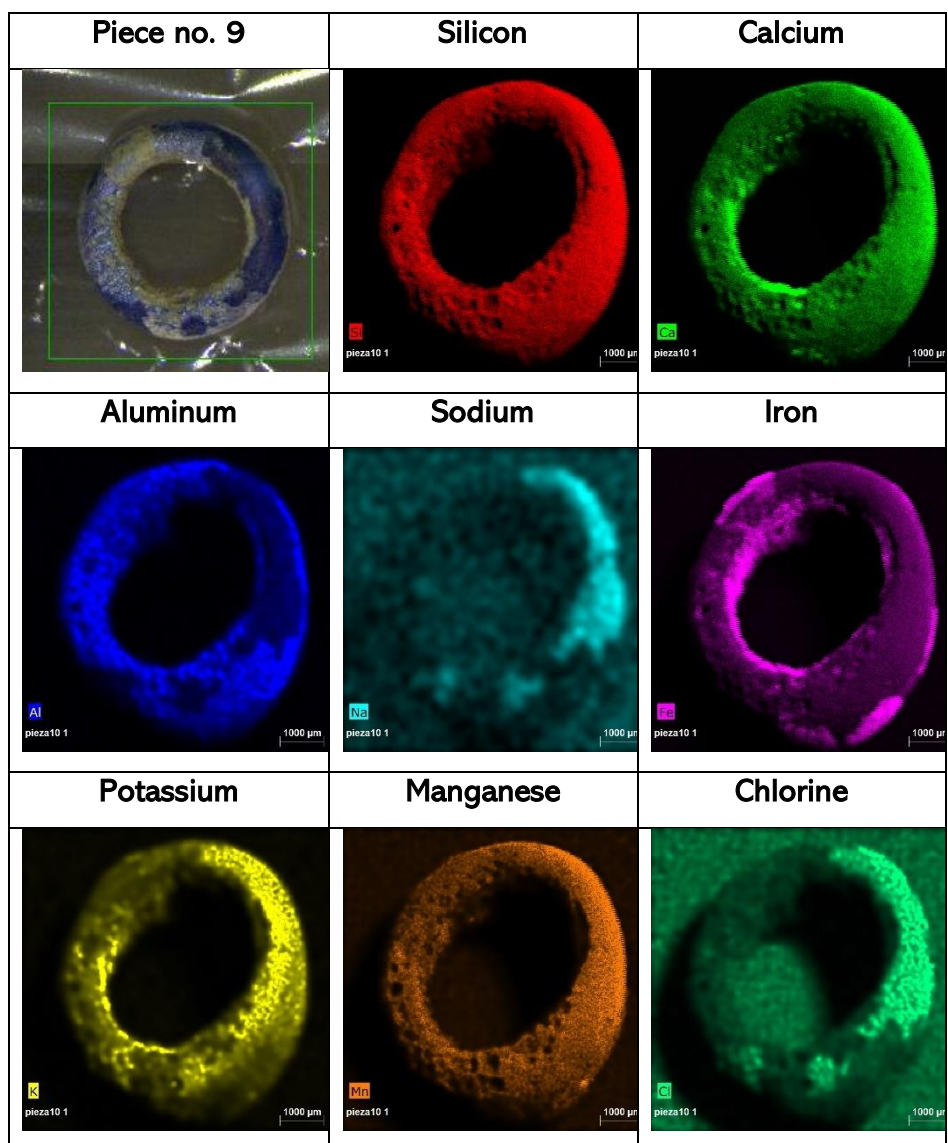


Figure 77 – Punctual analysis performed in yellow (above) and in blue area (down) in the piece no.8

In Figure 22 shows how the iron values on the yellow areas increased compared to the rest of the analyzed areas, being this the most significant difference between the analyzed areas.

The elemental distribution map obtained from the piece no. 9 is shown in the Figure 23 below.



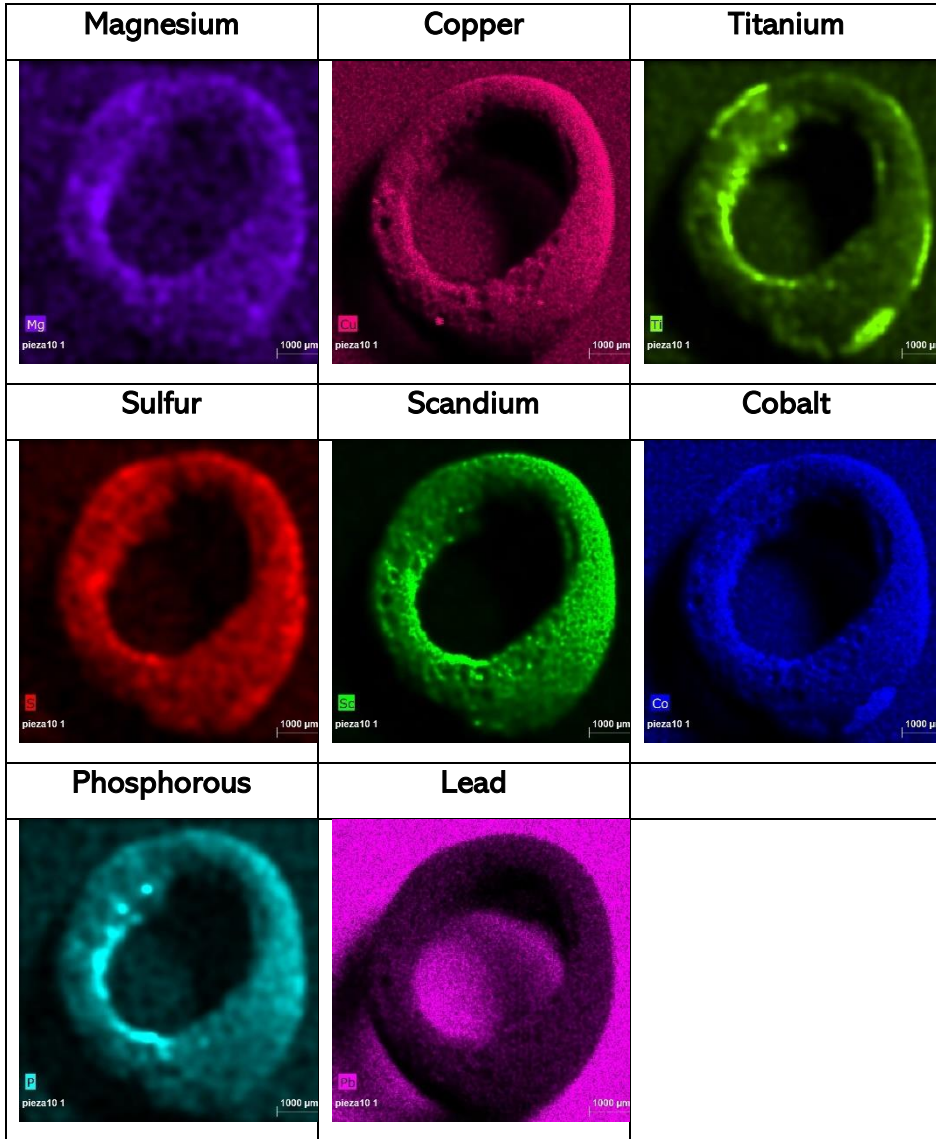


Figure 78 - Elemental image of the glass beads no. 9 by ED-XRF

Sample no. 9, shows, as observed for piece no. 8, a loss of color in a large part of the piece. However, the original blue color is still visible in the right area.

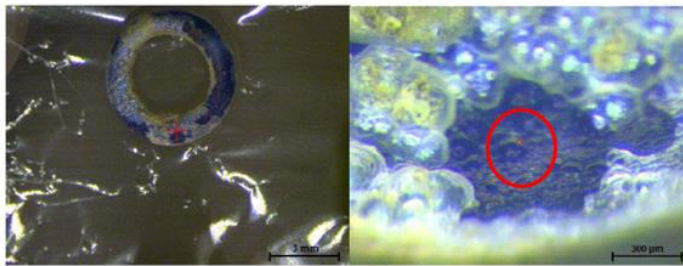
Elemental distribution analysis shows how silicon and manganese were present throughout the entire piece analyzed. Calcium and

potassium show a very similar distribution among them. Its presence is detected especially in the internal and in the upper right parts.

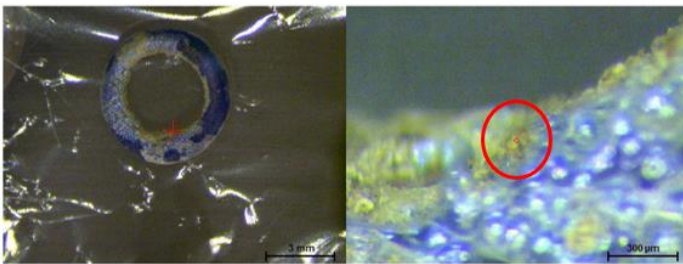
Aluminum is the element whose distribution is not similar to any other. Its presence is detected in most of the degraded area of the piece, in the white/brown area. In the case of sodium and chlorine, their distribution map is negatively correlated to the aluminum map, since in this case calcium and chlorine were only detected in the upper part of the piece, the blue area.

Iron, like titanium and cobalt, can be seen on the inside of the piece and in some specific areas on the outside of the piece. Magnesium, copper, and sulfur seem to be present throughout the piece, as well as silicon and manganese, but magnesium and copper seem to show a higher presence in the background than in the piece itself. Scandium and phosphorus have a very similar distribution that seems to show a higher presence of these elements in the internal area of the sample. Finally, lead shows a very high signal coming from the background, so its distribution is not reliable.

Point-by-point analysis performed in this sample demonstrated the same behavior of the elements commented in the sample no. 7. The results are showed in Figure 24.



| ELEMENT | NORM. C. (WT. %) |
|-----------|------------------|
| Silicon | 59.9 |
| Calcium | 16.4 |
| Sodium | 10.1 |
| Potassium | 4.5 |
| Aluminum | 2.5 |
| Chlorine | 2.1 |
| Iron | 1.7 |
| Manganese | 1.1 |
| Copper | 0.4 |
| Magnesium | 0.3 |
| Sulfur | 0.2 |
| Strontium | 0.2 |
| Cobalt | 0.2 |
| Scandium | 0.2 |
| Titanium | 0.1 |
| Antimony | 0.1 |
| Total | 100 |

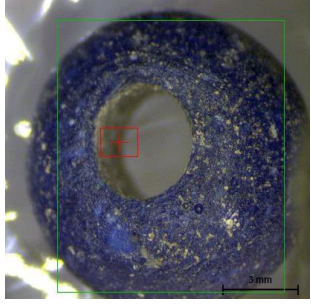
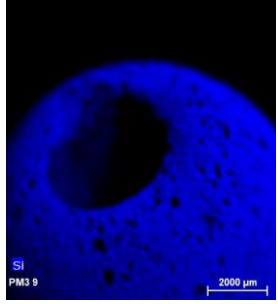
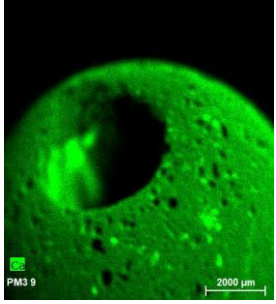
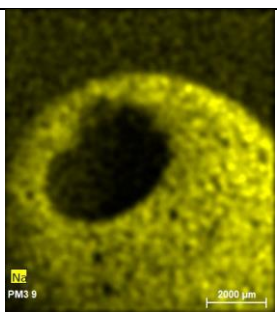
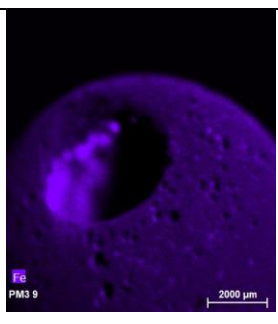
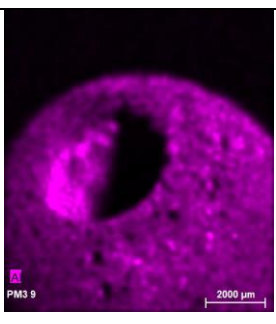
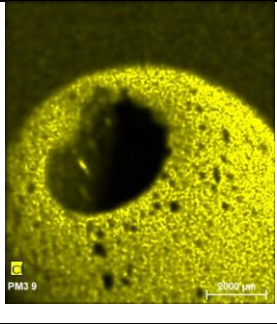
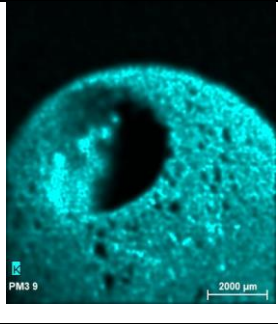
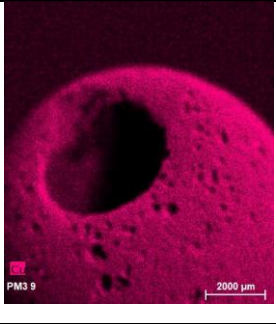
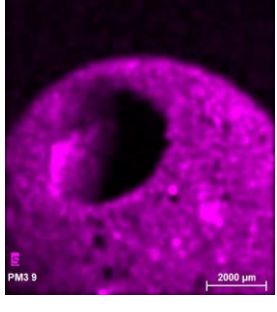
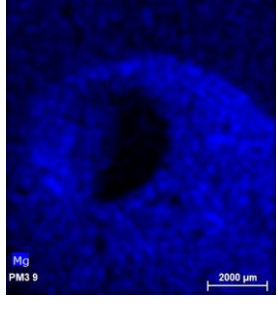
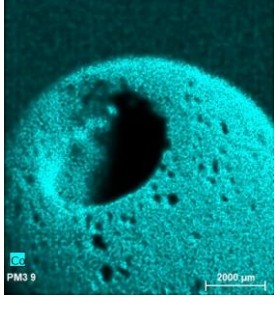


| ELEMENT | NORM. C. (WT. %) |
|------------|------------------|
| Silicon | 54.9 |
| Calcium | 20.2 |
| Aluminum | 9.3 |
| Iron | 8.0 |
| Potassium | 4.8 |
| Phosphorus | 1.1 |
| Sodium | 0.6 |
| Sulfur | 0.2 |
| Titanium | 0.2 |
| Manganese | 0.2 |
| Scandium | 0.1 |
| Chlorine | 0.1 |
| Strontium | 0.1 |
| Antimony | 0.1 |
| Copper | 0.1 |
| Total | 100 |

Figure 79 - Punctual analysis of the blue (above) and yellow (below) areas of the piece no.9

As commented before, the yellow area has the higher semi-quantitative values for iron and aluminum than the blue area.

The distribution map of the sample no. 10 can be distinguished in the Figure 25 below.

| | | |
|---|---|--|
| <p>Piece no. 10</p> | <p>Silicon</p> | <p>Calcium</p> |
|  |  |  |
| <p>Sodium</p> | <p>Iron</p> | <p>Aluminum</p> |
|  |  |  |
| <p>Chlorine</p> | <p>Potassium</p> | <p>Copper</p> |
|  |  |  |
| <p>Sulfur</p> | <p>Magnesium</p> | <p>Cobalt</p> |
|  |  |  |

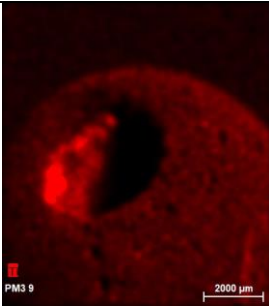
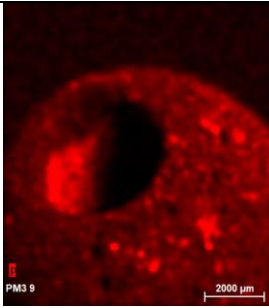
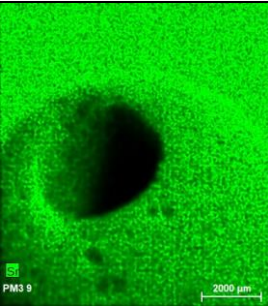
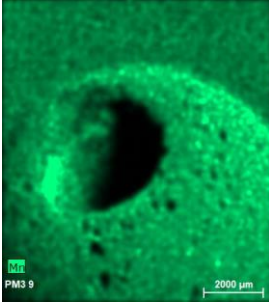
| Titanium | Phosphorus | Strontium |
|---|---|--|
|  |  |  |
| Manganese | | |
|  | | |

Figure 80 - Elemental image of the glass beads no. 10 by ED-XRF

This piece, as samples no. 6 and 7, has a blue color around the entire sample with little degraded areas with brown/white color.

The map distribution shows how silicon, sodium, chlorine, and copper have a homogeneous distribution around the entire piece. In contrast, calcium, iron, aluminum, potassium, sulfur, cobalt, titanium and phosphorus have a very similar distribution with little differences. All these elements were detected in the entire sample but some elements such as calcium, iron, aluminum, potassium, sulfur, titanium and phosphorus were also present in some degraded areas of the sample.

Magnesium, strontium and manganese show a high presence in all around the piece but showed a higher presence of these elements in the background. So, its detection was not reliable.

The results obtained by point-by-point analysis performed in different color of the pieces can be observed in the Figure 26.

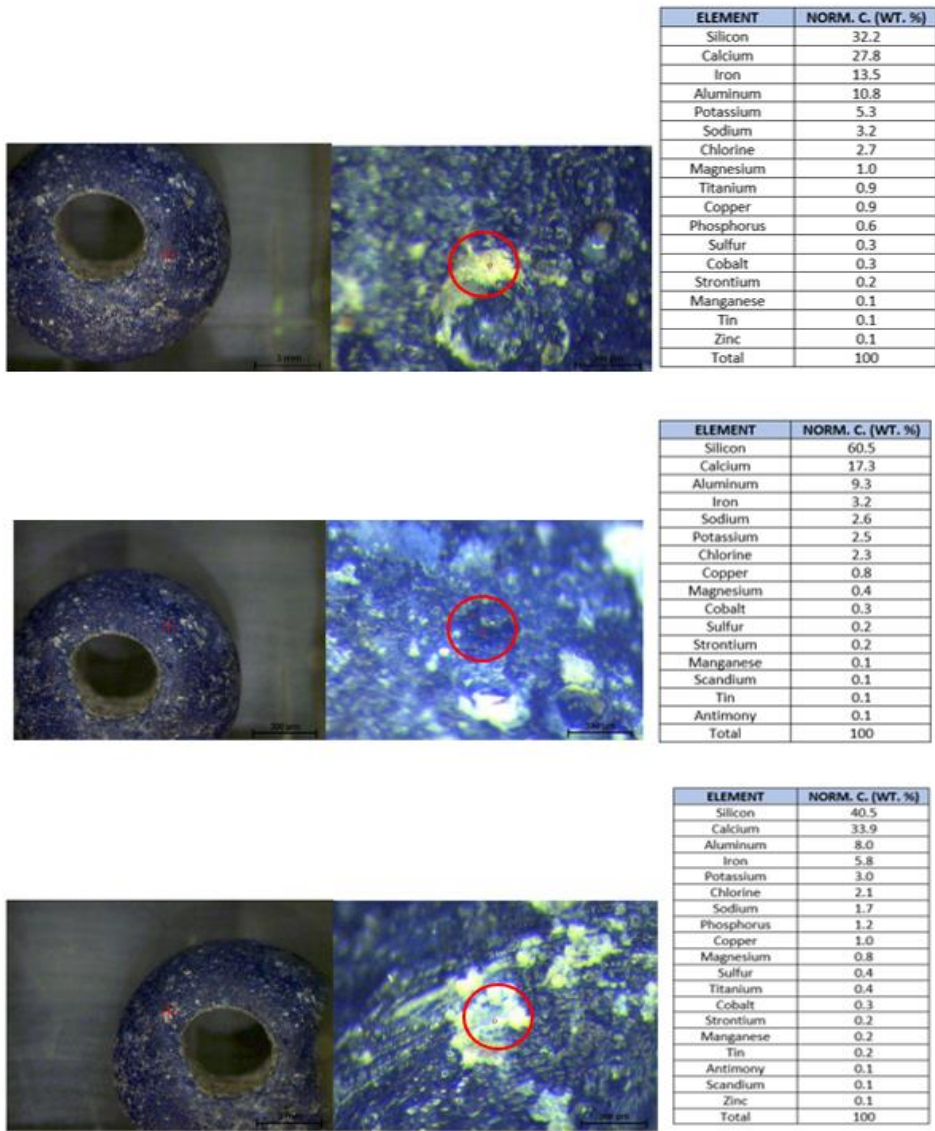
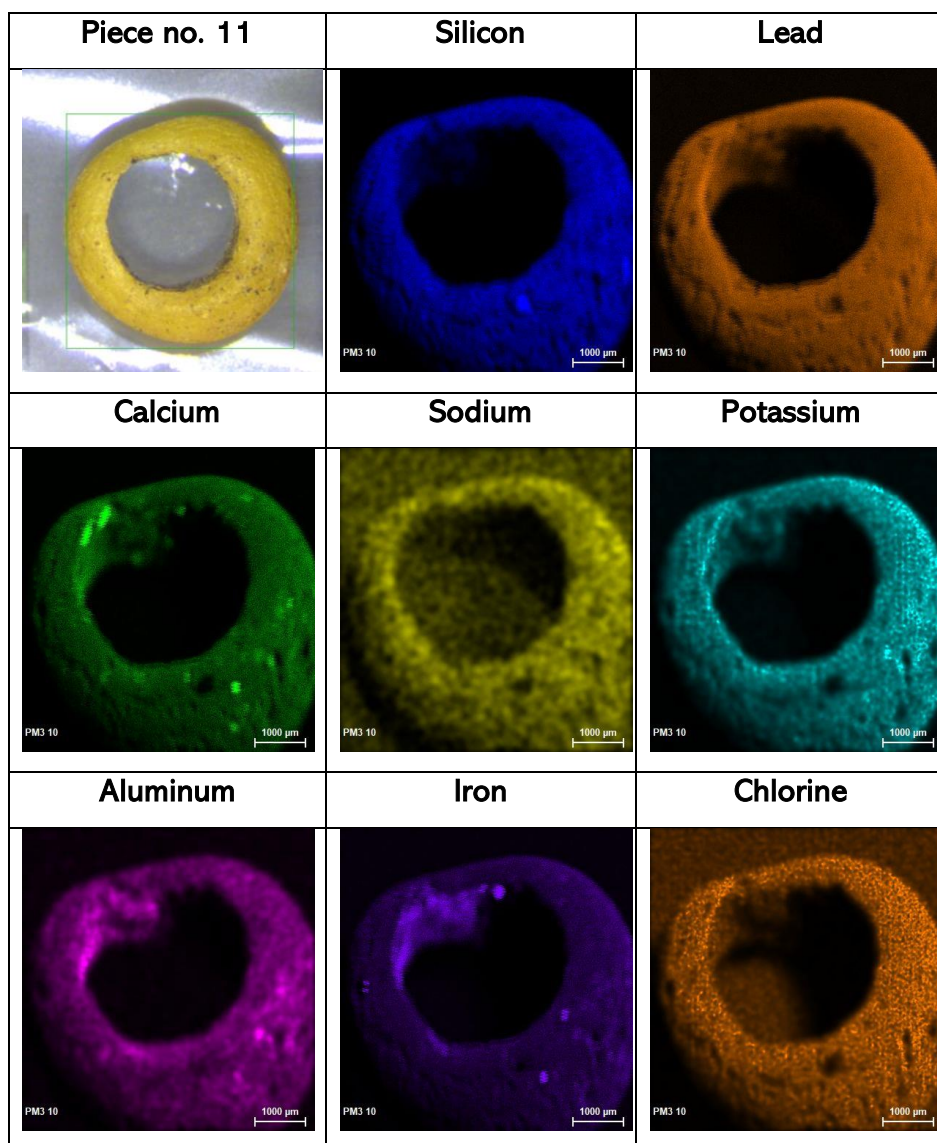


Figure 81 - Punctual analysis of the yellow (above), blue (intermediate) and yellow (below) areas of the piece no.10

In Figure 26 it can be observed how the semi-quantitative results obtained for iron were higher in yellow areas than in white and blue

ones. Furthermore, in the case of silicon, the main element of the samples, the obtained values decrease in the colored areas. That indicates that these areas are undergoing the process of degradation.

The elemental distribution map obtained from the piece no. 11 is shown in the Figure 27.



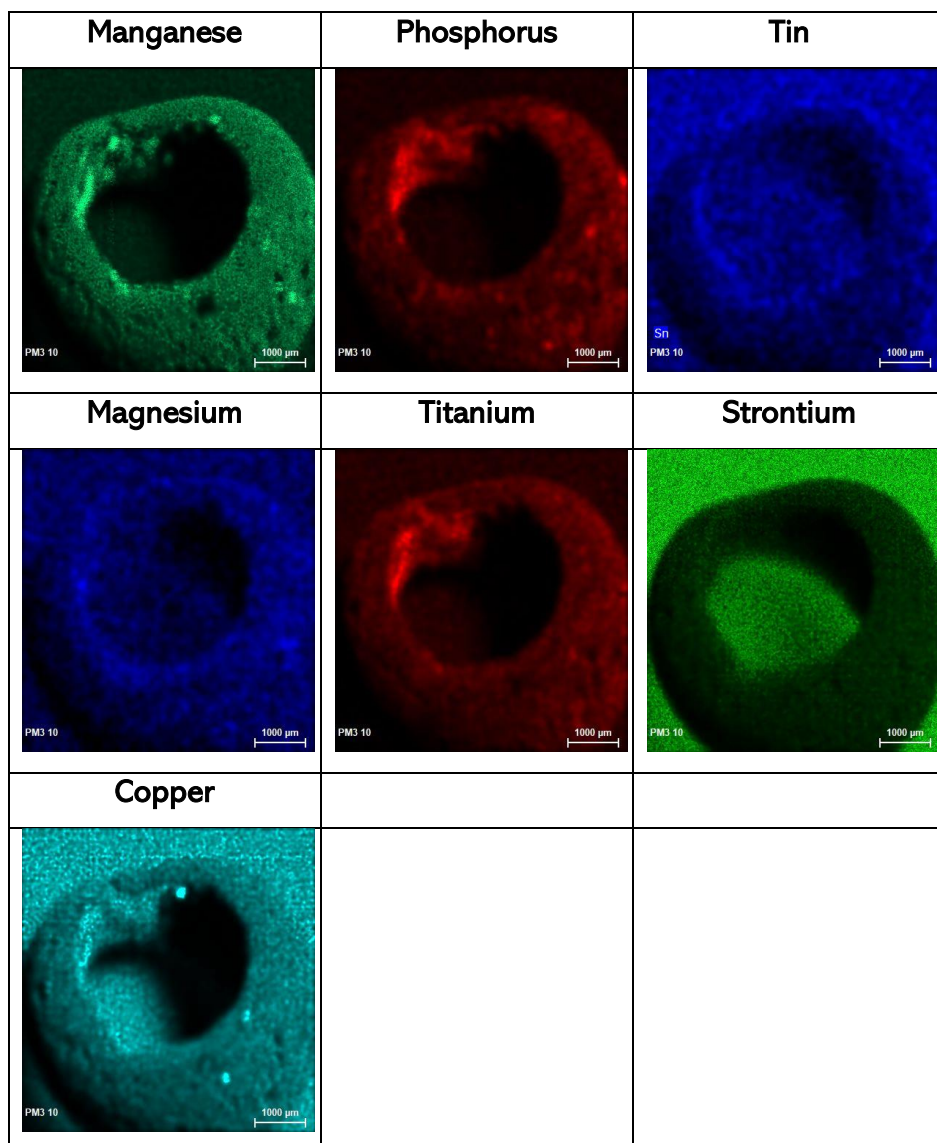


Figure 82 - Elemental image of the glass beads no. 11 by ED-XRF

As can be observed in Figure 27, this piece shows, unlike the rest, a homogeneous yellow color throughout the entire piece.

Due to the homogeneity of the color of the sample, there were not many differences in the distribution of the elements. However, there were certain differences. Aluminum, phosphorus, titanium, copper,

iron, and manganese were detected throughout the sample, but their higher presence was centered in the inner zone. It should be mentioned that in the specific case of copper, the signal obtained from the background is higher than the obtained from the piece, so it was not valid data.

On the contrary, silicon, chlorine, sodium, potassium and lead showed a similar and very homogeneous distribution equally distributed throughout the entire piece. In the case of calcium, this element had a particular distribution that was not similar to the rest of the elements. Its presence was found in several specific points of the piece, probably in the points that have some beginning of degradation process. Finally, in the case of magnesium, strontium and tin, their detection is higher in the spectral background than in the sample, so the distribution map obtained is not reliable.

To observe the possible elemental differences, present in the yellow color and in the points of degradation, point-by-point analysis were carried out. The semi-quantitative results obtained for these two areas can be observed in Figure 28.

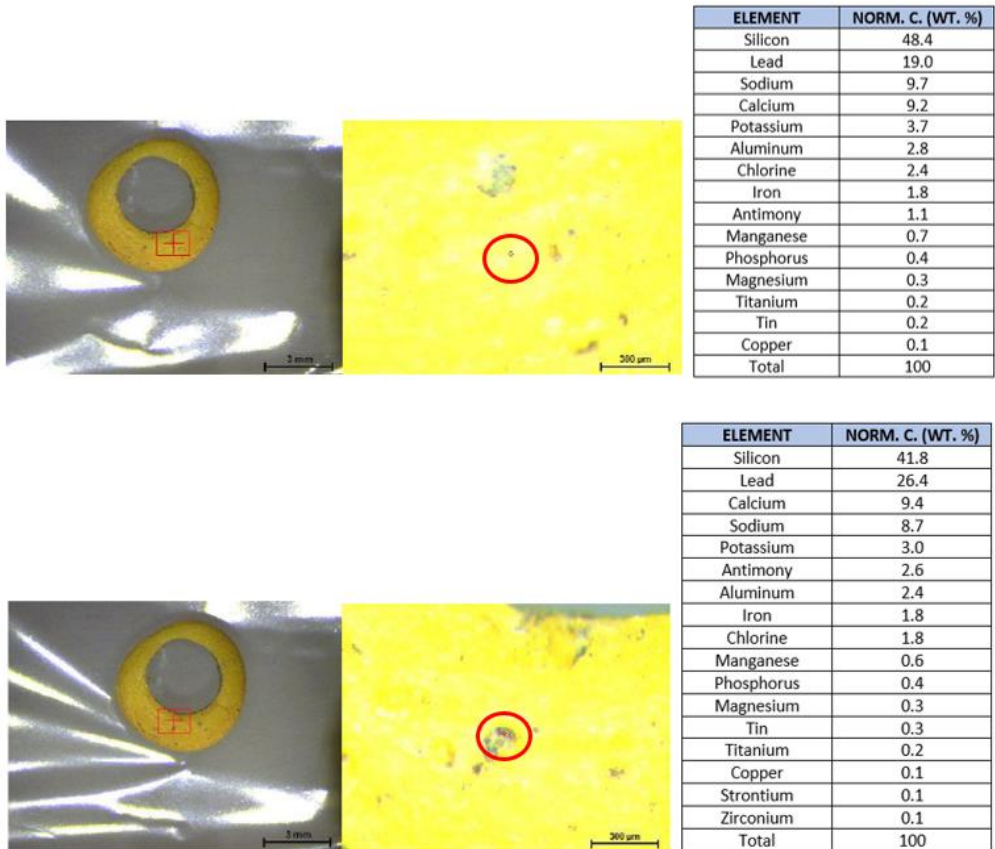
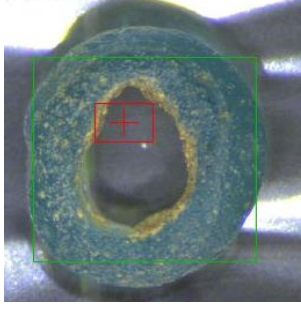
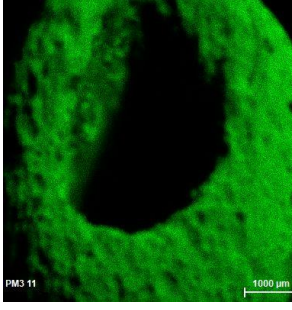
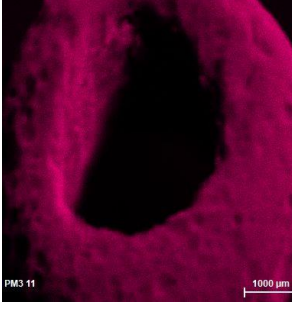
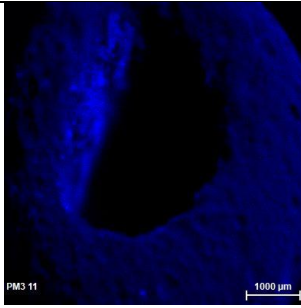
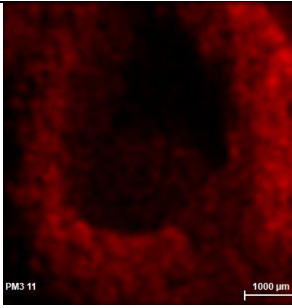
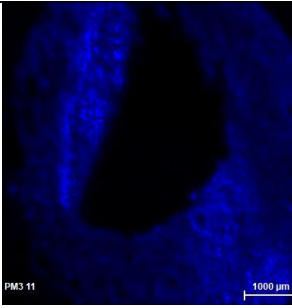
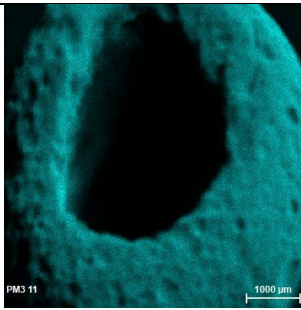
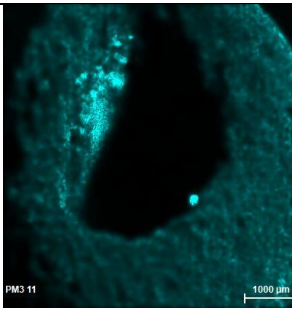
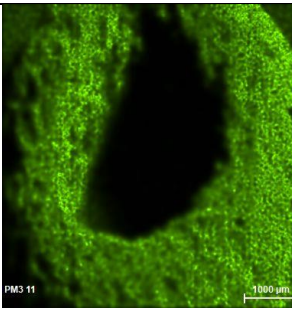
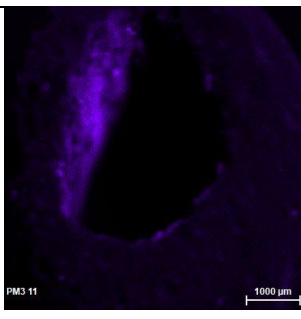
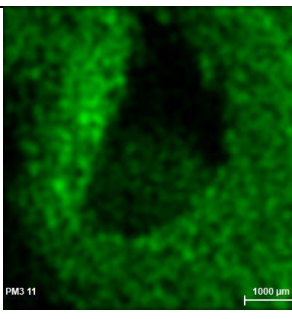
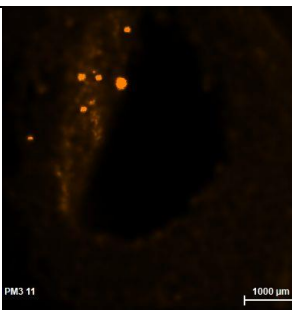


Figure 83 – Punctual analysis performed in yellow (above) and in brown degraded area in the piece no. 11

The results obtained demonstrated how semi-quantitative values of lead increases in the degraded areas. This was confirmed by performing several measurements at different points of degradation on the piece. The reason why lead signal was higher in degraded areas than in non-degraded areas may be due to a loss of the mayor element, in this case silicon.

In the case of the piece no.12, elemental map distribution results are showed in the Figure 29.

| Piece no. 12 | Silicon | Lead |
|---|---|--|
|  |  |  |
| Calcium | Sodium | Aluminum |
|  |  |  |
| Copper | Potassium | Chlorine |
|  |  |  |
| Iron | Magnesium | Titanium |
|  |  |  |

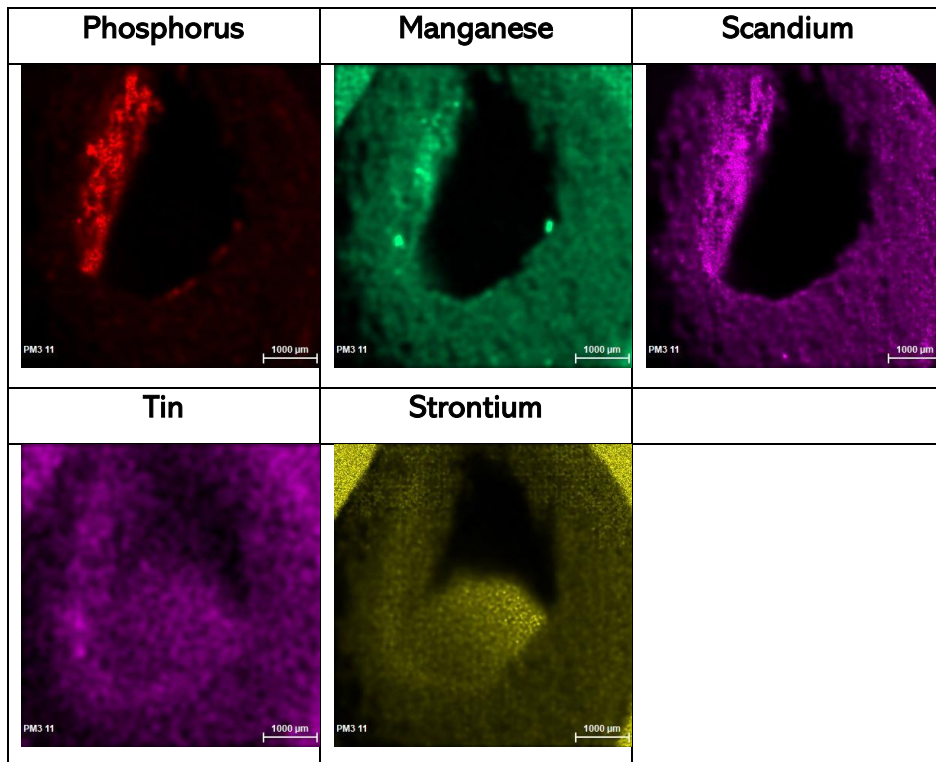


Figure 84 - Elemental image of the glass beads no. 12 by ED-XRF

Sample no. 12 has a greenish color along with small points of degradation on the surface and in the internal area of the sample.

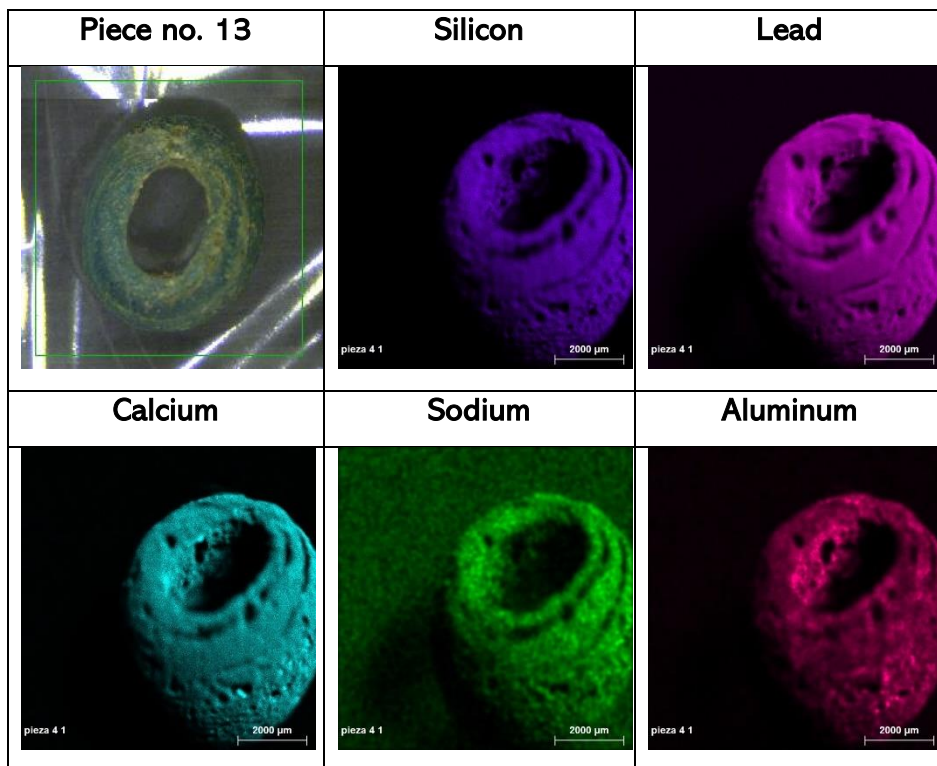
The elemental mapping results showed how the silicon was distributed homogeneously throughout the piece, except in the inner area, where it was barely present. In the case of calcium, aluminum, potassium magnesium, manganese and scandium, although their distribution was not the same for all, the presence of all of them was found throughout the entire piece but their higher presence is centered in the internal part.

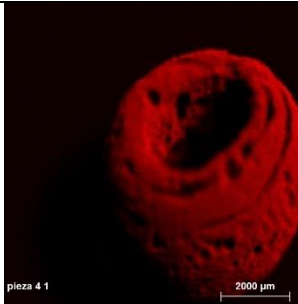
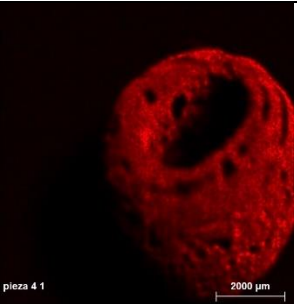
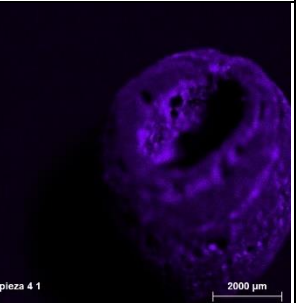
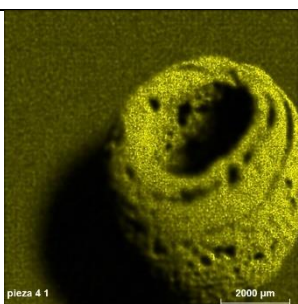
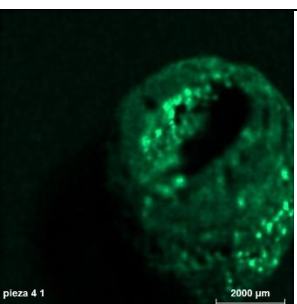
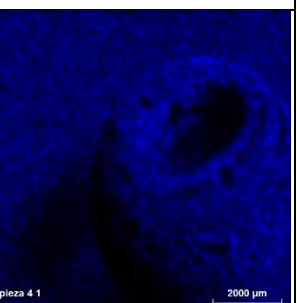
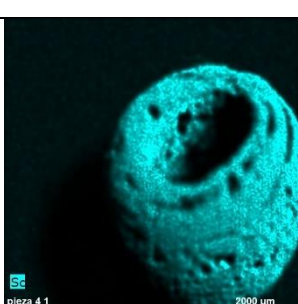
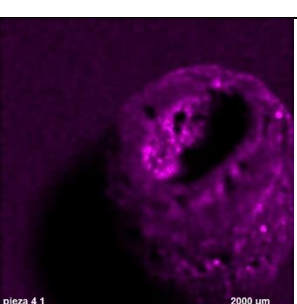
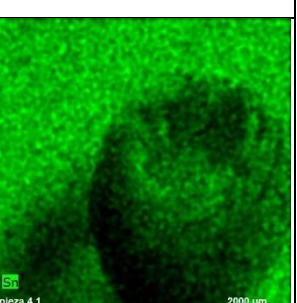

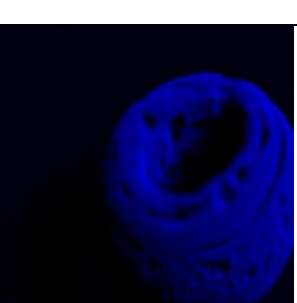
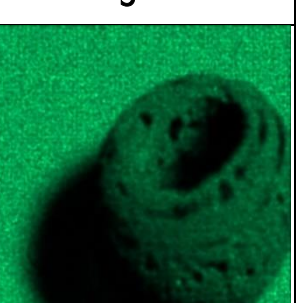
Lead, sodium, chlorine and copper, was detected in the entire piece, both internally and externally. On the contrary, iron, titanium, and phosphorus were only detected in the internal zone, in the most

degraded zone. Finally, tin and strontium seem to have a higher presence in the spectral background than in the piece itself, so their mappings were not valid.

Point-by-point measurements performed in different colored areas demonstrated again that the yellow zones have a higher semi-quantitative value of lead and blue areas have a similar semi-quantitative values than in other blue areas of other pieces.

The elemental mapping obtained from the analysis performed in the piece no.13 is shown in the Figure 30 below.



| | | |
|---|--|--|
| <p style="text-align: center;">Copper</p>  <p>pieza 4 1 2000 µm</p> | <p style="text-align: center;">Potassium</p>  <p>pieza 4 1 2000 µm</p> | <p style="text-align: center;">Iron</p>  <p>pieza 4 1 2000 µm</p> |
| <p style="text-align: center;">Chlorine</p>  <p>pieza 4 1 2000 µm</p> | <p style="text-align: center;">Phosphorus</p>  <p>pieza 4 1 2000 µm</p> | <p style="text-align: center;">Magnesium</p>  <p>pieza 4 1 2000 µm</p> |
| <p style="text-align: center;">Scandium</p>  <p>pieza 4 1 2000 µm</p> | <p style="text-align: center;">Titanium</p>  <p>pieza 4 1 2000 µm</p> | <p style="text-align: center;">Tin</p>  <p>pieza 4 1 2000 µm</p> |
| <p style="text-align: center;">Strontium</p>  <p>pieza 4 1 2000 µm</p> | <p style="text-align: center;">Arsenic</p>  <p>pieza 4 1 2000 µm</p> | <p style="text-align: center;">Manganese</p>  <p>pieza 4 1 2000 µm</p> |

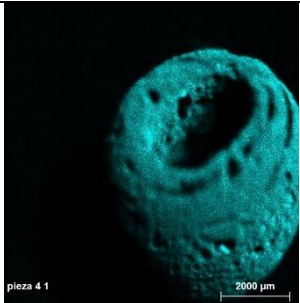
| Antimony | | |
|---|--|--|
|  | | |

Figure 85 - Elemental image of the glass beads no. 13 by ED-XRF

The color and the shape of this sample no. 13 was very similar to the sample commented before, sample 12.


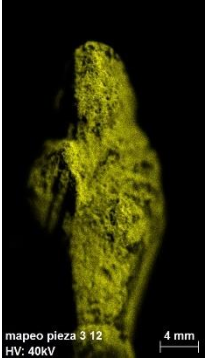
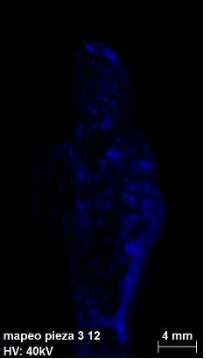
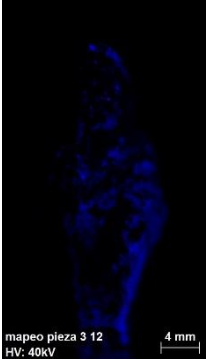
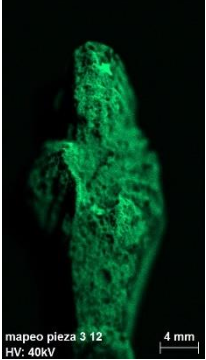
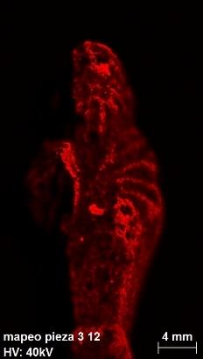
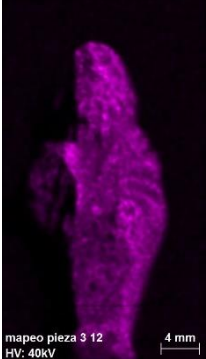
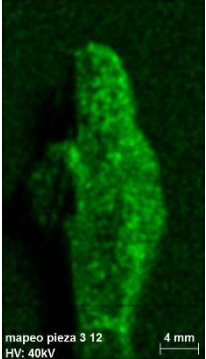
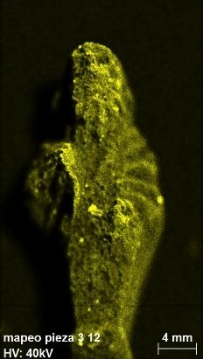
In this case, it can be observed how most of the detected elements showed a very similar distribution pattern. Silicon, lead, calcium, sodium, copper, chlorine, scandium, arsenic, and antimony were distributed throughout the piece.

On the contrary, the presence of aluminum, potassium, iron, phosphorus and titanium seems to be observed in the internal zone and in some specific points of the external zone of the piece, perhaps in yellow areas.

In the case of magnesium, tin, strontium and manganese, the signal obtained by these elements was higher in the spectral background than in the piece, so they were not taken into account.

The specific measurements made on this piece have not revealed new semi-quantitative information with the rest of the pieces. Silicon, lead and calcium were the elements detected mainly in all the analyzed points.

By last, the elemental map distribution of the tomb was performed, and the results obtained can be shown in the Figure 31.

| Togado's figure | Silicon | Calcium |
|--|--|---|
|  <p>mapeo pieza 3 12 HV: 40kV</p> <p>4 mm</p> |  <p>mapeo pieza 3 12 HV: 40kV</p> <p>4 mm</p> |  <p>mapeo pieza 3 12 HV: 40kV</p> <p>4 mm</p> |
| Sulfur | Copper | Potassium |
|  <p>mapeo pieza 3 12 HV: 40kV</p> <p>4 mm</p> |  <p>mapeo pieza 3 12 HV: 40kV</p> <p>4 mm</p> |  <p>mapeo pieza 3 12 HV: 40kV</p> <p>4 mm</p> |
| Aluminum | Magnesium | Iron |
|  <p>mapeo pieza 3 12 HV: 40kV</p> <p>4 mm</p> |  <p>mapeo pieza 3 12 HV: 40kV</p> <p>4 mm</p> |  <p>mapeo pieza 3 12 HV: 40kV</p> <p>4 mm</p> |

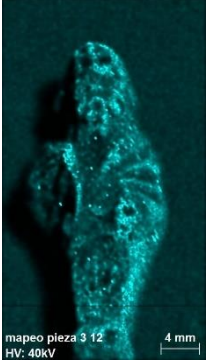
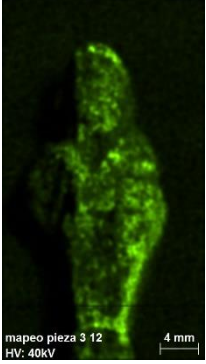
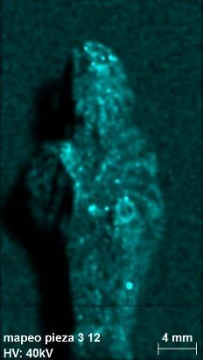
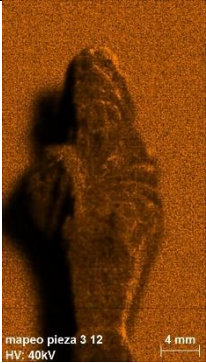
| Chlorine | Phosphorus | Titanium |
|--|---|---|
|  <p data-bbox="281 576 487 610">mapeo pieza 3 12 HV: 40kV 4 mm</p> |  <p data-bbox="596 576 802 610">mapeo pieza 3 12 HV: 40kV 4 mm</p> |  <p data-bbox="911 576 1117 610">mapeo pieza 3 12 HV: 40kV 4 mm</p> |
| Strontium | | |
|  <p data-bbox="281 1010 487 1044">mapeo pieza 3 12 HV: 40kV 4 mm</p> | | |

Figure 86 - Elemental image of the togado's figure by ED-XRF

This piece, as occurred with piece no.2 (the bifacial face), was of great archaeological interest. At first glance, it can be observed how the color of the piece is grayish, perhaps due to the deterioration it has suffered.

The results obtained show the presence of silicon, copper, aluminum and magnesium in the complete piece. Moreover, calcium and sulfur have the same distribution pattern; both seem to be present in much localized areas of the piece.

Potassium, iron, chlorine, titanium and phosphorus showed a very similar detection pattern that seems to focus on the darkest and most superficial areas of the sample, probably the most deteriorated ones.

Finally, in the case of strontium, once again, the signal obtained from this element was higher in the background of the sample than in the sample. So, the results obtained for strontium were not used.

The point-by-point analysis performed in different colored zones in this sample have the semi-quantitative results that can be observed in the Figure 32.

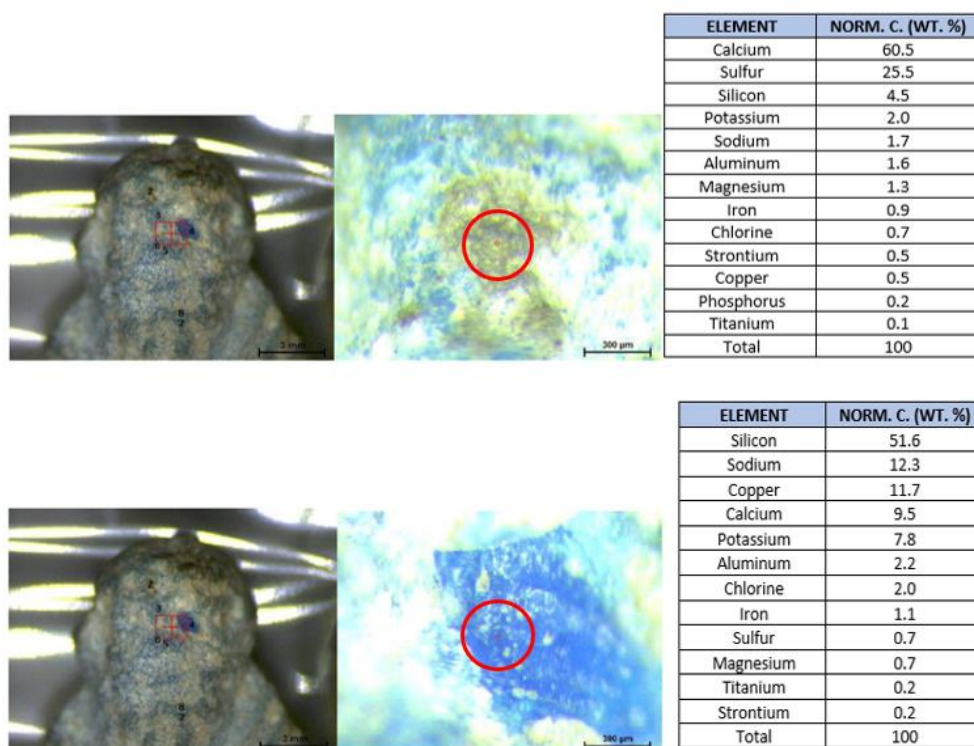


Figure 87 – Punctual analysis performed in yellow (above) and blue (below) areas of the togado's figure

These results showed in Figure 32 demonstrated how in some brown areas, sulfur and calcium have higher semi-quantitative values, but in other yellow ones, silicon and calcium have the higher values. In the case of original blue areas, silicon and sodium were the two elements with higher semi-quantitative values.

To sum up, it can be concluded that the presence of some elements could be related to the employment of some specific pigments. As it can be observed, phosphorous was detected in some specific pieces. Its presence could be concentrated in alterations, surface roughness, internal surface, etc. and could be related to surface adhered remains of the cremation ashes and not to the use of bone ash in the manufacture of these glasses.

In the case of lead, this element was detected in samples with a characteristic yellow color as in the case of sample no. 2 (bifacial piece), 3, and 11. These results confirm the use of lead in the yellow pigment employed as decoration of the pieces.

The presence of cobalt was detected as a pigment at trace level in the beads with dark blue color, as is the case with the pieces no. 1, 2, 3, 4, 6, 7, 8, 9 y 10.

Apart from this element, which could be related to a specific pigment, the rest of the elements detected have provided information related to their origin. Some elements seemed to correspond to a real component of the glass beads (based on the elemental imaging and point-by-point analysis) and in other cases they seemed to be the result of superficial alterations (contribution from the surrounding soil). Thus, it was possible to detect titanium as an exogenous element in pieces no. 1, 3, 4, 6, 7, 9, 10, 12 and 13. Tin was detected as an exogenous element in samples no. 2, 3, 11, 12 and 13.

Strontium was detected as an exogenous element in samples no. 3, 4, 5, 6, 7, 8, 9, 10, 11, 12 and 13. Sulfur was detected as another exogenous element detected in samples no. 1 and 5. Phosphorus was detected as an exogenous compound in samples no. 3, 6 and 8. Finally, zinc and manganese were detected as an exogenous elements in sample no. 10 and no. 4, respectively.

The identification of the mineral phases was performed by Raman spectroscopy by the team of the University of Valladolid. That group identified that the pigments used in the manufacture of these pieces were lead oxides, calcium antimonate, hematite and Naples yellow ($\text{Pb}_2\text{Sb}_2\text{O}_7$). Blue and green color seemed to be obtained with Fe (II) and Cu (II) based-compounds, although further works are needed to confirm if cobalt was used in a low concentration¹.

In addition, the study of several blue glass beads found in the same tomb (247a) with different levels of preservation was performed. The results obtained have provided valuable information about the cremation ritual, determining that the maximum temperature reached was about 600°C¹. As the analyzed glass beads were excavated from tombs, that temperature should be considered as the maximum one suffered by the pieces.

6.1.1 Discussion of glass beads of Vaccaei culture analyses

In general terms, it can be concluded that the physical condition of these pieces was somehow deteriorated. The vast majority of the pieces have visible cracks that can affect the shape of the piece and cause possible detaching of the pieces in the future. In addition to cracks, some samples have a worn color or were covered by degraded brown/white patinas.

Regarding the obtained results, the relationship between several of the colors used in the pieces and the presence of certain elements can be concluded in a general way. In the case of the yellow color, the presence of lead can be confirmed in all the pieces in which the yellow color was used, such as pieces 3, 11 and the piece of the bifacial face, in the inner zone. Moreover, in these yellow areas, antimony was also detected. This is consistent with the use of Naples Yellow as the yellow pigment, but the amount of Sb is much lower than the amount of Pb in Naples Yellow, suggesting the presence of another yellow containing Pb pigment, like massicot. In addition, other elements such as aluminum, iron, potassium, and chlorine were detected in such yellow color.

The white decorations of piece 3 and the bifacial face, located over the yellow surfaces, detected low amount of lead and always calcium and antimony, suggesting the use of calcium antimoniate (white compound identified by Raman spectroscopy) as the pigment used for the whites over the yellow surfaces.

The black/grey area that surrounds the yellow surfaces of these pieces has a clear and high presence of calcium, potassium, copper and sulfur. On the face A of the bifacial piece, a white area was detected next to the nose that was not similar to those obtained for the rest of the white areas. In this case, that area has a high presence of sulfur, suggesting the presence of a concretion rich in calcium sulfate, probably anhydrite as the face was found in a tomb with a clear presence of cremation remains.

The chemical composition of the glass beads is different to the face. Blue is the main color of such beads, but the degradations are so

important that white inner parts are visible. The white color of those degradations observed in several glass beads can be directly related to the presence of calcium, aluminum, potassium and iron, being absent antimony. Probably that detached areas allowed us to measure the bulk of the glass beads. In the case of the blue color, a color widely used in these beads, is directly related to the presence of cobalt, calcium, sodium and aluminum.

There was a glass bead that was different from the rest, and it was the tomb. It was the piece in which the highest presence of sulfur was detected (in degraded areas). In addition, the blue color of this piece was the color in which the highest amount of copper was detected.

Regarding the conservation state of the pieces, it could be concluded that most of the selected pieces present a quite good state of preservation because the degraded parts represent less than 5% of the overall material of the beads. In most of them, it was possible to identify the globular features typical of the vitreous paste, while only a few showed incipient crater phenomena or cracks and fractures with loss of surface material observable through the use of microscope.¹

6.2 LITHIC TOOLS

The analysis of the lithic tools, mostly arrowheads or knives, was possible thanks to the collaboration and participation of Dr. Juan José Ibáñez (CSIC, Barcelona). He provided us with the samples and allowed us to carry out the elemental and molecular analysis. The original material of the six analyzed tools was silex and they presented different color patterns from each other.

The main aim of this analysis was to know the elemental and molecular composition of the samples, to observe the distribution of the elements around the samples, contributing to find patterns related to the use of the tools, and to understand the possible degradation process that may be taken place. To perform these analyses, ED-XRF and Raman spectroscopy laboratory instruments were used.

All the tools were analyzed by performing first the elemental distribution mapping by ED-XRF of different areas of the samples and then performing point-by-point analysis with Raman spectroscopy. For all the analyses, a foam rubber base was used to keep the tools in a horizontal position which favored the analyses.

The results obtained for the elemental analysis of the samples already described in Chapter 4 are described.

At first, the upper face of the piece no.1 was analyzed, and its elemental distribution is shown in Figure 33. It can be observed how this piece has very characteristic colors, with beiges areas and reddish ones, as seen from the optical image. Regarding the elemental distribution maps, only silicon and aluminum distribution follow the entire silex tool.

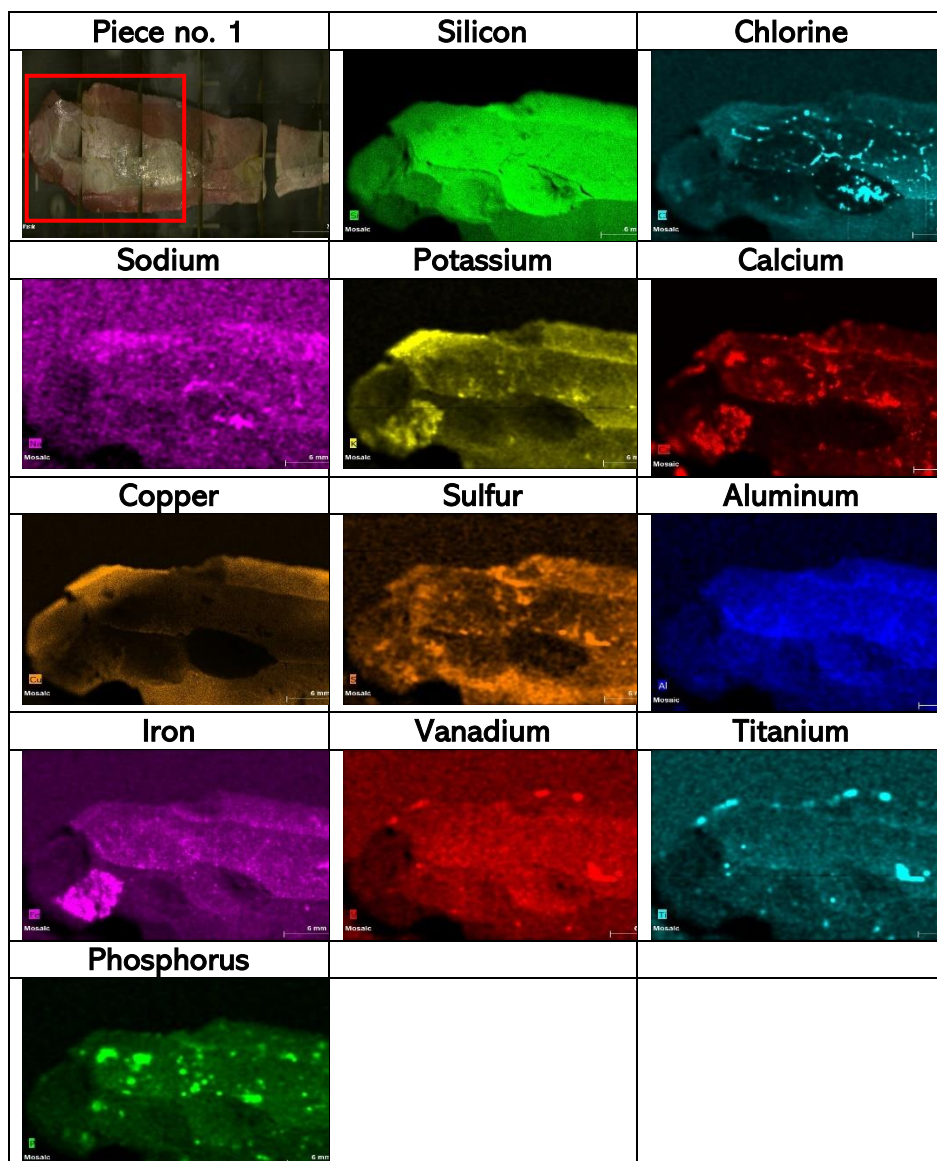


Figure 33 - Elemental image of the tool no. 1 by ED-XRF

The presence of chlorine was detected with a very different distribution from the rest of the elements. It seems to be detected in small cracks in the piece, suggesting an exogenous supply of this element, coming maybe from the use given to the tool.

Potassium and calcium have a very similar elemental distribution but only in some areas, which appears to be similar to the distribution of the red color in the piece. Copper was detected throughout the entire external area of the analyzed area, but not in the internal zone. It may be also related to the presence of red color in the piece. The presence of sulfur was found also in the entire analyzed area except in the inner part. The sulfur distribution map was very similar to the map obtained for potassium and calcium.

In the case of iron, it was detected mainly in one of the red points of the sample but not in the rest, so its distribution does not seem to be related to a specific color.

Vanadium and titanium were detected in the external zone of the piece and in some specific points of the internal zone. Their presence seems to be related to the cutting zones. Finally, phosphorus was present at various points inside the piece, but its distribution does not seem to be related to any particular color.

Apart from that area, the intermediate zone was also analyzed, and its map distribution is shown below (Figure 34). In this case, this area does not offer us as much information as the previous one. The distribution patterns observed were very similar to those discussed in the previous area.

The last area analyzed on the upper face of the piece no. X was the tip and its results are shown in Figure 34.

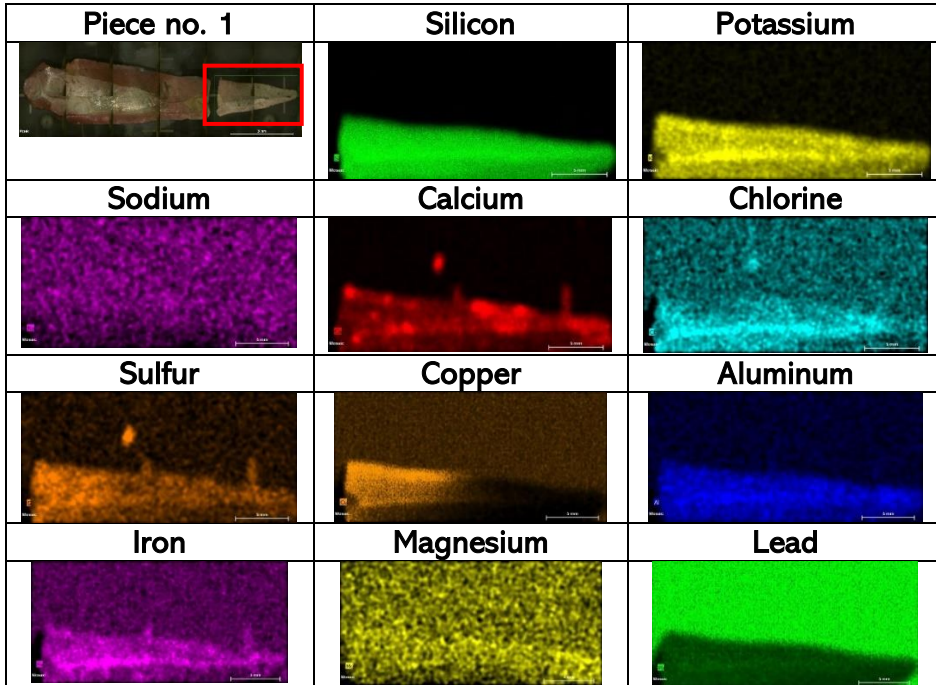
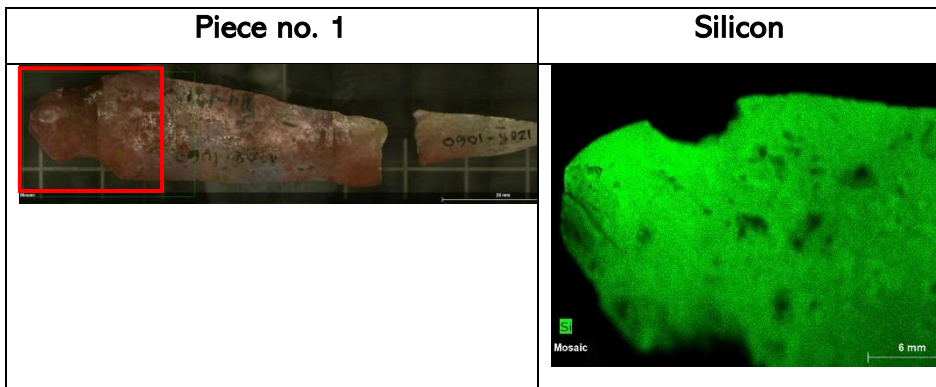
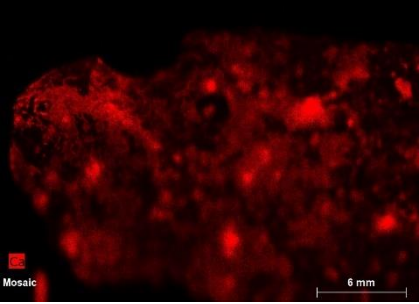
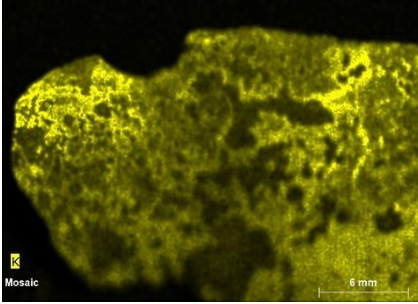
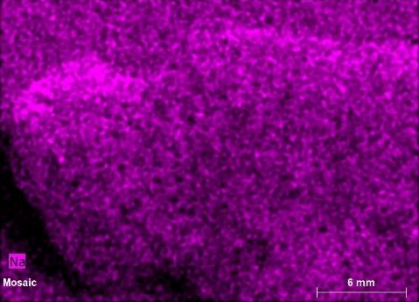
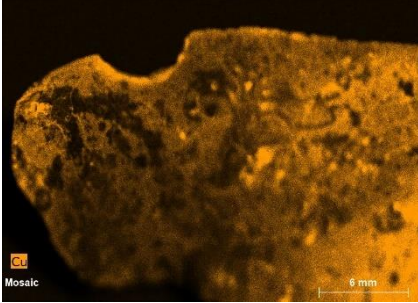
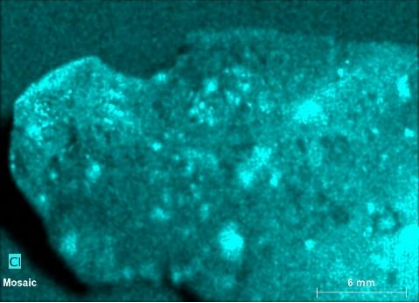
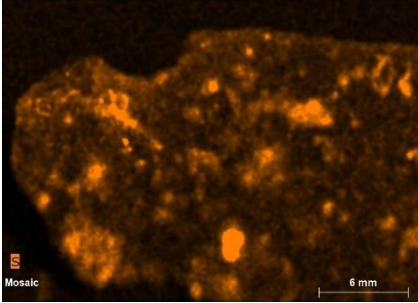
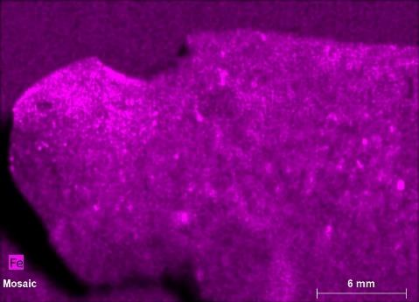
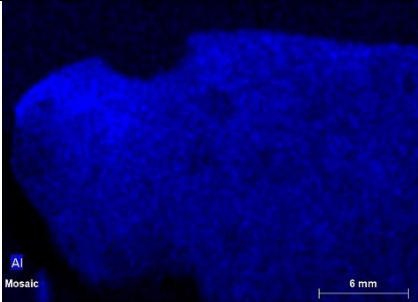


Figure 34 – Elemental image of the tip in the tool no. 1 by ED-XRF

The results obtained do not showed new information on this piece.

The elemental distribution map obtained for the back side of the piece, the rear area, can be observed in Figure 35.



| | |
|---|--|
| <p style="text-align: center;">Calcium</p> | <p style="text-align: center;">Potassium</p> |
|  |  |
| <p style="text-align: center;">Sodium</p> | <p style="text-align: center;">Copper</p> |
|  |  |
| <p style="text-align: center;">Chlorine</p> | <p style="text-align: center;">Sulfur</p> |
|  |  |
| <p style="text-align: center;">Iron</p> | <p style="text-align: center;">Aluminum</p> |
|  |  |

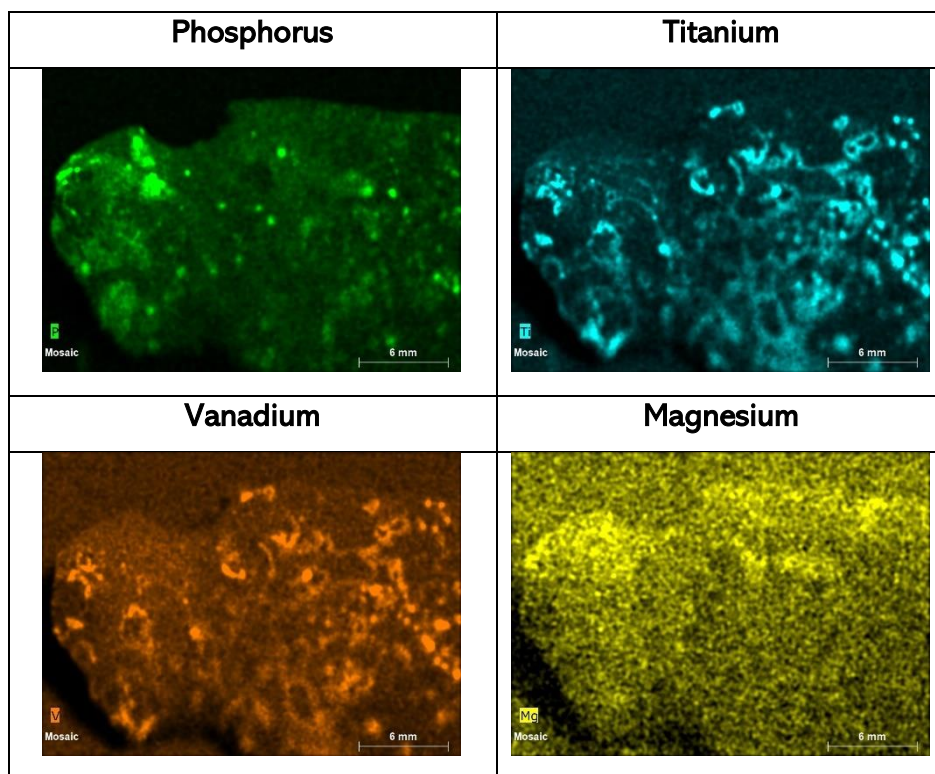


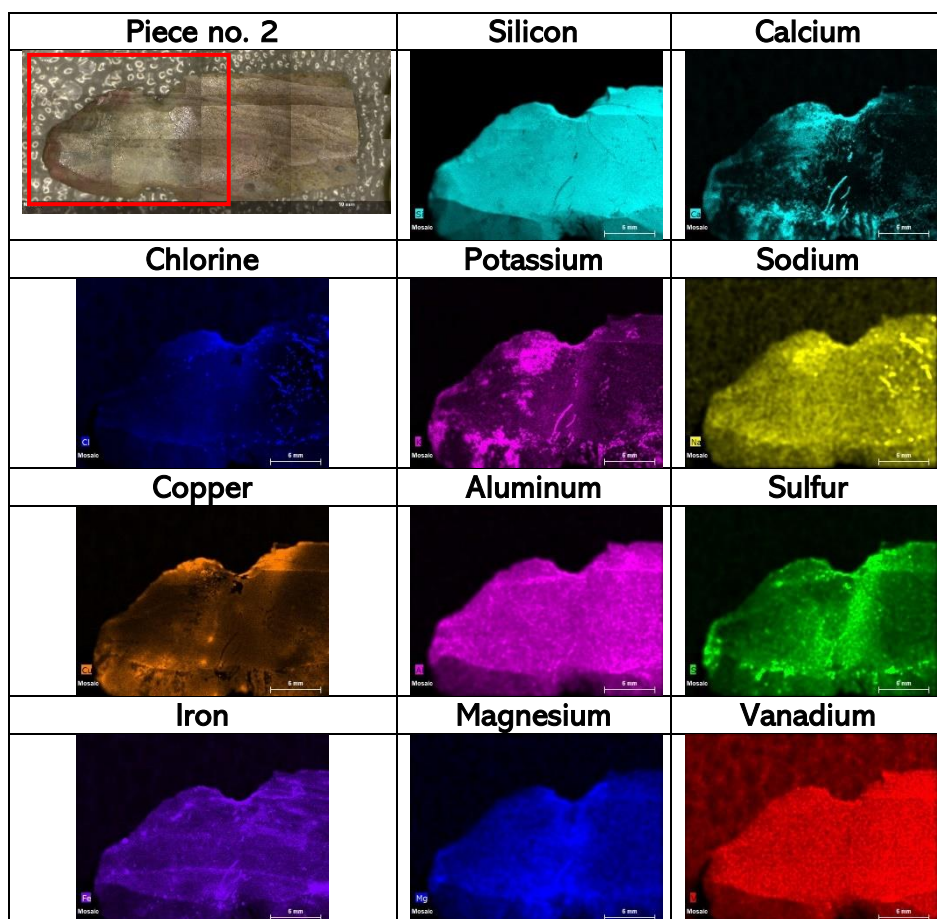
Figure 35 - Elemental image of the tool no. 1 by ED-XRF

In this case, silicon, sodium, iron, aluminum and magnesium were distributed in the same way throughout the entire piece. On the other hand, calcium chlorine and sulfur showed nearly the same distribution map. In addition, the areas where these elements were detected, the silicon, sodium, iron, aluminum and magnesium were not detected and vice versa.

Potassium was an element which was detected in specific areas of the piece, without being able to relate directly to any specific color. Copper showed up again in areas with a higher presence of red color. The presence of phosphorus was found in very specific points of the piece and its distribution was not similar to any of other elements. Vanadium and titanium again showed the same distribution pattern.

To sum up, a correlation can be made between some elements and certain areas of the pieces. For example, copper seemed to be related to the red color of the samples. Phosphorus, titanium and chlorine seemed to be concentrated in the most superficial roughness of the piece. Other elements, such as calcium, sulfur, iron, aluminum and silicon were observed almost all over the area of the piece.

The elemental results obtained from the piece no.2 are showed below in the Figure 36.



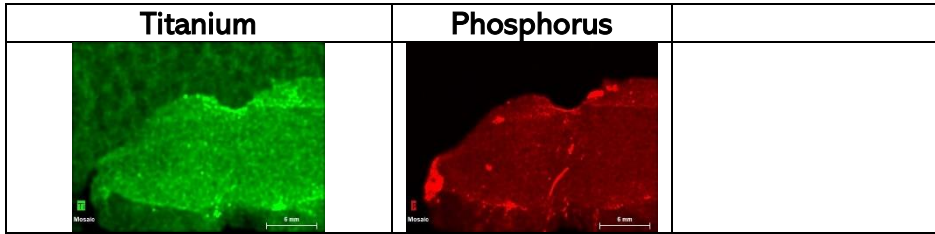
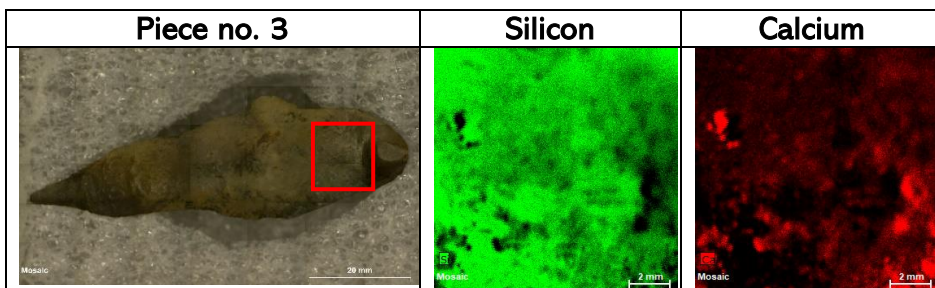


Figure 36 – Elemental image of the tool no. 2 by ED-XRF

In the marked area of the piece no. 2, silicon, sodium, aluminum, iron, magnesium, vanadium, titanium and phosphorus were detected. Among them, only silicon and vanadium showed the same distribution, The others, despite being present throughout the analyzed area, showed different hotspots where their presence was higher.

Calcium and potassium were both distributed in the external intermediate zone of the analyzed area. Chlorine was only found on one of the analyzed sides of this area. Copper was detected in the reddest areas of the piece and sulfur was present to a great extent in the red areas of the piece.

Regarding the piece no. 3, the elemental mapping obtained from the marked area is shown in the Figure 37.



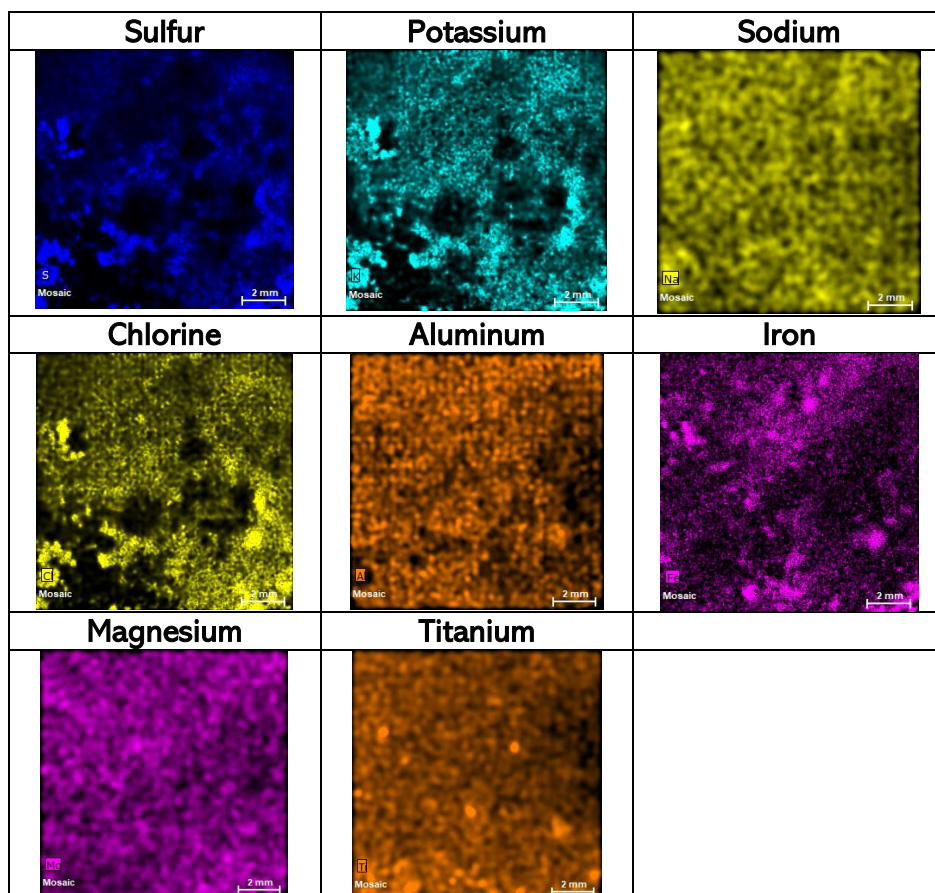


Figure 37 – Elemental image of the marked area in the tool no. 3 by ED-XRF

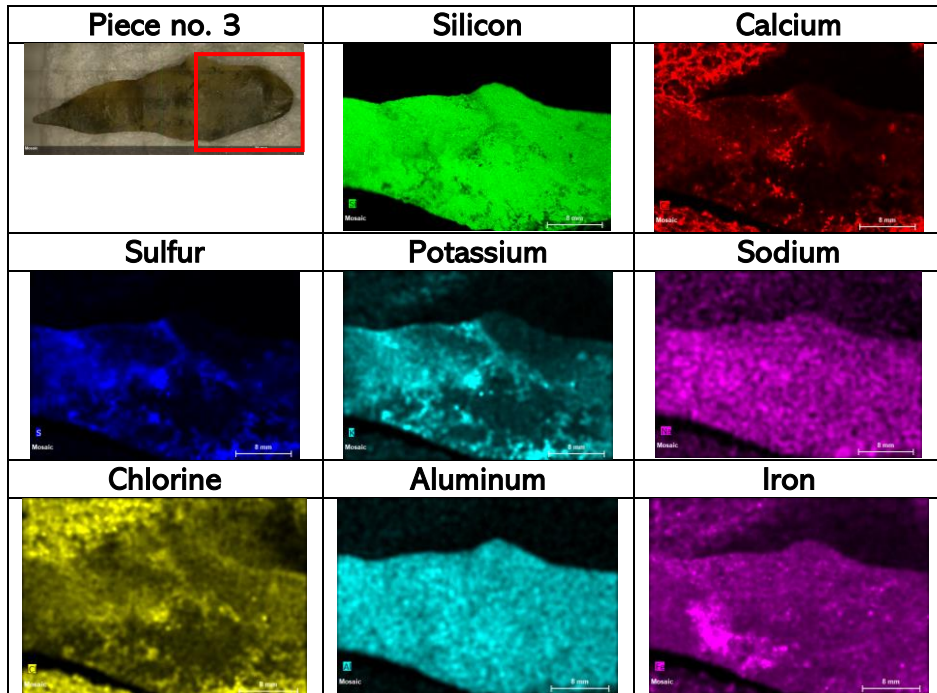
First of all, it is important to mention that this piece presents a blackish/brown color for most its surface. Four types of very clear patterns can be discerned in the analyzed area. In the first group, calcium, sulfur, potassium, and chlorine showed the same distribution map. On the other hand, silicon shows a different pattern. Its presence was detected throughout the entire analyzed area, and it was detected in areas where the elements of the first group were not detected.

Finally, sodium, aluminum, magnesium, and titanium showed a more homogeneous distribution than the rest of the elements mentioned.

In the specific case of iron, although its distribution was similar to this group of elements, it did not fully resemble any of the aforementioned patterns.

An analysis of the tip area was also carried out, which showed a very blackish color. The results showed a clear presence of silicon, sodium, sulfur, potassium, magnesium and aluminum in the tip area. The rest of the element, calcium, iron, titanium, chromium and zinc, showed a very different distribution pattern.

The results obtained for the area marked in red are shown below (Figure 38).


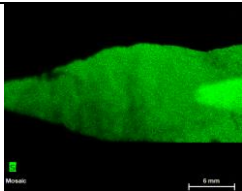
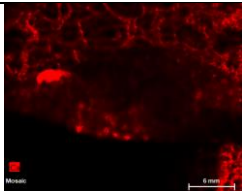
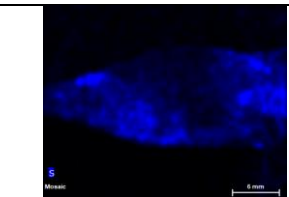
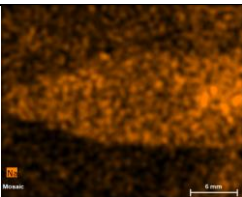
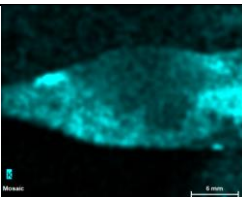


| Titanium | | |
|---|--|--|
|  | | |

Figure 38 - Elemental image of the marked area in the tool no. 3 by ED-XRF

In this case, silicon, sodium, aluminum and titanium were present throughout the entire analyzed area. Sulfur, potassium, chlorine and to a lesser extent, calcium, showed a very similar distribution pattern and its presence seems to be detected to a greater extent in the blackest areas. Finally, iron, despite being distributed in all the area analyzed, is detected to a greater extent in the brown surface.

Finally, the mapping of the intermediate zone of the piece no. 3 was carried out and its results are shown below in the Figure 39.

| Piece no. 3 | Silicon | Calcium |
|---|---|--|
|  |  |  |
| Sulfur | Sodium | Potassium |
|  |  |  |

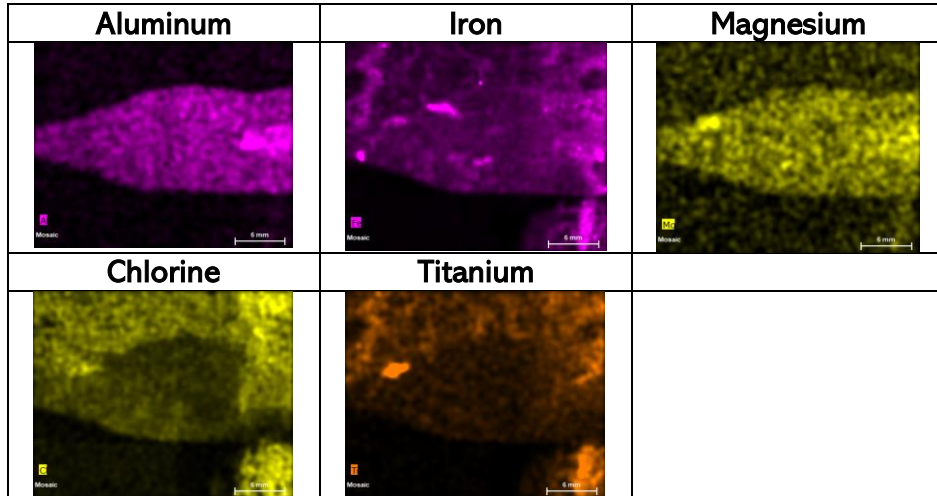


Figure 39 - Elemental image of the marked area in the tool no. 3 by ED-XRF

Once again, silicon was again present in all the entire area analyzed as expected. To a lesser extent, sodium aluminum, and magnesium were also present. Calcium, sulfur and potassium seem to have a similar distribution pattern, but it should be mentioned that part of the calcium detected outside the piece was due to the signal provided by the background.

In the case of iron, its distribution does not seem to be similar to the distribution of any other element. Moreover, chlorine and titanium were two elements whose signal was detected above all in the external part of the sample, due to the signal of the material used to place the sample when analyzing it.

In the case of the upper face of the piece no 4, the elemental mapping distribution results are exposed below in the Figure 40.

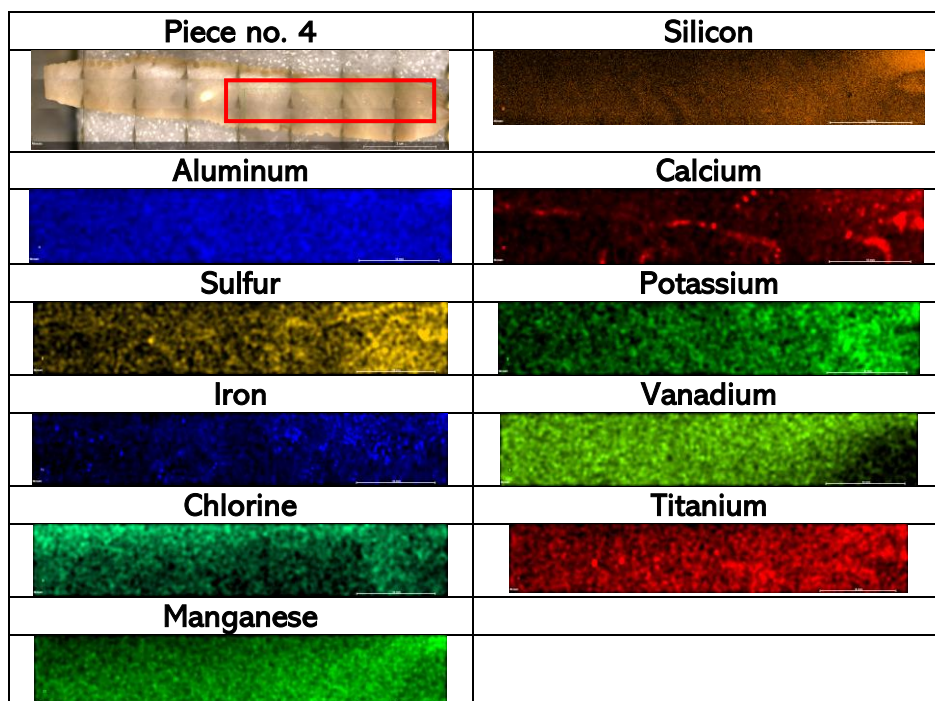


Figure 40 - Elemental image of the marked area in the tool no. 4 by ED-XRF

The results obtained for this piece showed how, in general terms, the detected elements were present throughout the entire piece, without a characteristic pattern. Calcium was the only elements which seemed to have a different pattern from the rest, and its detection seems to be present just on the roughness of the piece.

Elemental mapping results obtained for the back face of the piece no. 4 are the following ones (Figure 41).

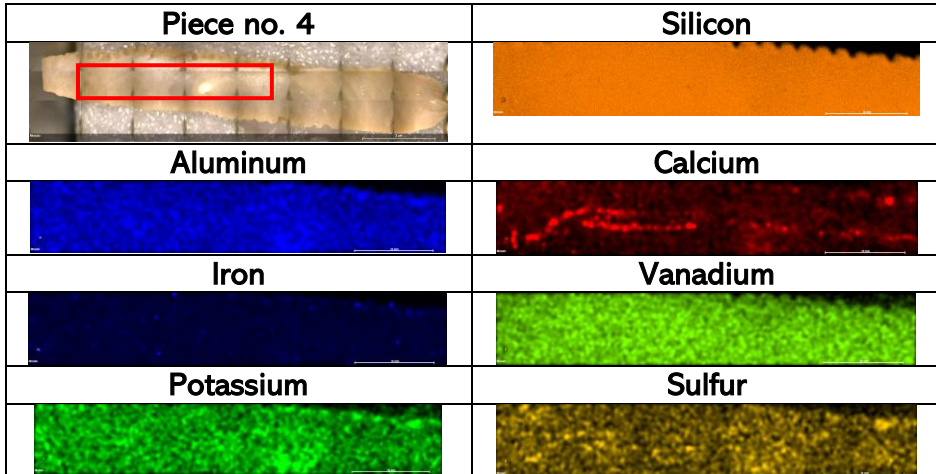
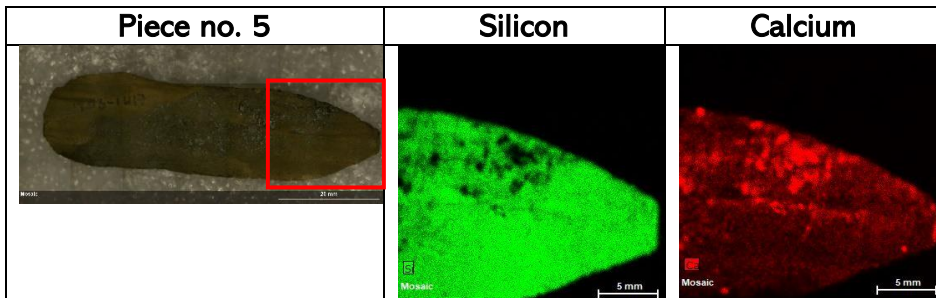


Figure 41 - Elemental image of the marked area in the tool no. 4 by ED-XRF

On this face of the piece, the same thing happens as mentioned above. All the elements detected showed the same pattern, except for calcium. Contrary to the rest of the pieces, this sample presented a homogeneous distribution of the elements.

For the piece no. 5, the elemental mapping results obtained are showed in the Figure 42.



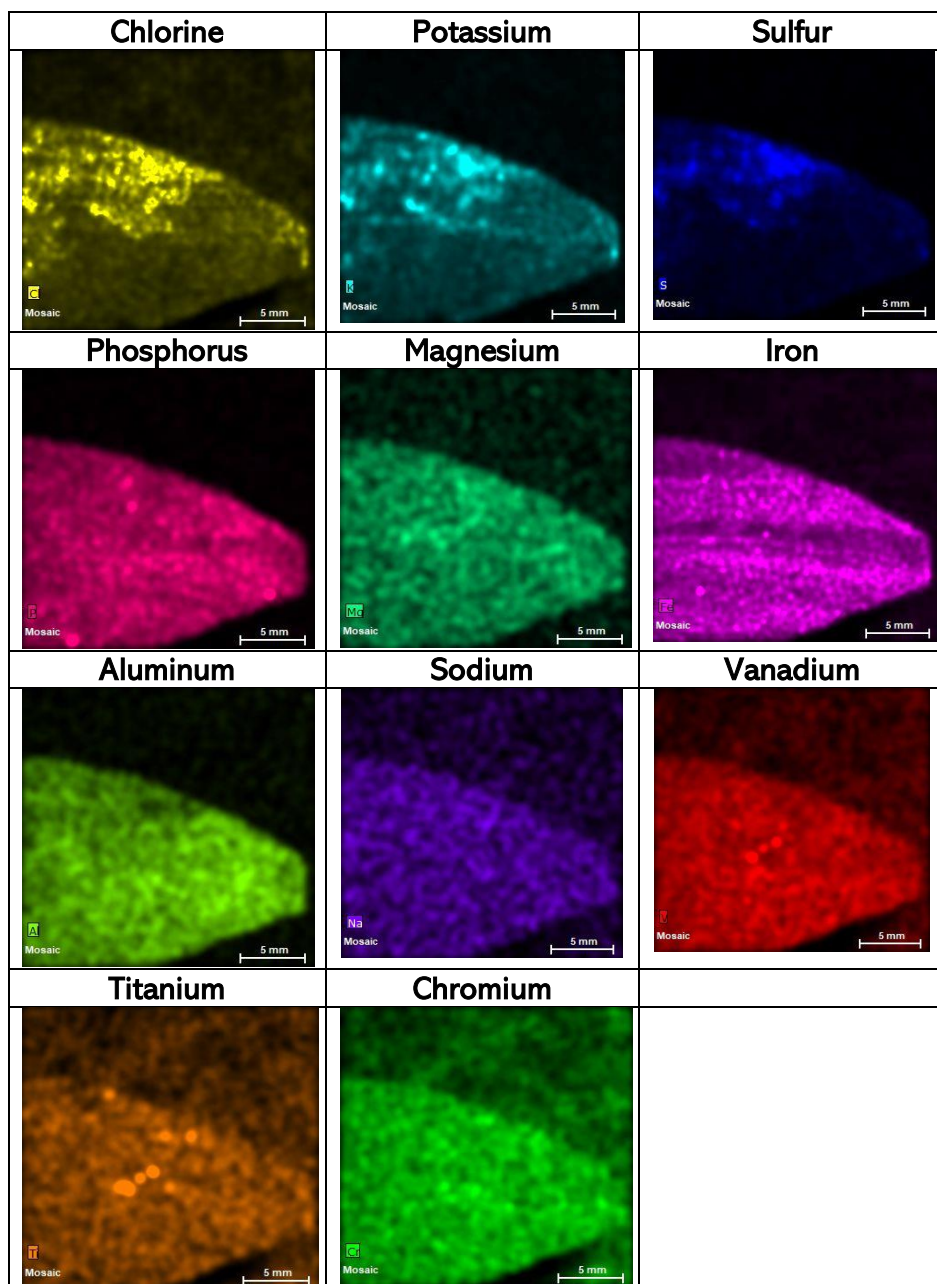


Figure 42 - Elemental image of the marked area in the tool no. 5 by ED-XRF

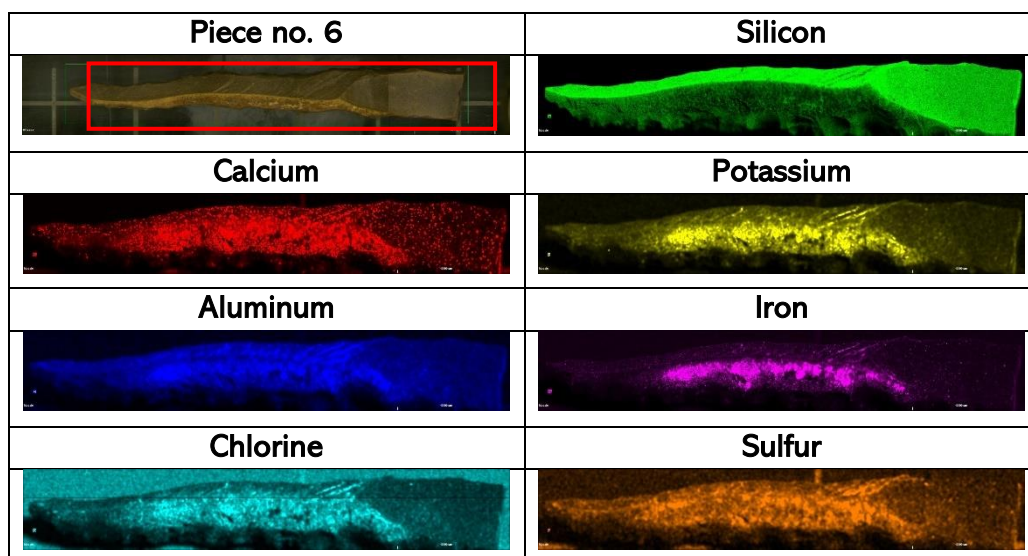
In the elemental mappings, a very similar distribution can be observed for calcium, chlorine, potassium and sulfur, whose detection seems to be in the upper cut-off area of the tool. On the contrary, in the areas

where these elements were not detected, the presence of silicon was detected, indicating that the four elements are over the silex of the tool.

Finally, the rest of the elements showed a completely homogeneous distribution throughout the entire analyzed area.

The elemental mapping carried out for the intermediate zone of the same piece did not show new information. The results obtained showed how the aforementioned distribution pattern in the tip area of this piece was maintained. Calcium, chlorine, potassium and sulfur were distributed in the same way and silicon, on the contrary, was detected in areas where these elements were not present. The rest of the detected elements showed a very homogeneous distribution throughout the entire piece.

In the case of the piece no. 6, the results obtained from the elemental distribution mapping are showed below in the Figure 43.



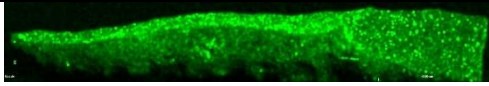
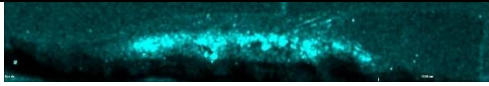


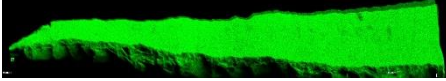
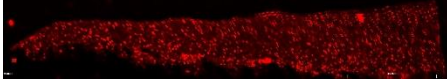
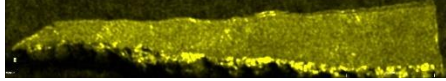
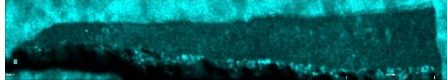
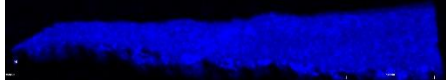
| | |
|---|--|
| Phosphorus | Titanium |
|  |  |
| Magnesium | |
|  | |

Figure 43 - Elemental image of the tool no. 6 by ED-XRF

The elemental distribution of this piece was very significant since it showed the precise distribution of several elements. As is the case of calcium, potassium, iron, chlorine, sulfur and titanium, whose detection occurs in the internal area of the upper part, in the central area of the piece.

On the other hand, silicon can be clearly seen throughout the entire area of the piece. Aluminum, phosphorus and magnesium were elements also observed throughout the entire piece, but with a higher presence in the central part of the piece.

In the case of the lower part of this piece, the results of the elemental mapping were represented in Figure 44.

| | |
|---|--|
| Piece no. 6 | Silicon |
|  |  |
| Calcium | Potassium |
|  |  |
| Chloride | Aluminum |
|  |  |

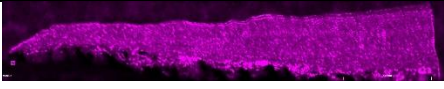
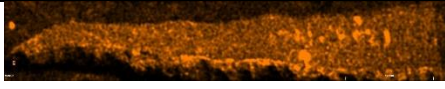
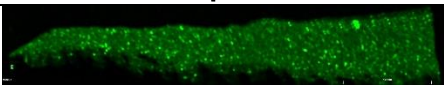
| Iron | Sulfur |
|---|--|
|  |  |
| Phosphorus | |
|  | |

Figure 44 - Elemental image of the tool no. 6 by ED-XRF

Contrary to the top side, the back side did not offer as clear element information because most of the elements had a similar distribution. As was the case of silicon, aluminum, iron, sulfur, titanium, vanadium and manganese. Despite the very similar results, there were little differences among them. For example, in the case of calcium and phosphorus, whose distribution seemed to be throughout the piece but more superficially than silicon. Potassium, chlorine, iron and sulfur seem to show a higher presence in the lower zone of the piece, in a possible cutting area.

After the elemental results of the arrowheads, areas of great interest, those with an unexpected elemental distribution, were located and identified and areas of interest for molecular analysis (using the Raman Spectroscopy laboratory equipment). Unfortunately, these samples produced fluorescence and the results obtained revealed scarce molecular information.

In all the samples analyzed, the presence of gypsum ($\text{CaSO}_4 \cdot 2\text{H}_2\text{O}$, main Raman band at 1006 cm^{-1}) and α -quartz ($\alpha\text{-SiO}_2$ main band 464 cm^{-1}) was only found in the most deteriorated areas. These compounds are not usually detected in non-degraded silex samples. For most of silex, the main mineral form is known as calcedonia, a microcrystalline variety of silica.

In the case of gypsum, the existence of this compound on the surface of the samples suggests the presence of infiltration or condensation water during the burial period. This presence could have caused the dissolution of the original material and the crystallization of this salt in the pores and on the surface of the flint sample. The formation of gypsum in these pieces could be due to or caused by the action of the infiltrated waters which contains sulfate ions. The same can explain the formation of α -quartz in the sample because it may be caused by alterations due to the contact of the tools with the sediments.

6.2.1 Discussion of arrowheads analyses

Regarding to these pieces, it can be roughly concluded that they were very delicate pieces (due to their low thickness) and due to the cracks found in many of them. In addition, one of the tips of the arrowheads (piece no. 1) was fallen and several arrowheads do not have a tip due to the breakage, which demonstrated their fragility.

The results obtained by XRF showed how there were several elements that can be directly related to the presence of a specific color. This was the case of copper and iron. This element was detected in the pieces with red areas. In addition, copper was also found in the outer areas of the pieces, the cutting areas of the tools. Due to the relationship between the red color and the presence of iron and copper, it was suggested that the red color could be the remains of red ochre added to the pieces as decoration².

In addition to the reddish color, no other elements were found that showed this relationship with another specific feature. It must be said that there were samples that were covered by a black color around

all the piece whose elemental information was more limited than in the pieces without that color. The origin of this black layer may be that those tools were burned but a variety of silex known as pedernal is blackish due to the organics trapped during the diagenetic process.

6.3 IRON ARCHAEOLOGICAL SLAGS

Iron has been a valuable resource since the Iron Age. This element has been used in a wide variety of areas. One of its first uses was the manufacture of weapons of war, as it guaranteed victory and protection from other civilizations not knowing the iron casting technology. The advances in the use of this metal were observed in agriculture, where iron was used for the manufacture of plow tips that allowed man to work in a better way the land and crops. His dominion allowed that in his free time they used it as a pastime for the elaboration of jewels, crafts and fabrics. In the industry it is one of the most used metals due to its hardness, especially in construction. Finally, one of the areas in which this element has acquired the most over time is archaeological research³.

In archaeological research, the remains of iron manufacturing are of great value because thanks to them you can get a lot of information about the production and consumption of this element in ancient times. A key requirement for obtaining this information is the development of new means to track iron objects to their production origins. Among them you can find the chemical analysis of the slags. Slags are waste material from mining or smelting sites and arise due to the process suffered by minerals for the production of melted iron⁴. Depending on the processes used and the composition of the minerals used, there are different types of slag, and this study will focus on the archaeological slag.

The reason why it is important to analyze the slags is because it can be obtained valuable information about the mineral sources of the iron and the technology used. In order to know this information, the main objective of this work has been to determine the original

composition of different archaeological slags. To carry out this task, elemental analysis of the pieces was performed using laboratory ED-XRF equipment and molecular analysis using laboratory Raman spectroscopy equipment.

The analyzed samples were described in Chapter 4. The results obtained by the use of Raman spectroscopy showed the presence of calcite and two different iron compounds, such as goethite and hematite, as can be seen in Figure 45.

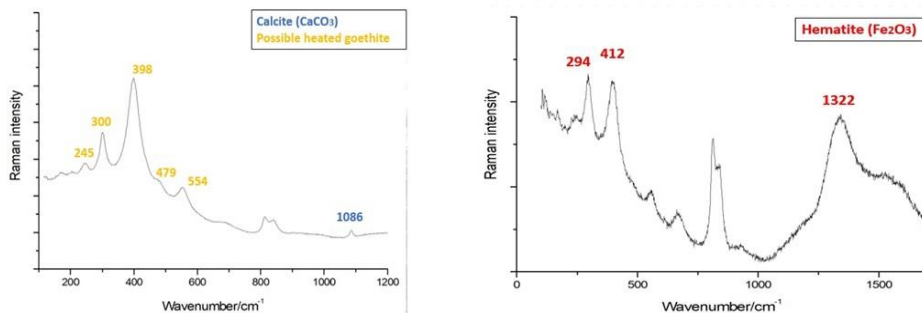


Figure 45 - The calcite and iron compounds identified in archaeological slags

The presence of calcite (CaCO₃) is an indication of the use of a flux salt (CaO in this case) to help the elimination of impurities through the formation of the slag. The use of goethite is referred as one of the most popular iron ores due to the low associated impurities of sulfur and phosphorus, two of the most harmful elements for a good iron metallic piece.

Furthermore, two different types of silicates were identified, as seen in Figure 46, one of them linked with iron named Fayalite (FeSiO₄)

and the other with manganese named tephroite (Mn_2SiO_4), both belonging to the family of olivine.

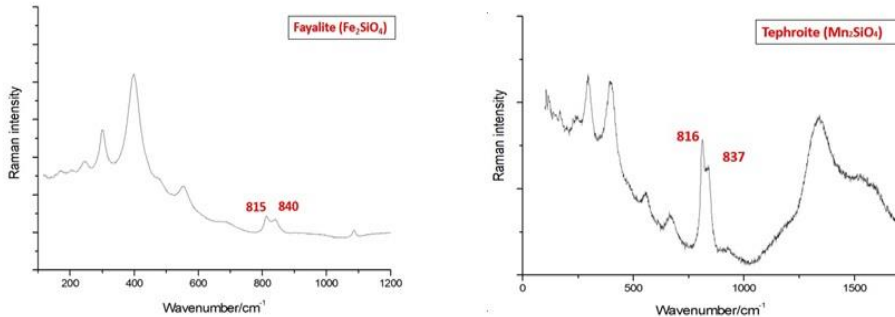
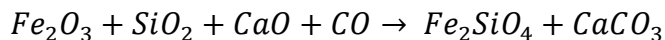
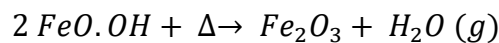
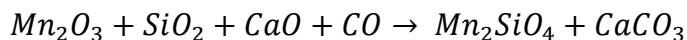


Figure 46 – Two different types of silicate identified in the slag samples

Fayalite is present in the same Raman spectrum where heated goethite and calcite were identified. The presence of this compound is a clear indication of the used of a flux salt (CaO in this case) that promotes the removal of silica (the slag) and the same time of obtaining the metallic iron:



And the other silicate which was identified was tephroite, a manganese silicate. Manganese is the typical element associated to iron. Its removal through the slag follows a similar reaction, ending with the formation of tephroite (Mn_2SiO_4):



The last interesting result that has been obtained from the Raman analysis was the identification of quartz and anatase, as showed in the Figure 47.

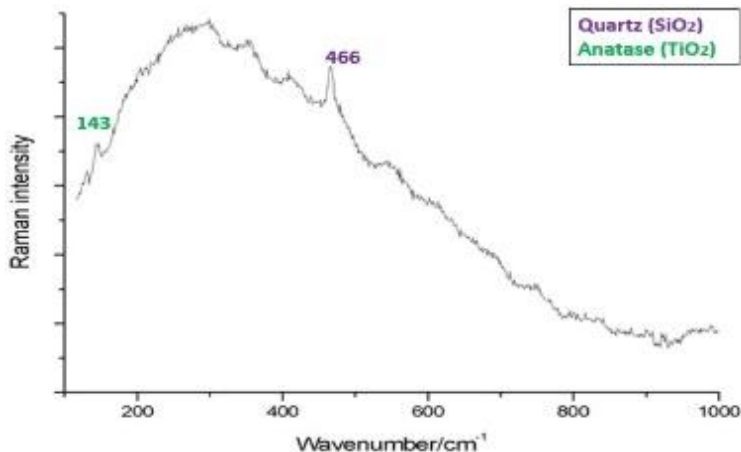
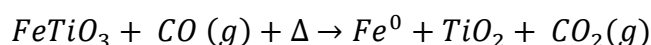


Figure 47 - Raman spectrum of quartz and anatase

The identification of anatase confirms the presence of ilmenite (FeTiO_3) as another raw compound present in the iron ore. Ilmenite can be reduced to metallic iron in the same process, obtaining as a side product titanium oxide. Depending on the temperature, anatase (low temperature) or rutile (high temperature polymorph) should be obtained:



In this case, anatase was detected. This mineral phase should pass irreversible to the stable rutile in the range of 400-1200°C. But as no rutile was detected in the slag, it could be corroborated that the temperature attained during the reduction process of the iron ores was not higher than 400°C⁵.

The ED-XRF analysis performed in the samples revealed in Figure 48 that the iron was the major element in all the slags.

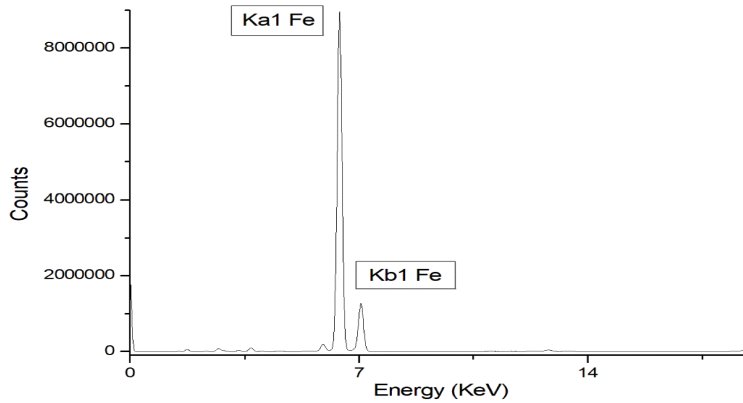


Figure 48 - X-Ray characterization of archaeological slags

The detected minor elements can be seen in Figure 49. In this spectrum it can be observed that the iron ore was accompanied by some impurities (removed through the formation of the slag). The principal impurity is usually silicon that should be removed through the slag, as well as other elements like sulfur, phosphorus, manganese, zinc, lead, and copper. The arsenic is an important element, despite not being detected, and must be taken into account due to its toxicity and to its presence in the area (the Biscay Iron Mountains) where the mineral was extracted.

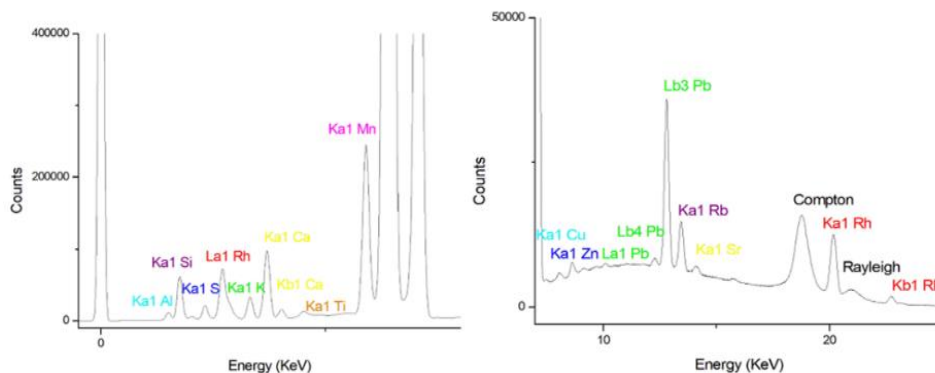


Figure 49 – Different regions of the same elemental characterization spectra of archaeological slags by the used of XRF

6.3.1 Discussion of iron archaeological slags analyses

In conclusion, regarding to the analytical non-destructive techniques used, both have been adequate for the analysis of slags without the destruction of them and for the determination of the molecular and elemental composition of the samples.

With respect to the results obtained by the use of Raman spectroscopy, it can be said that the detection of some key minerals in the slag allowed us to confirm the used of an iron ore composed of iron oxides (with associated manganese and ilmenite) as the primary minerals to produce the metallic iron. In addition, this technique has served as a thermometer of the iron slag formation process. The detection of calcite is an indication of the use of a fused salt (CaO) to remove the removal of impurities through the formation of the slag. Most of the silica/silicates, together with the iron excess and manganese were employed in the formation of fayalite, tephroite and quartz (probably also Ca and K aluminosilicates).

The results obtained have allowed us to evaluate the state of conservation of the pieces, concluding that they present a good state of conservation, since none of the techniques used allow us to confirm the contrary information.

6.4 CONCLUSIONS OF SAMPLES BURIED IN SOIL

In general terms it can be concluded that the methodology used is a good one for the characterization of these buried archaeological pieces. Regarding general results of lithic tools, it is true that Raman results have not been informative enough due to the associated fluorescence promoted by the excitation laser at 785nm. For future works, the use of UV lasers (325 nm) or Deep-UV ones (266 nm) is recommended to avoid such fluorescence related problems. In case of not having access to such ultraviolet lasers, another type of non-destructive technique such as SEM-EDS and UV-NIR analysis should be tested.

Making a comparison between the results using portable techniques and non-portable techniques, it could be said that there is not much difference as regards to the Raman spectra obtained. The laboratory equipment has allowed observing with a greater precision the spot of analysis thanks to the different objectives. In the case of X-Ray fluorescence results, the laboratory equipment was much more complete and offered interesting information such as the elemental distribution of the elements detected, even though its analysis time was longer. It also allows the detection of lighter elements that could not be detected with the portable equipment. However, in-situ analyzes have allowed us in this case and in the case of pieces buried in marine sediments to obtain elemental and molecular information in cases in which the pieces could not be moved and obtaining results in a relatively short time.

Regarding the pieces analyzed, the three kinds of pieces apparently have a possible incipient degradation. In the case of Vaccaei glass beads, a loss of color and small crack only visible under a microscope

can be observed in many of them. The presence of different type of oxides in the pieces could affect their state of conservation aggravating the cracks already present on the surface of the pieces. In the case of tools, several of them have some cracks visible to the naked eye, loss of color, a blackish coating and even several of them have a broken or cut tip. In addition, the presence of gypsum on the surface of these materials can be the cause of the present and future cracks. Finally, in the case of iron slags, these pieces also showed a beginning in corrosion process since they have several cracks and since small pieces of the original part have fallen of. The detection of different sulfates aggravated again the conservation state of the pieces.

In this chapter, three different types of materials were analyzed, glass materials, flint materials and ferrous/ferric materials. Despite having in common the origin as buried materials in soil, each one has its peculiarities regarding the results obtained.

In the case of glass beads, elemental mappings have offered very relevant information when studying their elemental composition. In addition, these analyzes have allowed the archaeologists of Valladolid group to carry out new analyzes using Raman spectroscopy technique in areas of great interest.

In the case of arrowheads, the elemental results obtained have offered more information than the molecular results, due to the fluorescence of these pieces.

And finally, in the case of archaeological slags, both techniques have provided accurate and complementary information when it comes to knowing both the elemental and mineral composition of the El Pobal slags.

6.5 BIBLIOGRAPHY

The references mentioned in this work are based on the bibliography format described below:

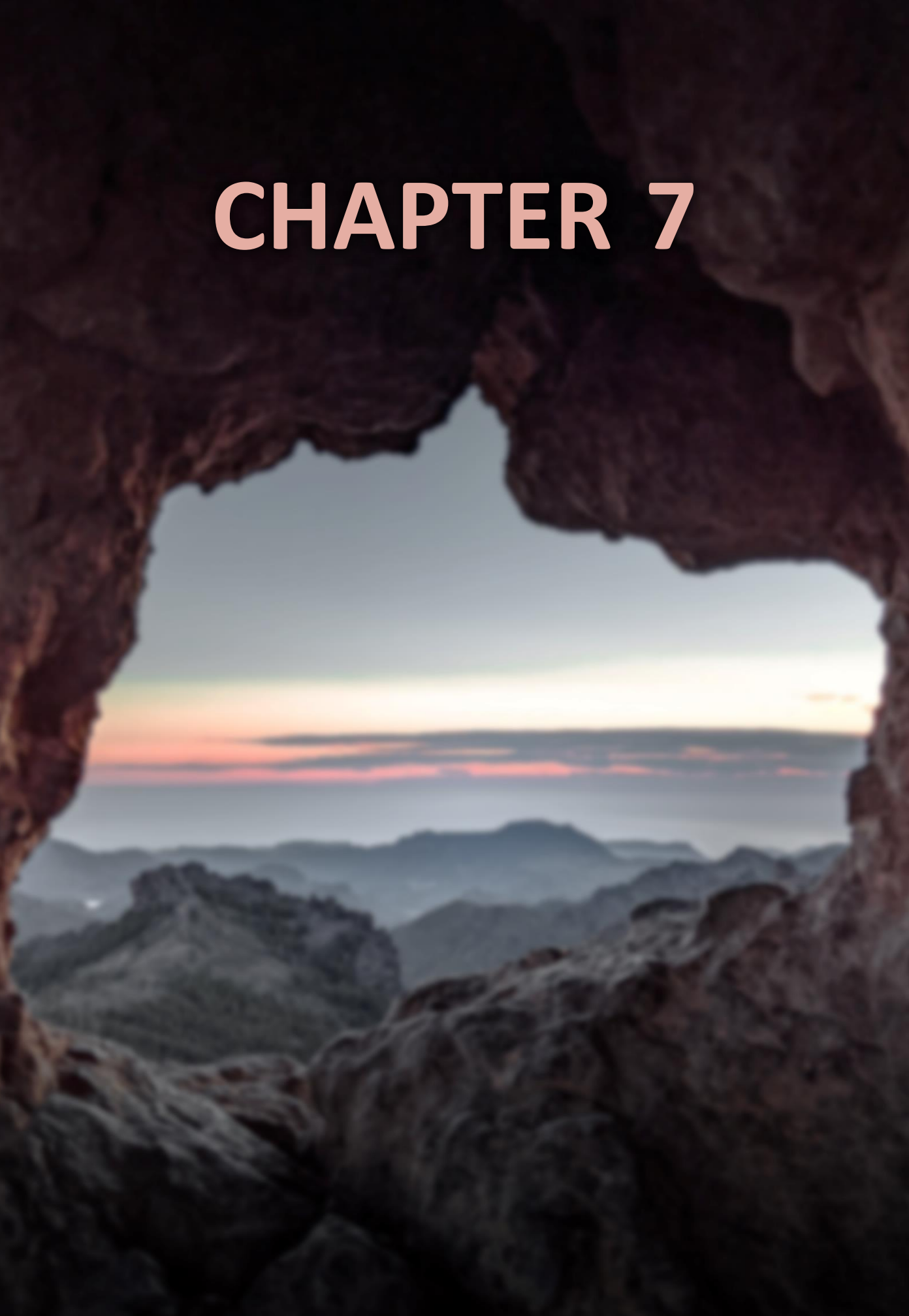
Journals: Estalayo, E. Aramendia, J. Bellot-Gurlet, L. Garcia L. Garcia-Camino, I. Madariaga, J.M. Article title. *Journal abbreviation*, volume, pages (year).

Books: Estalayo, E. Aramendia, J. Bellot-Gurlet, L. Garcia L. Garcia-Camino, I. Madariaga, J.M. *Book title*, (year). DOI number.

1. Pinto, J., Prieto, A. C., Coria-Noguera, J. C., Sanz-Minguez, C. & Souto, J. Investigating glass beads and the funerary rituals of ancient Vaccaei culture (S. IV-I BC) by Raman spectroscopy. *Journal of Raman Spectroscopy* **52**, 170–185 (2021).
2. Shaham, D., Grosman, L. & Goren-Inbar, N. The red-stained flint crescent from Gesher: New insights into PPNA hafting technology. *Journal of Archaeological Science* **37**, 2010–2016 (2010).
3. Blakelock, E., Martínón-Torres, M., Veldhuijzen, H. A. & Young, T. Slag inclusions in iron objects and the quest for provenance: an experiment and a case study. *Journal of Archaeological Science* **36**, 1745–1757 (2009).
4. Ettler, V., Johan, Z., Zavřel, J., Selmi Wallisová, M., Mihaljevič, M. & Šebek, O. Slag remains from the Na Slupi site (Prague, Czech Republic): Evidence for early medieval non-ferrous metal smelting. *Journal of Archaeological Science* **53**, 72–83 (2015).

5. Gómez-Nubla, L. PhD Thesis: Innovative analytical methodologies to characterize original and weathered materials of extraterrestrial origin and terrestrial analogues to meteorites. (2015).

CHAPTER 7



7. INTEGRATED DISCUSSION AND CONCLUSIONS

“All we have to decide is what to do with the time we are given” – “Todo lo que tenemos que decidir es qué hacer con el tiempo que se nos da”

In this final chapter, the integrated discussion, and general conclusions of all the results extracted in this work will be exposed.

The analysis of materials present in Cultural Heritage is always a complex task which needs a multianalytical approach¹. The combination of several analytical techniques is essential to an adequate characterization of CH materials.

The main objective of this PhD was to identify the problem present in different type of archaeological pieces exposed to different environments, manufactured in different materials and subjected to different conservation procedures. In this way, identifying the main reason for their current conservation state was also an aim.

For that purpose, non-destructive analytical techniques were employed with the combination of portable and non-portable equipment. These techniques were X-Ray Fluorescence Spectroscopy (μ -ED-XRF), Scanning Electron Microscopy with Energy Dispersive X-Ray Spectroscopy (SEM-EDS) and Raman Spectroscopy. In some specific cases, destructive analytical techniques were employed, such as X-Ray Diffraction (XRD).

The use of these techniques allowed us to obtain information about the problems present in these types of samples, and therefore, to improve future analyses of samples with similar composition and situation.

Regarding to the instrumental techniques used in this work, it is assessed that considering the obtained results, they were adequate techniques to define raw materials employed in the manufacture of the samples analyzed, to detect main degradation sources for different materials and in different environments and for the characterization and evaluation of the state of conservation of the archaeological pieces. On the one hand, X-Ray fluorescence has allowed us to know the distribution (laboratory equipment) and the elemental characterization of the pieces. On the other hand, Raman spectroscopy has allowed us to know the molecular characterization of the pieces. The use of XRD in specific cases allowed us to obtain more complete information on the samples.

The comparison between the portable and laboratory equipment, helped us to concluded that the portable equipment was of vital importance in this work because some pieces were not possible to transfer to the laboratory considering size or permit limitations. The laboratory equipment was essential to expand the results obtained through the results of portable techniques for example element/compound distribution studies. The combination of both was necessary for establishing a complete analytical methodology for the study and conservation of archaeological pieces and for evaluating the efficiency of different commonly used conservation treatments by the multi-analytical approach carried out.

The wide diversity of pieces studied has allowed us to obtain a broad field of vision regarding archaeological pieces of different origin. With the analysis of the pieces of underwater origin it has been possible to know with more precision which factors are directly related to their deterioration and therefore, which chemical elements participate in this corrosion process. In this way, it has been possible to know the problem with zinc and sulfur that was damaging the condition of the nails of the Urbieta shipwreck. On the other hand, in the case of the Bakio shipwreck, it was possible to know how the poor conditions of the pieces together with an inadequate treatment were affecting their state of preservation.

In the case of the buried samples in soils, these studies helped us to determine the different factors that affect this type of pieces, in comparison with the pieces of underwater origin. In the case of the beads, it was possible to appreciate a beginning of deterioration without being directly related to any element. In the case of the arrowheads, the presence of small cracks unrelated to the presence of any element could be observed. And finally, in the case of the slags, it was possible to observe how their state of conservation is relatively adequate.

In this sense, the possibility of carrying out an interdisciplinary work to obtain more complete results is proposed. Specialists in the field of geology, archaeology, biology, chemistry, and history can provide valuable information in the understanding and analysis of the data obtained.

The results obtained have been of great help in understanding the precise situation that each analyzed piece was suffering. In spite of

this, further analyses have been proposed for completing the characterization of each type of piece:

In the case of Urbieta nails, the wood of the shipwreck should have been measured with Raman spectroscopy to confirm the presence of sulfur and iron compounds in it and to assess its state of preservation. In the Bakio shipwreck, new methodologies have not been considered due to the deterioration of the pieces and the impossibility of being transferred to the laboratory (most of them).

Regarding the glass beads, given the delicacy of the pieces, it is considered that the techniques used have been the most appropriate ones. In the case of the arrowheads, the poor molecular information provided by Raman spectroscopy clearly indicated that it was not the most suitable technique for the proposed aim. However, the VIS-NIR technique could be used as the main molecular technique. VIS-NIR technique could be a non-destructive and accurate powerful tool for providing important information about the classification and the provenance of flint artefacts².

Finally, in the case of iron slags, the possibility of destructive analysis of the pieces has been considered. For this aim, a cross-section preparation of some of the slags would be made.

This PhD has served to characterize the materials used in these samples, to evaluate their state of conservation and the treatments carried out, and to propose a future universal methodology that promotes the best possible conservation for archaeological pieces. This universal methodology is based on developing an approach for archaeological centers that focuses on the elaboration of a general report on the current and future state of the archaeological pieces. In this way, correct handling, durability over time and heritage value

could be ensured. For that aim, the collaboration of different types of experts such as archaeologists, conservators, geologists, chemists, biologists, etc. would be necessary to conduct more complete studies.

7.1 BIBLIOGRAPHY

The references mentioned in this work are based on the bibliography format described below:

Journals: Estalayo, E. Aramendia, J. Bellot-Gurlet, L. Garcia L. Garcia-Camino, I. Madariaga, J.M. Article title. *Journal abbreviation*, volume, pages (year).

Books: Estalayo, E. Aramendia, J. Bellot-Gurlet, L. Garcia L. Garcia-Camino, I. Madariaga, J.M. *Book title*, (year). DOI number.

1. Madariaga, J. M. Analytical chemistry in the field of cultural heritage. *Analytical Methods* **7**, 4848–4876 (2015).
2. Moral, L. F. G. del, Morgado, A. & Esquivel, J. A. Reflectance spectroscopy in combination with cluster analysis as tools for identifying the provenance of Neolithic flint artefacts. *Journal of Archaeological Science* **37**, 1–8 (2021).

CHAPTER 8

The background of the page is a soft-focus photograph of a forest. Tall, slender trees with light-colored bark rise vertically, their leaves creating a dappled light effect. In the lower foreground, a large, weathered log lies horizontally, partially covered in moss and fallen leaves. The overall color palette is muted, with various shades of green, brown, and grey, giving it a natural and somewhat somber feel.

8. APENDIXES

“Nothing in life is to be feared, it is only to be understood” – “En la vida no existe nada que temer, solo cosas que comprender” – Marie Curie

8.1 SCIENTIFIC PUBLICATIONS

8.1.1 Articles

Estalayo, E., Aramendia, J., Matés Luque, J. M. & Madariaga, J. M. Chemical study of degradation processes in ancient metallic materials rescued from underwater medium. *Journal of Raman Spectroscopy* **50**, 289-298 (2019). Doi: 10.1002/jrs.5553

Estalayo, E., Aramendia, J., Bellot-Gurlet, L., Garcia, L., Garcia-Camino, I., & Madariaga, J. M. The interaction of sediments with the archaeological iron remains from the recovery shipwreck of Urbieta (Gernika, North of Spain). *Journal of Raman Spectroscopy* **52**, 230-240 (2021). Doi: 10.1002/jrs.5944

8.1.2 Book chapters

Estalayo, E., Aramendia, J., Castro, K. & Madariaga, J. M. Non-destructive study of the degradation processes in underwater metallic materials. *Conserving Cultural Heritage* 319-321 (2018). Doi: 10.1201/9781315158648-80

8.1.3 Congresses

-Technoheritage (International Congress Science and Technology for the Conservation of Cultural Heritage) in Cádiz, 21-24 May 2017.

Poster: E. Estalayo, J. Aramendia, L. García, K. Castro, I. García-Camino, J. M. Madariaga. *Non-destructive study of the degradation processes in underwater metallic materials.*

-RAA (International Congress on the Application of Raman Spectroscopy in Art and Archaeology) in Évora, 24-28 October 2017.

Poster: The combination of Raman spectroscopy and SEM-EDS techniques to obtain a different structure of iron oxides in archaeological iron nails from the Basque Country

Oral communication: E. Estalayo, J. Aramendia, J. M. M. Luque, J. M. Madariaga. *Chemical study of degradation processes in underwater metallic materials.*

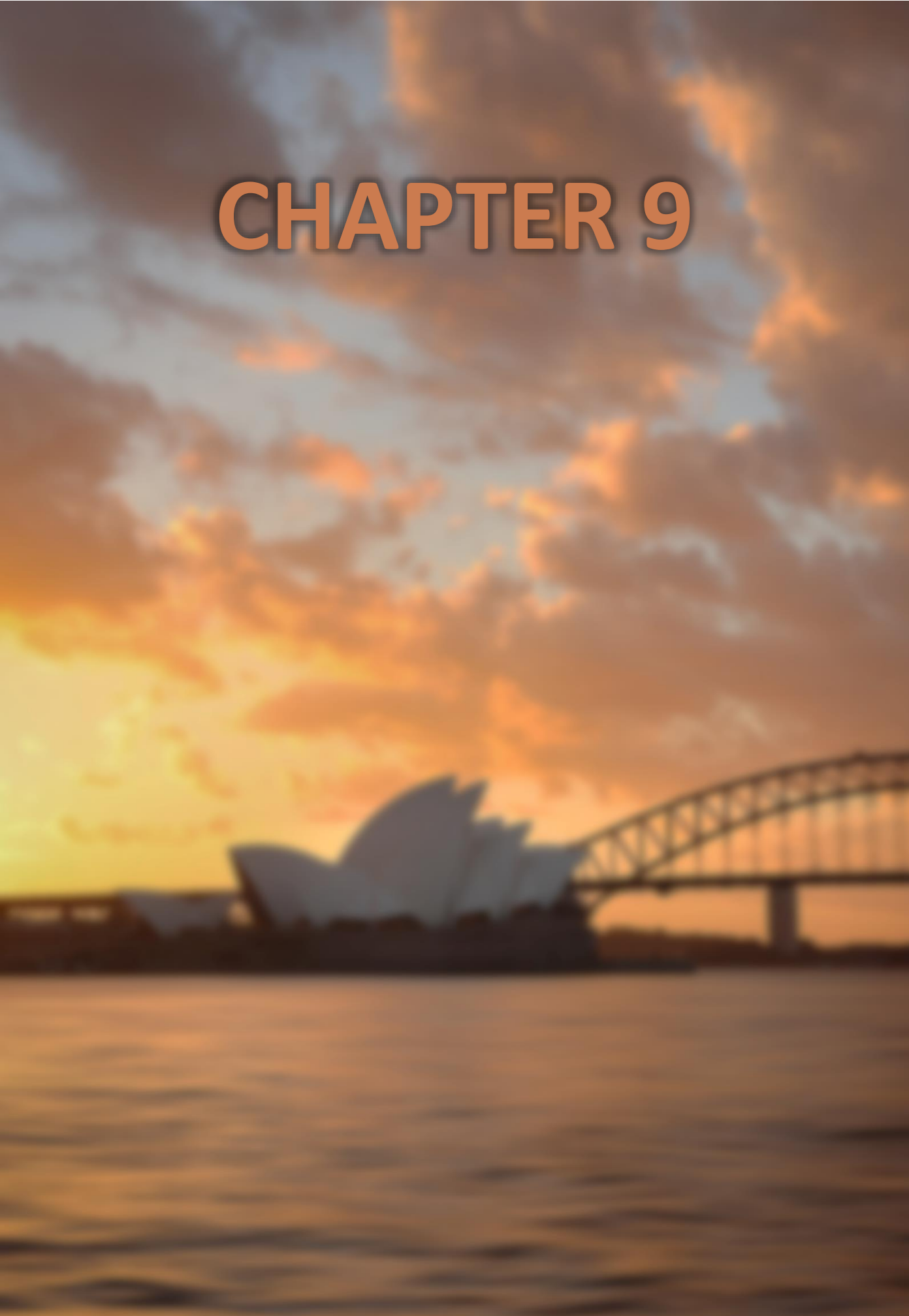
-EAA (24th Annual Meeting of the European Association of Archaeologists) in Barcelona, 5-8 September 2018.

Paper: J. Ibáñez, E. Estalayo, J. Aramendia, J. M. Madariaga, F. Borrel, M. Mozota, O. Bar-Yosef. *Lithic tools from Nahal Hemar Cave: Residue and use-wear analyses at a ritual site.*

-RAA (International Congress on the Application of Raman Spectroscopy in Art and Archaeology) in Potsdam, 3-7 September 2019.

Oral communication: E. Estalayo, J. Aramendia, L. Bellot-Gurlet, L. García, I. García-Camino, J. M. Madariaga. *The influence of sediments on some extracted iron nails from the recovered Urbieta shipwreck (Gernika, North of Spain).*

CHAPTER 9



9. ACKNOWLEDGEMENTS

“Strive to find things to be thankful for, and just look for the good in who you are” – “Esfuézate por encontrar cosas buenas por las que dar las gracias y busca lo bueno en lo que eres” – Bethany Hamilton

First and foremost, I would like to thank the department of Analytical Chemistry of the UPV/EHU Research Group, IBEA, for offering me the opportunity to carry out this PhD with them and for all the support they have shown me during all this time.

I must appreciate greatly the help offered by the archaeologist Jose Manuel Matés Luque at the beginning of this PhD, as well as that of Dr. Juan José Ibáñez, for providing us access to lithic tools and for allowing us to perform our non-destructive analysis.

Also mention the Department of “Física de la Materia Condensada, Cristalografía y Mineralogía” of Valladolid University (UVA) for the collaboration in the realization of this PhD and for allowing me to carry out the elemental study of the glass beads of Vaccaei culture.

I would like to acknowledge to the Archaeological Museum of Bilbao for providing us access to archaeological samples of Bakio’s and Urbietta’s shipwrecks, for giving us the opportunity to performed non-destructive analyses and even allowing us to take some archaeological pieces for the laboratory.

Last but not least, I would like to thank Francisco Javier Sangüesa for his aid in performing the analyses carried out in the General X-Ray Service of Rocks and minerals of the UPV/EHU (SGIKER).

Tras los agradecimientos oficiales, me dispongo a escribir los agradecimientos personales. Creo que intentar mencionar aquí a todas las personas que de una manera o de otra han ayudado a que esta tesis sea posible, va a ser complicado, pero debo intentarlo.

Primero de todo, me gustaría decir que, aunque parezca una tontería, hay tanta gente que ha ayudado a que esta tesis salga adelante... que nadie se lo imagina. Hasta el comentario más sencillo, un simple abrazo porque sabíais lo agobiada que estaba, darme mi espacio, preguntarme si podíais ayudarme a pesar de no saber cómo, llamarme por teléfono para que me despejase, hacerme salir de casa para que me diese el aire... podría dar tantos ejemplos de bondad y de empatía de los que jamás me habría podido imaginar. Y eso me llena el corazón de gratitud.

Me gustaría empezar por las primeras personas que hicieron que esto sea posible, y han sido mis directores, Juanma y Julene. Sabían de sobra que para mí el tema clave era el mar y fue por ello que se les ocurrió que mi tesis se basara en el análisis de piezas subacuáticas. Ellos han sido mi apoyo fundamental en este largo tramo. Me han escuchado cuando más lo he necesitado, han comprendido mi situación,

No podía dejar sin mencionar a Iñaki García-Camino, director del Museo Arqueológico de Bilbao y a mis queridas Laura y Sonia, arqueólogas del Museo. Siempre me habéis ayudado con todo lo que os he pedido, me habéis hecho el camino mucho más fácil y siempre ha sido un gusto hablar con vosotras. Sois unas personas encantadoras, muy profesionales y ha sido una maravilla poder trabajar con vosotras.

Las siguientes personas que me gustaría mencionar, son mi familia. Mi madre, mi hermano, mi padre, mis primos y tíos... Esas personas que siempre se han interesado y preocupado por mi bien. Que siempre me ayudan cuando lo necesito, que me apoyan en todo y me animan a seguir adelante. Mi ama sabe bien todo lo que me ha pesado este trabajo, lo difícil que me ha sido llevarlo con otros trabajos, las pocas fuerzas que he tenido para seguir adelante, pero ella siempre me ha dado todo lo que me faltaba para poder llegar. Gracias por nuestros paseos cada domingo, por escucharme siempre, por darme algo de comida siempre que voy a casa, quiera o no, por animarme eternamente en cada cosa que hago, por todos los consejos que me das, por los videos de crecimiento personal que me recomiendas ver. Y por supuesto, por creer en mí.

Al igual que mi hermano, puede que desde fuera parezcamos fríos y distantes, pero ambos sabemos que siempre estamos para lo que sea. Siempre has tenido tiempo para ayudarme a corregir mis trabajos, para mejorar mi inglés, para aconsejarme... Gracias por tu particular humor, por ayudarme con cosas informáticas a pesar de la hora que sea y a pesar de ser algo "sencillo", por nunca decirme un "no, búscate la vida" pero si un "que pesada". Gracias por estar presente en cada paso que doy, y por siempre estar dispuesto a ayudarme.

A mi aita, porque a pesar de nuestras diferencias, somos más parecidos de lo que jamás reconoceremos. Porque a pesar de entendernos pocas veces, yo siempre estoy ahí, y tú siempre estás ahí. Y eso es lo que de verdad importa y con lo que hay que quedarse.

Ha llegado tu momento, amor. Me gustaría decirte muchas cosas, pero no puedo extenderme mucho. De hecho, todo lo que te diría ya

lo sabes de sobra, pero no viene mal decirlo de nuevo. Desde que estas en mi vida, todo, repito, todo ha mejorado. Hemos mejorado cada uno por separado, pero hemos mejorado mucho más juntos. Tenemos una muy buena vida, como siempre te digo, y doy gracias a ello cada día.

Ahora llega el momento de darte las gracias por tanto que me das... Gracias por preocuparte por mi como lo haces. Por ser mi apoyo cuando lo necesito. Por escucharme e intentar ayudarme, aunque no sepas a veces como hacerlo (con la tesis por ejemplo 😊). Por creer siempre que puedo con todo. Por sorprenderme cuando no me lo espero. Por hacerme sonreír cuando quiero llorar. Por obligarme a descansar cuando llevo días sin hacerlo. Por ser quién eres, quererme como soy, aceptarme como soy y, aun así, aguantarme cada día. Cada día me eliges, a pesar de mi mal humor, mal despertar, mal carácter, mi poco tiempo en esta última temporada, mi estrés, mi agobio y mi ansiedad por todo. Porque resumiría todo con esta preciosa frase...

Me has dado paz, en tiempos de guerra

Y aquí llega el momento de mencionar a esas personas que estaban en mi día a día conmigo en el laboratorio. Empezar por mi trio calavera, como nos hacemos llamar, Imanol y Patri.

Imanol, tenemos tanta confianza que será que no hemos discutido veces por cosas del laboratorio o por cualquier tema político o social, será que no hemos tenido largas conversaciones sobre nuestras vidas, será que no nos hemos escuchado y aconsejado veces... me has aguantado taaaaantaaaas veces y cosas que a veces me pregunto cómo me sigues hablando. Me acuerdo muchas veces de tonterías que pasaban en el laboratorio, de nuestras charlas, cuando íbamos a

tomar un café y a que nos diese el sol, recuerdo las veces que estaba yo tan amargada que no quería hablar con nadie y vosotros siempre me entendisteis, sabíais que necesitaba tiempo y espacio y me lo dabais.

Patri, querida amiga, cuando tengo que escribir este párrafo me viene a la mente los juernes que nos pegábamos, nuestras fiestas en Vitoria en el máster y las buenas risas, eso jamás me faltaba. Al igual que con Imanol, has estado presente en mi vida desde el máster y espero que sigas siempre en ella. Habéis sido mi salvavidas durante toda la tesis. Me habéis dado la vida con cada conversación, cada risa, cada plan... Espero que a pesar de no compartir tiempo todos los días como antes (lo echo de menos) sigamos compartiendo tiempo, historias, quedadas, planes y, sobre todo, amistad.

Leti, Ilaria, Cris y Jenny. Mis cuatro reinas, al poner aquí vuestros nombres solo puedo sonreír. Me viene a la mente Cris diciendo alguna de sus cosas mientras trabajábamos concentrados y teníamos que parar para reírnos, recuerdo las largas conversaciones a la hora de la comida, en la hora del café, en cualquier momento... Recuerdo que siempre hablábamos de comida, o de cómo hacíamos las pizzas en Telepizza. Recuerdo que siempre que estabais el ambiente era inmejorable y si alguno/a uno estaba mal, nunca nos podía durar mucho rato porque le dabais la vuelta al día siempre. Echo de menos aquellos tiempos, los recuerdo más de lo que creéis y me encantaría volver a vivirlos. Espero seguir viéndoos, seguir haciendo planes de comidas y quedadas y espero y siempre esperare lo mejor para vosotras. Os lo merecéis más que de sobra.

Llega el momento de mis “sangre azul”. Mis compis en Decathlon. Esas buenas personas que se cruzan por tu vida, y no puedes dejar

escapar. Mi Josu y mi Gaby, de lo p. mejor que me llevo de allí. Siempre que recuerdo algo bueno, estabais vosotros.

Mi bebe, Ane, eres de lo mejor que he conocido. Una AMIGA en mayúsculas. Siempre has estado a mi lado, sobre todo en lo malo. Y eso jamás lo podría olvidar. Eres una persona increíble y espero poder estar muchísimos años a tu lado.

Por supuesto mis pequeñas, Olga, Mery y Lau. Esas buenas personas que conoces y sabes que van a estar en tu vida durante mucho tiempo. Que siempre se preocupan por tu bienestar y tú por el suyo.

Todos vosotros estuvisteis en un momento muy duro de mi vida, que jamás olvidaré. Me disteis apoyo aun arriesgando vuestro puesto, aun sabiendo que os podían perjudicar, pero vinisteis, porque sabíais que era lo justo. QUE GRANDES SOIS. Espero disfrutar de vosotros toda la vida.

Y no podía acabar este apartado sin mencionar a mi segurata favorito, Juane. Eres de las personas que más he echado de menos. Trabajar allí era duro, pero tener a personas como tu cerca siempre te ayuda a suavizar la carga. Hemos echado muy buenas risas, hemos vivido muy buenos momento y siempre que estabas tu allí al lado de recepción, estaba más tranquila. Gracias por cuidarme, por relajarme cuando me estaba enfadando o alterando y por entenderme, siempre lo has hecho. Has sido un apoyo enorme para mí.

Gaizkita a ti tampoco te olvido. Siempre tienes una sonrisa para mí, y siempre intentas sacarme alguna, hasta en mis peores días. Tu apoyo siempre ha sido de lo mejor que he tenido allí, y espero seguir teniéndolo durante toda la vida. Que, por cierto, tengo que conocer a Goku eh 😊

A mis grandes amigos de Telepizza, Nere, David y Patri. A mi Nere y a mi David, que sabía que, aunque nos fuéramos de aquel infierno, os seguiría teniendo en mi vida. Y así ha sido. Gracias por seguir en mi vida, por nuestras quedadas de gordos haciendo barbacoas los fines, y por seguir en contacto siempre. ¿Tenemos pendiente un home tour eh, David? Puede que, en poco tiempo, sean dos home tours 😊. Os quiero mucho.

Patri, mi fisio favorita, eres de lo mejor que saqué de aquel infierno. Menudas risas era estar contigo trabajando, cuando hacías las malditas pizzas mal, o cuando intentaban jodernos mandándonos limpiar cristales y demás y tu lo hacías siempre divertido. Gracias por seguir haciéndome llorar, aunque de dolor por mis contracturas, gracias por seguir en mi vida, eres muy grande amiga.

No podíais faltar todas aquellas personas importantes en mi vida que conocí en la carrera. Aitor, Dennis, Ainhoa, Rocío, Zuriñe, Asier, Peli... Desde que nos conocimos hicimos un buen equipo, que a pesar del tiempo y de los malos momentos, hemos sabido mantener siempre contacto. Espero que sigamos como hasta ahora, haciendo planes juntos, quedadas, cenas, home tours, y, sobre todo, ¡viajes!

Aunque parezca mentira, tengo que dedicar una pequeña parte de estos agradecimientos a unos amigos que siempre tienen tiempo para meterse con mi veganismo, que no paran de pedirme que venda droga porque es un buen trabajo y da mucho dinero, que se meten con mi manía de recoger plásticos del suelo y del mar... Si, hablo de vosotros, Negro y Bosko. Al final siempre me hacéis reír con vuestras tonterías y siempre pasamos un buen rato.

Por supuesto, mencionar a mi grupo de Buceo, Mundo Marino. Entre ellos a mi Juantxu y mi Jonatan, por preguntarme siempre como llevo la tesis y cuando narices la presento. Por preocuparos siempre por mi bienestar, por mi salud, y hasta por meterme prisa si voy lenta buceando, o gritarme bajo el agua (esto solo te incumbe a ti Jonatan). Mencionar también a Juanan, porque siempre te preocupas por mí y me das nuevas ideas para poder llevar a cabo en la tesis.

A mi pareja favorita, Desi y Julen. Igual ni os esperáis leer esto, pero no hay nada mejor que dedicarle unas bonitas palabras a las personas que hacen tu vida mejor, y vosotros sois un buen ejemplo de ello. Desde que os conocí me habéis dado luz, alegría y buenos momentos a patadas. Con vosotros nunca faltan planes, ni risas y eso me da la vida. Espero que me la sigáis dando siempre. Porque, de hecho, soy y seré la tita favorita del pequeño/a que llegue. La que le enseñará a bucear, aunque tenga a Sendoa al lado haciendo competencia con el maldito balón de futbol.

Llega el momento de mi Murcia querida. Belén. Siempre has estado a mi lado, a pesar de la distancia, del tiempo, de los problemas, siempre. Eso es amistad. Amistad es que me llames un día y nos tiremos 2 horas aproximadamente contándonos como nos va todo. Que hagamos videollamadas donde veas a la loca de Nieve subirse por las paredes. Que hable con la Lola sin saber que quiere decirme. Porque sé que puedo contar contigo para todo, al igual que tu conmigo. No necesitamos hablarnos cada día para saber lo que hay. Y como siempre te he dicho, te quiero mucho y siempre me tendrás a tu lado para todo, pequeña.

A mis bebes, mis gordis, mis gatis. Ellos me dan la vida a diario, sin pedir nada a cambio. Bueno si, comida y cariño, sobre todo comida.

Creo que no hemos podido tomar mejor decisión en nuestra vida que haberos adoptado. Sois lo mejor de nuestra vida, aunque a veces también nos la compliquéis mordiendo y rompiendo el cable de fibra óptica, arañando la televisión nueva, tirando las figuras de casa, comiendo folios, rompiendo las cajas de cartón, comiendo el plástico de la bolsa que dejas 5 segundos fuera sin querer, tirando el árbol de navidad, comiendo el maldito espumillón azul, rascando el sofá, sacando vuestras necesidades del arenero para jugar con ellas, mordiendo el cable del disco duro...

Da igual lo que hagáis, nos enfadaremos 5 segundos, y os amaremos eternamente y os perdonaremos siempre. Porque os queremos tal y como sois. A ti Nieve, por ser mi reina, mi bebe, mi loca favorita. Porque adoro cuando se te va la olla y vas corriendo de lado a lado de la casa, o cuando te subes por las paredes o trepas por las cortinas. Porque eres una reina, mimosa con todo el mundo, porque cuando me ves mal, vienes donde mí y no te separas hasta que me tranquilizo. A ti Nekko, mi gordito, mi locopan, mi gordilui. Por ser mi fiel seguidor. Por ser el pequeño más juguetón de la casa, y el más comilón. A pesar de seguir siendo asustadizo, te has vuelto un mimoso de la leche. Adoro como lloras cuando quieres pechuga de pavo o cuando quieres juego con la pelota de papel albal. Por no separarte nunca de mí. A los dos, aunque no podáis leer esto, lo sabéis porque os lo digo cada día. Gracias por estar en nuestra vida, os amaremos y protegeremos SIEMPRE.

Y por último y no menos importante, a la persona más importante de mi vida, a mí. Esto se lo dedico a la incansable luchadora que hay en mí. Por demostrar, una vez más, que puedes con todo lo que te plantees. Que por difícil que parezca, siempre te levantas. Por haberte

hundido en el pozo más oscuro que había, haberte perdido entre la nada y el olvido, y aun así, haber salido a buscar el último rayo de sol. Por tener esperanza, aun cuando todo el mundo la ha perdido. Por pensar siempre que algo mejor te espera. Por dar siempre todo lo que tienes y más, sin esperar nada a cambio. Por acabar todo lo que empiezas. Por ser tan terca y cabezona, de hacer siempre las cosas como tú quieres hacerlas. Por qué en el fondo, y lo sabes, te gusta complicarte la vida. Esto es para ti, pequeña.

“Desde la noche que sobre mi se cierne, negra como su insondable abismo, agradezco a los dioses si existen por mi alma invicta. Caído en las garras de la circunstancia nadie me vio llorar ni pestañear. Bajo los golpes del destino mi cabeza ensangrentada sigue erguida. Más allá de este lugar de lágrimas e ira yacen los horrores de la sombra, pero la amenaza de los años me encuentra, y me encontrará, sin miedo. No importa cuán estrecho sea el camino, cuán cargada de castigo la sentencia. Soy el amo de mi destino; soy el capitán de mi alma”, William Ernest Henley

CHAPTER 10



10. BIBLIOGRAPHY

"We cannot choose what happens to us. But what it turns us into" – "No Podemos elegir lo que nos pasa. Pero si en qué nos convierte"

The references mentioned in this work are based on the bibliography format described below:

Journals: Estalayo, E. Aramendia, J. Bellot-Gurlet, L. Garcia L. Garcia-Camino, I. Madariaga, J.M. Article title. *Journal abbreviation*, volume, pages (year).

Books: Estalayo, E. Aramendia, J. Bellot-Gurlet, L. Garcia L. Garcia-Camino, I. Madariaga, J.M. *Book title*, (year). DOI number.

UNESCO. UNESCO official web page. at
<<https://whc.unesco.org/en/faq/19>>

UNESCO. Records of the General Conference (Seventeenth Session) Paris 1972. *General conference seventeenth session 1*, 135–145 (1972).

UNESCO. *Convention concerning the protection of the world cultural and natural heritage. General Conference seventeenth session* (1972).

UNESCO. Operational Guidelines for the Implementation of the World Heritage Convention. *World Heritage Center 1–177* (2019).

UNESCO. *Records of the General Conference. Resolutions 1*, (2005).

Alonso, G. & Medici, M. in *Indicadores UNESCO de Cultural para el desarrollo. Manual Metodológico* 132–140 (2014).

- España, M. de C. y Deporte. G. de. UNESCO Patrimonio Mundial. at <https://www.culturaydeporte.gob.es/cultura/areas/patrimonio/mc/patrimoniomundial/unesco-patrimoniomundial.html>>
- Sandu, I., Vasilache, V. & Vrînceanu, N. Environmental Technologies in the Field of Scientific Conservation of Cultural Heritage. New Perspectives and Directions of Research. *Present Environment and Sustainable Development* **3**, 97–105 (2009).
- Europe, C. of. Concerning the Adaptation of Laws and Regulations To the. in *Resolution (76) 28* 1–7 (1976).
- Convention, E. C., Charter, E., Heritage, A., Assembly, P., No, R. & No, R. Council of Europe: Convention for the Protection of the Architectural Heritage of Europe. *International Legal Materials* **25**, 380–390 (1986).
- Sablier, M. & Garrigues, P. Cultural heritage and its environment: An issue of interest for Environmental Science and Pollution Research. *Environmental Science and Pollution Research* **21**, 5769–5773 (2014).
- Dastgerdi, A. S., Sargolini, M. & Pierantoni, I. Climate change challenges to existing cultural heritage policy. *Sustainability Heritage Management* **11**, (2019).
- Sesana, E., Gagnon, A. S., Ciantelli, C., Cassar, J. A. & Hughes, J. J. Climate change impacts on cultural heritage: A literature review. *Wiley Interdisciplinary Reviews: Climate Change* **12**, 1–29 (2021).
- UNESCO. Climate change and World Heritage. *Science* **314**, 632–635 (2006).

- Spiridon, P., Sandu, I. & Stratulat, L. The conscious deterioration and degradation of the cultural heritage. *International Journal of Conservation Science* **8**, 81–88 (2017).
- School, W. S. How Much Water is There on Earth? (2019). at <<https://www.usgs.gov/special-topics/water-science-school/science/how-much-water-there-earth>>
- Little, B. J., Lee, J. S., Briggs, B. R., Ray, R. & Sylvester, A. Examination of archived rusticles from World War II shipwrecks. *International Biodeterioration and Biodegradation* **143**, 1–6 (2019).
- Chadwick, A. v., Berko, A., Schofield, E. J., Smith, A. D., Mosselmans, J. F. W., Jones, A. M. & Cibir, G. The application of X-ray absorption spectroscopy in archaeological conservation: Example of an artefact from Henry VIII warship, the Mary Rose. *Journal of Non-Crystalline Solids* **451**, 49–55 (2016).
- Rogério-Candelera, M. Á. Science, technology and cultural heritage. *Science, Technology and Cultural Heritage* 1–501 (2014). doi:10.1201/b17802
- Naderi Beni, A., Lahijani, H., Tofighian, H., Guibal, F., Kabiri, K., Gambin, T., Djamali, M., Abaie, H. & Jahani, V. Geoarchaeology of the 18th century Qoroq shipwreck, Caspian Sea, Iran: A tale of sailing in a dynamic environment. *Journal of Archaeological Science: Reports* **34**, (2020).
- UNESCO. *Convention on the Protection of the Underwater Cultural Heritage*. (2001).
- Ricca, M. & la Russa, M. F. Challenges for the Protection of Underwater Cultural Heritage (UCH), from Waterlogged and Weathered Stone

Materials to Conservation Strategies: An Overview. *Heritage* **3**, 402–411 (2020).

23. Angelini, E., Grassini, S. & Tusa, S. Underwater corrosion of metallic heritage artefacts. *Corrosion and Conservation of Cultural Heritage Metallic Artefacts* 236–259 (2013). doi:10.1533/9781782421573.3.236

Florian, M.-L. E. *The underwater environment. Conservation of Marine Archaeological Objects* (Butterworth & Co. (Publishers) Ltd., 1987). doi:10.1016/b978-0-408-10668-9.50007-1

Memet, J. B. in *Corrosion of Metallic Heritage Artefacts: Investigation, Conservation and Prediction of Long Term Behaviour* 152–169 (2007). doi:10.1533/9781845693015.152

Science, S. Depth sea pH profile. at <<https://skepticalscience.com/print.php?n=918>>

Frankel, G. S. Pitting Corrosion of Metals: A Review of the Critical Factors. *Journal of The Electrochemical Society* **145**, 2186–2198 (1998).

Engineering, S. of M. S. and. Crevice corrosion. at <<https://www.materials.unsw.edu.au/study-us/high-school-students-and-teachers/online-tutorials/corrosion/types-corrosion/crevice-corrosion>>

Loto, C. A. Stress corrosion cracking: characteristics, mechanisms and experimental study. *International Journal of Advanced Manufacturing Technology* **93**, 622–640 (2017).

Shehadeh, M., Anany, M., Saqr, K. M. & Hassan, I. Experimental investigation of erosion-corrosion phenomena in a steel fitting due to plain and

- slurry seawater flow. *International Journal of Mechanical and Materials Engineering* **9**, 1–8 (2014).
- Yang, L. *Techniques for Corrosion Monitoring*. (2008).
- Černoušek, T., Ševců, A., Shrestha, R., Steinová, J., Kokinda, J. & Vizelková, K. in *The Microbiology of Nuclear Waste Disposal* 119–136 (2021).
doi:10.1016/b978-0-12-818695-4.00006-x
- Little, B. J., Blackwood, D. J., Hinks, J., Lauro, F. M., Marsili, E., Okamoto, A., Rice, S. A., Wade, S. A. & Flemming, H. C. Microbially influenced corrosion—Any progress? *Corrosion Science* **170**, 108641 (2020).
- Broda, M. & Hill, C. A. S. Conservation of waterlogged wood—past, present and future perspectives. *Forests* **12**, 1–55 (2021).
- Kibblewhite, M., Tóth, G. & Hermann, T. Predicting the preservation of cultural artefacts and buried materials in soil. *Science of the Total Environment* **529**, 249–263 (2015).
- Arriba-Rodriguez, L. de, Villanueva-Balsera, J., Ortega-Fernandez, F. & Rodriguez-Perez, F. Methods to evaluate corrosion in buried steel structures: A review. *Metals* **8**, (2018).
- Logan, K. H. The Bureau of Standards Soil-Corrosion Investigation. *Journal of American Water Works Association* **21**, 311–316 (1929).
- Singh, B., Cattle, S. R. & Field, D. J. Edaphic Soil Science, Introduction to. *Encyclopedia of Agriculture and Food Systems* **3**, 35–58 (2014).
- Ismail, A. I. M. & El-Shamy, A. M. Engineering behaviour of soil materials on the corrosion of mild steel. *Applied Clay Science* **42**, 356–362 (2009).

- Pereira, R. F. D. C., de Oliveira, E. S. D., Lima, M. A. G. D. A. & Brasil, S. L. D. C. Corrosion of galvanized steel under different soil moisture contents. *Materials Research* **18**, 563–568 (2015).
- Veleva, L. in *Corrosion Tests and Standards: Application and Interpretation* 882 (2005).
- Tiba, C. & de Oliveira, E. M. Utilization of cathodic protection for transmission towers through photovoltaic generation. *Renewable Energy* **40**, 150–156 (2012).
- Kibblewhite, M., Tóth, G. & Hermann, T. Predicting the preservation of cultural artefacts and buried materials in soil. *Science of the Total Environment* **529**, 249–263 (2015).
- Eric, D. & Price Clifford A. *Research in Conservation. Research in Conservation* (2010).
- Doehne, E., Selwitz, D., Carson, D. & Selwitz, C. The damage mechanism of sodium sulfate in porous stone. *European research on cultural heritage* **5**, 127–146 (2006).
- Tokmak, M. & Dal, M. Types of degradation observed in underwater stone artifacts. in *12th International Symposium on Underwater Research* 72–77 (2020).
- Farooq, M. Mycobial Deterioration of Stone Monuments of Dharmarajika, Taxila. *Journal of Microbiology & Experimentation* **2**, 29–33 (2015).
- Carmona, N., García-Heras, M., Gil, C. & Villegas, M. A. Chemical degradation of glasses under simulated marine medium. *Materials Chemistry and Physics* **94**, 92–102 (2005).

- Kibblewhite, M., Tóth, G. & Hermann, T. Predicting the preservation of cultural artefacts and buried materials in soil. *Science of the Total Environment* **529**, 249–263 (2015).
- Abd-Allah, R. Chemical cleaning of soiled deposits and encrustations on archaeological glass: A diagnostic and practical study. *Journal of Cultural Heritage* **14**, 97–108 (2013).
- Zacharias, N., Palamara, E., Kordali, R. & Muros, V. Archaeological Glass Corrosion Studies: Composition, Environment and Content. *Scientific Culture* **6**, 53–67 (2020).
- Palomar Sanz, T. El vidrio arqueológico: Problemas y metodología. in *Actas de las V Jornadas de Investigación del departamento de prehistoria y arqueología de la UAM: Jóvenes investigadores de la Comunidad de Madrid* 79–87 (2016).
- Palomar, T. & Llorente, I. Decay processes of silicate glasses in river and marine aquatic environments. *Journal of Non-Crystalline Solids* **449**, 20–28 (2016).
- Zurer, P. S. Archaeological chemistry. *Chemical and Engineering News* **61**, 26–44 (1983).
- Glascok, M. D. Compositional Analysis in Archaeology History of Compositional Analysis. *Oxford Handbooks Online* 1–25 (2016). doi:10.1093/oxfordhb/9780199935413.013.8
- Caley, E. R. Early history and literature of archaeological chemistry. *Journal of Chemical Education* **204**, 64–66 (1951).
- Harbottle, G. *Chemical Characterization in Archaeology. Contexts for Prehistoric Exchange* (Academic Press, Inc., 1982). doi:10.1016/b978-0-12-241580-7.50007-3

Pollard, A. M. & Heron, C. *Archaeological Chemistry*. (1996).

Caley, E. R. Klaproth as a pioneer in the chemical investigation of antiquities.
Journal of Chemical Education **26**, (1949).

Lamont-Brown, R. *Humphry Davy: Life beyond the lamp*. (Sutton, 2004).

Institute, S. H. Humphry Davy. at
<<https://www.sciencehistory.org/historical-profile/humphry-davy>>

Humphry Davy. Some experiments and observations on the colours used in painting by the ancients. *Philosophical Transactions of the Royal Society of London* **105**, 97–124 (1815).

Davy, H. XXI. Observations upon the Composition of the Colours found on the Walls of the Roman House discovered at Bignor in Sussex. By Sir Humphrey Davy, Knt. F.R.S. in a Letter to Samuel Lysons, Esq. V.P. *Archaeologia* **18**, 222–222 (1817).

Moshenska, G. Michael faraday's contributions to archaeological chemistry.
Ambix **62**, 266–286 (2015).

Wikipedia. Karl Christian Traugott Friedemann Goebel. at
<https://en.wikipedia.org/wiki/Karl_Christian_Traugott_Friedemann_Goebel>

Göbel, K. C. Über der Einfluss der Chemie auf die Ermittlung der Völker der Vorzeit. (1842).

Vélová, L. Jan Erazim Vöcel. (2012). at
<<https://www.archeologienadosah.cz/o-archeologii/dejiny-oboru/osobnosti-ceske-archeologie/jan-erazim-vocel-1802-1871>>

- Walter, E. Jan Erazim Vocel (1802-1871): A Pioneer of Czech-Danish Friendship. *Essays on the arts and sciences* 924–927 (2019). doi:10.1515/9783111562575-003
- Vocel, J. E. Stein- und Bronzealterthümer. (1869).
- France, S. G. de. Agustin Alexis Damour. at <<https://www.geosoc.fr/propos.html/historique/presidents-de-la-sgf/64-presidents-sgf/441-augustin-alexis-damour.html>>
- Damour, A. Sur la composition des haches en pierre trouvées dans les monuments celtiques et chez les tribus sauvages. *Revue Archéologique* 13, 190–207 (1866).
- Percy, J. *Metallurgy: The Art of Extracting Metals from their Ores.* (1861).
- Gilberg, M. Friedrich Rathgen: The father of modern archaeological conservation. *Journal of the American Institute for Conservation* 26, 85–104 (1987).
- Rathgen, F. The Preservation of Antiquities, a Handbook for Curators. *Nature* 73, 412–412 (1906).
- Orna, M. v. & Rasmussen, S. C. in *Archaeological Chemistry: A multidisciplinary analysis of the past* 509 (2020). doi:10.2307/504338
- Oddy, W. A. Chemistry in the conservation of archaeological materials. *Science of the Total Environment, The* 143, 121–126 (1994).
- Ullén, I., Nord, A. G., Fjaestad, M., Mattsson, E., Borg, G. C. & Tronner, K. The degradation of archaeological bronzes underground: Evidence from museum collections. *Antiquity* 78, 380–390 (2004).

- Lambert, J. B. Archaeological chemistry. *Journal of Chemical Education* **60**, 345–347 (1983).
- Jakes, K. A. Archaeological chemistry: Materials, methods, and meaning. *ACS Symposium Series* **831**, 1–7 (2002).
- Goffer, Z. *Archaeological Chemistry*. (2007).
- Doménech-Carbó, A. & Doménech-Carbó, M. T. Electroanalytical techniques in archaeological and art conservation. *Pure and Applied Chemistry* **90**, 447–461 (2018).
- Franquelo, M. L., Duran, A., Castaing, J., Arquillo, D. & Perez-Rodriguez, J. L. XRF, μ -XRD and μ -spectroscopic techniques for revealing the composition and structure of paint layers on polychrome sculptures after multiple restorations. *Talanta* **89**, 462–469 (2012).
- Bitossi, G., Giorgi, R., Mauro, M., Salvadori, B. & Dei, L. Spectroscopic techniques in cultural heritage conservation: A survey. *Applied Spectroscopy Reviews* **40**, 187–228 (2005).
- de Castro, M. D. L. & Jurado-López, A. The role of analytical chemists in the research on the cultural heritage. *Talanta* **205**, (2019).
- Committee, A. M. & No, A. Raman spectroscopy in cultural heritage: Background paper. *Analytical Methods* **7**, 4844–4847 (2015).
- Bezur, A., Lee, L., Loubser, M. & Trentelman, K. *Handheld XRF in Cultural Heritage. A Practical Workbook for Conservators*. (2020).
- Kendix, E. L., Prati, S., Mazzeo, R., Joseph, E., Sciutto, G. & Fagnano, C. Far Infrared Spectroscopy in the Field of Cultural Heritage. *e-Preservation Science* **7**, 8–13 (2010).

- van Hoek, C. J. G., de Roo, M., van der Veer, G. & van der Laan, S. R. A SEM-EDS study of cultural heritage objects with interpretation of constituents and their distribution using PARC data analysis. *Microscopy and Microanalysis* **17**, 656–660 (2011).
- Tereszchuk, K. A., Vadillo, J. M. & Laserna, J. J. Depth profile analysis of layered samples using glow discharge assisted Laser-induced Breakdown Spectrometry (GD-LIBS). *Spectrochimica Acta - Part B Atomic Spectroscopy* **64**, 378–383 (2009).
- Jiang, L., Sui, M., Fan, Y., Su, H., Xue, Y. & Zhong, S. Micro-gas column assisted laser induced breakdown spectroscopy (MGC-LIBS): A metal elements detection method for bulk water in-situ analysis. *Spectrochimica Acta - Part B Atomic Spectroscopy* **177**, (2021).
- Gonzalez, V., Cotte, M., Vanmeert, F., de Nolf, W. & Janssens, K. X-ray Diffraction Mapping for Cultural Heritage Science: a Review of Experimental Configurations and Applications. *Chemistry - A European Journal* **26**, 1703–1719 (2020).
- János, I., Szathmáry, L., Nádas, E., Béni, A., Dinya, Z. & Máthé, E. Evaluation of elemental status of ancient human bone samples from Northeastern Hungary dated to the 10th century AD by XRF. *Nuclear Instruments and Methods in Physics Research, Section B: Beam Interactions with Materials and Atoms* **269**, 2593–2599 (2011).
- Al-Eshaikh, M. A. & Kadachi, A. Elemental analysis of steel products using X-ray fluorescence (XRF) technique. *Journal of King Saud University - Engineering Sciences* **23**, 75–79 (2011).
- Vasilescu, A., Constantinescu, B., Stan, D., Radtke, M., Reinholz, U., Buzanich, G. & Ceccato, D. Studies on ancient silver metallurgy using SR XRF and micro-PIXE. *Radiation Physics and Chemistry* **117**, 26–34 (2015).

- Cruz, J., Manso, M., Corregidor, V., Silva, R. J. C., Figueiredo, E., Carvalho, M. L. & Alves, L. C. Surface analysis of corroded XV–XVI century copper coins by μ -XRF and μ -PIXE/ μ -EBS self-consistent analysis. *Materials Characterization* **161**, (2020).
- Castro, K., Knuutinen, U., Vallejuelo, S. F. O. de, Irazola, M. & Madariaga, J. M. Finnish wallpaper pigments in the 18th-19th century: Presence of $\text{KFe}_3(\text{CrO}_4)_2(\text{OH})_6$ and odd pigment mixtures. *Spectrochimica Acta - Part A: Molecular and Biomolecular Spectroscopy* **106**, 104–109 (2013).
- Turco, F., Davit, P., Cossio, R., Agostino, A. & Operti, L. Accuracy improvement by means of porosity assessment and standards optimization in SEM-EDS and XRF elemental analyses on archaeological and historical pottery and porcelain. *Journal of Archaeological Science* **12**, 54–65 (2017).
- Bello, J. F. A. PhD Thesis: Nuevo micro-análisis cuantitativo de metales empleando microscopía electrónica de barrido con dispersión de energías de rayos X. *Universidad Complutense de Madrid* (1999).
- Wolfgong, W. J. *Chemical analysis techniques for failure analysis: Part 1, common instrumental methods. Handbook of Materials Failure Analysis with Case Studies from the Aerospace and Automotive Industries* (Elsevier Ltd., 2016). doi:10.1016/B978-0-12-800950-5.00014-4
- Arafat, A., Na'es, M., Kantarelou, V., Haddad, N., Giakoumaki, A., Argyropoulos, V., Anglos, D. & Karydas, A. G. Combined in situ micro-XRF, LIBS and SEM-EDS analysis of base metal and corrosion products for Islamic copper alloyed artefacts from Umm Qais museum, Jordan. *Journal of Cultural Heritage* **14**, 261–269 (2013).

- Pendleton, M. W., Washburn, D. K., Ellis, E. A. & Pendleton, B. B. Comparing the detection of iron-based pottery pigment on a carbon-coated Sherd by SEM-EDS and by Micro-XRF-SEM. *Yale Journal of Biology and Medicine* **87**, 15–20 (2014).
- Eberhardt, K., Stiebing, C., Matthaüs, C., Schmitt, M. & Popp, J. Advantages and limitations of Raman spectroscopy for molecular diagnostics: An update. *Expert Review of Molecular Diagnostics* **15**, 773–787 (2015).
- Rémazeilles, C., Lévêque, F., Conforto, E. & Refait, P. Long-term alteration processes of iron fasteners extracted from archaeological shipwrecks aged in biologically active waterlogged media. *Corrosion Science* **181**, (2021).
- Aramendia, J., Gomez-Nubla, L., Bellot-Gurlet, L., Castro, K., Paris, C., Colomban, P. & Madariaga, J. M. Protective ability index measurement through Raman quantification imaging to diagnose the conservation state of weathering steel structures. *Journal of Raman Spectroscopy* **45**, 1076–1084 (2014).
- Rémazeilles, C., Saheb, M., Neff, D., Guilminot, E., Tran, K., Bourdoiseau, J. A., Sabot, R., Jeannin, M., Matthiesen, H., Dillmann, P. & Refait, P. Microbiologically influenced corrosion of archaeological artefacts: Characterisation of iron(II) sulfides by Raman spectroscopy. *Journal of Raman Spectroscopy* **41**, 1425–1433 (2010).
- Estalayo, E., Aramendia, J., Matés Luque, J. M. & Madariaga, J. M. Chemical study of degradation processes in ancient metallic materials rescued from underwater medium. *Journal of Raman Spectroscopy* **50**, 289–298 (2019).

- Kerns, J. G., Buckley, K., Parker, A. W., Birch, H. L., Matousek, P., Hildred, A. & Goodship, A. E. The use of laser spectroscopy to investigate bone disease in King Henry VIII's sailors. *Journal of Archaeological Science* **53**, 516–520 (2015).
- Abdurakhimov, B. A., Kichanov, S. E., Talmaṭchi, C., Kozlenko, D. P., Talmaṭchi, G., Belozerova, N. M., Bălăsoiu, M. & Belc, M. C. Studies of ancient pottery fragments from Dobrudja region of Romania using neutron diffraction, tomography and Raman spectroscopy. *Journal of Archaeological Science* **35**, (2021).
- Butler, H. J., Ashton, L., Bird, B., Cinque, G., Curtis, K., Dorney, J., Esmonde-White, K., Fullwood, N. J., Gardner, B., Martin-Hirsch, P. L., Walsh, M. J., McAinsh, M. R., Stone, N. & Martin, F. L. Using Raman spectroscopy to characterize biological materials. *Nature Protocols* **11**, 664–687 (2016).
- Vandenabeele, P. Raman spectroscopy in art and archaeology. *Journal of Raman Spectroscopy* **35**, 607–609 (2004).
- Rajiv, K. & Mittal, K. L. in *Developments in Surface Contamination and Cleaning* **12**, 23–105 (2019).
- Engler, P. & Iyengar, S. S. Analysis of mineral samples using combined instrument (XRD, TGA, ICP) procedures for phase quantification. *American Mineralogist* **72**, 832–838 (1987).
- Aramendia, J. PhD Thesis: Analytical diagnosis of the conservation state of weathering steel exposed to urban atmospheres. *Universidad del País Vasco (UPV/EHU)* (2013).
- Kamimura, T., Nasu, S., Tazaki, T., Kuzushita, K. & Morimoto, S. Mössbauer spectroscopic study of rust formed on a weathering steel and a mild

- steel exposed for a long term in an industrial environment. *Materials Transactions* **43**, 694–703 (2002).
- Castro, K. PhD Thesis: Pigment characterization on paper-based artworks by vibrational spectroscopic techniques. *Universidad del País Vasco (UPV/EHU)* (2004).
- Bitossi, G., Giorgi, R., Mauro., Salvadori, B. & Dei, L. Spectroscopic techniques in cultural heritage conservation: A survey. *Applied Spectroscopy Reviews* **40**, 187-228 (2005).
- Winkler, E. M. *Stone in Architecture*. *Stone in Architecture* (1997). doi:10.1007/978-3-662-10070-7
- de Castro, M. D. L. & Jurado-López, A. The role of analytical chemists in the research on the cultural heritage. *Talanta* **205**, (2019).
- Committee, A. M. & No, A. Raman spectroscopy in cultural heritage: Background paper. *Analytical Methods* **7**, 4844–4847 (2015).
- Bezur, A., Lee, L., Loubser, M. & Trentelman, K. *Handheld XRF in Cultural Heritage. A Practical Workbook for Conservators*. (2020).
- Kendix, E. L., Prati, S., Mazzeo, R., Joseph, E., Sciutto, G. & Fagnano, C. Far Infrared Spectroscopy in the Field of Cultural Heritage. *e-Preservation Science* **7**, 8–13 (2010).
- van Hoek, C. J. G., de Roo, M., van der Veer, G. & van der Laan, S. R. A SEM-EDS study of cultural heritage objects with interpretation of constituents and their distribution using PARC data analysis. *Microscopy and Microanalysis* **17**, 656–660 (2011).
- Tereszchuk, K. A., Vadillo, J. M. & Laserna, J. J. Depth profile analysis of layered samples using glow discharge assisted Laser-induced

- Breakdown Spectrometry (GD-LIBS). *Spectrochimica Acta - Part B Atomic Spectroscopy* **64**, 378–383 (2009).
- Jiang, L., Sui, M., Fan, Y., Su, H., Xue, Y. & Zhong, S. Micro-gas column assisted laser induced breakdown spectroscopy (MGC-LIBS): A metal elements detection method for bulk water in-situ analysis. *Spectrochimica Acta - Part B Atomic Spectroscopy* **177**, (2021).
- Gonzalez, V., Cotte, M., Vanmeert, F., de Nolf, W. & Janssens, K. X-ray Diffraction Mapping for Cultural Heritage Science: a Review of Experimental Configurations and Applications. *Chemistry - A European Journal* **26**, 1703–1719 (2020).
- János, I., Szathmáry, L., Nádas, E., Béni, A., Dinya, Z. & Máthé, E. Evaluation of elemental status of ancient human bone samples from Northeastern Hungary dated to the 10th century AD by XRF. *Nuclear Instruments and Methods in Physics Research, Section B: Beam Interactions with Materials and Atoms* **269**, 2593–2599 (2011).
- Al-Eshaikh, M. A. & Kadachi, A. Elemental analysis of steel products using X-ray fluorescence (XRF) technique. *Journal of King Saud University - Engineering Sciences* **23**, 75–79 (2011).
- Vasilescu, A., Constantinescu, B., Stan, D., Radtke, M., Reinholz, U., Buzanich, G. & Ceccato, D. Studies on ancient silver metallurgy using SR XRF and micro-PIXE. *Radiation Physics and Chemistry* **117**, 26–34 (2015).
- Cruz, J., Manso, M., Corregidor, V., Silva, R. J. C., Figueiredo, E., Carvalho, M. L. & Alves, L. C. Surface analysis of corroded XV–XVI century copper coins by μ -XRF and μ -PIXE/ μ -EBS self-consistent analysis. *Materials Characterization* **161**, (2020).

- Castro, K., Knuutinen, U., Vallejuelo, S. F. O. de, Irazola, M. & Madariaga, J. M. Finnish wallpaper pigments in the 18th-19th century: Presence of $\text{KFe}_3(\text{CrO}_4)_2(\text{OH})_6$ and odd pigment mixtures. *Spectrochimica Acta - Part A: Molecular and Biomolecular Spectroscopy* **106**, 104–109 (2013).
- Turco, F., Davit, P., Cossio, R., Agostino, A. & Operti, L. Accuracy improvement by means of porosity assessment and standards optimization in SEM-EDS and XRF elemental analyses on archaeological and historical pottery and porcelain. *Journal of Archaeological Science* **12**, 54–65 (2017).
- Bello, J. F. A. PhD Thesis: Nuevo micro-análisis cuantitativo de metales empleando microscopía electrónica de barrido con dispersión de energías de rayos X. *Universidad Complutense de Madrid* (1999).
- Wolfgong, W. J. *Chemical analysis techniques for failure analysis: Part 1, common instrumental methods. Handbook of Materials Failure Analysis with Case Studies from the Aerospace and Automotive Industries* (Elsevier Ltd., 2016). doi:10.1016/B978-0-12-800950-5.00014-4
- Arafat, A., Na'es, M., Kantarelou, V., Haddad, N., Giakoumaki, A., Argyropoulos, V., Anglos, D. & Karydas, A. G. Combined in situ micro-XRF, LIBS and SEM-EDS analysis of base metal and corrosion products for Islamic copper alloyed artefacts from Umm Qais museum, Jordan. *Journal of Cultural Heritage* **14**, 261–269 (2013).
- Pendleton, M. W., Washburn, D. K., Ellis, E. A. & Pendleton, B. B. Comparing the detection of iron-based pottery pigment on a carbon-coated Sherd by SEM-EDS and by Micro-XRF-SEM. *Yale Journal of Biology and Medicine* **87**, 15–20 (2014).

- Eberhardt, K., Stiebing, C., Matthaüs, C., Schmitt, M. & Popp, J. Advantages and limitations of Raman spectroscopy for molecular diagnostics: An update. *Expert Review of Molecular Diagnostics* **15**, 773–787 (2015).
- Rémazeilles, C., Lévêque, F., Conforto, E. & Refait, P. Long-term alteration processes of iron fasteners extracted from archaeological shipwrecks aged in biologically active waterlogged media. *Corrosion Science* **181**, (2021).
- Aramendia, J., Gomez-Nubla, L., Bellot-Gurlet, L., Castro, K., Paris, C., Colombar, P. & Madariaga, J. M. Protective ability index measurement through Raman quantification imaging to diagnose the conservation state of weathering steel structures. *Journal of Raman Spectroscopy* **45**, 1076–1084 (2014).
- Rémazeilles, C., Saheb, M., Neff, D., Guilminot, E., Tran, K., Bourdoiseau, J. A., Sabot, R., Jeannin, M., Matthiesen, H., Dillmann, P. & Refait, P. Microbiologically influenced corrosion of archaeological artefacts: Characterisation of iron(II) sulfides by Raman spectroscopy. *Journal of Raman Spectroscopy* **41**, 1425–1433 (2010).
- Kerns, J. G., Buckley, K., Parker, A. W., Birch, H. L., Matousek, P., Hildred, A. & Goodship, A. E. The use of laser spectroscopy to investigate bone disease in King Henry VIII's sailors. *Journal of Archaeological Science* **53**, 516–520 (2015).
- Abdurakhimov, B. A., Kichanov, S. E., Talmaçhi, C., Kozlenko, D. P., Talmaçhi, G., Belozerovala, N. M., Bălăşoiu, M. & Belc, M. C. Studies of ancient pottery fragments from Dobrudja region of Romania using neutron diffraction, tomography and Raman spectroscopy. *Journal of Archaeological Science* **35**, (2021).

- Butler, H. J., Ashton, L., Bird, B., Cinque, G., Curtis, K., Dorney, J., Esmonde-White, K., Fullwood, N. J., Gardner, B., Martin-Hirsch, P. L., Walsh, M. J., McAinsh, M. R., Stone, N. & Martin, F. L. Using Raman spectroscopy to characterize biological materials. *Nature Protocols* **11**, 664–687 (2016).
- Vandenabeele, P. Raman spectroscopy in art and archaeology. *Journal of Raman Spectroscopy* **35**, 607–609 (2004).
- Rajiv, K. & Mittal, K. L. in *Developments in Surface Contamination and Cleaning* **12**, 23–105 (2019).
- Engler, P. & Iyengar, S. S. Analysis of mineral samples using combined instrument (XRD, TGA, ICP) procedures for phase quantification. *American Mineralogist* **72**, 832–838 (1987).
- Aramendia, J. PhD Thesis: Analytical diagnosis of the conservation state of weathering steel exposed to urban atmospheres. *Universidad del País Vasco (UPV/EHU)* (2013).
- Kamimura, T., Nasu, S., Tazaki, T., Kuzushita, K. & Morimoto, S. Mössbauer spectroscopic study of rust formed on a weathering steel and a mild steel exposed for a long term in an industrial environment. *Materials Transactions* **43**, 694–703 (2002).
- Castro, K. PhD Thesis: Pigment characterisation on paper-based artworks by vibrational spectroscopic techniques. *Universidad del País Vasco (UPV/EHU)* (2004).
- Franquelo, M. L., Duran, A., Castaing, J., Arquillo, D. & Perez-Rodriguez, J. L. XRF, μ -XRD and μ -spectroscopic techniques for revealing the composition and structure of paint layers on polychrome sculptures after multiple restorations. *Talanta* **89**, 462–469 (2012).

- Castro, K., Pérez-Alonso, M., Rodríguez-Laso, M. D., Fernández, L. A. & Madariaga, J. M. On-line FT-Raman and dispersive Raman spectra database of artists' materials (e-VISART database). *Analytical and Bioanalytical Chemistry* **382**, 248–258 (2005).
- Lafuente, B., Downs, R. T., Yang, H. & Stone, N. in *Highlights in Mineralogical Crystallography* 1–30 (2016). doi:10.1515/9783110417104-003
- Morillas, H., Maguregui, M., Huallparimachi, G., Marcaida, I., García-Florentino, C., Lumbreras, L., Astete, F. & Madariaga, J. M. Multianalytical approach to evaluate deterioration products on cement used as consolidant on lithic material: The case of Tello Obelisk, Lima (Peru). *Microchemical Journal* **139**, 42–49 (2018).
- Aramendia, J., Gomez-Nubla, L., Castro, K., Fdez-Ortiz de Vallejuelo, S., Arana, G., Maguregui, M., Baonza, V. G., Medina, J., Rull, F. & Madariaga, J. M. Overview of the techniques used for the study of non-terrestrial bodies: Proposition of novel non-destructive methodology. *Trends in Analytical Chemistry* **98**, 36–46 (2018).
- Izaguirre, M. El Pecio de Urbieta (Gernika) País Vasco. *Heritage at Risk. Underwater cultural heritage at risk: managing natural and human impact*. 90–92 (1998).
- Bilbao, M. M. Memoria de actividades. *Cuadernos de Relaciones Laborales* **33**, 477–481
- Izaguirre, M. & Valdés, L. Avance de excavación del pecio del siglo XV de Urbieta (Gernika). *Itsas Memoria. Revista de Estudios Marítimos del País Vasco* **2**, 35–41 (1998).
- Unsain, J. M. *La memoria sumergida. Arqueología y patrimonio subacuático vasco. Untzi Museoa - Museo Naval* (2004).

- Loewen, B. The Red Bay vessel. An example of a 16th-century Biscayan ship. *Itsas Memoria. Revista de Estudios Marítimos del País Vasco* **168**, 193–199 (1998).
- Irabien, M. J. & Velasco, F. Heavy metals in Oka river sediments (Urdaibai National Biosphere Reserve, northern Spain): Lithogenic and anthropogenic effects. *Environmental Geology* **37**, 54–63 (1999).
- Madariaga, J. Modelización del estuario de Gernika (Urdaibai). *Kobie Serie Ciencias Naturales XX*, (1991).
- Mijangos, L., Ziarrusta, H., Ros, O., Kortazar, L., Fernández, L. A., Olivares, M., Zuloaga, O., Prieto, A. & Etxebarria, N. Occurrence of emerging pollutants in estuaries of the Basque Country: Analysis of sources and distribution, and assessment of the environmental risk. *Water Research* **147**, 152–163 (2018).
- Irabien, M. J. PhD Thesis: Mineralogía y geoquímica de los sedimentos actuales de los ríos Nervión-Ibaizabal, Butrón, Oka y Nieve. Índices de gestión ambiental. *Universidad del País Vasco (UPV/EHU)* (1993).
- Solaun, O., Rodríguez, J. G., Menchaca, I., López-García, E., Martínez, E., Zonja, B., Postigo, C., López de Alda, M., Barceló, D., Borja, Á., Manzanos, A. & Larreta, J. Contaminants of emerging concern in the Basque coast (N Spain): Occurrence and risk assessment for a better monitoring and management decisions. *Science of the Total Environment* **765**, (2021).
- Villate, F., Iriarte, A., Uriarte, I. & Sanchez, I. Seasonal and interannual variability of mesozooplankton in two contrasting estuaries of the Bay of Biscay: Relationship to environmental factors. *Journal of Sea Research* **130**, 189–203 (2017).

- Luque, J. M. M. Pecio de Bakio. *Arkeoikuska: Investigación Arqueológica* 370–373 (2004).
- Arqueología, M. N. de. Arqueología subacuática en Bizkaia. El pecio de Bakio, investigación y puesta en valor. in *Actas de las Jornadas de ARQUA 2011* (ed. Ministerior de Educación, C. y D.) 131–138 (2011).
- Luque, J. M. M. in *Actas de las V Jornadas de Jóvenes en Investigación Arqueológica. Arqueología para el siglo XXI* 250–255 (2012).
- Luque, J. M. M. Pecio de Bakio. *Arkeoikuska: Investigación Arqueológica* 95–99 (2005).
- Luque, J. M. M. Pecio de Bakio. *Arkeoikuska: Investigación Arqueológica* 145–156 (2012).
- Solaun, O., Garmendia, J. M., del Campo, A., González, M., Revilla, M. & Franco, J. *Perfiles de las aguas de baño de la zona litoral de la Comunidad Autónoma del País Vasco. URA* (2016).
- García, L. *Information provided by the archaeologist.*
- I.S.O. Preparation of steel substrates before application of paints and related products - Visual assessment of surface cleanliness. *International Organization for Standarization* (1988). at <<https://www.iso.org/standard/15711.html>>
- Pinto, J., Prieto, A. C., Coria-Noguera, J. C., Sanz-Minguez, C. & Souto, J. Investigating glass beads and the funerary rituals of ancient Vaccae culture (S. IV-I BC) by Raman spectroscopy. *Journal of Raman Spectroscopy* **52**, 170–185 (2021).
- Valladolid, U. de. La Necropolis de Las Ruedas: Estelas y tumbas. at <<https://pintiavaccea.es/seccion/la-necropolis-de-las-ruedas-estelas-y-tumbas>>

- Sanz, C. & Coria, J. C. in *Novedades arqueológicas en cuatro ciudades vacceas: Dessobriga, Intercatia, Pintia y Cauca* 129–156 (2018).
- Hernández, L., Rubiales, J. M., Morales-Molino, C., Romero, F., Sanz, C. & Gómez Manzanque, F. Reconstructing forest history from archaeological data: A case study in the Duero basin assessing the origin of controversial forests and the loss of tree populations of great biogeographical interest. *Forest Ecology and Management* **261**, 1178–1187 (2011).
- Borrell, F., Ibáñez, J. J. & Bar-Yosef, O. Cult paraphernalia or everyday items? Assessing the status and use of the flint artefacts from Nahal Hemar Cave (Middle PPNB, Judean Desert). *Quaternary International* **569–570**, 150–167 (2020).
- Porat, R., Davidovich, U. & Frumkin, A. in *Outdoor Qumran and the Dead Sea. Proceedings of the Hebrew University - COST Cultural Heritage Workshop* (2012).
- Ibáñez, J. J. *Information provided by the archaeologist*.
- Blakelock, E., Martín-Torres, M., Veldhuijzen, H. A. & Young, T. Slag inclusions in iron objects and the quest for provenance: an experiment and a case study. *Journal of Archaeological Science* **36**, 1745–1757 (2009).
- Franco Pérez, F. J. & Gener Moret, M. Early ironwork in Biscay: Survey, excavation, experimentation and materials characterization. An integral study of the mountainside ironworks (ferrerías de monte or “haizeolak”). *Materials and Manufacturing Processes* **32**, 876–884 (2017).

- Ettler, V., Johan, Z., Zavřel, J., Selmi Wallisová, M., Mihaljevič, M. & Šebek, O. Slag remains from the Na Slupi site (Prague, Czech Republic): Evidence for early medieval non-ferrous metal smelting. *Journal of Archaeological Science* **53**, 72–83 (2015).
- Franco, J. Haizeolak en Bizkaia: Una investigación de largo recorrido sobre la arqueología de la producción del hierro. *Kobie Serie Anejo* **13**, 21–37 (2014).
- Orueta, E. PhD Thesis: Análisis de los materiales de las ferrerías de Bengola (Munitibar) y Urtubiaga (Ea). *Universidad del País Vasco (UPV/EHU)* (2018).
- Franco Pérez, F. J., Etxezarragaortuondo, I. & Lonbide, X. A. The origins of iron technology in the Basque Country: mountainside ironworks or haizeolak. *Kobie Serie Paleoantropología* **34**, 267–282 (2015).
- Álvarez, J. L. I. Las ferrerías de monte: una revisión bibliográfica. *Kobie Serie Paleoantropología* **18**, 207–214 (1989).
- Uriarte, R. Gestión y cambio técnico en una empresa siderúrgica tradicional: la ferrería El Pobal (s. XVI-XX). *Revista Internacional de los Estudios Vascos* **54**, 411–463 (2009).
- Torrecilla, M. J. La ferrería de “El Pobal” (Muskiz, Bizkaia). *Kobie Serie Paleoantropología* **26**, 245–272 (2000).
- Franco, J. PhD Thesis: Arqueología y paleosiderurgia prehidráulica en Bizkaia (siglos III-XIII) Tras las huellas de los antiguos ferrones. *Universidad del País Vasco (UPV/EHU)* (2017).
- Pereda, I. La metalurgia prehidráulica del hierro en Bizkaia: el caso de los alrededores del pantano de Oriola (Trapagaran, Bizkaia). *Kobie Serie Paleoantropología* **XX**, 109–122 (1993).

- Sandstrom, M., Jalilehvand, F., Persson, I., Gelius, U., Frank, P. & Hall-Roth, I. Deterioration of the seventeenth century warship Vasa by internal formation of sulphuric acid. *Nature* **415**, 893–897 (2002).
- Fors, Y. & Sandström, M. Sulfur and iron in shipwrecks cause conservation concerns. *Chemical Society Reviews* **35**, 399 (2006).
- UNESCO. *Convention on the protection of the Underwater Cultural Heritage Unesco*. (2001).
- Dillmann, P., Watkinson, D., Angelini, E. & Adriaens, A. *Corrosion and conservation of cultural heritage metallic artefacts. Corrosion and Conservation of Cultural Heritage Metallic Artefacts* (Woodhead Publishing Limited, 2013). doi:10.1533/9781782421573
- Fors, Y. PhD Thesis: Sulfur-related conservation concerns for marine archaeological wood: The Origin, Speciation and Distribution of Accumulated Sulfur with Some Remedies for the Vasa. (2008).
- Rémazeilles, C., Saheb, M., Neff, D., Guilminot, E., Tran, K., Bourdoiseau, J. A., Sabot, R., Jeannin, M., Matthiesen, H., Dillmann, P. & Refait, P. Microbiologically influenced corrosion of archaeological artefacts: Characterisation of iron(II) sulfides by Raman spectroscopy. *Journal of Raman Spectroscopy* **41**, 1425–1433 (2010).
- Fors, Y. & Sandström, M. Sulfur and iron in shipwrecks cause conservation concerns. *Chemical Society Reviews* **35**, 399–415 (2006).
- Irabien, M. J. Vertido de escorias en el Rio Oka (Reserva Natural de la Biosfera de Urdaibai Vizcaya): Aspectos mineralógicos y geoquímicos. *Geogaceta* **25**, 111,113 (1999).

- Carlin, W. & Keith, D. H. An improved tannin-based corrosion inhibitor-coating system for ferrous artefacts. *International Journal of Nautical Archaeology* **25**, 38–45 (1996).
- Neff, D., Dillmann, P., Descostes, M. & Beranger, G. Corrosion of iron archaeological artefacts in soil: Estimation of the average corrosion rates involving analytical techniques and thermodynamic calculations. *Corrosion Science* **48**, 2947–2970 (2006).
- Selwyn, L. in *Proceedings of Metal 2004, National Museum of Australia Canberra ACT* 294–306 (2004).
- Schwertmann, U. & Taylor, R. M. The influence of silicate on the transformation of lepidocrocite to goethite. *Clays and Clay Minerals* **20**, 151–158 (1972).
- Hanesch, M. Raman spectroscopy of iron oxides and (oxy)hydroxides at low laser power and possible applications in environmental magnetic studies. *Geophysical Journal International* **177**, 941–948 (2009).
- Mielczarski, J. A., Atenas, G. M. & Mielczarski, E. Role of iron surface oxidation layers in decomposition of azo-dye water pollutants in weak acidic solutions. *Applied Catalysis B: Environmental* **56**, 289–303 (2005).
- Gutierrez, J. A. PhD Thesis: Analytical diagnosis of the conservation state of weathering steel exposed to urban atmospheres. *Universidad del Pais Vasco (UPV/EHU)* (2013).
- Bajt Leban, M. & Kosec, T. Characterization of corrosion products formed on mild steel in deoxygenated water by Raman spectroscopy and energy dispersive X-ray spectrometry. *Engineering Failure Analysis* **79**, 940–950 (2017).

- Schlegel, M. L., Bataillon, C., Brucker, F., Blanc, C., Prêt, D., Foy, E. & Chorro, M. Corrosion of metal iron in contact with anoxic clay at 90°C: Characterization of the corrosion products after two years of interaction. *Applied Geochemistry* **51**, 1–14 (2014).
- Aramendia, J., Gomez-Nubla, L., Castro, K. & Madariaga, J. M. Structural and chemical analyzer system for the analysis of deposited airborne particles and degradation compounds present on the surface of outdoor weathering steel objects. *Microchemical Journal* **123**, 267–275 (2015).
- Estalayo, E., Aramendia, J., Castro, K., Madariaga, J. M., Garcia, L. & Garcia-Camino, I. in *Conserving Cultural Heritage* 319–321 (2018). doi:10.1201/9781315158648-80
- Nims, C., Cron, B., Wetherington, M., Macalady, J. & Cosmidis, J. Low frequency Raman Spectroscopy for micron-scale and in vivo characterization of elemental sulfur in microbial samples. *Scientific Reports* **9**, 1–12 (2019).
- Muyzer, G. & Stams, A. J. M. The ecology and biotechnology of sulphate-reducing bacteria. *Nature Reviews Microbiology* **6**, 441–454 (2008).
- Rémazeilles, C., Neff, D., Bourdoiseau, J. A., Sabot, R., Jeannin, M. & Refait, P. Role of previously formed corrosion product layers on sulfide-assisted corrosion of iron archaeological artefacts in soil. *Corrosion Science* **129**, 169–178 (2017).
- Huisman, D. J., Manders, M. R., Kretschmar, E. I., Klaassen, R. K. W. M. & Lamersdorf, N. Burial conditions and wood degradation at archaeological sites in the Netherlands. *International Biodeterioration and Biodegradation* **61**, 33–44 (2008).

- Rémazeilles, C., Lévêque, F., Conforto, E. & Refait, P. Long-term alteration processes of iron fasteners extracted from archaeological shipwrecks aged in biologically active waterlogged media. *Corrosion Science* **181**, (2021).
- Rémazeilles, C., Lévêque, F., Conforto, E., Meunier, L. & Refait, P. Contribution of magnetic measurement methods to the analysis of iron sulfides in archaeological waterlogged wood-iron assemblies. *Microchemical Journal* **148**, 10–20 (2019).
- Rémazeilles, C., Tran, K., Guilminot, E., Conforto, E. & Refait, P. Study of Fe(II) sulphides in waterlogged archaeological wood. *Studies in Conservation* **58**, 297–307 (2013).
- Aramendia, J., Gómez-Nubla, L., Castro, K. & Madariaga, J. M. Spectroscopic speciation and thermodynamic modeling to explain the degradation of weathering steel surfaces in SO₂ rich urban atmospheres. *Microchemical Journal* **115**, 138–145 (2014).
- Höffler, F., Müller, I. & Steiger, M. Thermodynamic properties of ZnSO₄(aq) and phase equilibria in the ZnSO₄–H₂O system from 268 K to 373 K. *Journal of Chemical Thermodynamics* **116**, 279–288 (2018).
- Falgayrac, G., Sobanska, S. & Brémard, C. Raman diagnostic of the reactivity between ZnSO₄ and CaCO₃ particles in humid air relevant to heterogeneous zinc chemistry in atmosphere. *Atmospheric Environment* **85**, 83–91 (2014).
- Rudolph, W. W., Brooker, M. H. & Tremaine, P. R. Raman spectroscopy of aqueous ZnSO₄ solutions under hydrothermal conditions: Solubility, hydrolysis, and sulfate ion pairing. *Journal of Solution Chemistry* **28**, 621–630 (1999).

- Rémazeilles, C., Lévêque, F., Conforto, E., Meunier, L. & Refait, P. Contribution of magnetic measurement methods to the analysis of iron sulfides in archaeological waterlogged wood-iron assemblies. *Microchemical Journal* **148**, 10–20 (2019).
- Höffler, F., Müller, I. & Steiger, M. Thermodynamic properties of ZnSO₄(aq) and phase equilibria in the ZnSO₄–H₂O system from 268 K to 373 K. *Journal of Chemical Thermodynamics* **116**, 279–288 (2018).
- Labrenz, M., Druschel, G. K., Thomsen-Ebert, T., Gilbert, B., Welch, S. A., Kemner, K. M., Logan, G. A., Summons, R. E., de Stasio, G., Bond, P. L., Lai, B., Kelly, S. D. & Banfield, J. F. Formation of sphalerite (ZnS) deposits in natural biofilms of sulfate-reducing bacteria. *Science* **290**, 1744–1747 (2000).
- Neff, D., Reguer, S., Bellot-Gurlet, L., Dillmann, P. & Bertholon, R. Structural characterization of corrosion products on archaeological iron: an integrated analytical approach to establish corrosion forms. *Journal of Raman Spectroscopy* **35**, 739–745 (2004).
- Aramendia, J., Gómez-Nubla, L., Castro, K. & Madariaga, J. M. Spectroscopic speciation and thermodynamic modeling to explain the degradation of weathering steel surfaces in SO₂ rich urban atmospheres. *Microchemical Journal* **115**, 138–145 (2014).
- Rodriguez-Iruretagoiena, A., Elejoste, N., Gredilla, A., Fdez-Ortiz de Vallejuelo, S., Arana, G., Madariaga, J. M. & de Diego, A. Occurrence and geographical distribution of metals and metalloids in sediments of the Nerbioi-Ibaizabal estuary (Bilbao, Basque Country). *Marine Chemistry* **185**, 82–90 (2016).

- Carlin, W. & Keith, D. H. An improved tannin-based corrosion inhibitor-coating system for ferrous artefacts. *International Journal of Nautical Archaeology* **25**, 38–45 (1996).
- Pérez, T. Estudio de la efectividad del ácido tánico sobre piezas de hierro arqueológico. (2017).
- Chadwick, A. v., Berko, A., Schofield, E. J., Smith, A. D., Mosselmans, J. F. W., Jones, A. M. & Cibin, G. The application of X-ray absorption spectroscopy in archaeological conservation: Example of an artefact from Henry VIII warship, the Mary Rose. *Journal of Non-Crystalline Solids* **451**, 49–55 (2016).
- Memet, J. B. in *Corrosion of Metallic Heritage Artefacts: Investigation, Conservation and Prediction of Long Term Behaviour* 152–169 (2007). doi:10.1533/9781845693015.152
- Fors, Y., Grudd, H., Rindby, A., Jalilehvand, F., Sandström, M., Cato, I. & Bornmalm, L. Sulfur and iron accumulation in three marine-archaeological shipwrecks in the Baltic Sea: The Ghost, the Crown and the Sword. *Scientific Reports* **4**, (2014).
- Fors, Y., Jalilehvand, F., Damian, E., Björdal, C., Phillips, E. & Sandström, M. Sulfur and iron analyses of marine archaeological wood in shipwrecks from the Baltic Sea and Scandinavian waters. *Journal of Archaeological Science* **39**, 2521–2532 (2012).
- Björdal, C. G. & Fors, Y. Correlation between sulfur accumulation and microbial wood degradation on shipwreck timbers. *International Biodeterioration and Biodegradation* **140**, 37–42 (2019).
- Gjelstrup, C. & Fors, Y. International Biodeterioration & Biodegradation Correlation between sulfur accumulation and microbial wood

- degradation on shipwreck timbers. *International Biodeterioration and Biodegradation* **140**, 37–42 (2019).
- Jana, A., Jana, S. K., Sarkar, D., Ahuja, T., Basuri, P., Mondal, B., Bose, S., Ghosh, J. & Pradeep, T. Electro spray deposition-induced ambient phase transition in copper sulphide nanostructures. *Journal of Materials Chemistry A* **7**, 6387–6394 (2019).
- Milekhin, A. G., Yeryukov, N. A., Sveshnikova, L. L., Duda, T. A., Rodyakina, E. E., Gridchin, V. A., Sheremet, E. S. & Zahn, D. R. T. Combination of surface- and interference-enhanced Raman scattering by CuS nanocrystals on nanopatterned Au structures. *Beilstein Journal of Nanotechnology* **6**, 749–754 (2015).
- Lafuente, B., Downs, R. T., Yang, H. & Stone, N. in *Highlights in Mineralogical Crystallography* 1–30 (2016). doi:10.1515/9783110417104-003
- Jegdić, B., Polić-Radovanović, S., Ristić, S. & Alil, A. Corrosion stability of corrosion products on an archaeological iron artefact. *International Journal of Conservation Science* **3**, 241–248 (2012).
- Bastidas, D. M., Ressa, J., Martin, U., Bosch, J., la Iglesia, A. & Bastidas, J. M. Crystallization pressure and volume variation during rust development in marine and urban-continental environments: Critical factors influencing exfoliation. *Revista de Metalurgia* **56**, 1–15 (2020).
- Jegdić, B., Polić-Radovanović, S., Ristić, S. & Alil, a. Corrosion Stability of Corrosion Products on an Archaeological Iron Artefact. *International journal of conservation science* **3**, 241–248 (2012).
- Kostadinovska, M., Jakovleska Spirovska, Z. & Minčeva-Šukarova, B. A spectroscopic study of inks from a rare Old Slavic manuscript:

Liturgical Collection of chronicles, scriptures, etc. 311–316 (2013).
doi:10.13140/RG.2.2.11773.56808

Degrigny, C. & le Gall, R. Conservation of ancient lead artifacts corroded in organic acid environments: Electrolytic stabilization/consolidation. *Studies in Conservation* **44**, 157–169 (1999).

Florentino, C. G. PhD Thesis: Development of innovative analytical methodologies, mainly focused on X-ray fluorescence spectrometry, to characterise building materials and their degradation processes based on the study performed in the historical building Punta Begoña Gall. *Journal of Chemical Information and Modeling* **53**, 1689–1699 (2019).

Frost, R. L., Martens, W., Kloprogge, J. T. & Ding, Z. Raman spectroscopy of selected lead minerals of environmental significance. *Spectrochimica Acta - Part A: Molecular and Biomolecular Spectroscopy* **59**, 2705–2711 (2003).

Krause, K. *Arms and the State: Patterns of Military Production and Trade*. (Cambridge University Press, 1996).

Ciarlo, N. C., López, A. N., de Rosa, H. M. & Pianetti, M. Naval Crossfire: A Comparative Analysis of Iron Projectiles from Mid-18th to Early 19th Centuries European Warships. *Procedia Materials Science* **8**, 712–721 (2015).

Cvikel, D., Ashkenazi, D., Stern, A. & Kahanov, Y. Characterization of a 12-pdr wrought-iron cannonball from the Akko 1 shipwreck. *Materials Characterization* **83**, 198–211 (2013).

Tylecote, R. F. *A History of Metallurgy*. (1976).

- Stefanescu, D. M. Classification and Basic Metallurgy of Cast Iron. *Properties and Selection: Irons, Steels, and High-Performance Alloys* **1**, 3–11 (2018).
- Singh, R. in *Applied Welding Engineering* 65–81 (2016). doi:10.1016/B978-0-12-804176-5.00007-4
- Akil, C. & Geveci, A. Optimization of conditions to produce manganese and iron carbides from Denizli-Tavas manganese ore by solid state reduction. *Turkish Journal of Engineering and Environmental Sciences* **32**, 125–131 (2008).
- Duraisamy, R., Pownsamy, K. & Asgedom, G. Chemical Degradation of Epoxy-Polyamide Primer by Electrochemical Impedance Spectroscopy. *ISRN Corrosion* **2012**, 10 (2012).
- Soiński, M. S., Jakubus, A., Kordas, P. & Skurka, K. The effect of aluminium on graphitization of cast iron treated with cerium mixture. *Archives of Foundry Engineering* **14**, 95–100 (2014).
- Selwyn, L. Overview of archaeological iron: the corrosion problem, key factors affecting treatment, and gaps in current knowledge. *Proceedings of Metal 2004, National Museum of Australia Canberra ACT* 294–306 (2004).
- Réguer, S., Dillmann, P. & Mirambet, F. Buried iron archaeological artefacts: Corrosion mechanisms related to the presence of Cl-containing phases. *Corrosion Science* **49**, 2726–2744 (2007).
- Neff, D., Dillmann, P., Bellot-Gurlet, L. & Beranger, G. Corrosion of iron archaeological artefacts in soil: Characterisation of the corrosion system. *Corrosion Science* **47**, 515–535 (2005).

- Rémazeilles, C., Neff, D., Kergourlay, F., Foy, E., Conforto, E., Guilminot, E., Reguer, S., Refait, P. & Dillmann, P. Mechanisms of long-term anaerobic corrosion of iron archaeological artefacts in seawater. *Corrosion Science* **51**, 2932–2941 (2009).
- Veneranda, M., Aramendia, J., Gomez, O., Fdez-Ortiz de Vallejuelo, S., Garcia, L., Garcia-Camino, I., Castro, K., Azkarate, A. & Madariaga, J. M. Characterization of archaeometallurgical artefacts by means of portable Raman systems: corrosion mechanisms influenced by marine aerosol. *Journal of Raman Spectroscopy* **48**, 258–266 (2017).
- Kergourlay, F., Guilminot, E., Neff, D., Remazeilles, C., Reguer, S., Refait, P., Mirambet, F., Foy, E. & Dillmann, P. Influence of corrosion products nature on dechlorination treatment: case of wrought iron archaeological ingots stored 2 years in air before NaOH treatment. *Corrosion Engineering, Science and Technology* **45**, 407–413 (2010).
- Veneranda, M., Costantini, I., de Vallejuelo, S. F.-O., Garcia, L., García, I., Castro, K., Azkarate, A. & Madariaga, J. M. Study of corrosion in archaeological gilded irons by Raman imaging and a coupled scanning electron microscope–Raman system. *Philosophical Transactions of the Royal Society of London A: Mathematical, Physical and Engineering Sciences* **374**, (2016).
- Ashkenazi, D., Nusbaum, I., Shacham-Diamand, Y., Cvikel, D., Kahanov, Y. & Inberg, A. A method of conserving ancient iron artefacts retrieved from shipwrecks using a combination of silane self-assembled monolayers and wax coating. *Corrosion Science* **123**, 88–102 (2017).

- Pinto, J., Prieto, A. C., Coria-Noguera, J. C., Sanz-Minguez, C. & Souto, J. Investigating glass beads and the funerary rituals of ancient Vaccaei culture (S. IV-I BC) by Raman spectroscopy. *Journal of Raman Spectroscopy* **52**, 170–185 (2021).
- Shaham, D., Grosman, L. & Goren-Inbar, N. The red-stained flint crescent from Gesher: New insights into PPNA hafting technology. *Journal of Archaeological Science* **37**, 2010–2016 (2010).
- Blakelock, E., Martín-Torres, M., Veldhuijzen, H. A. & Young, T. Slag inclusions in iron objects and the quest for provenance: an experiment and a case study. *Journal of Archaeological Science* **36**, 1745–1757 (2009).
- Ettler, V., Johan, Z., Zavřel, J., Selmi Wallisová, M., Mihaljevič, M. & Šebek, O. Slag remains from the Na Slupi site (Prague, Czech Republic): Evidence for early medieval non-ferrous metal smelting. *Journal of Archaeological Science* **53**, 72–83 (2015).
- Gómez-Nubla, L. PhD Thesis: Innovative analytical methodologies to characterize original and weathered materials of extraterrestrial origin and terrestrial analogues to meteorites. (2015).
- Madariaga, J. M. Analytical chemistry in the field of cultural heritage. *Analytical Methods* **7**, 4848–4876 (2015).
- Moral, L. F. G. del, Morgado, A. & Esquivel, J. A. Reflectance spectroscopy in combination with cluster analysis as tools for identifying the provenance of Neolithic flint artefacts. *Journal of Archaeological Science* **37**, 1–8 (2021).